Application of Mentha Plant Ash derived from distilled *Mentha piperita* plant waste as adsorbent in removal of dyes and heavy metals from aqueous solutions

THESIS

SUBMITTED TO
BABASAHEB BHIMRAO AMBEDKAR UNIVERSITY
LUCKNOW

BABASAHEB
BHIMRAO
AMBEDKAR
UNIVERSITY
LUCKNOW
प्रज्ञा शील करुणा
ESTABLISHED 1996

FOR THE DEGREE OF
Doctor of Philosophy
IN
ENVIRONMENTAL SCIENCE

Submitted by
Abhay Prakash Rawat
Enrollment number: 282/08

Under the guidance of
Prof. (Dr.) D. P. Singh

DEPARTMENT OF ENVIRONMENTAL SCIENCE
SCHOOL FOR ENVIRONMENTAL SCIENCES
BABASAHEB BHIMRAO AMBEDKAR UNIVERSITY
(A CENTRAL UNIVERSITY)
VIDYA VIHAR, RAEBARELI ROAD
LUCKNOW-226 025

2018

Certificate

This is to certify that the thesis titled **"Application of Mentha Plant Ash derived from distilled *Mentha piperita* plant waste as adsorbent in removal of dyes and heavy metals from aqueous solutions"** submitted by Mr. **Abhay Prakash Rawat** is an original research work and has not been previously submitted in part or full for the award of any other degree or diploma to this or any other University.

The thesis submitted to Babasaheb Bhimrao Ambedkar University, Lucknow satisfies all the requirements as stipulated in the *Doctor of Philosophy (Ph.D.) regulations -1999 as amended in 2008/2010/2013* and it is fit for submission and evaluation for the award of the degree of Doctor of Philosophy of the University.

Date: 23/07/218

23.07.18

(Supervisor)

Dr. D.P. SINGH
Professor
Department of Environmental Sciences
Babasaheb Bhimrao Ambedkar Central University
Lucknow-226025 (U.P.)

23.7.18

Head of the Department

Head
Deptt. of Environmental Sciences
B. B. Ambedkar University
Rae Bareli Road, Lucknow-25

Declaration

I hereby declared that the work presented in the thesis entitled **"Application of Mentha Plant Ash derived from distilled *Mentha piperita* plant waste as adsorbent in removal of dyes and heavy metals from aqueous solutions"** has been conducted in the Department of Environmental Science, Babasaheb Bhimrao Ambedkar University, Lucknow-226025, Uttar Pradesh, India. It is also declared that the work presented herein, to the best of my knowledge and original in nature. It has not been submitted earlier in part or full to any other University or Institute for the award of any other degree or diploma.

Date: 23/07/2018

Abhay Prakash Rawat

Dedicated to

My parents and Teachers

PREFACE

Adsorption is one of the most efficient methods for removal of dyes and heavy metals from aqueous solutions. Since last few years, adsorption technique has drawn greater attention of the scientists due to its cost effective nature, highly efficient and simple operation. The present work is an attempt in the direction of using low cost solid waste byproduct of mentha oil distillation units. The Mentha plant after distillation is air dried and used as source of cheap fuel. The ash generated after burning is simply a useless byproduct. In the present investigation, the powdered dry ash of Mentha plant has been used as an adsorbent for removal of dyes and chromium metal. The present investigation entitled "Application of Mentha Plant Ash derived from distilled *Mentha piperita* plant waste as adsorbent in removal of dyes and heavy metals from aqueous solutions'' includes VIII chapters:

Chapter-I: It describes general introduction about water pollution, role of dyes in water pollution, classification of dyes based on composition and application, heavy metal chromium and its occurrence in the environment.

Chapter-II: This chapter relates to review of literature concerning the research topic. It includes the work done by earlier workers carried out in relation to dyes/metals using various sorbents.

Chapter-III: It describes detailed methodology including chemicals and solutions, collection of Mentha Plant Ash (MPA), use of various instrumental techniques required for removal of dyes and Cr(VI). It also incorporates details of kinetic and thermodynamic studies related to adsorption of dyes and Cr(VI) metal.

Chapter-IV: This chapter describes general characterization of Mentha Plant Ash (MPA) as an adsorbent. The results of MPA characterization are based on SEM, EDX, BET, TGA, XRD and FTIR analysis of the sample.

Chapter-V: It includes removal of cationic dyes by Mentha Plant Ash (MPA). In this chapter, the results in section A pertains to removal of malachite green (MG) dye by Mentha Plant Ash (MPA), whereas in section B, removal of methylene blue (MB) dye by Mentha Plant Ash (MPA) has been described. The data on optimization of dye removal are also discussed with reference to temperature, pH, dose of dye/adsorbent etc. Further, data were analyzed for adsorption isotherms, kinetics and thermodynamic parameters.

Chapter-VI: It describes the removal of Cr(VI) by Mentha Plant Ash (MPA). The adsorption mechanisms involved in Cr(VI) adsorption by MPA has been worked out using different analytical tools such as FTIR, XPS, XRD, cyclic voltammetry etc. The kinetic and thermodynamic parameters were analyzed to explain the nature of adsorption.

Chapter-VII: This chapter describes the general discussions regarding characterization of Mentha Plant Ash (MPA) before and after adsorption of cationic dyes (MG and MB) and Cr (VI), factors affecting the adsorption of cationic dyes/Cr(VI).

Chapter-VIII: It mentions summary of the thesis work and important conclusions as evident from the findings of present investigation.

Finally, the most important outcome of the present investigation is that the Mentha Plant Ash (MPA) can be cheap, ecofriendly and excellent adsorbent for removal of cationic dyes and chromium metal due to it electronegative surface active ligands involving chemisorption process. At the same time, finding revealed that MPA also worked as

chemical catalyst catalyzing the reductive chemical transformation of dyes/metals as evident from the results of redox reaction.

Acknowledgements

I wish to express my deep sense of gratitude and reverence to the supervisor, Prof. D. P. Singh, Department of Environmental Science, Babasaheb Bhimrao Ambedkar University, Lucknow, Uttar Pradesh, India for his invaluable encouragement, helpful suggestions and supervision throughout the course of this work.

It is indeed, a great pleasure for me to express my heartfelt gratitude to Prof. S. K. Diwedi, Head, Department of Environmental Science and Director, University Science Instrumentation Centre (USIC), Babasaheb Bhimrao Ambedkar University, Lucknow, Uttar Pradesh, India for availing laboratory facilities to perform the experiments during the experimental work.

I am very thankful to Director, IIT, Kanpur for his kind permission for availing laboratory facilities to perform the experiments regarding characterization of adsorbent. The financial assistance provided to me as RGNF by the University Grant Commision, New Delhi, during the period of my research is gratefully acknowledged.

I would like to thanks all the faculties of Department of Environmental Science, Babasaheb Bhimrao Ambedkar University, Lucknow, Uttar Pradesh, India for their constant inspiration and encouragement. I am also thankful to all the staff members of Department of Environmental Science, Babasaheb Bhimrao Ambedkar University, Lucknow, Uttar Pradesh, India for their kind cooperation during the work period.

I acknowledge with thanks the help rendered by my colleagues, friends and technical staff Dr. Mukesh Kumar, Dr. Prem Chandra, Amit Kumar Rawat, Vinay Kumar, Vijay Singh, Ranjeet Sharma, A. K. Jain while carrying out instrumental analysis and experiments.

Lastly, I would like to thank my family members and friends for providing physical and moral support throughout the research work.

22/07/18

Abhay Prakash Rawat

Contents

Chapter-6

Chapter–7

Chapter–8

List of Tables

List of Figures

CHAPTER-I

General Introduction

1.1. Introduction

Nature does not produce anything that is harmful and cannot be decomposed and returned to the fresh pool resources present on earth. Nature returns organic and inorganic wastes to the soil in the form of manure and fertilizers. People often dump such wastes in the rivers and oceans, and thus treat the nature as a commodity. The detrimental effect of pollutants caused to water, air, land and other natural resources are referred as environmental pollution. Rivers and lakes nurture early civilization and human life without disturbing the ecosystems and nature. However, modernization has altered the trend of the environment and damaged its original state. The cities and villages developed along the rivers and lakes are discharging large quantities of different type of sewage into natural water bodies, virtually changing them into an open sewers. The industries established in urban and sub-urban areas discharge large quantity of industrial wastewater into natural water streams and oceans. Environmental pollutants coming from industrial effluents are of major concern because of their high toxicity potential and threat to human beings and environment. The discharge of untreated industrial effluents to the natural water bodies has raised high risk of health hazards associated with the entry of toxic pollutants into the food chains of animals and humans. Probably, the overpopulation is the main cause of environmental deterioration. The total land area available for cultivation is shrinking day by day due to desertification, soil erosion, changes in the weather conditions, fast growth of road systems and reduction in irrigation water. It is necessary for all of us to be aware of all such dimensions of the biosphere that are fixed and has limited ability to absorb pollutants. Socio-economic development is the main key to secure water availability in an increasing water-stressed conditions where huge quantity of wastes are being produced as an inseparable part of many human activities. Administrative, technical

processes and effective management are important parameters to gain water security, but it is not possible to produce them without support of economic resources.

1.2. Water Pollution

Water is a most precious natural resources available on the earth. It covers about 70% of the earth's surface, but only 0.7% of the fresh water is used for human consumption. Due to gradual increase in the global population by 2020, the water demand may also increase by about 50% in developing countries and approximately 18% in developed countries by 2020 (UN-Water, 2013). Saving water to save the earth and to make the future of mankind safe is a primary concern of environmentalists. The growth of mankind, society, science and technology is reaching to new horizons, but the environmental cost which we are going to pay in near future will surely be too high. Water scarcity is going to affect every society and it is estimated that about 1.8 billion people world over will be living with absolute water scarcity by the end of 2020. The water requirement by agriculture, industry, domestic purposes and energy sector would be very high (UN-Water, 2013). The United Nations World Water Development Report, UNESCO reported that industrial, agricultural and domestic sectors are consuming about 70, 22 and 8% of the available fresh water, respectively, which has resulted in the generation of large quantity of wastewater (Krishnan et al., 2011). Water pollution is the major global environmental problem at present day. Ever increasing contamination of natural water reserves such as rivers, lakes, oceans and ground water is adding to India's water woes. About 70% of the surface water and an increasing percentage of groundwater is being contaminated by organic and inorganic toxic pollutants. The sources of such pollution include point and nonpoint sources such as industrial waste water, domestic waste water and agriculture. The health implications of poor quality of water are enormous and water related diseases are responsible for

more than 60% of the health burden in India (UNICEF, FAO and SaciWATERs, 2013). Among all the toxic pollutants, the most important classes of the pollutants are dyes and heavy metals present in various industrial effluent. It is important to note that water pollution by dyes and heavy metals is considered as a serious environmental problem because these pollutants tends to modify the physico-chemical properties of water and are very toxic to aquatic life, animals and human beings (Sciban et al., 2011).

1.3. Dyes and their role in water pollution

Different dyes present in the industrial wastewaters are considered one of the major class of water pollutants. Many textile processing industries discharge a large amount of textile effluents into natural water bodies as shown in Fig. 1.1. Dyes cause severe environmental disposal problems due to their persistent and non-biodegradable nature (Chen et al., 2013).

Fig. 1.1. Discharge of textile effluents into natural water bodies by textile processing industry.

Synthetic dyes are types of toxic organic pollutants mainly used in paper industry, dye houses, textile and printing industries (Mittal et al., 2010). Synthetic dyes can cause serious environmental pollution due to their extensive application and large scale

production (Forgacsa et al., 2004). Food industries, printing, textiles, dyeing and dye manufacturing units are the main sources of dye release into natural water bodies (Mittal et al., 2010). Among various industries, the textile industry stands as frontline user of coloring dyes. It has been estimated that approximately 15% of the total dye stuff is lost to industrial effluents during manufacturing processes (Chakraborty et al., 2011). It has been reported that more than 1, 00,000 commercial dyes producing industrial units are available with an annual production of over 7×10^5 tons (Khandegar and Saroha, 2013). The synthetic organic dyes are known to cause serious health problems as number of dyes produced in industrial processes are found to be quite stable against photobleaching and are also persistent against aerobic digestion because of their structural complexity and large molecular size (Dincer et al., 2007). Depending on the ionic charges of the dye molecules, dyes can be categorized as cationic, anionic and non-ionic forms, and the cationic dyes have more toxicity potential as compared with anionic dyes (El-Sayed, 2011). Among various synthetic dyes, basic cationic dyes (crystal violet, methylene blue and malachite green) have drawn much more attention of researchers towards its complex structure, toxicity potential and its removal from their aqueous solutions.

1.4. Classification of dyes based on composition and application

The organic compounds which absorb electromagnetic/light energy with the wavelengths in the visible range (350–700 nm) are referred as colored compounds. Generally, the dyes contain two basic components which include chromophores and auxochromes. The chromophores may be defined as the delocalized electron systems with conjugated double bonds whereas auxochromes are electron donating or electron withdrawing groups that enhance the color of the chromophore by varying the total energy of the electron system. The common chromophores include –C=N–, –C=C–, –

N=N–, $–NO_2$, –C=O, and quinoid rings whereas common auxochromes are –COOH, $–NH_3$, –OH, and $–SO_3H$ (van der Zee et al., 2003). Various chromophore groups present in synthetic dyes are listed in Table 1.1. Further, all the synthetic dyes can be classified either according to their mode of application or its composition.

The chemical structures of dyes decide the properties, colors and its uses, and provide only the rational basis for the classification of synthetic dyes (Kiernan, 2001). A number of dyes groups based on the availability of different chemical structure/structural units/chromophores are reported currently. A very important dyes groups includes azo (monoazo, diazo, triazo, polyazo), arylmethane (diarylmethane, triarylmethane), anthraquinone, naphthoquinone, phthalocyanine and polymethine dyes. Other important dye groups are indigoid, thiazine, xanthene, azine, oxazine, nitro, nitroso, lactone, thiazole, indamine, indophenol, aminoketone and hydrxyketone dyes and dyes with undetermined chemical structures such as sulphur and stilbene dyes (Kiernan, 2001).

Dyes and colorants are classified depending on its mode of applications. They include basic dyes, acid dyes, direct dyes, reactive dyes, disperse dyes, azo dyes, mordant dyes and vat dyes (Hao et al., 2000).

Generally, the reactive dyes contain some reactive groups which are actively participate in the formation of covalent bonds with hydroxyl (OH^-), amine (NH_2^-) and thiol groups (–SH) in the fibers. Reactive dyes are widely used in the textile industry due to their wide range of color shades, easy application and low energy consumption (Singh et al., 2011). The hydrolysis of the reactive groups is an unwanted side reaction and it minimizes the extent of fixation onto fibers. Thus, it has been estimated that about 10–50% of reactive dyes do not react with fibers and it is hydrolyzed in the aqueous phase.

The problem of colored wastewater is therefore identified mainly with application of reactive dyes.

According to the color index, the acid dyes group is the largest class of dyes and it has been estimated that about 2300 different acid dyes are currently listed and currently about 40% of them are in production. The acid dyes are commonly referred as anionic organic compounds and mainly used for dyeing basic groups containing wool and silk fibres. Application of these dyes is usually favoured under acidic conditions due to protonation of basic groups present in the fibers. The dyeing process of acid dyes is reversible in nature and they are usually removed from fabrics by washing. The presence of different chromophore groups such as azo, anthraquinone and triarylmethane in acid dyes exhibit varying nature and behavior in aqueous media.

Direct dyes are referred as large and linear organic molecules which have high binding affinity towards cellulosic fibers. The dyes bind with the cellulosic fibers through weak Van der Waals forces of attraction. It has been suggested that the common salt is often used with the direct dye to promote dyeing, because the presence of excess sodium ions favours establishment of equilibrium stage with the minimum concentration of direct dye. The dyeing process of the direct dyes is reversible in nature and exhibit poor wash fastness. A typical example of direct dye is Congo red dye.

Mordant dyes are the compounds which attach to the fiber and then bind with the dye molecules to form an insoluble complex. It has been estimated that about 600 different mordant dyes are listed in the color index. Nowadays the usage of mordant dyes is gradually decreased to about 23%, but still they are used for dyeing silk, paper, wool, leather and modified cellulosic fibers. These dyes have poor affinity for the fibers. However, these dyes need a pretreatment of the fiber with the mordants (usually metal

salts such as chromium and iron salts). Azo, oxazine and triarylmethane compounds are generally referred as mordant dyes.

Table 1.1. Different chromophore groups present in synthetic organic dyes.

CLASS	CHROMOPHORE	EXAMPLE
Nitro dyes	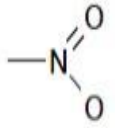	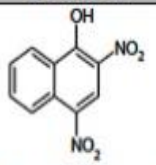 C.I. Acid Yellow 24
Nitroso dyes		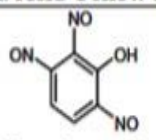 Fast Green O
Azo dyes		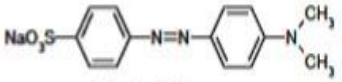 Methyl Orange
Triphenyl methyl dyes	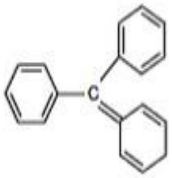	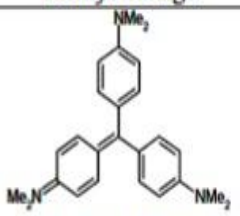 C.I. Basic Violet 3
Phthalein dyes	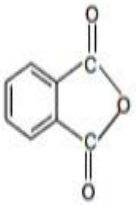	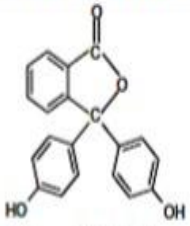 Phenolphtaleine
Indigoid dyes	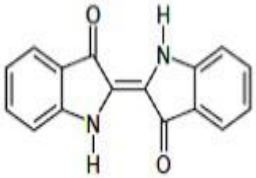	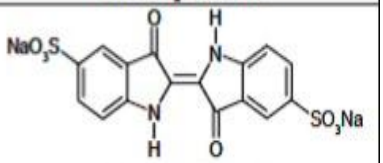 C.I. Acid Blue 71
Anthraquinone dyes	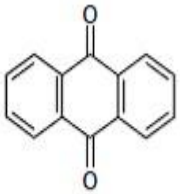	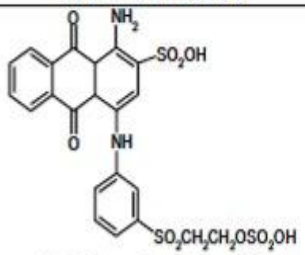 C.I. Reactive Blue 19

The disperse dyes are less soluble and specifically used to color synthetic fibers like cellulose acetate, polyester, polyamide, acryl and etc. The diffusion of dye molecules requires swelling of the fiber and it is achieved either by high temperature (>120˚C) or with the help of chemical softener. Disperse dyes form the third largest group of dyes in the color index. It has been estimated that about 1400 disperse dyes are listed currently and out of which about 40% are currently manufactured by the industries.These dyes are commonly azo or nitro compounds (yellow to red), anthraquinones (blue and green) or metal complex azo compounds (all colors).

Vat dyes are insoluble in water but their reduced forms are more soluble in water. These dyes are basically applied on fibers in their reduced forms and this form can be obtained by treating the compound with reducing agent (alkaline sodium dithionite). When the reduced form of dye is adsorbed on the fiber; the original insoluble dye is reformed upon oxidation with air or chemicals. Vat dyes offer excellent fastness but these dyes are quiet expensive and need some extra care during application. The vat dyes contain indigo and anthraquinone type of chromophore groups.

The sulphur dyes are heterocyclic polymeric aromatic compounds. Dyeing process of sulfur dyes involves reduction and oxidation process. Sulfur dyes become water soluble after reduction with sodium sulfide and exhibit great affinity towards cellulosic fibers. After exposure to air, the dyes are oxidized to insoluble dye inside the fibers. Sulfur dyes are basically used in textile industry to color cellulose fibers.

Solvent dyes (lysochromes) are nonionic dyes which are used for dyeing substrates in which they can easily dissolve, e.g. plastics, varnish, ink, waxes and fats. Most solvent dyes are diazo compounds and have found very less application in textile industry.

1.5. Basic cationic dyes

The cationic dyes are mainly employed in dyeing of wool, acrylic, nylon and silk fibres. Based on different substituted aromatic groups, cationic dyes have different molecular structures (Eren and Afsin, 2007). These dyes are commonly known as basic dyes and mainly depend on a positive ions like hydrochloride or zinc chloride complexes (Tyagi et al., 2002). Generally, cationic dyes have a positive charge in their chemical structure, furthermore these are soluble in water and produce colored cations in aqueous solution. Cationic functionality is found in number of dyes, especially in cationic azo dyes and methane dyes. Various other dyes such as anthraquinone, phthalocyanine dyes, di- and tri-arylcarbenium, various polycarbocyclic and solvent dyes also show cationic functionality. The anthraquinone dyes are expensive and weak as compared to low cost, strong cationic azo dyes (Hunger, 2003). Basic cationic dyes are highly visible even in very low concentration and have high color intensity and brightness (Mishra and Tripathi, 1993). Cationic dyes such as Crystal violet, Malachite green, Methylene blue, Basic blue 41 and Basic red 46 have been used intensely as model in dye adsorption studies. Among thsese dyes, Methylene blue is an important basic cationic dye which is widely used in the textile industry. It has been estimated that the basic dyes represent about 5% of all the dyes listed in the color index. These dyes give intense and brilliant shades to fibers but have poor light fastness. Further, basic dyes can be applied for dyeing silk and wool fibres directly.

The crystal Violet (CV), malachite green (MG) and methylene blue (MB) dyes are basic cationic dyes mostly used in the textile industry, manufacturing of paints, printing inks, leather, wool, jute and silk due to its low cost, easy availability, efficacy and lack of a proper alternatives (Zhang et al., 2008; Chakraborty et al., 2011). The chemical structures of CV, MG and MB dye have been shown in Fig. 1.2. The CV, MG and MB dye have been considered as a persistent recalcitrant organic molecule in the

environment as it is poorly metabolized by the microbes (Chakraborty et al., 2011; Shayesteh et al., 2015). In addition to it, the CV, MG and MB dye are found to be relatively more carcinogenic, genotoxic, mutagenic, and teratogenic as compared to anionic dyes due to its aromatic ring with delocalized electrons (Shayesteh et al., 2015; Suwandi et al., 2012). If these dyes are absorbed in higher amounts through the skin, it can cause skin irritation, digestive tract irritation, respiratory and kidney failures (Mittal et al., 2010; Ahmad, 2009; Shayesteh et al., 2015).

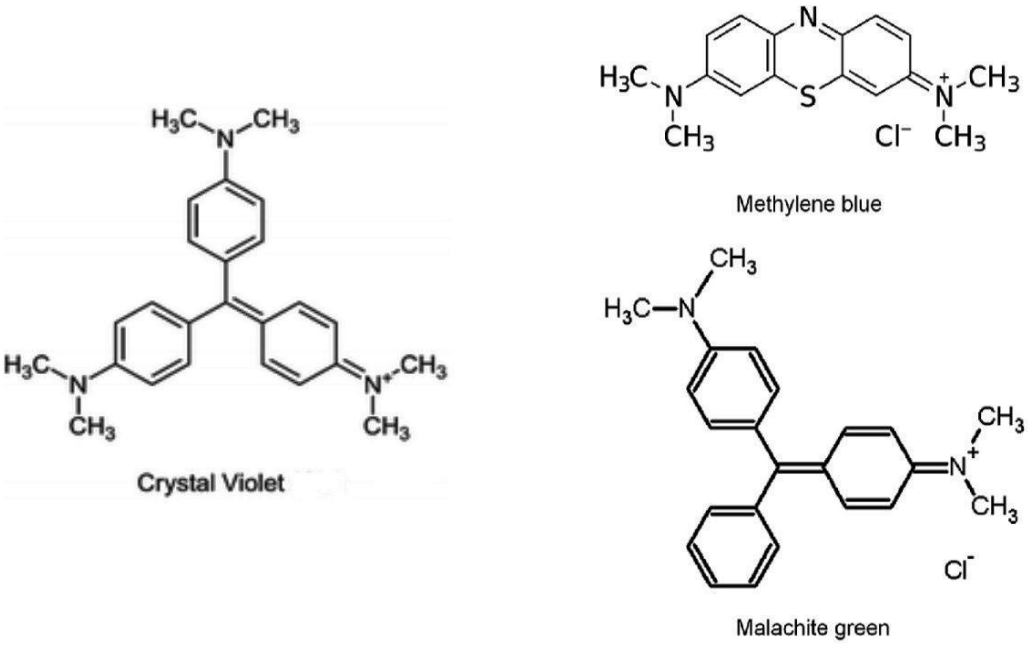

Fig. 1.2. Chemical structures of cationic dyes (crystal violet, malachite green and methylene blue).

1.6. Heavy metals

Heavy metals include copper (Cu), chromium (Cr), cobalt (Co), iron (Fe), manganese (Mn), molybdenum (Mo), magnesium (Mg), nickel (Ni), zinc (Zn), selenium (Se), mercury (Hg), arsenic (As) and lead (Pb). Among them, some are required as essential mineral nutrients for healthy physiological and biochemical functions of living beings while the other heavy metals such as cadmium, chromium, lead, mercury, arsenic, copper and cobalt are found to be extremely toxic for living beings even when ingested in very little amounts and are considered as major environmental pollutants because of

their high toxicity potential, non-biodegradable nature and accumulative behaviors (Anjum et al., 2011). A number of industries such as mining ore processing, metal processing, metal polishing, paint and battery manufacturing industries discharge large amount of industrial wastes and contribute to increase metal loads in the natural water bodies. A large amount of metal-loaded industrial effluent from various industries are discharge into natural water bodies and disturb the functioning of aquatic systems by causing metal toxicity in aquatic life and human beings (Babarinde et al., 2006). The main sources of heavy metals into the environment are listed in Table 1.2. The United States Environmental Protection Agency has estimated that 4,65,237 kg $year^{-1}$ of chromium, 5500 kg $year^{-1}$ of arsenic, 78,382 kg $year^{-1}$ of lead and 3,67,278 kg/year of nickel are released into the environment in the form of wastewater (USEPA, 1995). Industrial wastewater containing different metal pollutants (chromium, lead, mercury, nickel, copper and cadmium) causing direct toxicity to human and animals due to their concentration beyond the specified permissible limits (Xuejiang et al., 2006). Even at very low concentrations, these heavy metals are known to cause developmental abnormalities, cardiovascular diseases, neurologic disorders, hematologic and immunologic disorders. These heavy metals are also considered as potential carcinogens for living beings according to the U.S. Environmental Protection Agency. The presence of toxic heavy metals in natural water bodies due to discharge of untreated metal containing effluent from the associated industries, is considered to be as one of the most serious environmental problems (Hawari and Mulligan, 2006). Among various toxic heavy metals, Cr(VI) has drawn much more attention of environmentalists and many research groups are involved in the study of sources, application and toxicity potential of Cr(VI). In order to minimize the concentration of toxic metals in water and

wastewater, it is very necessary to treat industrial effluents to permissible levels before their discharge and cycling into the environment.

Table 1.2. Presence of heavy metals in industrial wastewater of different industries.

Industry	**Heavy metals present**
Electroplating	Cu, Cr, Zn, Ni
Batteries	Pb, Hg, Cd
Leather	Cr
Fertilizers	As, Cd, Cr, Mn, Hg, Cu, Zn, Pb
Paints, dyes and pigments	Cr, Cd, Pb, Cu, Ti, Se
Mining and metallurgy	Cd, Cr, As, Hg, Cu, Pb, Zn, Ni

1.7. Chromium and its occurance in the environment

Chromium is the most abundant element present on the earth crust in different valance states (-2 to +6), but among these the Cr(III) and Cr(VI) are commonly present in the natural environment. The two different oxidation states of chromium have different biological, chemical and environmental characteristics (WHO, Geneva, 1988). The Cr(II) compounds are very unstable and readily change to Cr(III) compounds whereas Cr(III) compounds are most stable. Most of the Cr(III) compounds are sparingly soluble in water, whereas the majority of Cr(VI) compounds are highly soluble in water and their presence in the environment has associated with the industrial activities. A list of water soluble Cr(VI) compounds are given in Table 1.3. The Cr(III) is present in vegetables, fruits, meat, grains and is often added to vitamins as a dietary supplement, whereas Cr(VI) produce by various industrial processes is considered as major environmental pollutants. The most stable state of chromium is Cr(III) which is comparatively less toxic than Cr(VI) (Wang et al., 2009). The trivalent state Cr(III) is comparatively insoluble in aqueous systems and required by microorganisms in very

small amounts as an essential trace metal nutrient (Saner, 1980), while hexavalent form of Cr(VI) is a major concern because of its high toxicity potential. Cr(VI) has been considered as a primary contaminant to animals, plants, humans and microorganisms and it is known to be carcinogenic for all living beings (Golonka, 1995).

Table 1.3. Different Cr(VI) compounds and their solubility in water.

Chromium compounds	Colour crystalline forms	Water solubility
Na_2CrO_4	Yellow	Soluble
$CaCrO_4$	Yellow	Slightly soluble
$Na_2Cr_2O_7$	Orange red	Soluble
K_2CrO_4	Yellow	Soluble
CrO_3	Dark red brown	Soluble
$K_2Cr_2O_7$	Orange red	Soluble
$SrCrO_4$	Yellow	Slightly soluble

Generally, the Cr(VI) occurs in combination with other elements in the form of chromium salts which are soluble in water. It has been estimated that about 80% of the Cr(VI) is used in stainless steel industry and various metallurgical applications. It is used to produce ferrous and non-ferrous alloys in chemical industry for the production of pigments, tanning of leather, electroplating and as a catalyst in the synthesis of many chemicals (Opperman and Van Heerden, 2007). The general physical characteristics of chromium are listed in Table 1.4.

A large amount of chromium is discharged into the environment by the textile dyeing, leather tanning, electroplating, steel fab-rication, mining, aluminium conversion coating operations, wood treatment units, paints and pigments leading to serious water pollution (Nriagu and Nieboer, 1988). Most of the industrialized countries have instituted the discharge limits for both Cr(III) and Cr(VI) due to their environmental concerns. The permissible limits for chromium in drinking water and industrial

wastewater are listed in Table 1.5 (BIS, 2012; EPA, 2010; USEPA, 2012; WHO, 2011). In order to meet the standard limit, it is important that the industries treat their effluents to reduce the concentration of Cr(VI) in wastewater to permissible levels before its disposal and cycling into the environment. Therefore, the concentration of Cr(VI) in industrial effluent can be minimized by the application of suitable methods.

Table 1.4. General physical characteristics of chromium.

General properties		**Physical properties**	
Symbol, Atomic number	Cr, 24	Density	7.19 g/cm^3
Elemental category	Transition metal	Melting point	2180 K
Group, Period, Block	VI, 4, d	Boiling point	2944 K
Standard atomic weight	51.9961	Heat of vaporization	339.5 KJ mol^{-1}

Table 1.5. Permissible limits for chromium in drinking water and industrial wastewater.

Permissible limits in drinking water (mg/L)				**Permissible limits for industrial wastewater discharge (mg/L)**
BIS	**EPA**	**USEPA**	**WHO**	**BIS**
0.05	0.05	0.1	0.05	0.1–2.0

1.8. Removal of dyes and heavy metals

Growing environmental concern and strict government policies have drawn an increasing attention of many research groups towards removal of dyes and heavy metals from the industrial wastewater. A number of methods are utilized to remove organic

and inorganic contaminants from the industrial wastewater. These methods include ion exchange (Tiravanti et al., 1997), electrochemical precipitation (Kongsricharoern and Polprasert, 1996), reduction (Seaman et al., 1999), adsorption (Calace et al., 2002), solvent extraction (K. Pagilla and Canter, 1999), membrane separation (Chakravarti et al., 1995, reverse osmosis and bio-sorption (Aksu and Kutsal, 1990; Aksu et al., 1996) and reduction followed by chemical precipitation (Zhou et al., 1993) and etc. All the treatment methods for the removal contaminants from aqueous systems can be divided into three categories viz. biological, chemical and physical methods. All of these methods have some advantages as well as drawbacks due to uneconomical high cost and disposal problems.

1.8.1. Biological treatment

Biological treatment is often used as an economical alternative method when compared with other physical and chemical processes of wastewater treatment. Biodegradation methods such as fungal decolorization, microbial degradation and adsorption by using both living and dead biomass are commonly employed methods of treatment of industrial wastewater. Many microorganisms such as bacteria, yeasts, algae and fungi are known to accumulate and degrade different toxic pollutants (Chakraborty et al., 2011). However, the application of microbes is often restricted because of technical constraints. Biological treatment requires a large land area and is constrained by sensitivity of microorganisms toward toxicants and growth limiting factors. Less operational flexibility in design and operation of biological treatment do not provide satisfactory results with biological treatment processes. Though many organic molecules are degraded, but many other compounds/chemicals are recalcitrant due to their complex chemical structure and highly toxic nature such as azo dyes which are never completely degraded (Shayesteh et al., 2015).

1.8.2. Chemical treatment

Chemical methods include coagulation or flocculation combined with floatation and filtration, precipitation, electrofloatation, electrokinetic coagulation, conventional oxidation by oxidizing agents and electrochemical processes. These chemical techniques are often expensive in treatment of industrial wastewater and create disposal problems due to accumulation of concentrated sludge. There is often a possibility of causing secondary pollution problem due to the excessive use of chemicals. Recently, other emerging techniques, known as advanced oxidation processes, which are based on the generation of powerful oxidizing agents such as hydroxyl radicals, have been successfully applied in degradation of various pollutants (Krishnan et al., 2017). Although chemical method is an efficient treatment process for industrial wastewaters but they are not cost effective and ecofriendly. The demand of high electrical energy and the consumption of many chemical reagents are most common problems of these method which make them commercially unattractive (Krishnan et al., 2017).

1.8.3. Physical methods

A number of physical methods such as membrane-filtration processes (nano-filtration, reverse osmosis, electro-dialysis) and adsorption techniques are commonly employed for removal of dyes and heavy metals from industrial wastewater (Dermont et al., 2008). Limited time, membrane fouling and the cost of periodic replacement of membranes are some of the major disadvantages of the membrane processes. So, among all the physical methods, adsorption method has been found to be superior to other techniques of wastewater treatment in terms of initial cost, flexibility and simplicity of design, easy operation and insensitivity to toxic pollutants (Babel and Kurniawan, 2003).

1.9. Adsorption and adsorbents

Adsorption is a well-known equilibrium separation process and is found to be an effective method for water decontamination applications. In accordance with literature, the liquid-phase adsorption is one of the most popular methods for the removal of pollutants from wastewater as the adsorption process results into a high-quality treated effluent (Gisi et al., 2016). The adsorption process provides an attractive alternative for the treatment of contaminated waters, especially if the sorbent is inexpensive and does not require an additional pre-treatment step before its application. Adsorption is the process of accumulating the dissolved substances in solution on a suitable solid-liquid interface. It is a mass transfer operation wherein the constituents of liquid phase get transferred to the solid phase. The substance which is being separated from liquid phase is called 'adsorbate' and the substance which accumulates the substance is called 'adsorbent' (Metcalf and Eddy, 2004). Adsorption is one of the simple and cost effective techniques for removal of dyes and heavy metals from their aqueous solutions. High efficiency, easy handling, high selectivity, low operating cost, minimum use of chemicals and regeneration of adsorbent are the main advantages of this method. However, initial dye/metal ion concentration, adsorbent dose, contact time, pH and temperature are the few process optimizing factors that influence the rate of adsorption. Applicability of different adsorbents is often limited as they are usually prepared from non-renewable materials and they are still found to be expensive. In recent years, different waste biomass have been applied for removal of dyes and heavy metals from wastewater and that is considered as good step in the direction of reducing the cost of adsorbent (Zhang et al., 2014). Activated carbon is one of the most commonly used adsorbent for the removal of dyes/heavy metals because of its large surface area, micro-porous nature, high adsorption capacity and surface reactivity. However, commercially available activated carbon is still found to be very expensive and has high cost of

regeneration (Waranusantigul et al., 2003). This has led many researchers to find some cheap and efficient alternative materials for this purpose. Researchers are always in search for developing more efficient, cheap and easily available types of adsorbents, particularly from the waste materials. A range of biological materials such as agricultural by-products, biomass and activated sludge have been utilized as sorbents in wastewater treatment. These adsorbents exhibit varying degree of efficiency in the removal of dyes and heavy metals from wastewater (Shi et al., 2015).

1.9.1. Agricultural wastes as adsorbents

Among several bio-materials, agricultural waste materials have shown significant dye/metal removal efficiency at minimum cost as they are readily and abundantly present in nature. Agricultural waste materials have little or no economic value and often pose a disposal problem. Agricultural waste materials always contain certain biomolecules like hemicellulose, polysaccharides, lignin, lipids, proteins, sugars, water, hydrocarbons and starch which are actively involved in the process of ionic adsorption (Bhatnagar and Sillanpaa, 2010). The utilization of agricultural waste is of great significance in removal of toxicants. Agricultural wastes used as an adsorbent for the removal of pollutants are mainly applied in the form of raw materials (Guiza, 2017), biochar (Wang et al., 2016) and chemically activated or modified biosorbent materials (Chen et al., 2013). In the form of raw materials, the product is washed, ground and sieved until the desired particle size of adsorbents are obtained, which can be subsequently used in batch adsorption experiments. But in the case of activated or modified form, the product is pre-treated by using suitable modification techniques (Bhatnagar and Sillanpaa, 2010). The main aim of the pretreatments is to modify the surface functional group and, consequently, increase the number of active sites on the surface of adsorbents. Application of agricultural waste materials and optimization of

adsorption efficiency are being studied for removal of different dyes and heavy metals from aqueous solutions. The common agricultural wastes used as adsorbents in the removal of dyes and heavy metals are listed in Table 1.6.

Table 1.6. Agro-waste based adsorbents used in the removal of dyes and heavy metals.

Adsorbents	References	Adsorbents	References
Coir pith	Parab et al. (2006)	Bagasse fly ash	Memon et al. (2009)
Orange peel	Feng et al. (2011)	Hemp fibres	Gupta and Ali (2000)
Rice husk	Rajeswari et al. (2001)	Corn cob	Buasri et al. (2012)
Sugarcane bagasse	Malik (2003)	White ash	Chou et al. (2001)
Wheat straw	Soliman et al. (2011)	Wood derived biochar	Kizito et al. (2015)
Banana peel	Farooq et al. (2011)	Barley straw	Pehlivan et al. (2012)

1.9.2. Industrial wastes as adsorbents

Nowadays, many industrial activities produces a large amount of solid waste materials as by-products. Some parts of solid waste materials are reused while remaining portion is dumped in the landfills. Therefore, the possibility of reuse of industrial waste by-products in the sorption process represent an interesting alternate choice for wastewater treatment mainly because of the excess availability of industrial waste materials without any cost. During last few years, a number of industrial wastes have been employed as potential adsorbents for removal of the toxicants from industrial wastewaters (Bhatnagar and Sillanpaa, 2010). Generally, industrial waste materials can be divided

into five sub-groups: (i) Steel industry waste (ii) Fly ash (iii) Fertilizer industry waste (iv) Aluminium industry waste and (v) Paper industry and leather industry. Fly ash is a type of waste material generated during combustion processes in thermal power plants. Fly ash is commonly used in the construction of roads, cement, bricks etc. It has been estimated that the high percentage of alumina and silica in fly ash make it suitable for the utilization as a low cost adsorbent for wastewater treatment (Bhatnagar and Sillanpaa, 2010). The steel industry wastes such as sludge, blast furnace slag and dust are the most investigated adsorbents with reference to their high adsorption potential and easy recovery processes. Red mud, an aluminium industry wastes, has drawn more attention of environmentalists in removal of contaminants from wastewater. Red mud is a type of waste material generated during the production of alumina. The toxicity potential and colloidal nature of red mud particles create a serious environmental problems. Red mud is widely used in the manufacture of red mud bricks, as filler in asphalt road construction and as a source of various minerals (Ali et al., 2012). It has been reported that red mud after pre-treatment is found suitable for the treatment of Congo red dye from aqueous solutions (Bhatnagar et al., 2011). Fertilizer industry also generates a number of waste by-products in large amounts which deteriorate the quality of nearby environment and create serious disposal problems. So, their utilization as adsorbents for the removal of toxicants offer a good alternatives in wastewater treatment.

1.9.3. Soil and ore minerals as adsorbents

Soil, clays, zeolites, sediment and ore materials fall in this group of adsorbent materials. The adsorption potential of clay depend on the negative charges on the surface of fine powder silicate minerals. The negative charges present on clays particles can be neutralized by the binding of positively charged cationic dyes. The clays has large

specific surface area ranging up to 800 m^2 g^{-1} which contributes to its high adsorption potential (Ali et al., 2012). Among many types of clays, only montmorillonite clays are considered as an efficient adsorbent and expected to have the highest adsorption capacity in comparison to other. Further, the clay particles can be modified by using suitable chemicals to enhance its adsorption efficiency for the removal of contaminants from aqueous solutions. Zeolites are naturally occurring silicate minerals and it can also be synthesized at commercial level. The adsorption characteristics of zeolites mainly depend on their ion-exchange behavior. Soil, sand and sediment can also be utilized for the removal of organic contaminants from industrial wastewater. Soils have been applied as an adsorbents to remove the organic and inorganic pollutants from aqueous solutions. The high adsorption efficiencies of soils for the removal of glyphosate, pesticides and phenolic compounds have been reported by earlier workers (Morillo et al., 2000; Kibe et al., 2000; Gao et al., 2011). It has been reported that ore minerals are more suitable for the removal of organic contaminants from wastewater. Ali et al. (2012) and Bouyarmane et al. (2010) have investigated the adsorption potential of natural phosphate rock and synthetic mesoporous hydroxyapatites for the removal of pyridine and phenol from aqueous solutions. Both, natural and synthetic apatites showed similar phenomenon in the sorption of pyridine whereas the adsorption of phenol was directly proportional to their respective specific surface area of adsorbents. In order to reduce the material cost of adsorbents, plant waste is used as low cost adsorbents. Undoubtedly the agro-waste can offer low cost adsorbents for the removal of toxic substances from aqueous medium. But the disposal of plant waste and toxic adsorbate after the wastewater treatment is still big question. Can we find an adsorbent which not only adsorb/separates the toxicants from aqueous phase, but also convert the toxic waste into less toxic form which may easily be disposed off or recycled in

ecofriendly manner. The researchers will have to make multifaceted approach with main focus on cost reduction and ecofriendly technology, so that water treatment is commercially acceptable and environmentally sustainable.

The present work is an attempt in the direction of using low cost solid waste byproduct of mentha oil production i.e. Mentha Plant Ash (MPA) and harnessing the adsorption efficiency of biomaterial (MPA) derived from distilled mentha plant waste by studying the optimization of process. Further attempts are made in the present study to exploit the physicochemical characteristics of MPA for catalytic transformation of toxic dyes and metals into less toxic forms.

1.10. Objectives of the study

- To investigate the adsorption and reduction potential of ash derived from *Mentha piperita* plant waste in removal of cationic dyes (malachite green, methylene blue) and Cr(VI) from their aqueous solutions.
- To determine the various physicochemical characteristics of Mentha Plant Ash (MPA) as an adsorbent using Zeta Potential Analyzer, Scanning Electron Microscope (SEM), Energy Dispersive Spectroscopy (EDS), X-Ray Photoelectron Spectroscopy (XPS), Brunauer-Emmett-Teller (BET), Fourier Transform Infrared Spectroscopy (FTIR), X-Ray Diffraction (XRD), Thermo gravimetric Analyzer (TGA) and Cyclic Voltammetry (CV).
- To study the effect of various physicochemical factors affecting the efficiency and nature of adsorption including such as initial dye/metal ion concentration, contact time, pH, temperature, adsorbent dose and other desorption characteristics to evaluate the applicability and efficiency of MPA as low cost adsorbent for the removal of cationic dyes and Cr(VI).
- To carry out studies on equilibrium, kinetic and thermodynamic parameters for explaining the nature of adsorption process and to define the applicability of various isotherms and kinetic models for the sorption of cationic dyes and Cr(VI).

CHAPTER-II

Review of Literature

2.1. Environmental occurence and toxicity potential of synthetic dyes

The manufacturing of synthetic organic compounds and their application for different purposes is need of the industries but unwanted discharge of non-biodegradable organic wastes from different manufacturing processes such as petroleum refining, coal conversion, dyes and other synthetic organic compounds manufacturing, textile and dyeing, paper and pulp are harmful to the environment (Husain and Jan, 2000). A number of synthetic dyes are widely used as coloring agents by paper, textiles, hair, leather, plastics, cosmetics bases and various foodstuffs industries (O' Neill et al., 1999). A number of dyes used for dyeing operations in textile industry are listed in Table 2.1. However, inefficient conditions in various dyeing processes results into discharge of huge quantity of dyestuffs to industrial effluent, which causes serious harms to the environment (Robinson et al., 2001). Approximately 10,000 commercial dyes are available and about 7×10^5 tons/year of dye stuff produced by the coloring industries. It is estimated that about 2% of dyes produced annually is directly discharged in industrial effluents from the associated industries (Allen and Koumanova, 2003). Textile and dyestuff industries discharge a large amount of wastewater which contains various synthetic and complex organic compounds, which make them more resistant and difficult to degrade into simpler ones (Padmesh et al., 2005). Among many industries, textile industry stands at first position in usage of dyes for coloration of fiber and other products. The total dye consumption by the textile industry is about 107 kg/year in all over the world and it is estimated that about 90% of this ends up on coloration of fabrics. Consequently, 1,000 tons/year or more of synthetic dyes are released into waste streams by the textile industry in all over the world (Marc, 1996). Moreover, textile effluents commonly contains different chemicals that may be very

toxic, mutagenic and carcinogenic to human beings, aquatic animals and various microbes (Verma et al., 2010).

Keen interest in the dye remediation has been primarily encouraged by the concern over their possible toxicity potential and carcinogenicity (Novotny et al., 2006). It has been estimated that about 60–70% of the dyes used in textile industrial operations are mainly azo compounds (molecules with one or more azo –N=N– bridges) (Stolz, 2001). According to their solubility in water, the azo dyes are divided into two sub-groups. Water soluble azo dyes are referred as anionic (acidic dyes) or cationic (basic dyes), while the dyes insoluble in water are non-ionic dyes or neutral dyes.

Table 2.1. Dyes used in dyeing operations in textile industry (Demirbas, 2009).

Dye class	**Description**
Acid	Soluble in water, anionic organic compounds
Basic	Water-soluble, used in slightly acidic dyebaths, high brightness
Direct	Anionic compounds, water-soluble, applied directly to cellulosic fibres without any mordants or metals like chromium and copper
Disperse	Insoluble in water
Reactive	Largest dye class, soluble in water, anionic organic compounds
Sulfur	Sulfur or sodium sulfide containing organic compounds
Vat	Insoluble in water, chemically complex oldest dyes

Dyes are highly visible even at very low concentration, some dyes can be detected in concentration below 1.0 mg L^{-1} and are produced to be photolytically and chemically stable, thus persist in environments (Nigam et al., 2000). However, many of the azo dyes are not toxic in nature by themselves but after their discharge into natural water bodies, these organic compounds can be transformed into carcinogenic amines and other aromatic compounds (Lima et al., 2007). Consequently, the discharge of

potentially toxic dyes in the aquatic environment can create an ecotoxic risk and affect all the human beings and animals through food chain (Mondal, 2008). The ecotoxic risk, which the dyes exhibit in wastewater, mainly depends on their concentration, exposure time, chemical and physical properties (Robinson et al., 2001). Fish mortality and algal growth is not severely affected by the dye concentration less than 1 mg L^{-1}. The most extremely toxic dyes for fish, algae and other aquatic organisms are basic and acid dyes, especially those which have a triphenylmethane structure (Greene and Baughman, 1996). Dyes have ability to absorb and reflect sunlight entering the water and so it can interfere with the growth of aquatic plants and disturb the process of photosynthesis in aquatic plants. Dyes can have acute and chronic effects on the living beings depending on the exposure to dye concentration and duration of exposure. Dyes can cause serious allergic dermatitis, cancer, mutation, and etc. in human beings. The problems of dye pollution become serious and degradation of dyes remains ineffective due to complex aromatic structures of the dyes (Pearce et al., 2003). A highly colored textile effluents contain mixture of different dyes discharged by textile and dye manufacturing industries. The textile and dyestuff manufacturing industries are the main sources which release dye-loaded wastewater into natural water bodies. Textile effluent contains high ionic strength, salt concentrations and high pH values (Nigam et al., 1995). Toxic, non-biodegradable and complex structure of dyes pose serious threat to aquatic life and human beings. Textile dyes have been considered as major pollutants of aquatic systems due to their toxicity potential, carcinogenic and mutagenic nature. Most of the synthetic dyes are made from carcinogens such as benzidine and other aromatic compounds which contribute to carcinogenicity of dyes (Clarke and Anliker, 1980). Basic dyes and anthraquinone based dyes are the most resistant to degradation due to their complex aromatic structures and remain in coloured form in aqueous

systems for longer durations. Metal-based complex dyes release toxic metal ions like chromium into the environment which poses serious threat to aquatic bodies and human beings. Some of the disperse dyes have the tendency to accumulate in living components of the environment (Banat et al., 1996). A huge amount of azo dyes present in the textile industrial effluent are the major concern for the environmentalists due to their toxic, mutagenic and carcinogenic behavior. The nitro group present in azo dyes make it mutagenic and produce many toxic degradation products like 1,4-phenylenediamine and ortho-tolidine, etc. (Chung and Cerniglia, 1992). It has been reported that sulphonated azo dyes show no mutagenic effect in comparison to the unsulphonated azo dyes (Jung et al., 1992). Due to the various ill effects of azo dyes on the living beings, the entry of these toxic dyes into the environment can be minimized using an efficient method such as bio-sorption to minimize or remove the dyes from the industrial wastewaters. In biosorption, the nature and type of dye molecules (anionic and cationic) may effect the sorption of dye onto the surface of adsorbent. The negatively charged surface of adsorbents favours adsorption of the basic cationic dyes, whereas the positively charged surface of adsorbents enhances adsorption of anionic dyes. The Van der Waals interaction and ion exchange processes are commonly involved in the sorption of cationic and anionic dyes (Zhu and Ma, 2008).

2.2. Environmental occurence and toxicity potential of chromium

Generally, the hexavalent chromium exists in monomeric form ($HCrO_4^-$ and CrO_4^{2-}) and bimeric form ($Cr_2O_7^{2-}$). Presence of monomeric and dimeric forms of chromium impart yellow and orange colors to aqueous systems, respectively (Palmer and Puls, 1994). The concentration of Cr(VI) mainly depends on the pH of the solution. The fractions of Cr(VI) species in aqueous solution as a function of different pH and total

Cr(VI) concentration has been shown in Fig. 2.1(a) and 2.1(b), respectively, (Palmer and Puls, 1994).

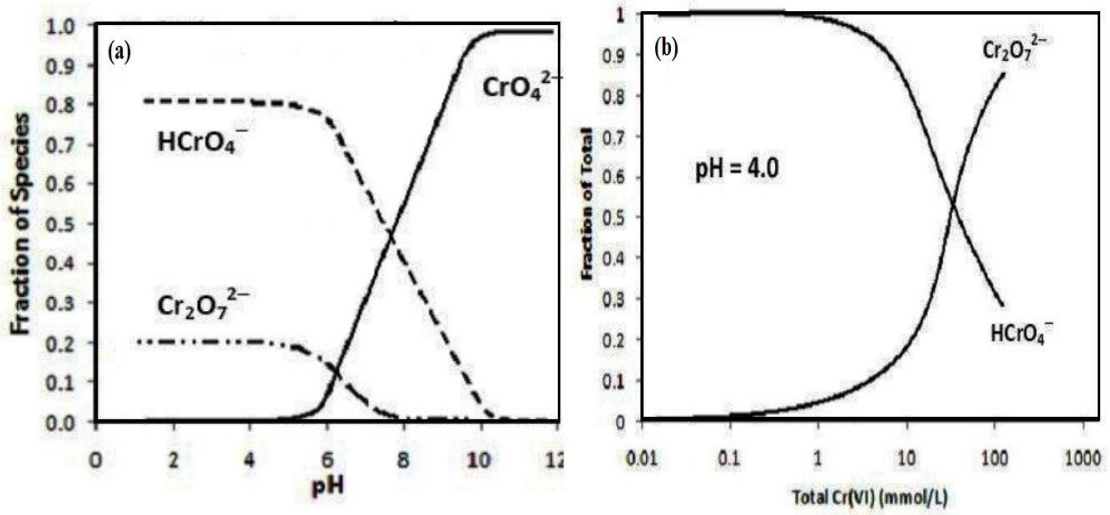

Fig. 2.1. Fractions of $HCrO_4^-$ and $Cr_2O_7^{2-}$ species as a function of (a) different pH and (b) total Cr(VI) concentration [$Cr(VI)_{tot}$ = 5 m mol/L] (Palmer and Puls, 1994).

Chromium is commonly present in hexavalent form [Cr(VI)] under oxidizing conditions. At concentrations below 10 mM or at pH 7.0, the Cr(VI) exists as monomeric (H_2CrO_4, $HCrO_4^-$, CrO_4^{2-}) and dimeric species ($Cr_2O_7^{2-}$). It has been reported that CrO_4^{2-} predominates above pH 6.5 and $HCrO_4^-$ dominates in the pH range (1.0–6.5) as shown in Fig. 2.1 (a). The Cr(VI) concentration in different industrial effluents are given in Table 2.2.

Table 2.2. The concentration of Cr(VI) in different industrial effluents.

Industrial effluents	Cr(VI) conc. (mg/L)	References
Leather industry	10.3 – 34.5	Dhungana and Yadav (2009)
Metal finishing	20.0	Sarin and pant (2006)
Electroplating	3.0	Ganguli and Tripathi (2002)
Chrome plating	28.2	Selvaraj et al. (2003)
Electropolishing	42.8	Davis et al. (1995)

The adsorption of Cr(VI) is mainly affected by pH of the aqueous solution, which dominates the rate control steps of sorption process, ionization and reduction of Cr(VI) to Cr(III) form (Zhou et al., 2016). A high pH value reduces sorption efficiency of Cr(VI), since the abundant OH^- ions led to generation of $Cr(OH)^3$, which inhibits the transfer of Cr(VI) ions and interact with surface functional groups (Chen et al., 2015). A low pH condition increases protonation of Cr(VI) during adsorption (Zhou et al., 2016). The sorption of Cr(VI) increases with increase in temperature due to favorable endothermic reactions (Yang et al., 2017). Zhou et al. (2016) reported that the sorption mechanisms of Cr(VI) include adsorption and reduction processes in which the Cr(VI) ions are adsorbed onto the surface of adsorbent via electrostatic attractions, further the adsorbed Cr(VI) is partially reduced to Cr(III) form and discharge into the solution. The Cr(VI) shows various types of pH dependent equilibrium sorption in aqueous solutions. A high adsorption at low pH and low adsorption at high pH exhibits by Cr(VI) in aqueous solution. The Cr(VI) is present in different stable states such as $HCr_2O_7^-$, $HCrO_4^-$ and CrO_4^{2-} in aqueous solution and the relative availability of a particular metal complex depends on the the pH of the solution and concentration of the chromium ions. At acidic pH, the sorbent has positively charged surface due to the protonation of amino groups, whereas the sorbate (dichromate ion) is available mostly as an anion enhancing electrostatic attraction between sorbent particles and sorbate molecules. Subsequently, biosorption of Cr(VI) increases at low pH, but increase in the pH favours deprotonation of the sorbent and reduces adsorption capacity.

Since last few years, most of the Indian tanneries adopt the chromium tanning process due to its low cost, processing speed, light color and high stability of the leather. In the chromium tanning process, the leather uses about 60–80% of applied chromium, and the rest part of chromium is usually discharged into the sewage water causing serious

negative impacts on evironment. Generally, chromium metal ions in liquid tanning wastes occurs in the form of Cr(III), which gets further oxidized to Cr(VI) form due to the presence of organic molecules (Sarin and Pant, 2006). The hexavalent form of chromium is considered as strong oxidizing agent in acidic media and tends to associate with oxygen during the formation of chromate and dichromate (Lai and Lo, 2008). The Cr(VI) is rarely present in the environment in the form of crocoite ($PbCrO_4$) and only a small fractions of hexavalent chromium is formed in the soil due to the oxidation of Cr(III), the rest parts of Cr(VI) is introduced into the environment by the human activities as a result of many industrial processes (Barceloux, 1999). The Cr(VI) is a potential toxicant in soil, sediments and water. It is well known mutagenic and carcinogenic toxicant as well as strong oxidizing agent which harms animal and plant tissues even in very low concentrations. The Cr(III) form can not penetrate the biological membranes while the Cr(VI) form penetrates through it and reduced to Cr(III) form in the cell organelles (mitochondria, nuclei and cytoplasm) which forms insoluble hydroxides of chromium at pH 7.5. The Cr(III) form may be generated inside the living cell, binds to protein molecules and interacts with nucleic acids (Petrilli and Deflora, 1977).

The toxic effects of Cr(VI) in human beings and animals are caused by direct skin contact and inhalation of fumes and mist release during welding and hot-cutting of stainless steel or other chromium-containing metal alloys. The drinking water from chromium contaminated sites cause severe health problems in human beings. It has been estimated that the permissible limit for Cr(VI) into inland surface waters and potable water is 0.1 and 0.05 mg/L, respectively (EPA, 1990). The short term exposure to Cr(VI) on human beings cause acute toxicity, irritation, ulceration of the nasal septum and respiratory sensitization (asthma), but exposure to Cr(VI) for longer

durations cause severe perforation of the nasal septum and structural damage to DNA, leading to genotoxicity. It has been reported that Cr(VI) induces DNA damage, altered gene expression and inhibition of DNA replication and transcription in humans and animals (Cohen et al., 1993). Cr(VI) is known to be very toxic to plants and animals in the form of dichromate and chromate anions in aqueous medium (Demirbas et al., 2004). The surface and ground water contamination depends on the mobility of Cr(VI) ions in different medium (Cohen et al., 1993). It has been reported that the soluble Cr(VI) form cause serious toxic effect to human and animals due to its oxidizing potential and easy permeability to biological membranes (Outridge and Scheuhammer, 1993). The Cr(VI) has been considered as more toxic metal having high toxicity potential and therefore it has drawn greater attention of environmentalists towards its removal using suitable method like bio-sorption. Keeping the essentiality of dyes and metal ions removal, concerned industries are required to treat the industrial effluents before dumping them into the natural water bodies. Thus, the scientific community should have the responsibility of wastewater treatment by developing cost effective technologies.

2.3. Techniques for removal of dyes and heavy metals from aqueous solution

During last years, a number of technologies have been employed for the removal of dyes and heavy metals from industrial wastewater. These techniques include chemical precipitation (Ku and Jung, 2001), ion exchange (Alyuz and Veli, 2009), adsorption (Guo et al., 2010), ultrafiltration (Sampera et al., 2009), reverse osmosis (Shahalam et al., 2002), coagulation (Chang and Wang, 2007), flocculation (Chang et al., 2009), floatation (Lundh et al., 2000) and electrochemical process etc. (Heidmann and Calmano, 2008). Among all the removal methods, adsorption seems to be a significant

promising technique in removal of dyes and heavy metals due to its wide applications, easy operation, economical feasibility, wide availability of adsorbent materials and simplicity of design (Faust and Aly, 1987).

2.3.1. Chemical precipitation

It is a very simple and common method used to remove dyes and heavy metals due to inexpensive and easy operation (Ku and Jung, 2001). This technique is commonly employed for the treatment of metal-laden wastewater by forming an insoluble precipitate through the addition of some chemicals (Karthikeyan et al., 1996). Many other chemical precipitation techniques such as hydroxide precipitation, sulfide precipitation and heavy metal chelating precipitation are also used in treatment of industrial wastewater. Lime and limestone are commonly used as precipitating agents in chemical precipitation due to effective, convenience and simple process in removal of inorganic contaminants from industrial effluents at higher concentrations (Aziz et al., 2008). Generally, the heavy metal hydroxides are not soluble in aqueous media, so lime is widely employed for precipitating metal hydoxides. The valence states of heavy metals in aqueous media play a vital role in the precipitation of heavy metal. The chromate (CrO_4^{2-}), a hexavalent form of chromium is considerably more soluble in water than Cr(III) form of chromium. In this event, the chromate, in which Cr is available in the form of Cr(VI), which must be reduced with SO_2 of sodium metabisulphite at acidic pH for removal of chromium as Cr(III) form by precipitation (Sarin and Pant, 2006). Disadvantages of this method include the requirement of an excess amount of chemicals, generation of excessive sludge and the problem of sludge disposal into the environment.

2.3.2. Ion exchange

An ion exchange method has been widely applied for the removal of toxic metal ions and dyes from their aqueous medium (AWWA and ASCE, 2012). It is a reversible chemical reaction in which an ion is exchanged from their solution in the leiu of similar charged ion attached on an immobile solid phase. Natural materials (alumina, carbon, silicates) and synthetic materials (zeolites and resins) have been used as ion exchangers. Among them, zeolites are the most commonly employed ion exchange material (Fernandez et al., 2005). Generally, an ion exchange process takes place by the transfer of anions and cations in an aqueous medium. The Dowex 50x4, Dowex 50x2 and Dowex M-4195 have been used for removal of Ni(II) ions from synthetic wastewater (Dave et al., 2011). It was observed that Ni(II) was completely removed at pH 5.0 with Dowex 50x4 and Dowex M-4195. Removal of dyes (acid orange 7 and direct blue 71) from wastewater using amberlite IRA 478RF have been studied by the earlier workers (Wawrzkiewicz, 2012). The maximum removal efficiencies were found to be about 97 and 69.5% at 20°C in 72 and 96 hours for acid orange 7 and direct blue 71, respectively. The easy handling of concentrated metal ion solutions cannot be possible in this method because the matrix gets fouled by organics chemicals and other solid particles in wastewater. Further, an ion exchange method is non-selective and highly sensitive to pH of the aqueous medium (Barakat, 2011).

2.3.3. Reverse osmosis

Reverse osmosis is basically used for the separation and fractionation of organic and inorganic toxicants from aqueous and non-aqueous medium. This method has been used to treat different types of industrial effluents discharge from chemical, textile, electrochemical, petrochemical, food, paper and tannery industries (Mohsen-Nia et al., 2007). In combination with the membrane reactor, this technique has been found to be more efficient in removal of heavy metals (Dialynas and Diamadopoulos, 2009). In this

process, water tends to move from higher saline solution to weaker solution through the semipermeable membrane. Since the salt molecules are comparatively larger than water molecules and thus membrane inhibits the entry of salt particles. The end result corresponds to the presence of desalinated water on one side of membrane and concentrated saline solution on the other side of membrane (Parmar and Thakur, 2013). The process of reverse osmosis has been employed for the treatment of chromium-loaded wastewater from electroplating industry (Mohammadi et al., 2009). The removal efficiency of Cr(VI) has been reported to be about 99% at pH 6.0 and 25°C. Removal of dyes (acid red, reactive black and reactive blue) from industrial wastewater has been performed using both reverse osmosis and nanofiltration techniques by earlier workers (Abid et al., 2012). They have reported removal efficiencies of 97.20, 99.58 and 99.9 % for acid red, reactive black and reactive blue, respectively. The reverse osmosis process was found to be more efficient as compared to nanofiltration. The disadvantages of this process include frequent cleaning due to fouling of membrane, consumes high power and involves high cost in replacement of membrane (Al-Jlil and Alharbi, 2010).

2.3.4. Coagulation/flocculation

Coagulation is a most common method used to separate contaminants from wastewater. The mixing and addition of some chemicals are involved in this process for the removal of toxicants. During this process, the particles destabilization and charge neutralization occurs by the addition of differently charged ions which allows the particles to agglomerate. Generally, flocculation is used in combination with coagulation which links the stabilized particles to each other and form bigger aggregates of particles. In this process, the slow mixing allows the particles to collide and stick with each other until heavy enough to get settle down (Sharma and Sanghi, 2012). Aluminum sulphate,

polyaluminium chloride and magnesium chloride along with coagulant (Koaret PA 3230) have been used for the removal of Pb(II) from aqueous solution (Pang et al., 2009). The removal of dyes (Blue bezaktiv S-GLD 150 and Black novacron R) from synthetic wastewater has been investigated using coagulation/flocculation and nanofiltration techniques (Khouni et al., 2011). The consumption of large quantity of chemicals and generation of large quantity of toxic sludge are the main disadvantages of the method (Verma et al., 2012).

2.3.5. Adsorption

The accumulation of large number of molecular species at the surface of solid phase occurs in the process of adsorption. The attachment of the adsorbate molecules to the available binding sites on the surface of adsorbent occurs due to the presence of unbalanced residual forces at the surface of liquid or solid phase (Markandeya et al., 2017). The unbalanced residual forces have tendency to attract the molecular species with which it comes in contact with the solid surface. Adsorption is a surface phenomenon in which two components (adsorbent and adsorbate) are involved in the process. The term adsorbent can be defined as the substance on which adsorption occurs whereas the substance which is being adsorbed on the surface of adsorbent called as adsorbate. Forces of attraction involves in the surface process occurs between adsorbate and adsorbent. The weak forces of attraction (Vander Waal forces of attraction) and strong forces of attraction (chemical bond) involves in the adsorption. Surface adsorption can be divided into two sub-types (physical and chemical adsorption) on the basis of type of forces of attraction involve between adsorbent and adsorbate molecules (Bajpai and Rajpoot, 1999)

In physical adsorption, the intermolecular attractions between adsorbate molecules and binding sites of adsorbent take place and therefore this process is independent on

electronic behaviour of the adsorbate and adsorbent particles. Adsorption occurs due to weak Van der Waals forces of interaction between the adsorbate molecules and adsorbent particles. Physical adsorption takes place with formation of multilayer of adsorbate molecules on the surface of adsorbent (Kapoor, 2009). The energy released in this process is of the same order of magnitude as the enthalpy of condensation. The enthalpy of physical adsorption can be determined by monitoring the rise in temperature of a sample of known heat capacity. It has low enthalpy of adsorption i.e. ΔH adsorption is 20–40 KJ/mol. The process is reversible in nature and attains equilibrium rapidly at low temperature below boiling point of adsorbate. The process of physisorption decreases with increase in temperature (Atkins and Paula, 2006).

Chemical adsorption or chemisorption involves an exchange of electrons between specific surface sites of adsorbent and adsorbate molecules, and as a result the formation of chemical bond takes place between active sites of adsorbent and adsorbate molecules. In chemisorption, the adsorbate molecules bind to the active sites of adsorbent by forming a chemical bond. The enthalpy of chemisorption is much greater than that of physisorption. The process occurs at high temperature with attainment of equilibrium stage and it is an irreversible nature of monolayer adsorption with involvement of high activation energy (Kapoor, 2009). It has high enthalpy of adsorption i.e. ΔH adsorption is 200–400 KJ/mol. Chemisorption increases with increases in temperature (Kapoor, 2009).

2.4. Factors affecting adsorption

2.4.1. Effect of pH

The pH of a solution has been found to be an important parameter in adsorption of dyes and metal ions from aqueous solution, as the surface charge of the adsorbent and adsorbate molecules both depend on the pH of solution. The pH of solution controls the

magnitude of electrostatic charges which are imparted by the ionized adsorbate molecules (Onal et al., 2006). The pH of an aqueous solution can be adjusted by using dilute acid (0.1 N HCl) and base (0.1 N NaOH) or by appropriate phosphate buffers. Generally, a low pH solution, the dye removal capacity decreases for cationic dye while increases in case of anionic dyes adsorption. In contrast, at a high pH condition, the removal efficiency increases for cationic dye and decreases for anionic dyes due to adsorption (Salleh et al., 2011). In case of metal ions adsorption, pH dependent removal of metals may occur due to changes in the ionic state of the various oxygen containing functional groups present on the surface of adsorbent, as well as metal ion speciation (Djouider, 2012). It has been investigated that the removal of Cr(VI) is favoured at low pH conditions (3–5) because the functional groups of adsorbents become positively charged and form complex with Cr(VI) ions that mainly exist in solution as species of $HCrO_4^-$ and $Cr_2O_7^{2-}$ through electrostatic attraction and an ion exchange process (Guo et al., 2017). Osma et al. (2007) studied the effect of pH ranging from 2.0 to 4.0 on the sorption of Reactive black 5 dye by using sunflower seed shells as adsorbent and they found that the rate of dye removal was minimum at pH 4.0. Hameed et al. (2008a) investigated the sorption of cationic methylene blue (MB) dye by banana stalk and they observed that the adsorption of MB dye onto banana stalk was minimum at pH 2.0 and maximum at pH 4.0.

2.4.2. Effect of adsorbent dose

The effect of adsorbent dosage on the adsorption can be assessed by preparing adsorbent–adsorbate solution containing varying doses of adsorbent and fix dose of adsorbate at equilibrium (Salleh et al., 2011). It has been investigated that the percentage removal of dyes and metal ions increases with increase in the dose of adsorbent. Initially the rate of removal has been found to be rapid followed by slowing

down of adsorption with increasing dose of adsorbent. But after a certain dose of adsorbent, increase in the rate of removal is insignificant because the rate of adsorption becomes limiting factor at higher doses of adsorbent (Salleh et al., 2011). A sluggish increase in the removal capacity at higher doses of adsorbent may be due to less availability of adsorbate molecules per unit concentration of adsorbent. Otherwise it may state that the clustering of adsorbent particles per unit volume might be hindering the free mobility of the adsorbate molecules approaching to the binding sites on the surface of adsorbent (Garg et al., 2003). The possible clustering effect may not be the sole reason for decrease in the adsorption capacity at higher doses of adsorbent. It has been investigated that the percentage removal of Cr(VI) increases from 45.34% to 99.97%, with further increase in adsorbent dose, a reduction in the adsorption capacity of Cr(VI) is observed with further increase in the dosage of biochar (Guo et al., 2017). The effect of adsorbent concentration on the removal of malachite green (MG) dye by maize cob has been studied by Sonawane and Shrivastava (2009). They observed that the % dye removal increased from 90% to 98.5% with increase in the concentration of adsorbent from 0.5 to 12 g/L at dye concentration of 20 mg/L and 25 min of contact time.

2.4.3. Effect of contact time

The effect of contact time on adsorption has been carried out by preparing adsorbent–adsorbate solution with fixed dose of adsorbent and dyes/metal ions concentration for various time durations and shaken until equilibrium is reached. It has been investigated that the adsorption capacity increases with an increase in contact time to a certain extent, but further increase in the contact time does not increase the adsorption capacity due to saturation of all the active sites on the surface of adsorbent (Ansari and Mosayebzadeh, 2010). The time needed to reach the equilibrium stage is termed as

equilibrium time and the amount of dye/metal ion adsorbed at the equilibrium time reflects the maximum adsorption capacity of the adsorbent (Bello et al., 2010). The adsorption of both Cr(VI) metal ions and methylene blue (MB) dye are found to increase with increase in contact time, until the equilibrium stage of adsorption is reached. A biphasic pattern in the adsorption of Cr(VI) and methylene blue dye onto biochar includes a rapid step, attributes to the surface adsorption of contaminants onto the adsorbent surface; while the later step is slow and relates to adsorption of contaminants onto the inner surfaces of the adsorbent (Thirumavalavan et al., 2011).

2.4.4. Effect of initial dye/metal ions concentration

The initial dye/metal ion concentration in the solution is an important parameter in the sorption process. Since a given mass of adsorbent material can be adsorbed to a fixed amount of adsorbate molecules (Benaissa, 2005). The effect of initial dye/metal ion concentration has been carried out by preparing adsorbent–adsorbate solution with fixed adsorbent dose and different initial dye/metal ion concentrations for varying time intervals and shaken until the stage of equilibrium (Salleh et al., 2011). The percentage dye removal is mainly dependent on the initial adsorbate concentration in solution. The effect of the initial concentration on adsorption mainly depends on the immediate contact between the adsorbate molecules and active sites of adsorbent (Salleh et al., 2011). The availability of increased vacant sites on the surface of adsorbent particles would be possible at low concentration of adsorbate molecules per unit mass of the adsorbent but less availability of active sites for the binding of the adsorbate molecules may be due to increase in dye/metal ion concentration (Kannan and Sundaram, 2001). Low and Lee (1990) have reported that the time taken to attain equilibrium stage is increased with increasing adsorbate concentration, but the actual amount of dye/metal ion adsorbed per unit mass of adsorbent increases with increase in concentration. This

may be attributed to the higher driving force required for mass transfer at a high initial dye/metal ion concentration (Bulut and Aydin, 2006). Garg et al. (2004) investigated the sorption of methylene blue dye onto sulphuric acid treated sawdust at a fixed dose of adsorbent (0.4 g/100 mL), neutral pH (7.0) and temperature (26±1 °C). They observed that the amount of dye adsorbed increased from 12.49 mg/g to 51.4 mg/g with increase in initial dye concentration from 50 mg/L to 250 mg/L, while the percentage of dye removal decreased from 99.9% to 82.2% in the selected range of dye concentration. Original textile wastewaters having high concentration of synthetic dyes, which is comparatively higher than the dye concentrations used in previous reported work, therefore many research groups used an empirical design procedures based on equilibrium adsorption conditions in order to evaluate the size of adsorbent particles as well as sorption efficiency. Vadivelan and Kumar (2005) studied the sorption design in removal of methylene blue (MB) dye by using rice husk as an adsorbent. They observed that the doses of adsorbent (rice husk) needed to remove 90% of MB dye from solution (100 mg L^{-1}) were found to be 3.828, 7.655, 11.482 and 15.309 g for dye solution of volumes 1, 2, 3 and 4 L, respectively.

2.4.5. Effect of temperature

A study about the effect of temperature on adsorption provides important information about the enthalpy and entropy changes during adsorption. Temperature indicates the nature of adsorption whether it is an endothermic or exothermic process (Salleh et al., 2011). An increase in the adsorption capacity with increase in temperature indicates an endothermic process. The kinetic mobility of the adsorbent particles and adsorbate molecules increases with increase in temperature (Senthilkumaar et al., 2006). It has been reported that the increase in adsorption capacity of the adsorbent (activated carbon) at higher temperatures is attributed to the expansion of pore size of the particles

and surface activation of the adsorbent. Various structural changes occur in the adsorbate molecules and adsorbent particles during the sorption process (Hema and Arivoli, 2007). The adsorbed water molecules displaced by the adsorbate molecules and gain more translational entropy than it lost by the adsorbate molecules, thus allowing the predominance of randomness in the system. An increase in temperature may decrease the adsorptive forces between the active sites of adsorbent and adsorbate molecules as a result of decreasing adsorption capacity of adsorbent (Ofomaja and Ho, 2007). It has been reported that the adsorption of cationic dyes (methylene blue, malachite green and crystal violet) onto carbon derived from waste apricot increases with an increase in temperature (Önal, 2006). Hameed and Ahmad (2009) investigated the sorption behavior of garlic peel in the removal of methylene blue (MB) dye and they reported that the sorption capacity of garlic peel was increased from 82.64 to 142.86 mg g^{-1} with increase in temperature from 30°C to 50°C, indicating an endothermic adsorption process.

2.5. Adsorption mechanisms

The identification of the underlying mechanisms of the adsorption is needed to evaluate the adsorption potential of adsorbents in the removal of organic and inorganic contaminants from aqueous solutions. The sorption behavior of adsorbents for different contaminants are different and it is well correlated with the physico-chemical properties of the contaminants. Different physico-chemical properties of adsorbents such as surface functional groups, specific surface area, porous structure and mineral compositions affect the adsorption mechanisms of dyes and heavy metals as reported earlier workers (Kumar and Ahmad, 2011). Generally, the processes like particle diffusion and exchange of mass-action controlled mechanisms are commonly involved in sorption and ion-exchange process of contaminants (Singh et al., 2003). Generally,

the external transport process is the rate-limiting step in the systems with low concentration of adsorbate molecules, poor mixing, small particle size and high affinity of the adsorbate molecules towards adsorbent. In contrast, the intra-particle diffusion step limits the overall mass transfer in the systems which have high concentration of adsorbate molecules, good mixing, large particle size and low binding affinity of the adsorbate molecules for the adsorbent (Singh et al., 2003). Three main successive steps such as film diffusion (transport of the adsorbate molecules to the external surface of the adsorbent), particle diffusion (transport of the adsorbate molecules within the pores and external surface of adsorbent) and transport of the adsorbate molecules into the interior surface of the adsorbent take place during adsorption of adsorbate molecules onto a porous adsorbent (Gupta et al., 2004). Kumar and Ahmad, (2011) investigated the removal mechanisms of crystal violet dye onto treated ginger waste. They found that various factors such as chemical structure of dye, surface properties of bio-sorbent, steric effect, hydrogen bonding and Van der Waals forces of attraction influence the sorption process. The chemical structure of the crystal violet dye was found to be a prominent factor for its sorption process. The binding between dye molecules and adsorbent particles might occurr due to weak and strong forces of attraction. The weak interactions between adsorbate molecules and adsorbent particles may be attributed to the Van der Waals forces, while the strong interactions among them occur due to hydrogen bonding and electrostatic interaction between the cationic dye and negatively charged surface of adsorbent in alkaline medium. A four-stage sorption mechanism (Fig. 2.2) is involved in the removal of dyes (Acid Blue 92, Basic Red 29, Reactive Red 4 and Direct Blue 53) by using precursor wood as an adsorbent has been reported by earlier workers (Sivakumar and Palanisamy, 2010).

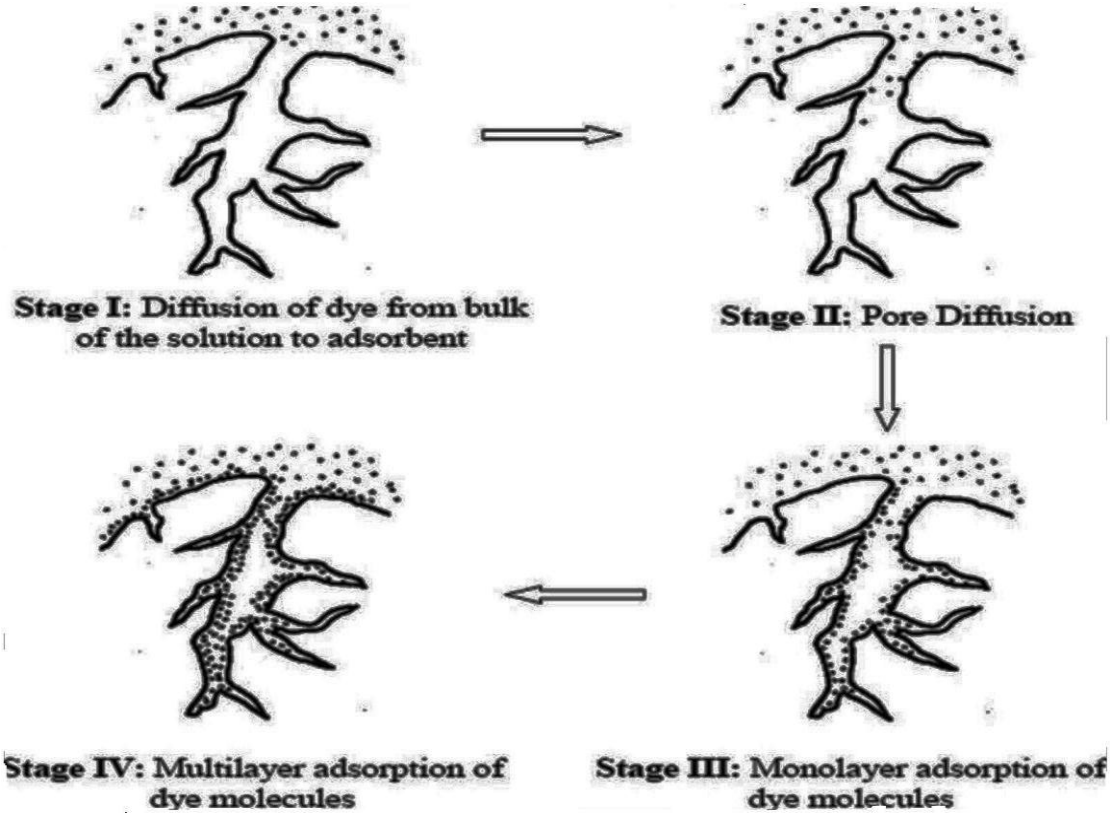

Fig. 2.2. A four-stage sorption mechanism involved in dye removal (Sivakumar and Palanisamy, 2010).

Different types of interactions (Fig. 2.3) are involved in the binding of dye molecules and adsorbent particles. A number of factors such as hydrophobic effect, electrostatic interaction, hydrogen bonds and pore-filling may be involved in the sorption mechanisms of dyes onto biochar particles (Cao et al., 2009). Generally, the surface properties of adsorbents play a crucial role in the adsorption of dyes from aqueous solutions. The biochars have heterogeneous surface due to the presence of carbonized and non-carbonized fractions and these fractions exhibit different sorption mechanisms in dye removal. The adsorption of dyes can occurr due to both the non-carbonized and carbonized organic matter present in biochar (Cao et al., 2009). A number of previous studies suggested that an electrostatic attraction is the dominant mechanism involved in the sorption of dyes onto the biochars (Inyang et al., 2014). The mechanism of dye adsorption onto a straw-based biochar has been investigated by Qiu et al. (2009). They observed that the mechanisms of dye adsorption involved various interactions such as

π– π interactions between graphene layers of biochar particles and dye molecules, the electrostatic attraction and the intermolecular hydrogen bonding.

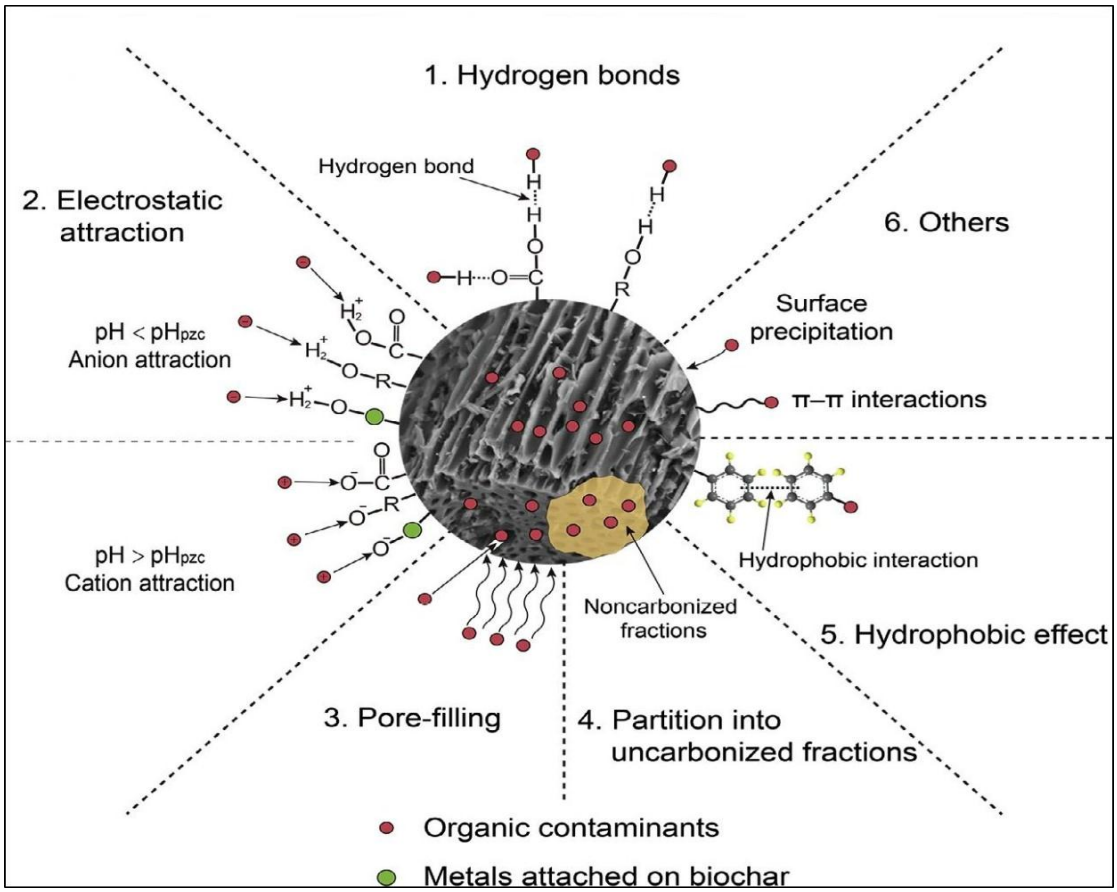

Fig. 2.3. Sorption mechanisms involved in the adsorption of dyes (Tan et al., 2015).

The removal of heavy metals by biochars commonly involved integrative effects of various types of interactions including ion-exchange, physical adsorption, electrostatic attraction, precipitation and surface complexation. The various sorption mechanisms (Fig. 2.4) have been proposed for the chemical interaction of biochar particles and heavy metals. The nature of specific sorption mechanisms for different heavy metals is different and the appropriate surface characteristics of biochars make it suitable for the adsorption of heavy metals. A large number of surface functional groups such as carboxylate (–COOH) and hydroxyl group (–OH) are available on the surface of biochar and are involved in various strong interactions such as electrostatic attraction, ion-exchange and surface complexation with heavy metal ions. The binding of metal

ions with surface binding ligands of biochar particles is known to occur due to changes in surface functional groups of biochar after metal ion adsorption (Khare et al., 2013). The process of electrostatic attraction of Cr(VI) with biochar has been the main factor in the removal of Cr(VI) using sugar beet tailing biochar as reported earlier (Dong et al., 2011).

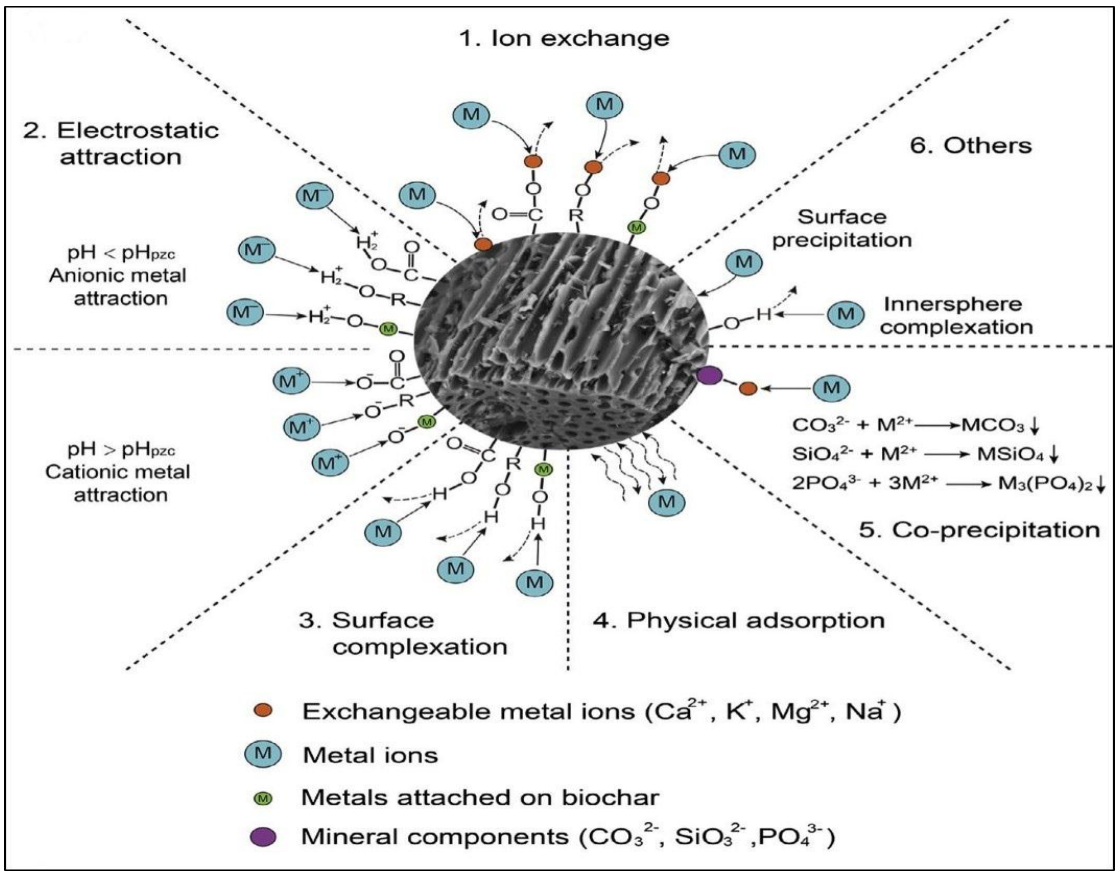

Fig. 2.4. Sorption mechanisms for adsorption of heavy metals (Tan et al., 2015).

2.6. Agricultural solid wastes as low-cost adsorbents

During the last few years, many research groups have used various adsorbents to remove toxic pollutants from industrial wastewaters, especially those that remain unaffected by conventional biological wastewater treatment. However, among all the reported sorbent materials, activated charcoal has been considered as most effective adsorbents for the removal of dyes and metal ions from industrial wastewater. As the world's most powerful adsorbent, it can cope with a wide range of contaminants. A high

adsorption potential of activated carbon is mainly due to their structural characteristics and porous nature which offers a large surface area for the adsorption of toxic pollutants (Bangash and Alam, 2009). The surface of activated carbon can be easily modified by chemical treatment in order to increase their surface properties. However, activated carbon exhibits several disadvantages in the field of adsorption because it is quite expensive, higher cost for good quality, non-selective and ineffective against some toxic dyes (disperse and vat dyes). The regeneration of activated carbon after treatment results in loss of the adsorbent characteristics and it is considered as an expensive process to recover the activated carbon in its original form. The use of carbons based adsorbents derived from relatively expensive materials is also uneconomical for the wastewater treatment applications. This has led many researchers to find some best alternatives of expensive adsorbents which have low cost and high adsorption potential for the removal of toxicants from aqueous solutions.

The solid agricultural wastes include almond shell (Aygun et al., 2003), barley straw (Pehlivan et al., 2012), cashew nut shell (Kumar et al., 2011), corncob (Juang et al., 2002), fruit juice residue (Yadav et al., 2015), garden grass (Hossain et al., 2012), garlic peel (Liu et al., 2014), grapefruit peel (Zou et al., 2012), hazelnut shell (Aygun et al., 2003), mango peel waste (Iqbal et al., 2009), Mosambi (Citrus limetta) peel (Saha et al., 2013), groundnut shell (Malik et al., 2007), olive stone (Fiol et al., 2006), plum kernel (Juang et al., 2002), pomegranate peel (Moghadam et al., 2013), pomelo peel (Tasaso, 2014), potato peel (Aman et al., 2008), rice shell (Aydin et al., 2008), rice straw (Ding et al., 2012), sugarcane bagasse (Tsai et al., 2001), banana peel (Annadurai et al., 2002), orange peel (Li et al., 2007), rice husk (Yadav et al., 2015), white rice husk ash (Tavlieva et al., 2013), wood derived biochar (Kizito et al., 2015) etc. These agrowaste have been investigated for removal of dyes and heavy metals from aqueous

solutions. The main structural components of agricultural waste materials include lignin, lipids, hemicelluloses, simple sugars, proteins, hydrocarbons, water and starch, which contain different functional groups with high sorption potential for various contaminants (Bhatnagar and Sillanpaa, 2010). The natural and modified form of agricultural wastes are commonly used in removal of toxicants from industrial wastewater. In the natural form of adsorbent, the agro-waste material is washed with distilled water, grounded and sieved until it reaches to the uniform particle size. Finally, they are used for batch adsorption experiments. But in the case of modified form of adsorbent, the resource material is pre-treated by means of well-known surface modifying agents (Bhatnagar and Sillanpaa, 2010), which increases the surface functional group and, consequently, enhances the number of active binding sites on the surface of activated adsorbents. Application of agricultural waste products as an adsorbents have been extensively studied in removal of contaminants from aqueous solutions.

Further, the application of biochar derived from agricultural wastes as an adsorbent has drawn more attention of many research groups towards toxicants removal from industrial wastewater. The use of biochar offer a low-cost efficient technology for the removal of dyes and heavy metals from aqueous solutions. Biochar is a by-product of slow pyrolysis of lignocellulosic biomass containing large number of oxygen-carrying functional groups (–OH and –CO groups), which are active functional groups in the binding of metal ions and dye molecules (Manya, 2012). Biochar exhibits differing physical and chemical properties depending on the feedstock and the temperature for pyrolysis. The feedstock for the preparation of biochar are mainly obtained from agricultural biomass, which is widely available in plenty as a renewable resources on the earth. A number of feedstock materials including crop residues, wood biomass,

animal litters and solid wastes are commonly used to produce biochar via various thermochemical processes (slow pyrolysis, fast pyrolysis, hydrothermal carbonization (HTC), flash carbonization and gasification) (Meyer et al., 2011). However, biochar has some notable drawbacks as an adsorbent, due to its low specific surface area and loss of porosity after repeated use, resulting in an inadequate removal of toxicants and decreased stability, making biochar inefficient in long term for large scale wastewater treatment. The structural stability and adsorption capacity of these agro-waste adsorbents can be significantly improved by activation or chemical modification. It has been reported that the adsorption capacity of adsorbents can be greatly enhanced by the activation or modification of raw materials or biochar with acidic or basic compounds, or polymers with specific functional groups such as an amine group (Chen et al., 2013). The benefits and application of biochar as an efficient adsorbent in wastewater treatment has been shown in Fig. 2.5.

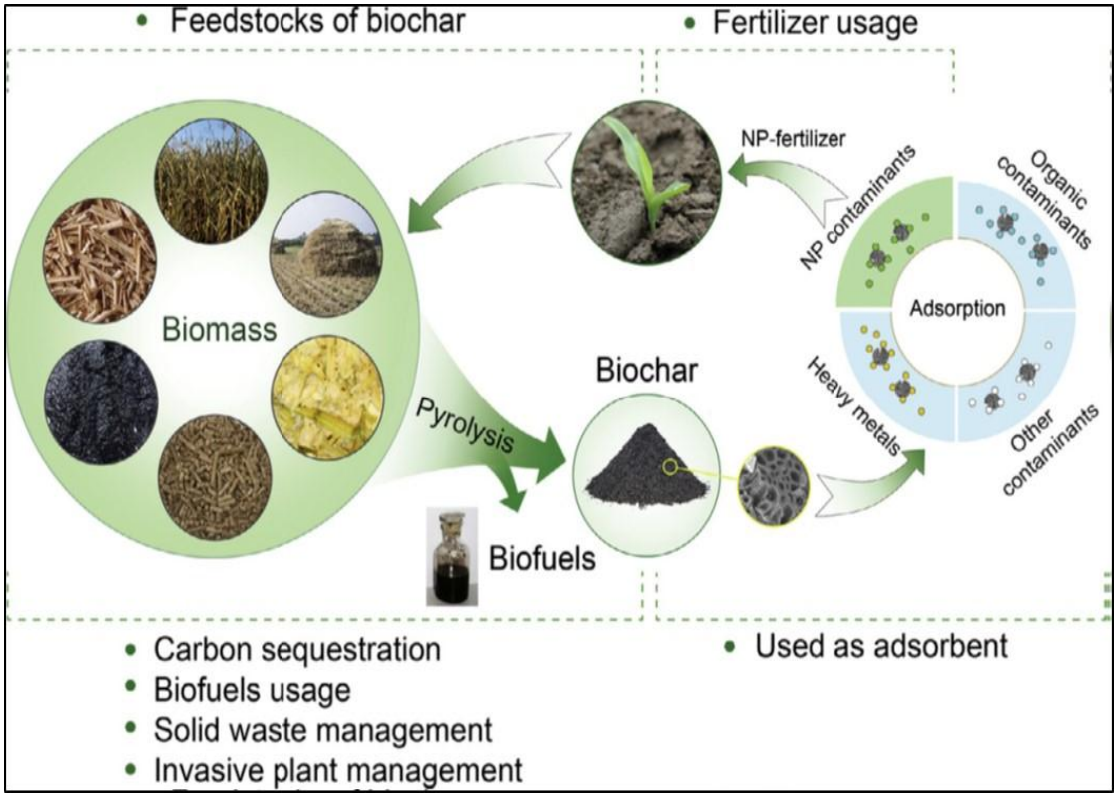

Fig. 2.5. The application of biochar as an effective adsorbent in wastewater treatment (Tan et al., 2015).

2.7. Physico-chemical characteristics of sorbents and specificity for sorbates

Kadirvelu et al. (2005) studied the sorption process of Rhodamine B using activated carbon derived from industrial solid sago waste. The physico-chemical characteristics of activated carbon contributed to effectiveness of the adsorbent in the sorption process. A high concentration of lactonic group followed by phenolic, carboxyl and carbonyl groups were observed in activated carbon. They reported a considerable increase in sorption capacity of Rhodamine-B dye at pH range (pH 3.0 – 7.0) due to dissociation of carboxyl groups. A maximum dye removal of 91% and 100% was reported at pH 5.7 and 7.0, respectively. An ion exchange sorption mechanisms was predominantly involved in the removal of RB dye from aqueous solution.

Bello et al. (2013) investigated the removal of Eosin dye from aqueous solution using powdered activated carbon and raw coal fly ash. The maximum time to attain the equilibrium stage was found to be about 120 min for both the adsorbents. The maximum monolayer adsorption capacities of activated carbon and raw coal fly ash were found to be 62.28 and 43.48 mg g^{-1}, respectively. They reported that the hydroxyl (–OH), carboxyl, amine and methyl groups were particularly were involved in adsorption of Eosin dye. They found that activated carbon was more efficient than fly ash as adsorbent for Eosin dye adsorption. The oxygen donor sites such as hydroxyl and carbonyl groups were present on the surface of raw coal fly ash adsorbent. The adsorption of Eosin dye onto raw coal fly ash was found to increase with decrease in pH due to nucleophilic nature of functional groups.

Nasuha et al. (2010) studied the sorption of methylene blue onto rejected tea (RT) as a low cost adsorbent from aqueous solution. They reported lower adsorption of MB dye at acidic pH condition was due to the presence of excess H^+ ions competing with the cation groups of MB dye for binding sites of adsorbent. But at higher pH, they found

that negatively charged surface of RT adsorbent enhanced the cationic dye adorption through electrostatic forces of attraction. Further, they observed that the three significant bands were detected at wavenumbers 3430, 1630 and 608 cm^{-1}, which indicated the C=O stretching, bonded –OH groups, –C–C– group and aromatic nitro compound. These three surface functional groups on the surface of RT were mainly involved in MB dye adsorption. In their studies, the monolayer sorption capacity of RT adsorbent was found to increase from 147 to 156 mg g^{-1} with increase in temperature from 30 to 50ºC due to increase in kinetic mobility of dye molecules at higher temperature.

Babu et al. (2010) studied the adsorption of malachite green dye using activated carbon prepared from dried *Borassus flabellofer* male flower. The optimum pH and activation temperatures were found to be 7.5 and 45 ºC, respectively. The percent adsorption of MG dye at pH 7.5 and 9.0 was found to be 94.67% and 93.39%, respectively. Further, they reported maximum dye removal at adsorbent dose of 0.05 mg/100 mL and its equilibrium time. They suggested that the decrease in dose-dependent percent dye removal can be attributed to decrease in the surface area of adsorbent and availability of active binding sites. The overlapping or aggregation of adsorbent particles at higher dose of adsorbent resulting in decrease in the total surface area available to MG dye and an increase in diffusion path length.

Ahmad and Alrozi, (2011) investigated the removal of malachite green dye from aqueous solution by using rambutan peel based activated carbon (RPAC) as an adsorbent. The mechanism of dye adsorption onto adsorbent was well explained by the intra-particle diffusion model. The average pore diameter (nm) of RPAC adsorbent was found to be 2.56 nm, which indicated mesoporous naure of adsorbent. They reported a high specific surface area and average pore volume of adsorbent due to the activation

of RPAC by using CO_2 and KOH. The content of volatile organic matter was found to decrease whereas the content of fixed carbon increased after activation and carbonization of RPAC adsorbent. This was due to the pyrolytic effect where most of the biomolecules have been degraded and discharged as liquid tars and gas molecules, leaving a material with high carbon purity. During activation of RPAC, the KOH–carbon and CO_2–carbon reactions was occurred, which enhanced the pores size of adsorbent particles thus increase the specific surface area and sorption capacity of the adsorbent. Further, they observed that the heterogeneous pores structures were distributed on the surface of RPAC adsorbent.

Zhang et al. (2008) used carbon derived from *Arundo donax* root (ADRC) in removal of malachite green dye from aqueous solutions. The BET specific surface area of the adsorbent was found to be 158 m^2 g^{-1} as determined by N_2 adsorption/desorption isotherm. They reported that the color of MG dye was more stable over the pH range (pH 3.3–7.0) and minimum dye removal (28.4%) by ADRC was recorded at pH 3.3, which found to increase about 41.8% at the pH 7.0. A lower percent removal of dye was due to the small dose of adsorbent (0.2 g/100 mL). They suggested that the surface of ADRC adsorbent may contain large number of surface binding sites and the binding of MG dye could be related to the active sites of adsorbent particles. The optimum pH range and optimum adsorbent dose for dye removal was found to be 5–7 and 0.6g/100 mL, respectively. Further, they observed that ADRC showed negative values of zeta-potential at the selected pH range (i.e., pH > 3.3). As the solution pH increased, the number of positively charged binding sites decreased and negatively charged binding sites increased. The positive value of enthalpy change indicated spontaneous and endothermic nature of the adsorption.

Yagub et al. (2013) studied the removal of methylene blue from aqueous solution using pine cone powder treated with NaOH. Surface characteristics of raw and NaOH modified pine cone powder were investigated using IR-spectroscopy and scanning electron microscope (SEM). They observed several IR peaks in the FTIR spectra, exhibited several functional groups (hydroxyl, amino and carbonyl) on the surface of pine cone powder and these functional groups played a crucial role in the binding of cationic MB dye. The point of zero charge, pH_{PZC}, of pine cone powder in aqueous media was found to be 4.4, as determined by Dawood and Sen (2012), and negative surface charge was found to increase with increase in pH of solution. The maximum monolayer adsorption capacity (q_{max}) of raw pine cone powder was found to be 129.87 mg g^{-1} at pH 9.0. But the NaOH modified pine cone powder showed the higher q_{max} value (142.25 mg g^{-1}) as compared with raw pine cone powder.

Crini et al. (2007) studied the removal of cationic malachite green dye from its aqueous solution using cyclodextrin based powder material as an adsorbent. The equilibrium stage in the sorption of dye was attained in about 120 min. They observed that the sorption of MG dye was strongly pH-dependent and the maximum adsorption capacity was reported at pH 8.0, but above pH 8.0, the sorbent material attained the same value of sorption capacity. The sorption capacity was increased from 3.1 to 8.2 mg g^{-1} with increase in pH from 5.0 to 8.0. The amount of dye adsorption was lower at lower pH alues (pH 5.0 – 6.0). They reported that the sorption mechanism of cyclodextrin based sorbent was quite different from other adsorbent materials due to its specific characteristics (presence of cyclodextrin molecules, small surface area and complexing chemical groups). The sorption mechanism involved both hydrogen bonding and surface adsorption due to the complex formation between the cyclodextrin molecules

and the dye molecules through host–guest interactions including hydrogen bonding and hydrophobic interactions.

Baccar et al. (2013) studied the adsorption potential of activated carbon prepared derived from agricultural byproduct for the removal of a tannery dye from simulated waste water. The q_{max} value of adsorbent was found to be 146.31 mg g^{-1} at 25ºC.

Li et al. (2013) investigated the adsorption of methylene blue from aqueous solution using graphene oxide (GO)/calcium alginate (CA) as an adsorbents. The maximum monolayer adsorption capacity calculated from Langmuir isotherm equation was found to be 181.81 mg g^{-1}. The kinetic models and thermodynamic parameters indicated that the adsorption of methylene blue dye onto calcium alginate immobilized graphene oxide composites was spontaneous and exothermic in nature. They observed a strong IR peak at 3426 cm^{-1} was assigned to stretching vibration of hydroxyl groups (–OH). The IR peak at wavenumber 1625 and 1400 cm^{-1} indicated the presence of symmetrical and asymmetrical stretching of C=O groups. Further, the IR peak was observed at wavenumber 1110 cm^{-1} assigned to C–O groups. A higher sorption capacity of adsorbent (GO/CA) was reported due to that the addition of GO enhanced the specific surface area of adsorbent particles and thus allowed more surface functional groups for binding of MB dye molecules, which increased the sorption efficiency of the composites. They found higher percent desorption at acidic condition because more H^+ ions competed the active binding sites present on GO/CA adsorbent with the cationic dye molecules and replaced the adsorbed MB dye molecules through an ion exchange process resulting in more percent desorption of MB dye.

Hameed et al. (2009) studied the adsorption of basic methylene blue dye from aqueous solution using pine apple stem (PS) as an adsorbent. The maximum dye removal occurred in alkaline medium and maximum adsorption capacity of pine apple stem was

about 119.05 mg g^{-1}. They reported a considerable numbers of heterogeneous layer of pores on the surface of PS adsorbent which facilitated dye adsorption onto the surface of adsorbent. The amount of dye adsorption was found to increase from 13.29 to 104.50 mg g^{-1} with increase in pH from 2.0 to 10.0. A negatively charged surface of PS at higher pH enhanced the adsorption of positively charged dye molecules through electrostatic attraction process. The adsorption capacity of the PS adsorbent was found to increase with an increase initial dye concentration, but the percent (%) removal of MB dye showed the reverse trend. The sorption capacity of PS increased from 18.33 to 116.95 mg g^{-1} with increase in initial dye concentration from 25 to 300 mg L^{-1}, where the percent removal was found to decrease from 96.70 to 54.50%.

Hameed and El-Khaiary (2008a) investigated adsorption potential of pumpkin seed hull (PSH) in the removal of basic cationic dye malachite green from aqueous solution, thereby making an attempt to overcome the economic disadvantages of activated carbon. The maximum monolayer adsorption capacity of PSH was found to be 149.35 mg g^{-1} at 30 ºC. They found that the rate of adsorption was almost controlled by film diffusion for a short time durations. However, for long duration, only pore-diffusion controlled the rate of adsorption. Pore diffusion occured in two particular regimes, corresponds to diffusion in macropores and mesopores. The adsorbent displayed a number of IR absorption peaks in the IR-spectra, reflecting the complex nature of the adsorbent. The FTIR spectrum of PSH exhibited a number of surface functional groups such as hydroxyl, methyl, amino, phenyl, carbonyl and carboxyl groups on the surface of adsorbent and these were actively participated in the removal of cationic malachite green dye. The sorption capacity was found to increase from 9.67 to 15.33 mg g^{-1} with increase in pH from from 6.0 to 11.0. At low pH condition, the surface of adsorbent become positively charged, thus making H^+ ions competed with cationic dye molecules

causing decreased in adsorption capacity. The amount of MG dye adsorption increased with increase in pH of solution due to electrostatic interaction between MG dye molecules and negatively charged surface of PSH adsorbent.

Mall et al. (2006) utilized bagasse fly ash for the removal of Orange-G (OG) and Methyl violet (MV) from aqueous solution. Results indicated that the maximum removal of OG occurred at acidic pH 4.0 whereas MV dye adsorption was maximum at alkaline pH 9.0. The percentage of dye removal was found to be higher at low initial dye concentration and high dose of adsorbent. The Effective pH for OG and MV dye removal were found to be pH 4.0 and 9.0, respectively. A high percentage of dye adsorption was observed with decrease in the initial dye concentration, and increasing dose of adsorbent. The percent removal of OG dye (anionic) was maximum at acidic pH (pH 3.0 – 4.0) and minimum at higher pH (above 5.0). Firstly, the acid dye dissolved in the aqueous solution and its sulphonate groups (D–SO_3Na) changed to dye anions after dissociation. A number of oxides (alumina, calcium, silica etc.) in the BFA adsorbent developed positive charges in contact with H_2O. Except silica, all the oxides present in BFA had positive charge for the selected pH range because zero point charge (ZPC) of SiO_2, Al_2O_3 and CaO were found to be 2.2, 8.3 and 11.0, respectively. The negatively charged sites of silica in BFA adsorbent neutralized by H^+ ions thereby minimizing hindrance to diffusion of anionic dye molecules. At pH below 4.0, a high electrostatic attraction between the positively charged surface of the BFA and anionic dye molecules enhanced the adsorption capacity.

Han et al. (2007) investigated adsorption potential of Phoenix tree leaf as an adsorbent in removal of methylene blue dye from aqueous solution. They suggested that the adsorption process was found to be more efficient due to the presence of various active functional groups such as carboxyl, hydroxyl and amide in Phoenix tree leaves powder,

which might be actively involved in the binding of dye molecules with the adsorbent particles. Various other agro-waste materials such as de-oiled soya, coir pith, sawdust, banana pith, corncob and orange peel have been successfully employed for the removal of dyes from their aqueous solutions (Mittal et al., 2005; Parab et al., 2009).

Sciban et al. (2011) investigated the removal of metal ions such as copper, zinc, cadmium and chromium from aqueous solution using kraft lignin as an adsorbent. The BET Specific surface area and average pore diameter were found to be 0.75 $m^2 g^{-1}$ and 4.3 nm, respectively, indicated mesoporous adsorbent. They reported that the surface area and porosity of kraft lignin adsorbent was comparatively lower than commercial activated carbon, but textural characteristics of kraft lignin was almost comparable to a number of lignocellulosic adsorbents such as palm shell and wood sawdust. The adsorption of cations (Cu, Zn and Cd) onto the surface of kraft lignin was better explained by the Freundlich sorption isotherm whereas the adsorption of Cr(VI) by Langmuir sorption isotherm. They reported heterogenous and homogeneous surface of lignin with equal adsorption sites which involved in adsorption of metal cations and chromium anions. The impact of examined interfering ions on decreasing sorption efficiency of Cu(II) followed the trend Ni(II) > Cd(II) > Pb(II).

Wang et al. (2012) investigated the adsorption potential of bamboo based charcoal (MBC) and cobalt-coated bamboo based charcoal (Co-MBC) adsorbent impregnated with $Co(NO_3)_2$ and HNO_3 by microwave irradiation. Both the bamboo charcoals were characterized by using XRD, SEM, EDX, FTIR, BET and point of zero charge (PZC) measurements. The results exhibited the higher surface area of 263 $m^2 g^{-1}$ of Co-modified bamboo charcoal. The adsorption of Cr(VI) ions onto Co-modified bamboo charcoal was a spontaneous process and an ion exchange mechanism played a vital role in the removal of metal ions from aqueous solution. The surface physical parameters

suggested that the BET specific surface area and total pore volume improved significantly due to the addition of HNO_3 and $Co(NO_3)_2$ during pyrolysis. The BET specific surface area and total pore volume of Co-MBC adsorbent increased from 15 to 263 $m^2\ g^{-1}$, and 0.14 to 0.27 $cm^3\ g^{-1}$, respectively, as compared to MBC adsorbent. They suggested that HNO_3 and $Co(NO_3)_2$ could improved the porosity of the bamboo based charcoal under microwave heating for short time duration.

Gupta et al. (2013) investigated the adsorption potential of activated carbon derived from *Ficus carica* fiber (FCF) as an adsorbent for the removal of Cr(VI) from aqueous system. The adsorbent was prepared by the process of carbonization of *F. carica* fiber, followed by H_3PO_4 activation under microwave radiations. The maximum adsorption capacity of *Ficus caria* activated carbon for the removal of Cr(VI) was found to be 44.84 mg g^{-1}. The IR peak at wavenumber 3435 cm^{-1} indicated free and hydrogen-bonded hydroxyl (–OH) groups on the surface of FCF biosorbent. The presence of several functional groups such as amine, carboxyl, hydroxyl groups, etc., were mainly responsible for the binding of Cr(VI) metal ions onto the surface of FCF biosorbent. The amount of Cr(VI) adsorption was found to increase from 12.98 to 13.41 mg g^{-1} with increase in pH from 1.0 to 3.0. The percent adsorption decreased to 10.52 mg g^{-1} with increase in pH from 3.0 to 5.0 and further decreased to 6.99 mg g^{-1} at pH 8.0. Below pH 6.0, the Cr(VI) exists in aqueous media mainly in the form of dichromate ($Cr_2O_7^{2-}$). The concentration of $Cr_2O_7^{2-}$ increased with decrease in pH from 6.0 to 2.0 and thus, FCF biosorbent became more positively charged; as a result, the amount of adsorption increased. Above pH 6.0, the Cr(VI) was present in aqueous solution in the form of CrO_4^{2-} and the concentration of CrO_4^{2-} increased with increase in pH. Moreover, at high pH, negatively charged surface of FCF biosorbent did not favor the adsorption of metal ions due to electrostatic repulsions.

Sobhanardakani et al. (2013) applied an untreated rice husk as an adsorbent for the removal of Cr(III) and Cu(II) from simulated wastewater. The q_{max} value of rice husk for the removal of Cr(III) and Cu(II) were found to be 22.5 and 30 mg g^{-1}, respectively. They reported high adsorption rate of Cr(III) and Cu(II) metal ions onto the surface of adsorbent (rice husk) in the pH range from pH 2.0 to 5.0. They observed that the percent removal of Cr(III) or Cu(II) was found to increase with increase in pH and recorded maximum 55% of Cr(III) and 65% of Cu(II) removal at pH 6.0. At low pH conditions, the surface of the rice husk was overlapped by hydronium ions (H^+), which inhibited the metal ions from approaching the active binding sites on the surface of rice husk sorbent. The optimum range of initial pH was recorded as pH 5.0–6.0. The rate of adsorption for Cr(III) and Cu(II) metal ions increased with decrease in initial metal ion concentration with increased contact time and dose of adsorbent.

Jalali and Aboulghazi, (2013) investigated the feasibility of sunflower stalks for the sorption of lead (Pb) and cadmium (Cd) ions from their aqueous solution. The q_{max} value of adsorbent for the removal of Pb(II) and Cd(II) was found to be 182 and 70 mg g^{-1}, respectively. The optimum pH for the sorption of heavy metals (Pb and Cd) onto sunflower stalks was found to be pH 5.0. The percent removal of Pb and Cd by sunflower residues at pH 5.0 was calculated to be 99.2 and 90.1 %, respectively. They reported that the sorption capacity for metal ions was found to increase with increase in concentration of adsorbents due to the availability of more active binding sites or specific surface area at higher dose of adsorbent. They recorded about 97% of Pb and 87 % of Cd removal from their aqueous solutions within 150 mins of contact time. A high rate of percent removal of metal ions was recorded in the beginning due to availability of more active binding sites on the surface of the adsorbent.

Zheng et al. (2012) used corn stalk as an adsorbent derived after modification by graft polymerization for the removal of Cd(II) ion from their aqueous solution. The q_{max} value derived from Langmuir equation was found to be 21.37 mg g^{-1}. A high adsorption potential was observed in case of modified corn stalk due to the presence of surface functional groups (–CN and –OH) as compared to unmodified corn stalk. The surface functional groups (–CN and –OH) played a vital role in adsorption of Cd(II), because the oxygen and nitrogen of –OH and –CN group, respectively, have been considered strong Lewis base due to the presence of vacant pair electrons. The vacant pair of electrons can be found more helpful in the formation of coordination complex with metal ions. Thus both functional groups –CN and –OH group in the grafted polymer chains and cellulose, respectively, were actively involved in the binding of Cd(II) metal ions. The amount of adsorption was found to be increase with increase in pH of the solution. A rapid increase in Cd(II) adsorption was observed in the pH range between pH 1.0 to 3.0 but no significant adsorption found between pH 3.0 and 7.0. At low pH condition (below pH 3.0), the H_3O^+ ions competed with the Cd(II) ions for the active binding sites of adsorbent, hence H_3O^+ ions occupied the surface active sites of adsorbent.

Sarin and Pant (2006) applied eucalyptus bark (EB) as an adsorbent on the removal of Cr(VI) and Cr(III) ions from the aqueous solution. The maximum monolayer adsorption capacity (q_{max}) was found to be 45 mg g^{-1} at acidic pH 2.0. They reported that the maximum percent removal of Cr(VI) was found to be 100% at acidic pH 2.0 and initial Cr(VI) concentration (50 ppm). At lower pH 2.0, the Cr(VI) is mainly present in the form of bichromate ($HCrO_4^-$) but increase in pH condition can change $HCrO_4^-$ form to other forms of Cr(VI) such as $Cr_2O_7^{2-}$ and CrO_4^-. They found that the $HCrO_4^-$ form of Cr(VI) was actively adsorbed on the surface of EB adsorbent. The EB adsorbent derived

from cellulose based plant fibers containing a number of hydroxyl (–OH) groups which might be involved in the binding of Cr(VI) metal ions. Further, the pretreatment of eucalyptus bark with formaldehyde promote crosslinking of compounds to form a phenol–formaldehyde copolymer which favours adsorption of cations.

Bhatti et al. (2010) studied the adsorption potential of *Daucus carota L.* waste biomass in the removal of chromium from aqueous solution. The maximum monolayer adsorption capacity for the removal of Cr(III) and Cr(VI) as determined by the Langmuir equation was found to be 85.65 and 88.27 mg g^{-1}, respectively. The maximum metal ions removal was occurred in 240 minutes at initial metal ion concentration (100 mg/L) with adsorbent dose (0.1g/100 mL) at room temperature. The equilibrium adsorption capacity of *D. carota L.* (carrot) waste biomass for Cr(III) and Cr(VI) at pH 5.0 and 1.0 were found to be 86.06 and 88.28 mg g^{-1}, respectively. The results on analysis of variance of the data exhibited that pH had significant ($P < 0.01$) effect on the sorption of Cr(III) and Cr(VI) by biosorbent (carrot waste biomass). A significant increase in Cr(III) adsorption by *D. carota L.* (carrot) waste biomass was observed with increase in pH from 4.0 to 5.0. At low pH conditions, the positively charged surface of waste biomass prevents the binding of positively charged metal ions due to electrostatic repusion. They suggested that the different functional groups on the surface of biosorbent and their ionic states at pH 4.0 and 5.0 determined the extent of sorption process.

Koroki et al. (2010) used bamboo grass treated with concentrated H_2SO_4 for the removal of Cr(VI) from aqueous solutions. They found that the removal of Cr(VI) was highly dependent on pH of the solution and a physico-chemical sorption mechanism was involved in the removal of Cr(VI). An irreversible nature of adsorption was observed due to strong bonding between bichromate form ($HCrO4^-$) and active sites

available on the surface of adsorbent. The IR peaks at wavenumbers 950 and 760 cm^{-1} were absent in the IR-spectrum (FTIR) of Cr-laden sorbent but their presence in the IR-spectra of sorbent before adsorption of Cr(VI) indicated chemical interaction between $HCrO4^{-}$ and the surface functional groups of the sorbent. The chemical interaction involved the reduction of Cr(VI) to Cr(III) through electron transfer process. The sorption of Cr(VI) onto the surface of adsorbent was found to increase with increase in the pH of solution and the amount of adsorption of Cr(VI) by the sorbent might be responsible due to depletion of protons in the system. Further, the utilization of protons in the aqueous system was described by ion exchange mechanisms with hydroxyl ions (–OH) during sorption.

Shibi and Anirudhan, (2006) investigated the adsorption potential of banana peel for the removal of Pb(II) and Cd(II) ions from aqueous solution. A pH range (5.5 –8.0) was found to be more effective in removal of both Pb(II) and Cd(II). The equilibrium stage for the adsorption of Pb(II) and Cd(II) was attained in 180 min of contact time. The maximum monolayer adsorption capacity of banana peel for the sorption of Pb(II) and Cd(II) ions was found to be 185.34 and 65.88 mg g^{-1}, respectively. Adsorption of metal ions was found to decrease with increase in ionic strength due to formation of chloro complexes and expansion of the diffuse double layer. They found that the isosteric heat of sorption process was found to be independent of surface coverage of metal ions.

Jimoh et al. (2012) studied the adsorption behavior of *Delonix regia* (Flamboyant) flower in removal of Co(II), Cu(II) and Pb(II) ions from aqueous solutions. The maximum removal of Co(II), Cu(II) and Pb(II) ions from aqueous solution was found to occur at acidic pH 5.0. The equilibrium stage was attained within 60 min of contact time. The adsorption capacity was increased with increase in dose of adsorbent and initial metal ion concentration. The amount of metal ions adsorption by the adsorbent

at pH 1.0, 2.0 and 3.0 were found to low as compared to pH 4.0 and 5.0 due to increase in competition between the H^+ ions and the metal ions, because at low pH condition (1.0 to 3.0), the high concentration of H^+ was observed. They suggested that at low pH condition, the surface of the adsorbent was surrounded by H_3O^+ ions, thereby inhibiting the metal ions from approaching the active binding sites of the sorbent material.

Kaikake et al. (2007) investigated the feasibility of degreased coffee beans (DCB) as an adsorbent for removal of Cu(II), Zn(II), Pb(II), Fe(III) and Cd(II) from their aqueous solutions. The various surface characteristics of the adsorbent was characterized by using FTIR, SEM and fluorescent X-ray instruments. Batch adsorption experiments were conducted at different pH in order to explain the selectivity of metal ions. All the selected metals were efficiently removed from aqueous solution at acidic pH conditions (3 – 5). They reported porous structure of DCB adsorbent and the BET specific surface area was found to be 1.2 m^2 g^{-1}. The percent desorption of Cd(II) was attained about 90% by a single batch treatment with desorbing solution of HCl or HNO_3 at more than 0.01 mol dm^{-3}. Based on these results they suggested that DCB was used as a cation exchanger.

Han et al. (2010) studied the adsorption characteristics of modified wheat straw in removal of copper ion from industrial wastewater. The thermo-gravimetric analysis of wheat straw confirmed the presence of moisture, cellulose and lignin in the material. The surface functional groups (carbonyl and hydroxyl) present on the surface of adsorbent were confirmed by the FTIR analysis. Kinetic studies indicated that the adsorption of Cu^{2+} followed the pseudo-second order kinetic model. The maximum adsorption capacity of modified wheat straw for Cu^{2+} was found to be 39.17 mg g^{-1} at 293 K. The thermodynamics studies indicated spontaneous and endothermic nature of sorption process.

Bhatnagar et al. (2010) evaluated the feasibility of lemon peel waste as an adsorbent in the removal of cobalt ions from aqueous solutions. The maximum monolayer adsorption capacity of lemon peel adsorbent for cobalt ion was found to be 22 mg g^{-1}. It was found that the adsorption of cobalt ion onto lemon peel adsorbent could be explained more favorably by the pseudo-second order kinetic model. Initially, the rate of adsorption was rapid and about 50% of the metal ions adsorption reached in 120 min. Equilibrium adsorption of cobalt ions was attained within 7 hours. They suggested that the sorption of cobalt ions onto the surface of biosorbent occurred in the form of monolayer adsorption. The overall sorption mechanism of cobalt ions by lemon peel adsorbent involved the binding of cobalt ions with carboxyl and hydroxyl groups present in the biomolecules (hemicellulose, cellulose and lignin) of lemon peel waste. An initial part of cobalt adsorption by adsorbent might be related to intra-particle movements of cobalt ions controlled by surface diffusion process while the later part controlled by pore diffusion.

Chen et al. (2018) investigated the adsorption potential of biochar derived from macroalgae residue in removal of dyes from wastewater. The effect of varying temperature from 400 °C to 800 °C on surface characteristics of biochar was investigated. Among the chosen biochars, biochar derived from macroalgae exhibiting high thermal stability, special surface properties and highly porous material was found to be more efficient in removal of crystal violet (CV), malachite green (MG) and congo red (CR) from aqueous media. The biochar produced at 800 °C exhibited the highest sorption capacity for basic dye malachite green (5306.2 mg g^{-1}). They reported stretching vibration of C=O, –CONH– and C=C in carbonyl, carboxyl groups and aromatic rings corresponded to the IR peak at around wavenumber 1600 cm^{-1}. They suggested that the biochar prepared at 800°C had lower pH_{pzc} and higher pH in aqueous

solution, which could enhance the sorption capacity of cationic dyes (MG and CV) through electrostatic attractions due to the negative potential effect of biochar.

Nautiyal et al., (2016) studied the utilization of residual biomass of *Spirulina platensis* algae (solid waste residue of biodiesel industry) in the preparation of biochar. Adsorption capacity of prepared biochar was examined for removal of Congo red dye from the aqueous solution. The adsorption results were compared with other adsorbents (commercial activated carbon, original algae biomass) used in the study. Various surface characteristics of biochar were studied by using elemental analysis, IR-spectroscopy, SEM and powder XRD techniques. The selected adsorbents showed better adsorption potential in removal of Congo red dye from aqueous solutions. The highest dye uptake onto surface of biochar was observed at acidic pH 2.0, adsorbent dose 0.2 g/100 mL and initial dye concentration (90 mg/L). The algal cell wall is composed of several biomolecules such as cellulose, carbohydrates, proteins, lipids, etc. which comprised of polar surface functional groups (hydroxyl, aldehydic, phenolic, carboxylic, ketonic, etc.) acting as the active binding ligands for the dye molecules.

Oladipo and Ifebajo, (2018) studied the application of magnetic chicken bone biochar (MCB) as an adsorbent in removal of rhodamine B dye and tetracycline from aqueous solutions. The specific surface area and point of zero charge (pH_{pzc}) of the chosen biochar were found to be 328 $m^2 g^{-1}$ and 8.3, respectively. The adsorption potential of biochar in removal of tetracycline (TC) and rhodamine B dye (RB) was evaluated in a single and double stage stirred adsorber. Based on the comparative adsorption studies, the magnetic chicken bone biochar has been considered as an efficient alternative adsorbent. In the acidic conditions, the sorption of TC onto MCB was not favoured due to the electrostatic repulsion between the positively charged surface of MCB (pH < pHpzc) and the cationic TC molecules. As the pH increased above pH 3.3, the sorption

efficiency increased, which was perhaps due to ion exchange mechanisms involved between the zwitter ion form of TC species and the MCB adsorbent. The sorption efficiency of RB dye increased with increase in pH, and maximum adsorption of RB dye (85%) was occured at pH 10.0. In acidic medium, the extent of dye removal was lower due to high interference of H^+ ions and electrostatic repulsion between the dye molecules and active sites on MCB adsorbent.

Lyu et al. (2018) synthesized novel adsorbents from different feedstock materials and pyrolysis temperature using a planetary ball mill. The removal efficiency and sorption mechanisms of methylene blue onto the biochar were examined. Biochar derived from ball milled sugarcane bagasse biomass prepared at 450ºC exhibited highest adsorption capacity for methylene blue dye as compared to unmilled bagasse biochar. A large specific surface area, pore volume, short hydrodynamic radius, more negative zeta potential and abundant oxygen-containing surface functional groups were common features in ball milled sugarcane bagasse. These physico-chemical characteristics resulted in high adsorption capacity (354 mg g^{-1}) for methylene blue dye.

Sewu et al. (2017) investigated adsorption potential of biochar derived from rice straw (RS), Korean cabbage (KC) and wood chip (WC) and used them as alternative adsorbents and compared them with commercial activated carbon (CAC) in removal of dyes from aqueous solutions. In their experiments, crystal violet (CV) and Congo red (CR) were used as a model cationic and anionic dye, respectively. Initial pH of the solution had less effect on adsorption of CV and CR dye onto all chosen biochars except for CR dye adsorption onto CAC. A chemisorption process was involved in the sorption of cationic and anionic dye. Korean cabbage derived biochar exhibited higher adsorption capacity (1304 mg g^{-1}) than RS (620.3 mg g^{-1}), CAC (271.0 mg g^{-1}) and WC (195.6 mg g^{-1}) for the removal of CV dye. The KC derived biochar may be a cheap and

effective alternative adsorbents to commercial AC for the removal of basic cationic dyes from aqueous solution.

Choudhary and Paul, (2018) investigated the adsorption isotherms and kinetics for the removal of Cr(VI) from aqueous solution by using *Eucalyptus globulus* bark biochar (EBB) prepared by the pyrolysis of residual bark biomass at 500 °C. Various process optimizing parameters such as contact time (15–240 min), initial Cr(VI) concentration (1–240 mg L^{-1}), and temperature (303–323 K) were studied to recognize the EBB–mediated efficient Cr(VI) adsorption. The maximum sorption capacity was found to be 21.3 mg g^{-1}. The percent removal of Cr(VI) at pH 2.0 was found to increase from 85% to 99% with increase in dose of EBB from 1 g/L to 5 g/L. It might be possible due to availability of large number of active binding sites at higher dose of adsorbent. A positive value of zeta potential (ζ = 15.6 mV) of EBB adsorbent at pH 2.0 favoured the adsorption of Cr(VI). Further, the isoelectric point (pH_{IEP}) of EBB sorbent was calculated to be at pH 3.18.

Zhao et al. (2018) studied the sorption efficiency of biochars derived from corn straw at different temperatures to remove Cr(VI) from aqueous solution in the presence of salts. In their experiments, X-ray absorption and X-ray photoelectron near edge spectra confirmed that Cr(VI) was reduced to Cr(III). Effect of persistent free radicals on biochars were found to play a vital role in the reduction of Cr(VI) at neutral pH 7.0, which was confirmed by free radical quenching and electron spin resonance. The biochar with persistent free radicals disclosed a highly selective method for the removal of Cr(VI) with potential implications for the detoxification of industrial wastewater. They suggested that oxygen containing functional groups (carboxylic and hydroxyl) on the surface of biochars were found to decrease as the pyrolysis temperature increased. They found that the addition of NaCl enhanced the sorption of Cr(VI) onto the surface

of biochar due to minimization of thickness of the diffuse double layer present around solid and liquid phases.

Zhang et al. (2018) synthesized magnetic biochar (MMABC) from *Melia azedarach* wood and applied as an adsorbent for the removal of Cr(VI) from aqueous solution. The specific surface area of mesoporous MMABC adsorbent was found to be S_{BET} 5.219 m^2 g^{-1}. Based on Raman spectroscopy and IR-spectroscopy (FTIR), the benzene-ring adjacent to carbonyl group did not show clear positive effects on Cr(VI) adsorption. However, adsorption coupled reduction was found to occur in the removal of Cr(VI) from aqueous solution using MMABC adsorbent. The effect of adsorbent (MMABC) dosage on adsorption of Cr(VI) was chiefly depended on surface active sites of adsorbent. The number of active adsorption sites was proportional to per unit mass of adsorbent. However, after adsorbent dosage (0.5 g/100 mL), the sorption efficiency was constant to 99.8% and indicated that adsorbent dose (5 g/L) was optimum dosage for the removal of Cr(VI). They found that the surface functional groups (υC-O, C–H and C–C) were disappeared in the FTIR spectrum of Cr-laden sorbent, indicating involvement of these functional groups in the removal of Cr(VI).

CHAPTER-III

Materials and Methods

3. Materials and methods

3.1. Chemicals

In the present investigation, a number of analytical grade chemicals were used to perform the experiments such as characterization of adsorbents, stock solutions and preparation of adsorbate-adsorbent solutions for adsorption/desorption experiments. A list of used chemicals, their sources and molecular weight (g mol^{-1}) are given in Table 3.1. Double distilled water (pH 7.0) was used in the preparation of buffers, stock and working solutions of different chemicals throughout the experimental study.

Table 3.1. Sources and molecular weight (g mol^{-1}) of chemicals used in the present study.

Chemicals	**Sources**	**Molecular weight (g mol^{-1})**
Malachite green ($C_{23}H_{25}ClN_2$)	Aldrich	463.50
Methylene blue ($C_{16}H_{18}ClN_3S$)	E Merck Ltd.	319.85
Potassium dichromate ($K_2Cr_2O_7$)	E Merck Ltd.	294.18
Sodium borate ($Na_2B_4O_7.10H_2O$)	Himedia	381.38
Citric acid ($C_6H_8O_7$)	Himedia	192.13
Dibasic sodium phosphate ($Na_2HPO_4.7H_2O$)	Himedia	268.07
Monobasic dihydrogen phosphate (KH_2PO_4)	Himedia	136.08
Dibasic monohydrogen phosphate (K_2HPO_4)	Himedia	174.18
Sodium hydroxide (NaOH)	Himedia	39.99
Hydrochloric acid (HCl)	E Merck Ltd.	36.46
Acetic acid (CH_3COOH)	E Merck Ltd.	60.05
Sulfuric acid (H_2SO_4)	E Merck Ltd.	98.07
Potassium bromide (KBr)	E Merck Ltd.	119.00

3.2. Preparation of adsorbate solutions

3.2.1. Malachite green solution: The stock solution (1000 mg L^{-1}) was prepared by mixing 1.0 g of malachite green ($C_{26}H_{27}N_2O_6$) in 1000 mL of double distilled water. The stock solution was diluted in phosphate buffer (20 mM, pH 6.0) to prepare the working solutions of malachite green (MG) dye with different initial dye concentration and further batch adsorption experiments were carried out as a function of different physico-chemical controlling factors.

3.2.2. Methylene blue solution: The stock solution (1000 mg L^{-1}) was prepared by mixing 1.0 g of methylene blue (MB) dye ($C_{16}H_{18}ClN_3S$) in 1000 mL of distilled water (pH 7.0). The stock solution was diluted in phosphate buffer (20 mM, pH 7.0) to prepare the working solutions of MB dye of different initial dye concentrations and further batch adsorption experiments were carried out under different process optimizing parameters (contact time, pH, adsorbent dose, temperature and initial dye concentration) to define the optimum conditions for the removal of MB dye from aqueous solution.

3.2.3. Cr(VI) solution: The stock solution (1000 mg L^{-1}) of Cr(VI) was prepared by dissolving 2.828 g of $K_2Cr_2O_7$ in 1000 mL of double distilled water with addition of l mL of dilute H_2SO_4. The stock solution was diluted in citrate phosphate buffer (20 mM, pH 3.0) to prepare the working solutions of Cr(VI) with different initial concentrations and further batch adsorption experiments were carried out under different physico-chemical controlling factors.

3.3. Preparation of buffer solutions

Due to excess alkalinity caused by the adsorbent (MPA) in aqueous solution, the pH of dye/heavy metal solution with fixed concentration was adjusted to pH 3.0, 4.0, 5.0, 7.0, 9.0 and 10.0 by using appropriate citrate-phosphate, phosphate and borate buffer (20

mM, each) to study the effect of pH on the sorption of cationic dyes and Cr(VI). In the present study, acid (HCl) or base (NaOH) was not used to fix the pH of dye and heavy metal solution. According to the preparation methods of different buffers (Gomori, 1955), the preparation of all the selected buffers are described as follows:

3.3.1. Citrate-phosphate buffer: The stock solutions of citric acid (0.1M) and dibasic sodium phosphate (0.2M) were prepared by dissolving 19.21 g (citric acid) and 53.65 g (dibasic sodium phosphate) in 1000 mL of distilled water. In order to obtain the pH range (3–5), a fixed quantity (mL) of solution was taken from each stock solutions and diluted to a total of 100 mL of distilled water to get required pH (Gomori, 1955).

3.3.2. Phosphate buffer: The stock solutions of monobasic sodium phosphate (0.2M) and dibasic sodium phosphate (0.2M) were prepared by dissolving 27.8 g and 53.65 g, respectively, in 1000 mL of distilled water. In order to obtain the pH range (6 – 8), a fixed quantity (mL) of solution was taken from each stock solution and diluted to a total of 200 mL of distilled water to get required pH (Gomori, 1955).

3.3.3. Borax-NaOH buffer: The stock solutions (0.02M) of sodium borate was prepared by dissolving 19.05 g in 1000 mL of distilled water. Further, a stock solution (0.2M) of NaOH was prepared by dissolving accurately weighed NaOH in 1000 mL of distilled water. In order to obtain the pH 10.0 of aqueous medium, the stock solution were diluted by adding 50 mL of sodium borate and 43.0 mL of 0.2 M NaOH to a total of 200 mL of distilled water (Gomori, 1955).

3.4. Collection of Mentha Plant Ash (MPA)

Mentha (mint) Plant Ash (MPA), a waste byproduct of the mentha oil production, was collected from local mentha oil distillation units, Barabanki, Uttar Pradesh, India. The geographical location of sampling site Barabanki, Uttar Pradesh (latitude 26º 56’ N and longitude 81º 13’ E) has been shown in Fig. 3.1. The oil extracted mentha plant residue

is dried and used by the farmers as a cheap source of fuel for heating of the oil distilllating units. The resulting plant ash is left in the field as a dumping waste with no subsequent application. Further, MPA is an unattended waste byproduct of mentha distilling industry and it is easily available in plenty in the vicinity of the industrial plant. A schematic diagram representing the generation of MPA as a waste byproduct of mentha oil distillation unit has been shown in Fig. 3.2. Prior to use, MPA was kept in hot air oven at a temperature of 80°C for 6 – 8 hours to remove the moisture from material. The material was homogenized to a fine powder with a pestle and mortor. Finally the powder was sieved (< 0.21 mm) by using 70-mesh size sieve so that all the particles were of almost of similar size. The sieved MPA powder was placed in air tight glass bottle so that it could be used for further application and characterization.

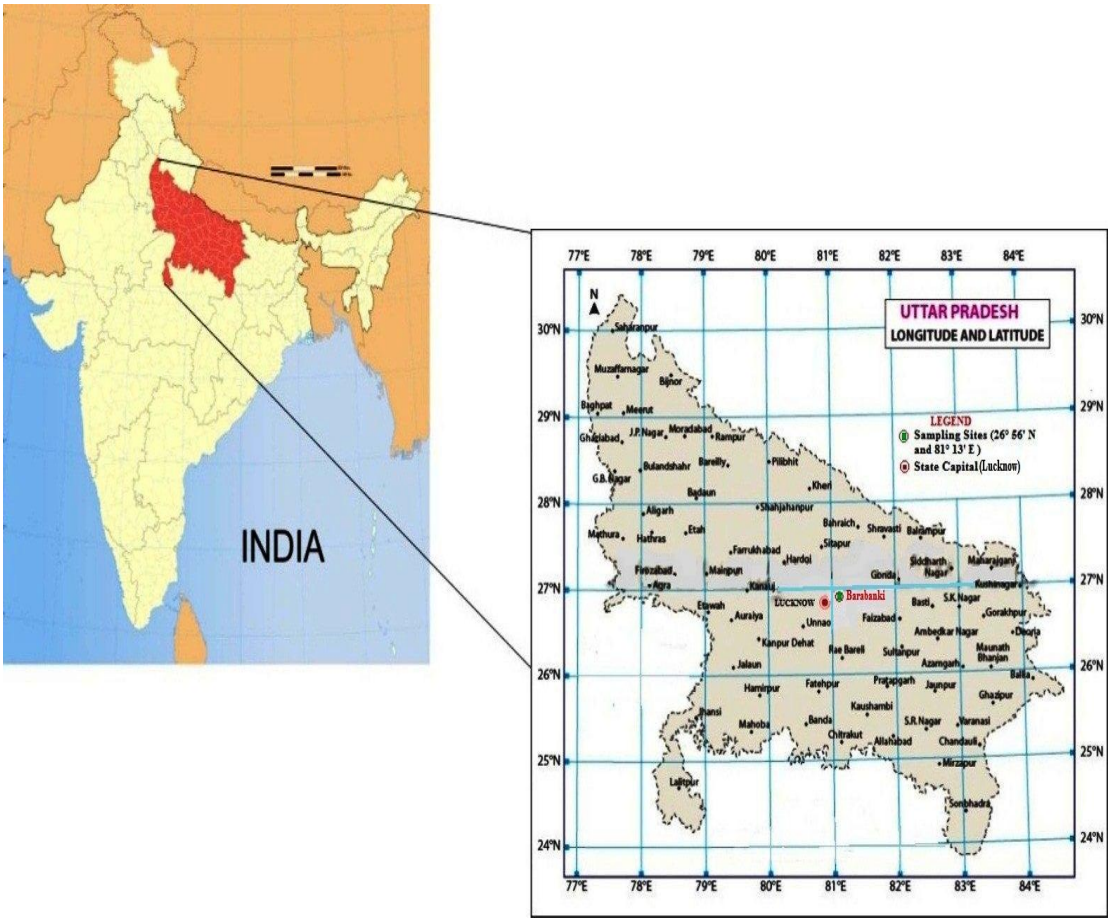

Fig. 3.1. Geographical location of sampling site Barabanki, Uttar Pradesh (latitude 26º 56' N and longitude 81º 13' E).

Fig. 3.2. A schematic diagram representing the generation of Mentha Plant Ash as a waste byproduct of mentha oil distillation unit.

3.5. Characterization of MPA adsorbent

3.5.1. Zeta potential

Zeta potential analysis of adsorbent (MPA) provides an important information about the surface potential of MPA particles and the type of sorption mechanisms (electrostatic attraction and ion exchange) occurring on the surface of MPA particles. In general terms, the surface potential of any adsorbent may be defined as the potential difference established between the mobile and stationary phase of the dispersion medium attached to the dispersed particles. The pH of the aqueous medium affects zeta potential and the values of zeta potential changes with the change in pH of the aqueous

medium. Some other factors such as ionic strength, temperature and concentration of any additives may also affect zeta potential value of adsorbent particles (Basar, 2003). Zeta potential measurements are mainly associated with stability of emulsions (short and long-term stability). A high value of surface potential (negative or positive) of emulsions indicate electrically stabilized emulsions while low value of zeta potentials of emulsions tend to coagulate or flocculate leading to poor physical stability. In general, the value of surafce potential of an emulsion is high as the repulsive forces exceed the attractive forces, resulting in a relatively stable system (Losso et al., 2005). In order to define the sorption mechanisms (chemical binding) of cationic dyes and Cr(VI), the zeta potential of MPA particles was determined by using zeta potential analyzer (Malvern Instruments Ltd, Serial Number: MAL1010294). The samples for zeta potential analysis were prepared by dissolving 1.0 mg of MPA adsorbent in 10 mL deionized water at chosen pH and was sonicated before analysis. The zeta potential spectrums were recorded in the range of –200 to 200 mV (Cao et al., 2007).

3.5.2. SEM and EDX analysis

Scanning electron microscopy (SEM) is one of the most commonly used technique to analyze surface morphology of adsorbents derived from agricultural waste materials. SEM is a type of electron microscope which is used to produce an image of a sample by passing a focused beam of electrons over the sample for scanning through it. SEM analysis provides direct observation of surface structure and elemental composition of powder materials. The ability to create an actual image of solid surface makes this technique very helpful in obtaining morphological features of bio-sorbents (Yuvaraja et al., 2014). It has been considered to be very popular technique for the characterization of adsorbents to determine the surface morphology and general physical characteristics. In the present study, the surface morphology and mineral composition of MPA

adsorbent was investigated using a JEOL JSM-6490 LV scanning electron microscope equipped with an energy dispersion X-ray spectroscopy (EDX). SEM micrographs were taken at 15 kV under 5000 time's magnification (Bello et al., 2017). Energy dispersive X-ray spectroscopy (EDX) is primarily used for the elemental and chemical characterization of adsorbent materials. The elemental/chemical characterization of adsorbents is based on the principle which may state that each element has a unique atomic structure and thus permit unique set of peaks on its X-ray spectra of adsorbent materials. Thus, EDX analysis was carried out to determine elemental composition of MPA adsorbent (Bello et al., 2017).

3.5.3. BET specific surface area

Brunauer-Emmett-Teller (BET) and Barrett-Joyner-Hanlenda (BJH) methods are the most widely studied analytical procedures for N_2 adsorption/desorption isotherms measured at 77 K to determine specific surface area and pore size distribution of adsorbent, respectively (Clarkson et al., 1997). Both BET and BJH method are used to determine specific surface area and other textural characteristics of adsorbents such as pore volume, pore size and average pore diameter of adsorbent particles. In the BET method, the nitrogen multilayer adsorption is determined as a function of relative pressure using a fully automated Brunauer-Emmett-Teller (BET) instrument. The BET method covers pore area and external surface area estimations to determine the total specific surface area (m^2g^{-1}) which provide an important information in studying the effects of porosity, specific surface area, and particle size of adsorbent particles in the sorption process (Alothman, 2012). In the present study, specific surface area and other textural characteristics of adsorbent (MPA) were determined using a Brunauer-Emmett-Teller (BET) instrument (BEL Master^{TM} Ver.2.3.1, BEL Japan, INC.). The BJH method is used to determine pore size distribution independent of external surface

area due to particle size of the adsorbent materials. The pore-size distributions of MPA adsorbent was determined by using the BJH method (Clarkson et al., 1997).

3.5.4. IR-spectroscopy (FTIR)

The presence of several functional groups on the surface of adsorbents derived from different waste biomass is the most attracting chemical characteristic of an adsorbent. Fourier Transform Infrared Spectroscopy (FTIR) is an important instrument which is commonly used in the determination of surface functional groups particularly involved in the binding of dyes and heavy metals. The surface functional groups of agro-waste based adsorbents can be easily determined by using FTIR instrument through the monitoring of the vibrations of the functional groups and these vibrations characterize molecular structure of various organic molecules present in the adsorbent materials (Mohan, 2005). In the present investigations, the IR-spectrum (400 – 4000 cm^{-1}) of MPA adsorbent before and after adsorption of cationic dyes (crystal violet, malachite green, methylene blue) and Cr(VI) were obtained by using Fourier Transform Infrared Spectroscopy (FTIR, Thermo Scientific, USA; Model: Nicolet^{TM} 6700). Samples were prepared for analysis by mixing 1 mg of samples before and after adsorption with 100 mg of spectroscopy grade potassium bromide (KBr) and pellets were made by hydraulic press (15 tons). The spectra were corrected for background KBr absorption (Bello et al., 2017).

3.5.5. X-Ray diffraction (XRD) analysis

X-Ray diffraction (XRD) technique is commonly used to determine the mineralogical composition as well as qualitative and quantitative phase analysis of multiphase mixtures in the adsorbent materials. The existence of different minerals in adsorbent materials can be confirmed by their inter-atomic distance (*d*) in the random powder

diffraction pattern of the adsorbents (Singh et al., 2010). The XRD pattern of adsorbent material is unique for a particular crystalline material because the XRD patterns reflects the various spacing of planes of atoms within the crystal lattice. The position of different peaks of minerals in the XRD pattern are related to lattice spacing in the crystal according to Bragg's law (McQuarrie, 1997):

$$n\lambda = 2d_{hkl} \sin\theta \quad \textbf{(3.1)}$$

Where n is an integer represent order of the reflection; λ (nm) is the wavelength; d is the interatomic distance between the (hkl) diffracting planes in the crystal and θ is the angle between the incident X-ray beam and the diffracting planes. In order to confirm the mineralogical compositions of adsorbent, the X-Ray diffraction (XRD) analysis of the MPA sample was carried out using a PAN alytical XRD instrument (Model/Supplier: Panalytical), operated at 30 mA and 40 kV. The XRD data was collected over in the range of $2\theta = 5–50^{\circ}$ by step scanning using Cu Kα ($\lambda = 0.154$ nm) radiation (Singh et al., 2010).

3.5.6. Cyclic Voltammetry analysis

Cyclic voltammetry (CV) is a type of potentio-dynamic electrochemical measurement of an analyte in electrolytic solution and commonly used to study the redox (reduction/oxidation) behavior of an analyte in the electrolytic solution (Ngamukot et al., 2006). The working electrode potential in a cyclic voltammetry test is ramped linearly versus time. In the present study, cyclic voltammetry analysis was carried out to see whether a rapid decolourization/color change of dye and metal ion solution in the presence of adsorbent (MPA) was simply adsorption or something else like reduction and oxidation of contaminants. Cyclic Voltammetry (BASi EC Epsilon) instrument was used to determine electrochemical behavior of basic cationic dyes (malachite green,

methylene blue) and Cr(VI) in aqueous solution after treatment of adsorbent MPA. The cyclic voltammetry test was performed in a single compartment with 50 mL of dye/metal ion solution (50 mg L^{-1}) treated with MPA for 75 min at room temperature. In cyclic voltammetry test, Ag/AgCl electrode, glassy carbon and a platinum wire were used as a reference electrode, working electrode and counter electrode, respectively. The redox behavior of cationic dyes and Cr(VI) was studied over a potential range from –1.5V to +1.5V (vs. Ag/AgCl) with a scan rate of 100 mVs^{-1} and step potential of 0.002V (Ngamukot et al., 2006).

3.5.7. Thermo-gravimetric analysis (TGA)

Thermo-gravimetric analysis (TGA) is widely used to determine the rate of change in the weight of adsorbent material as a function of varying temperature or time in a controlled conditions. TGA analysis is also very helpful in determination of composition of materials and their thermal stability at temperatures up to 1200°C. Further, TGA technique can also be used to characterize the biomaterials which exhibit weight loss or gain due to oxidation, dehydration and decomposition at varying temperature (Qi et al., 2010). In order to confirm the thermal behavior of organic and inorganic content present in MPA adsorbent, the thermogram (TG) of MPA was obtained by using Thermo-gravimetric Analyzer (Netzsch Germany) under N_2 flow of 100 mL min^{-1}, heating rate of 10°C min^{-1} and temperature ranges (30–850°C). The composition of adsorbent (MPA) and their thermal stability at temperature up to 850°C was determined by using TG analysis. In the preparation of sample for TG analysis, one grams of the powder adsorbent sample was placed into the platinum pan of the TGA analyzer and the sample was degassed for a few minutes. Further, N_2 gas was allowed to pass through the chamber furnace of TGA analyzer to confirm an inert atmosphere and the sample was heated at required temperature until a constant weight

is obtained for the determination of moisture content and volatile organic matter (Bello et al., 2017; Qi et al., 2010).

3.5.8. X-Ray Photoelectron Spectroscopy (XPS)

X-ray Photoelectron Spectroscopy (XPS) is a quantitive spectroscopic technique used to analyze the surface chemistry of an adsorbent sample and determine its elemental composition, atomic concentrations, and chemical states of elements present at the surface of samples (Wen et al., 2011). In XPS instrument, a soft X-ray source (AlKα) is commonly used to ionize electrons from the surface of a solid sample. The binding energy (eV) of ionized electrons are measured to determine valence state of various metal ions. In the removal of Cr(VI) by MPA, the composition and valence state of the Cr(VI) metal ions on the surface of MPA was analyzed to confirm the reduction of Cr(VI) during sorption process (Wen et al., 2011). The surface chemistry, composition and valence state of the Cr(VI) on the surface of MPA was determined by performing the experiments using X-ray photoelectron spectroscopy instrument (XPS, Thermo Fisher Scientific, UK) with Al Kα radiation ($h\upsilon$ = 1486.6 eV) (Wen et al., 2011).

3.6. Batch adsorption experiments

3.6.1. Batch adsorption experiments for removal of cationic dyes

Batch adsorption experiments were carried out to examine the adsorption potential of MPA adsorbent in the removal of basic cationic dyes (malachite green and methylene blue) from their aqueous solutions, using an orbital shaking incubator (Model UTS: 1.21) at 180 rpm and conical flasks of 250 mL. The sorption of malachite green (MG) and methylene blue (MB) dye by MPA was carried out as a function of different contact time (0 – 45 min for MG; 0 – 30 min for MB), adsorbent dose (0.05–0.3g/100 mL for both MG and MB), pH condition in each (pH 4.0 – 10.0) and initial dye concentration

(20 – 100 mg L^{-1} of MG; 5 – 50 mg L^{-1} of MB). To study the effect of contact time, pH and initial dye concentrations on the sorption of MG and MB dye, an amount of 0.1 g of MPA was added to 250 mL conical flasks containing 100 mL of 50 mg L^{-1} of MG and 25 mg L^{-1} of MB dye solutions (pH 6.0 for MG; pH 7.0 for MB). Further, the resulting solutions were placed under shaking condition (180 rpm) at an incubation temperature of 32°C (approximately room temperature) for various time durations (0 – 45 min for MG; 0 – 30 min for MB). Due to excess alkalinity caused by the adsorbent (MPA) in aqueous solution, the pH range of dye solution (25 mg L^{-1} for MB; 50 mg L^{-1} for MG) was adjusted to pH 4.0, 5.0, 7.0, 9.0 and 10.0 by using appropriate citrate-phosphate, phosphate and borate buffer (20 mM, each) to study the effect of pH on the sorption of cationic dyes. An amount of 0.1g of MPA was added to the dye solution to start the adsorption process at room temperature (32°C) for varying time intervals. All the working solutions were centrifuged (Remi Instruments LtD: AXCI-7182) at 5000 rpm for 10 min to separate dye-loaded adsorbent from the suspension. The final dye concentration in the supernatant was evaluated by measuring the concentration of MG and MB dye at a wavelength of 618 and 668 nm, respectively, using a UV–visible double beam spectrophotometer (Shimadzu UV–1601).

3.6.2. Batch adsorption experiments for removal of Cr(VI)

Batch adsorption experiments were carried out to examine the adsorption potential of MPA for the removal of Cr(VI) from their aqueous solution using an orbital shaking incubator (Model UTS: 1.21) at 180 rpm and conical flasks of 250 mL. The sorption of Cr(VI) by MPA was carried out as a function of different contact time (0 – 90 min), adsorbent dose (0.1 – 0.5g/100 mL), pH condition (pH 3.0 – 8.0) and initial Cr(VI) concentration (10 – 50 mg L^{-1}). To study the effect of contact time, pH and initial Cr(VI) concentration on the sorption of Cr(VI), an amount of 0.1 g of adsorbent (MPA) was

added to 250 mL conical flasks containing 100 mL of Cr(VI) solution (10 mg L^{-1}; pH 3.0) and the resulting solutions were placed under shaking condition (180 rpm) at 32°C (approximately room temperature) for various time durations ranging from 5 min to 90 min. To study the effect of pH, the Cr(VI) metal ion solution was prepared using appropriate buffer (20 mM) and shaken at 32°C for 90 minutes. All the working solutions were centrifuged (Remi Instruments LtD: AXCI-7182) at 5000 rpm for 10 min to separate Cr-loaded adsorbent from the suspension. The final Cr(VI) concentration was determined at 540 nm wavelength using a UV–visible double beam spectrophotometer (Shimadzu UV–1601) and the total chromium concentration was measured by fast sequential atomic adsorption spectrometer (Varian; AA240FS).

All the samples measured three times and the mean values were considered for the calculation of adsorption capacity and percent removal of cationic dyes and Cr(VI) metal ions. The amount of dye/metal ion adsorbed at equilibrium, q_e (mg g^{-1}) and percent removal were calculated by following equations (Hameed et al., 2008):

$$q_e = \frac{(C_i - C_e)V}{m} \quad \textbf{(3.2)}$$

$$\text{Percent removal (\%)} = \frac{C_i - C_e}{C_i} \times 100 \quad \textbf{(3.3)}$$

Where, q_e (mg/g) is the amount of dye/metal ion adsorbed per unit weight of adsorbent, C_i, C_e, V and m represent initial dye/metal ion concentration (mg L^{-1}), final dye/metal ion concentration in solution (mg L^{-1}), volume (Litre) of the solution and mass (grams) of the adsorbent, respectively.

3.7. Desorption studies for cationic dyes

Desorption studies were carried out to see the recovery of adsorbent (MPA) as well as re-use potential of adsorbate. If the dye desorption occurs by desorbing agents such as acids (H_2SO_4, HCl and CH_3COOH) or alkali (NaOH), then it indicates chemisorption process (Rawat and Singh, 2017). If the adsorbed dye is desorbed by using neutral pH

water, then the attachment of the dye molecules with the adsorbent particles is by weak bonds and it indicates physical adsorption of adsorbate molecules (Ansari & Mosayebzadeh, 2010).

In the present desorption studies, 100 mL of MG (50 mg L^{-1}) and MB dye (25 mg L^{-1}) solutions was mixed with adsorbent MPA (0.1g/100 mL) at pH 6.0, and 7.0, respectively. The resulting dye solutions were placed under shaking (180 rpm) at 32°C for different time intervals (45 min for MG; 30 min for MB). The dye-loaded MPA was separated by centrifugation and the residual concentration of dyes (MG and MB) in the supernatant was measured to determine the amount of dye adsorbed by MPA particles. Thereafter, 0.1 g of dye-loaded dried MPA (dried at 70ºC for 6 – 8 hours) was added to 100 mL of desorbing solution (1.0 N each of HCl, CH_3COOH, H_2SO_4 and NaOH) and the mixture was shaken at 180 rpm for 60 minutes. The amount of dye released in the desorbing solution was determined by using UV-visible double beam spectrophotometer (Shimadzu UV-1601) as described earlier. The adsorbent (MPA) separated from the desorbing solution was washed with the distilled water 3 to 4 times to remove the desorbing solution from the surface of MPA. The washed MPA particles were dried at 70°C for 6 – 8 hours for further use in wastewater treatment. In the present study, use of 1N desorbing solution of acids or alkali to desorb the MG and MB dye was preferred so that the surface characteristics of MPA were not severely modified. The percent desorption of dye was calculated at regular time interval by the following equation (Ansari & Mosayebzadeh, 2010):

$$\text{Percent desorption (\%)} = \frac{\text{Amount of dye desorbed}}{\text{Amount of dye adsorbed}} \times 100 \qquad \textbf{(3.4)}$$

3.8. Adsorption isotherms

The adsorption isotherms (Langmuir and Freundlich) are well known equilibrium adsorption models applied on equilibrium adsorption data and clarifies the sorption

mechanisms of dyes and heavy metals onto the surface of adsorbent. Generally, the adsorption isotherms describe the relation between the equilibrium concentration of adsorbate molecules in the solution and the amount of adsorbate molecules adsorbed onto the surface of adsorbent (Ozdes et al., 2011). A number of adsorption isotherm models are available that describe the process of equilibrium adsorption of contaminants (dyes and heavy metals) onto the surface of adsorbents. In the present study, the two well studied adsorption isotherm models (Langmuir and Freundlich) were applied on equilibrium adsorption data of cationic dyes and Cr(VI).

3.8.1. Langmuir isotherm model

The Langmuir adsorption model is mainly applicable on those adsorbent materials that have uniform surface and sorption energies (Nava et al., 2011). Absence of particles interactions between adsorbent and adsorbate molecules with no any transmigration of the adsorbate molecules on the surface of adsorbent material (single layer adsorption) are the most common features of Langmuir isotherm (Nava et al., 2011).

The Langmuir adsorption isotherm (Langmuir, 1915) assumes monolayer adsorption onto a surface of adsorbent having a finite number of active sites. It is applicable on homogeneous surface of adsorbent and the calculation of the maximum adsorption capacity (q_{max}) conforming to whole monolayer coverage on the surface of adsorbent. The Langmuir isotherm equation is represented in linear form as follows (Langmuir, 1915):

$$\frac{C_e}{q_e} = \frac{1}{q_{max}\, b} + \frac{C_e}{q_{max}} \qquad \textbf{(3.5)}$$

Where, C_e is the equilibrium dye/metal ion concentration (mg L^{-1}) in solution; q_e is the amount of dye/metal ion adsorbed onto the surface of adsorbent at equilibrium (mg g^{-1}); q_{max} is the Langmuir constant known as the maximum adsorption capacity (mg g^{-1}) of the adsorbent and b is called as adsorption free energy (L mg^{-1}). A plot of $1/q_e$ versus

$1/c_e$ was used to calculate the Langmuir constants q_{max} (mg g^{-1}) and b (L mg^{-1}) from the slope and intercept of the plot, respectively.

3.8.2. Equilibrium parameter or separation factor (R_L)

The effect of shape of Langmuir isotherm on adsorption of dyes and heavy metals was studied to understand whether a sorption process is favorable or unfavorable. Further, the analysis of Langmuir equation can be made on the basis of equilibrium parameter or separation factor (R_L) which is a dimensionless constant and it can be used to determine the feasibility of sorption process in a given range of dye/metal ion concentrations over the adsorbent (Hall et al., 1966). It is represented by the following equation:

$$R_L = \frac{1}{1+bC_i} \quad \textbf{(3.6)}$$

The R_L value indicates the nature of sorption process to be either linear adsorption (R_L = 1), favorable adsorption (0 < R_L< 1), unfavorable adsorption (R_L > 1) or irreversible sorption process (R_L = 0) (Ho and Mckay, 2000).

3.8.3. Freundlich isotherm model

Freundlich proposed an adsorption isotherm based on the hypothesis that the uptake of adsorbate molecules onto a heterogeneous surface of adsorbent with multilayer adsorption and the amount of adsorbate molecules adsorbed onto the surface of adsorbent increases infinitely with the increase in concentration of adsorbate molecules in solution (Arfaoui et al., 2008). The Freundlich isotherm equation is given as follows:

$$q_e = K_F C_e^n \quad \textbf{(3.7)}$$

Where, K_F is a Freundlich constant related to adsorption capacity of the adsorbent $(mg/g)/(mg/L)^{1/n}$ and n is an empirical parameter related to intensity of adsorption. The values of n varies with the heterogeneity of adsorbent particles and n value between 0.0

– 1.0 indicates favorable adsorption of dyes and heavy metals (Arfaoui et al., 2008). The Freundlich isotherm equation can be written in linear form as:

$$\log q_e = \log K_F + 1/n \log C_e \quad \textbf{(3.8)}$$

Where, K_F is the adsorption capacity and n represents the intensity of adsorption. Thus, a plot of log q_e versus log C_e is a straight line and values of Freundlich constants (K_F and n) are calculated from the intercept and slope of the linear plot.

3.9. Adsorption kinetics

The adsorption kinetics describe the uptake rate of adsorbate molecules onto the surface of adsorbent, sorption mechanisms and reaction pathways of adsorbate molecules-adsorbent particles interaction untill equilibrium is attained. Further, the kinetic parameters derived from different kinetic models (Pseudo-first order, Pseudo-second order and Intra-particle diffusion model) provide valuable information about designing, optimization, and modeling of the batch adsorption process (Bektas et al., 2011). A number of kinetic models are available in order to investigate the adsorption mechanisms of dyes and heavy metals onto the surface of adsorbent. In the present work, kinetic studies were carried out by applying pseudo-first order, pseudo-second order kinetic model and intra-particle diffusion model on time dependent experimental data to know the extent of dye/metal ion adsorption as a function of time. The amount of dye/metal ion adsorption at time t, q_t (mg g^{-1}), was calculated by the following equation (Hameed et al., 2008):

$$q_t = \frac{(C_i - Ct)V}{m} \quad \textbf{(3.9)}$$

Where C_i is the initial dye/metal ion concentration (mg L^{-1}) in solution and C_t is the dye/metal ion concentration (mg L^{-1}) at time t in solution.

3.9.1. Pseudo-first order kinetic model

In Pseudo-first order kinetic model, the rate of adsorption is proportional to the number of vacant sites on the surface of adsorbent (Liu and Liu, 2007), which can be described by the following equations:

$$dq_t/d_t = k_1 (q_e - q_t) \quad \textbf{(3.10)}$$

Where, q_e and q_t are the amount of dye/metal ion adsorbed (mg g^{-1}) onto the surface of adsorbent at equilibrium and at time t, respectively and k_1 (1/min) is the pseudo-first order rate constant.

After integration and applying boundary conditions t=0 to t=t and $q_t = 0$ to $q_t = q_t$, a linear form of pseudo-first order kinetic equation can be described in the following form (Liu and Liu, 2007):

$$\log (q_e - q_t) = \log q_e - k_1 t/2.303 \quad \textbf{(3.11)}$$

Where q_e and q_t are adsorption capacity (mg g^{-1}) at equilibrium and after time (t), respectively and k_1 (min^{-1}) is the first order rate constant. The constants k_1 and q_e of pseudo-first order kinetics can be calculated from the slope and intercept of the plot of log ($q_e - q_t$) versus t. The value of intercept in the plot is equal to the log q_e.

3.9.2. Pseudo-second order kinetic model

Pseudo-second order kinetic model is most commonly studied model applied in liquid-phase adsorption systems to describe the sorption kinetics in removal of dyes and heavy metals from aqueous solution. The Pseudo-second order equation for the analysis of adsorption kinetics can be expressed in linear form as (Ho and Mckay, 2000):

$$\frac{t}{q_t} = \frac{1}{K_2 q e^2} + \frac{t}{q_e} \quad \textbf{(3.12)}$$

Where k_2 is the rate constant (g mg^{-1} min^{-1}) of Pseudo-second order kinetic model. The plot between t/q_t and t should give a linear relationship from which k_2 and q_e can be derived from the slope and intercept of the plot, respectively.

The Pseudo-second order kinetic model can also be applied on adsorption kinetic data to calculate initial adsorption rate h (mg g^{-1} min^{-1}) for the sorption of dye and heavy metal onto the surface of adsorbents, which can be written as:

$$h_{0,2} = k_2 q_e^2 \quad \textbf{(3.13)}$$

3.9.3. Intra-particle Diffusion Model

The intra-particle diffusion (IPD) model is commonly applied on time dependent experimental data to describe sorption kinetics involved in the removal of dyes and heavy metals. There are two or three steps are mainly involved to follow the overall sorption process of contaminants (Sun and Yang, 2003). The adsorption of adsorbate molecules on external surface of adsorbent (instantaneous adsorption) takes place in the first step where as the second step in sorption process is the gradual adsorption step and during which the intra-particle diffusion is in controlled conditions. The third step in the sorption process is the final equilibrium stage where the solute particles seem to move slowly from macropores to micropores causing a decline in the rate of adsorption. The time required for the second step of sorption process usually depends on the variations in the physico-chemical parameters including adsorbate-adsorbent concentration, temperature, and particle size of adsorbent. Generally, IPD model is studied to investigate the rate controlling steps and sorption mechanisms affecting the efficiency and nature of sorption process (Weber and Morris, 1962). IPD model can be explained by the following equation:

$$q_t = k_{id} t^{1/2} + C \quad \textbf{(3.14)}$$

Where, C is the intercept and k_{id} is the intra-particle diffusion rate constant (mg/g $min^{1/2}$). The constant C and k_{id} can be derived from the slope of the linear plot of q_t versus $t^{1/2}$.

3.10. Activation energy

The activation energy (*Ea*) provides valuable information about the types and nature of sorption processes which are generally occur in the removal of dyes and heavy metals from their aqueous solutions. Based on value of activation energy, the sorption process can be classified as physical and chemical adsorption. The value of *Ea* for the physical adsorption is usually < 40 kJ mol^{-1}, since the forces involved in physical adsorption are weak whereas the *Ea* value > 40 kJ mol^{-1} indicates chemisorption which is more specific and involves forces much stronger than in physisorption process (Saha et al., 2012). In the present study, the activation energy (*Ea*) for the sorption of basic cationic dyes by MPA adsorbent was calculated using Arrhenius equation (Chowdhury and Saha, 2010):

$$\ln k = \ln A - \frac{E_a}{RT} \quad \textbf{(3.15)}$$

Where k is the velocity constant, A the Arrhenius constant, *Ea* (kJ mol^{-1}) the activation energy for surface binding, R (8.314 J $mol^{-1}K^{-1}$) is called gas constant and T is the temperature (K). The value of velocity constant (k) was determined by the following equation:

$$k = \frac{C_0}{C_f} \quad \textbf{(3.16)}$$

Where C_0 (mg L^{-1}) and C_f (mg L^{-1}) are the initial and final dye concentration in solution at temperature (K), respectively. Activation energy (*Ea*) was calculated from the slope of linear plot of lnk versus 1/T.

3.11. Thermodynamic studies

The effect of temperature on the sorption process can be conducted by preparing adsorbate-adsorbent solution with varying initial dye/metal ion concentration and temperature. Temperature has been considered as an indicator for nature of sorption process whether it is an endothermic or exothermic process. If the amount of adsorption increases with increase in temperature then the sorption process is an endothermic in

nature. The kinetic mobility of the adsorbate molecules and the number of active sites for the adsorption increases with increase in temperature (Senthilkumaar et al., 2006). The decrease in adsorption capacity with increasing temperature indicates that the sorption process is an exothermic in nature (Nandi et al., 2009). Increase in temperature may decline the adsorptive forces between the adsorbate molecules and the active sites present on the surface of adsorbent which causes decline in adsorption capacity (Ofomaja and Ho, 2007).

In temperature-dependent adsorption process, it is very useful to define the thermodynamic parameters such as standard enthalpy change (ΔH°), free energy change (ΔG°) and entropy change (ΔS°) (Ahmad and Kumar, 2010). In the present study, the Gibbs free energy change for sorption of dye and heavy metal onto the adsorbents as studied in a selected range of temperature (20 – 50 ºC) can be calculated by the following equation:

$$\Delta G = -RT \ln Kc \qquad \textbf{(3.17)}$$

ΔH° and ΔS° of sorption process can be derived from Van't Hoff equation, which can be written as:

$$\ln Kc = \frac{\Delta S^\circ}{R} - \frac{\Delta H^\circ}{RT} \qquad \textbf{(3.18)}$$

Where Kc is equilibrium constant for adsorption, R is the gas constant, T is absolute temperature (K). The value of ΔH° and ΔS° were calculated from the slope and intercept of the linear plot of lnKc versus 1/T. The Kc value is determined by the following relation:

$$K_c = \frac{q_e}{C_e} \qquad \textbf{(3.19)}$$

Where q_e is the amount of dye/metal ion adsorbed (mg g^{-1}) onto the adsorbents at equilibrium and C_e is equilibrium dye/metal ion concentration (mg L^{-1}) in solution.

CHAPTER- IV

General characterization of Mentha Plant Ash (MPA)

4.1. Introduction

Adsorption is an efficient and effective method for the removal of dyes/heavy metals from aqueous solution and activated carbons derived from different waste biomass is one of the most studied adsorptive materials in wastewater treatment (Singh et al., 2003). The adsorption capacity of the various adsorbent materials mainly depends on its physico-chemical properties such as porosity, specific surface area, surface functional groups, organic and inorganic contents (Barbooti et al., 2004). The surface characteristics of adsorbent materials play a vital role in sorption processes and it is mainly dependent on the method of preparation and type of precursor used. Therefore, proper characterization of the adsorbents using suitable techniques is crucial to the adsorption and separation processes used to remove organic and inorganic contaminants from wastewater. During last few years, the surface chemistry of many adsorbent materials including biochar and activated carbon has been explored to interpret results of dyes and heavy metals adsorption (Al-Degs et al., 2003). The application of activated carbon as an adsorbent has been found more expensive in treatment of industrial wastewater, particularly for the removal of dyes and heavy metals. Due to low price and high efficiency, the usage of non-conventional adsorbents such as natural materials, bio-sorbents and waste materials from industry and agriculture have been preferred in adsorption of toxicants by earlier workers (Crini, 2006).

4.2. Materials and Methods

In the present study, Mentha Plant Ash (MPA), a waste byproduct of the mentha oil production, was collected from local mentha oil distillation units, Barabanki, Uttar Pradesh, India. The characterization of MPA as an adsorbent was carried out by using various instrumental techniques such as Scanning Electron Microscope (SEM), Energy

Dispersive X-Ray Spectroscopy (EDX), IR-Spectroscopy (FTIR), Thermo-gravimetric Analysis (TGA), Brunauer-Emmett-Teller (BET), Barret-Joyner-Halenda (BJH) method and zeta potential analyzer to study various physico-chemical characteristics of MPA as adsorbent for dyes and heavy metals. For general characterization of the MPA adsorbent, the detailed methodology including collection of MPA; chemicals and solutions; type of instruments used and samples preparation has been described earlier in Chapter-3- Materials and Methods.

4.3. Results and Discussions

4.3.1. SEM and EDX analysis

The surface morphology of adsorbent particles play a crucial role in the sorption of organic and inorganic contaminants from aqueous solutions. SEM image of MPA showed irregular surface and crushed ends with dawdle deposits on the surface of MPA particles. The surface morphology of MPA has been shown in Fig. 4.1.

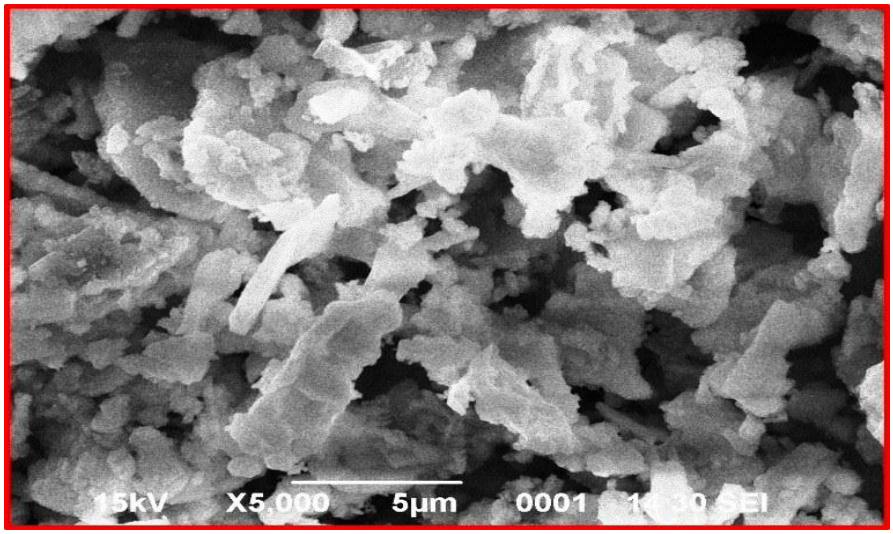

Fig. 4.1. SEM micrograph of MPA (Accelerating voltage = 15 kV; Magnification = 5000X).

Presence of small pores on the surface of MPA particles might be due to the volatilization and decomposition of various biomolecules present in the plant waste

material. Generally, the waste plant materials contain high content of volatile matter and low lignin content which directly affects the pore formation on the surface of adsorbent particles (Lehmann et al., 2011). The surface morphology of MPA particles became more complex and showed fibrous structures due to aggregation of mineral compounds at higher temperature (850ºC) (Yargicoglu et al., 2014). The fibrous structure of adsorbent particles might be developed from various cellulosic structures during combustion process as suggested by earlier workers (Fernandez et al., 2012). The volatization of organic matter during thermal change (450 – 800 ºC) may cause variation in particle surface, shrinking and splitting of adsorbent particles. Further results on EDX analysis (Table 4.1) of the MPA exhibited chemically rough surface of adsorbent particles due to presence of high content of clay minerals. The mineral composition of MPA (Fig. 4.2) showed major contribution of C, O, Mg, Cl, K, Si, Fe and Ca, which registered several fold increase in the mineral contents than that in earlier reported adsorbents (Lehmann et al., 2011).

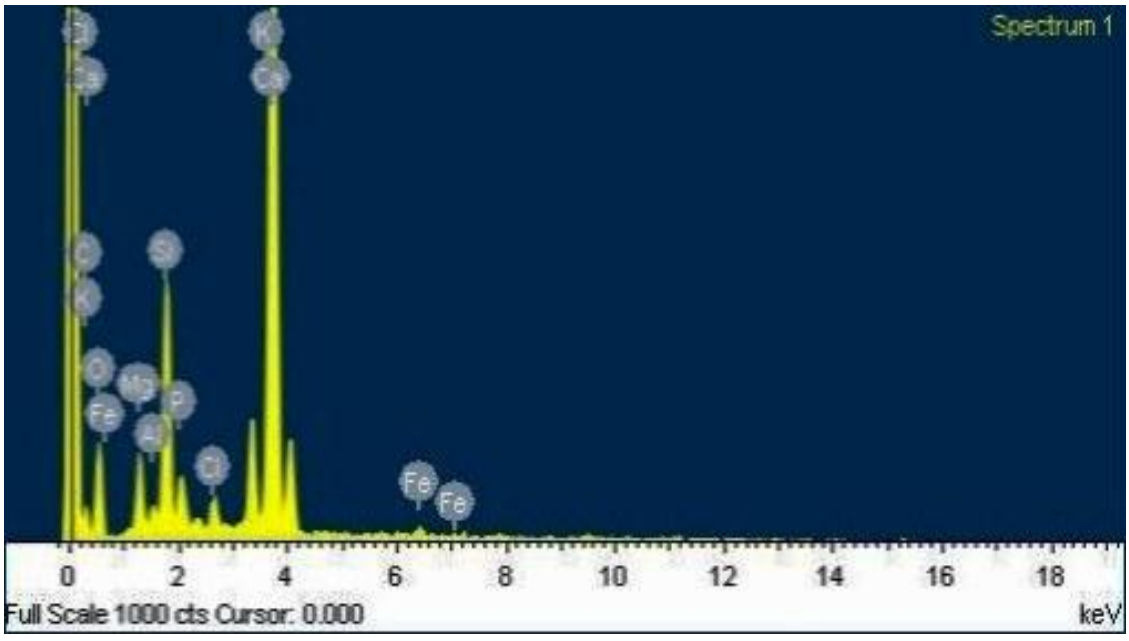

Fig. 4.2. EDX analysis showing mineral composition of MPA.

Table 4.1. Mineral composition of MPA (EDX analysis).

Elements	Percent (%) contribution	
	Weight %	**Atomic %**
C	18.93	31.85
O	32.53	41.08
Mg	2.5	2.08
Al	0.52	0.39
Si	6.7	4.82
P	1.63	1.06
Cl	1.09	0.62
K	3.98	2.06
Ca	31.02	15.64
Fe	1.11	0.4

4.3.2. BET specific surface area

The Brunauer-Emmett-Teller (BET) analysis of the N_2 adsorption-desorption isotherm provides valuable information about sorption process, specific surface area and porosity of the adsorbent material (Mall et al., 2006). Based on previous studies, all the N_2 adsorption/desorption isotherms would follow only one of the five basic types of adsorption isotherms (Types I to V) as suggested by earlier workers (Brunauer et al., 1940). The adsorbent materials are supposed to have certain porosity for a specific type of N_2 adsorption/desorption isotherm. The N_2 adsorption-desorption isotherms measured on MPA sample at temperature of 77 K has been shown in Fig. 4.3 (a). The shape of the isotherm matches the Type IV shape of adsorption isotherm (IUPAC classification), indicating a mesoporous structure of MPA adsorbent. The specific features of Type IV isotherm correspond with monolayer-multilayer adsorption and are indicative of relatively strong interaction between adsorbent particles and adsorbate molecules as suggested by earlier workers (Sing et al., 1985). The surface and other textural properties of MPA are listed in Table 4.2. In the present study, the BET specific

surface area of MPA adsorbent was found to be 7.169 m^2 g^{-1}. The small BET specific surface area of MPA might be due to filling of pores largely with resins and minerals, which interfere with diffusion of nitrogen molecules (Rawat and Singh, 2017). The total pore volume and average pore diameter of MPA were found to be 3.414 cm^3 g^{-1} and 12.915 nm, respectively.

Barret-Joyner-Halenda (BJH) method is a very common method for the determination of the mesopore size distribution of adsorbent particles. According to the International Union of Pure and Applied Chemistry (IUPAC), the pore size of adsorbent particles can be classified as macropores (d > 50 nm), meso-pores (2 < d < 50 nm) and microporous particles (diameter, d < 2 nm) (IUPAC, 1982). Further, microporous particles can be classified as super-micropores (0.7 < d < 2 nm) and ultra-micropores adsorbent particles (d < 0.7 nm). For a gas-phase sorption process, adsorbents consisting mainly of microporous particles as most of the gaseous contaminants vary from 0.4–0.9 nm in diameter, while in liquid-phase sorption process, adsorbents are preferred to have significantly more mesoporous structures because of the larger sizes of liquid molecules. The pore size distribution of MPA particles, as determined by BJH method, was found to be in the range of 3–25 nm indicating mesoporous material. The BJH plot measured on MPA at temperature of 77 K has been shown in Fig. 4.3 (b). A pore diameter in adsorbent particles between 2 to 50 nm indicates a mesoporous material (Sing et al., 1985). The results suggested that the adsorbent MPA is a mesoporous material. The International Union of Pure and Applied Chemistry (IUPAC) has classified the meso-pore diameter (d) ranging between 2 to 50 nm, micropores ranging < 2 nm and macropores ranging > 50 nm (Rawat and Singh, 2017).

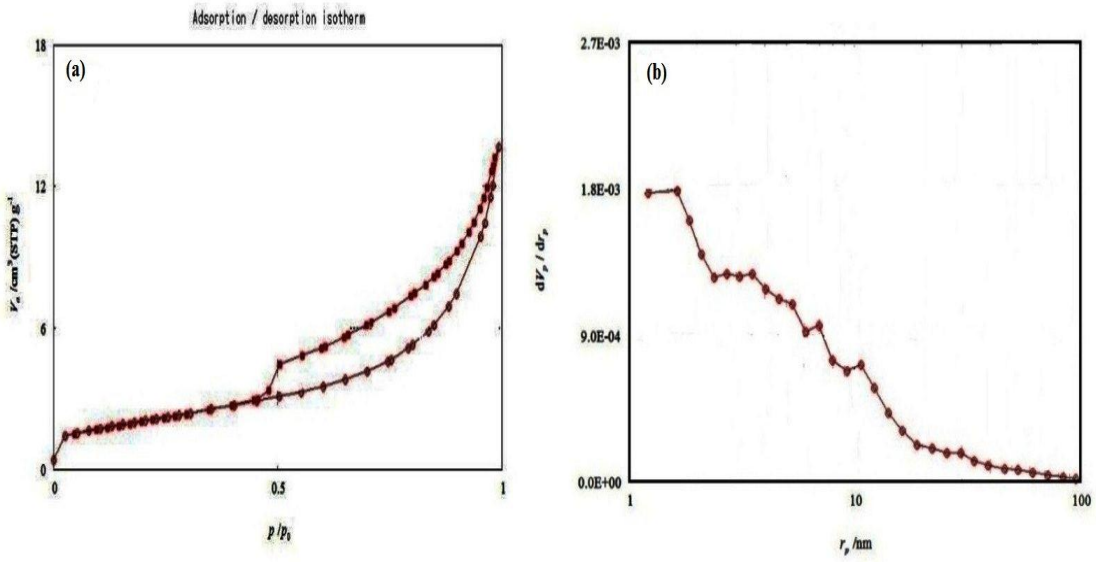

Fig. 4.3. (a) N_2 adsorption-desorption isotherm and (b) BJH plot measured on MPA at 77 K.

Table 4.2. Surface and other textural properties of MPA.

Property	**Magnitude**
Specific surface area (BET-plot; m^2g^{-1})	7.169
Total pore volume (BET-plot; cm^3g^{-1})	3.414
Average pore diameter (nm)	12.915
Pore area (BJH-plot; $m^2\ g^{-1}$)	7.258
Pore volume (BJH-plot; $cm^3\ g^{-1}$)	2.025

4.3.3. Thermo-gravimetric analysis (TGA)

Thermo-gravimetric analysis (TGA) was carried out to investigate the organic and inorganic contents by analyzing the thermal behavior of adsorbent (MPA). The recorded thermograms (TG) of MPA obtained by using Thermo-gravimetric Analyzer at different temperature ranges from 0 to 850ºC has been shown in Fig. 4.4.

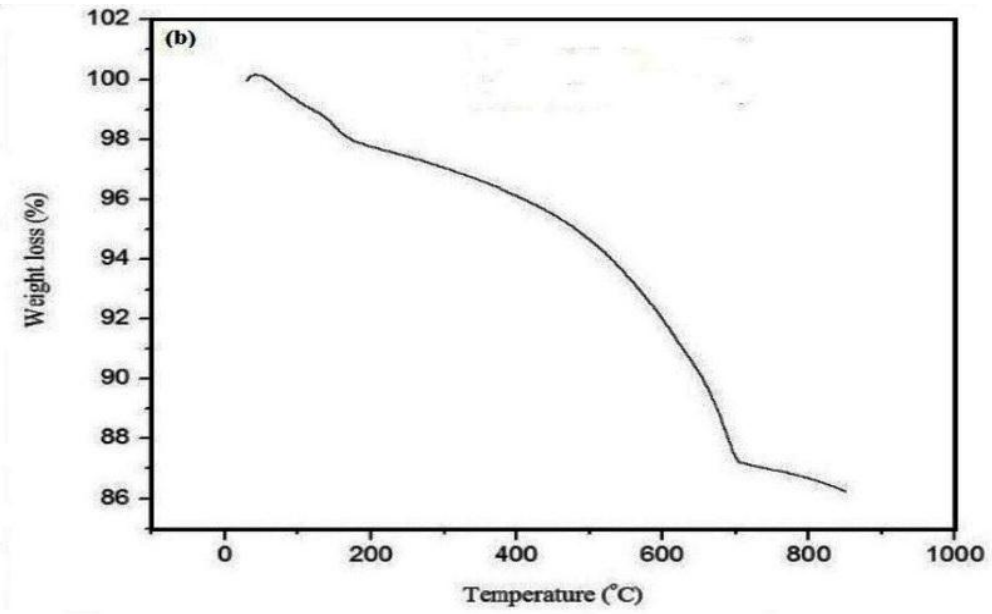

Fig. 4.4. Thermogram of MPA (Nitrogen flow = 100 mL/min; Heating rate = 10°C/min).

The TG analysis of MPA exhibited three main stages of weight loss in different temperature ranges (0 – 180ºC, 180 – 700ºC and 700 – 850ºC) during combustion of post-distillation mentha plant residues. The results showed that the first phase of weight loss in recorded thermogram of MPA corresponds to release of water molecules and low boiling volatile organic matter (Zhang et al., 2006; Liu et al., 2012). Approximately 3% of weight loss was recorded in first phase of TG analysis, indicating moisture content and low amount of volatile compounds present in the plant waste material. The second phase of weight loss at temperature range (180 – 700°C) might be related to the decomposition of hemicellulose (200 – 300°C), cellulose (300 – 400°C) and lignin (200 – 700°C) and its conversion into CO_2, CO and CH_4 (Xu and Chen, 2013). In second phase, approximately 10% of weight loss was recorded in thermogram of MPA (Chen and Chen, 2009; Kim et al., 2012; Xu and Chen, 2013). Further, the third phase of weight loss at temperature range 700 – 850°C was indicative of thermal decomposition of lignin (160 – 900°C) (Xu and Chen, 2013). The CO_2 evolution after thermal

decomposition of calcite ($CaCO_3$) resulting in material of greater thermal stability during the third phase of weight loss as suggested by earlier workers (Qi et al., 2010).

4.3.4. Powder X-Ray Diffraction (XRD) analysis

The XRD pattern of MPA adsorbent produced from mentha plant waste at about 800 – 900ºC of temperature is shown in Fig. 4.5. The presence of calcite, quartz, crystalline cellulose and dolomite were confirmed by their corresponding peaks represented as interplaner distance (*d*) in the XRD pattern of MPA (Fig. 4.5).

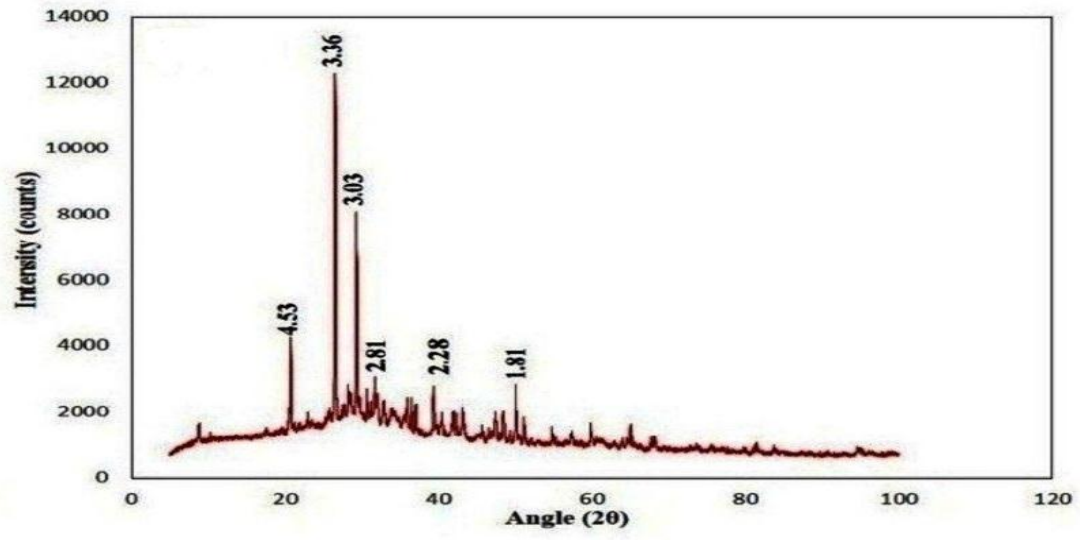

Fig. 4.5. X-ray diffraction pattern of MPA [Interplaner distance (*d*) values are given in Å].

The presence of quartz and crystalline cellulose were detected by peaks at 3.36 and 4.53 Å, respectively, whereas the existence of calcite was exhibited by peaks at 3.03, 1.81 and 2.28 Å in the XRD pattern of MPA (Yuan et al., 2011). Further, the presence of dolomite, CaMg $(CO_3)_2$ was detected by peak at 2.81 Å in the XRD spectra of adsorbent. The intense sharp peaks at 3.03 Å, 4.53 Å and 3.36 Å indicated well crystalline form of calcite, crystalline cellulose and quartz, respectively, and available in high content as compared with other minerals of MPA adsorbent (Yuan et al., 2011). A high peak intensity at 3.36, 4.53 and 3.03 Å in the XRD pattern of MPA, also

suggested that the quartz, crystalline cellulose and calcite content was found to increase with increase in temperature from 450 to 850ºC during combustion of post-distillation mentha plant residues. Further, the XRD pattern and a high carbonates content in adsorbent material suggested that different carbonates forms were the main alkaline constituents in the MPA adsorbent produced from mentha plant waste at the high temperature (800ºC) (Yuan et al., 2011).

4.3.5. Zeta potential analysis

The surface-potential of adsorbent (MPA) is an essential factor which affects the extent of dye/metal ion adsorption on the surface of adsorbent particles. In order to see the role of surface charge potential on adsorption of dyes and heavy metals, the zeta potential (ZP) of MPA adsorbent was recorded as a function of different pH in a buffered medium. The ZP values for the MPA powder ranged from –24.3 mV at pH 4.0 to – 40.1 mV at pH 10.0 (Fig. 4.6). The ZP value of MPA particles (Fig. 4.7) at neutral pH (7.0) was found to be –37.1 mV, indicating negatively charged surface of MPA particles. The results on zeta potential values of MPA particles at different pH condition (pH 4.0 to pH 10.0) indicated a highly negatively charged surface with little effect of pH condition. As the pH of ambient condition increases, the zeta potential of MPA became slightly more negative. A highly electronegative surface along with little effect of changing pH condition on the zeta potential suggested about larger contribution of salts and clay minerals in determining the zeta potential was suggested by earlier workers (Aksoy and Kaya, 2011). This could be the reason for high binding efficiency of MPA for cationic dyes (malachite green and methylene blue) and Cr(VI) metal ions (Bootharaju and Pradeep, 2013). Similar observations have been made by earlier workers on zeta potential of quartz powder with isoelectric point (iep) at around pH 2.0 and zeta potential ranging from –15 mV at pH 4.0 to –56 mV at pH 10.5 (Huang and

Fuerstenau, 2001). Johnson (1999) reported that the quartz has iep at pH below 2 and the zeta potential is about –50 mV at neutral pH and – 60 mV at pH 10 in the presence of 1×10^{-3} M KCl. In the present investigation, the iep of the used adsorbent (MPA) could not be found within the selected range of pH, but perhaps a low pH condition (below 3.0) might be more helpful in determination of iep of MPA adsorbent. However, hydrated ionic radius of minerals may also affect the zeta potential; the larger is the ionic radius and thicker the layer, the value of zeta potential shifts towards negative side as in the case of MPA adsorbent (Aksoy and Kaya, 2011).

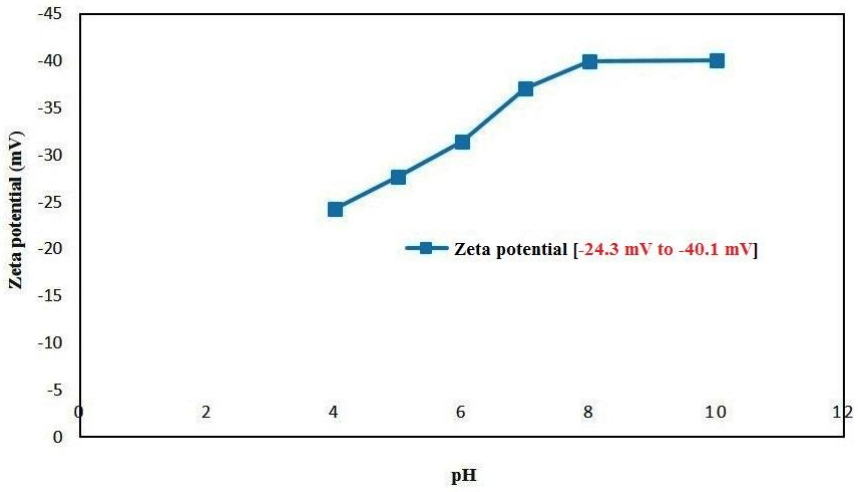

Fig. 4.6. Zeta potential values of MPA at different pH condition (pH 4.0 to 10.0).

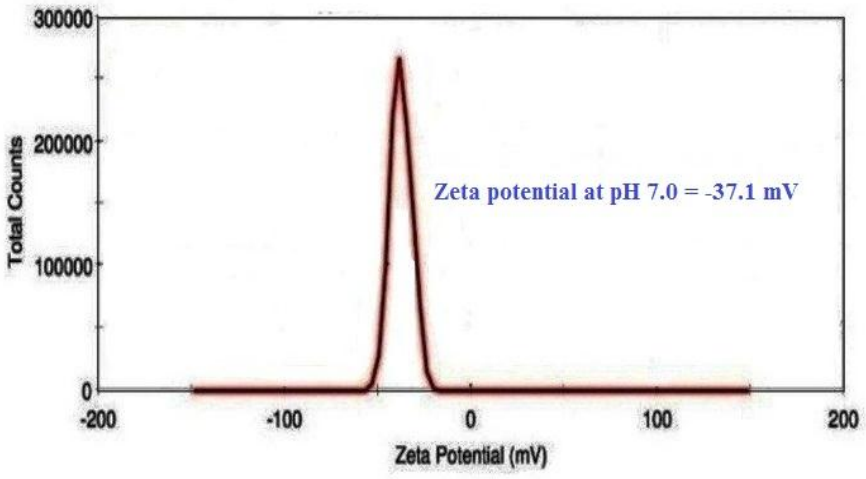

Fig. 4.7. Zeta potential curve measured on MPA at neutral pH condition (pH 7.0).

4.3.6. IR-spectroscopy (FTIR)

The FTIR spectra (4000 to 500 cm^{-1}) of MPA adsorbent (Fig. 4.8) before adsorption of cationic dyes and Cr(VI) was recorded to analyze the presence of several functional groups on the surface of MPA particles. The results displayed a number of oxygen containing functional groups present on the surface of adsorbent particles.

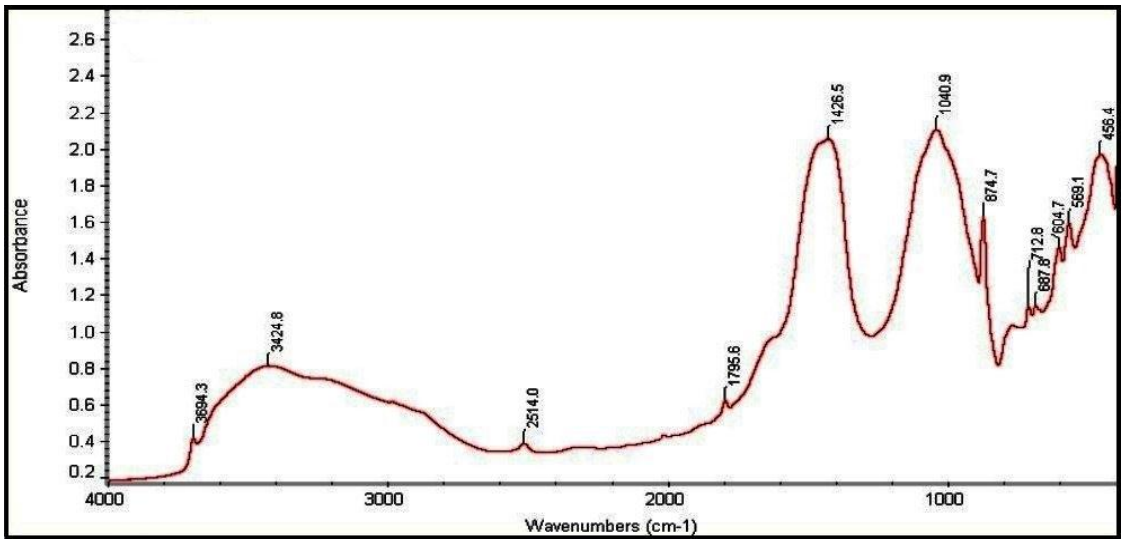

Fig. 4.8. IR-spectra (FTIR) of MPA before adsorption of cationic dyes and Cr(VI).

The IR absorption spectrum of MPA showed different IR peaks at wavenumbers 3694.3, 3424.8, 1795.6, 1426.5 and 1040 cm^{-1} which correspond to hydroxyl (–OH) and amine groups ($–NH_2$), acid chloride with C=O stretching of amines, C=O stretching of carboxyl groups and carbonyl groups, respectively (Mary et al., 2016; Mohan, 2005; Ding et al., 2016). These surface functional moieties, not only contributing to negative surface potential of MPA particles but may play a crucial role in the adsorption/reduction of cationic dyes and Cr(VI) metal ions. The oxygen-containing functional groups are actively involved in the binding of cationic dyes and Cr(VI) as suggested by earlier workers (Guo et al., 2017). The band at 1426.5 cm^{-1} and 1040.9 cm^{-1} are characteristic of C–O stretching and vibrations of lignin and carbohydrates as

reported earlier in wood samples (Poletto et al., 2012). Further, it has been suggested that the IR absorption peak at wavenumber 1040.9 cm^{-1} pertains to C–O stretching in carbohydrates (Reznik et al., 2008). The observed IR peaks and their corresponding functional groups of MPA adsorbent are listed in Table 4.3. The IR peaks around at 674 – 685.6 cm^{-1}, 500 – 600 cm^{-1} and 675 – 1000 cm^{-1}, assigned to strong bend C–H phenyl rings, alkyl halide (–C–Br stretch) and alkene (=C–H bending), respectively (Akerholm et al., 2004). The overall results on IR spectra of MPA exhibit that hydroxyl, ester, amine, phenyl, carboxyl and carbonyl groups are the surface functional moieties, not only contributing to negative charge on surface of MPA particles, but may be actively involved in the binding of cationic dyes and Cr(VI) as well as its reduction through electron transfer process.

Table 4.3. Observed frequencies (cm^{-1}) and surface functional groups of MPA adsorbent.

Frequency range (cm^{-1})	**Observed peaks (cm^{-1})**	**Band assignment**
3800–3550	3694.3	O–H stretching of alcohol (Mohrig et al., 2006)
3550–3250	3424.8	N–H stretching of amine (Farhan, 2015)
3200–2500	2514.0	O–H stretching of carboxylic acid (Mohan, 2005)
1815–1770	1795.6	C=O stretching of acid chloride (Mohan, 2005)
1435–1405	1426.5	C–O stretching of carbonyl group (Poletto et al., 2012)
1300–1000	1040.9	C–O stretching of ester (Mohrig et al., 2006)
920–830	874.7	CO_3^{2-} group (Smidt and Schwanninger, 2005)
770–620	712.8	CO_3^{2-} group (Smidt and Schwanninger, 2005)
675–1000	874.7	Alkene (= C–H) (Akerholm et al., 2004)
500–600	569.1	Alkyl halide (–C–Cl) (Akerholm et al., 2004)

CHAPTER-V

Removal of cationic dyes by Mentha Plant Ash (MPA)

5.1. Introduction

Food industries, printing, textiles, dyeing and dye stuff manufacturing are the main sources of dye-containing wastewater discharges into natural water bodies (Mittal et al., 2010). Large-scale production and application of organic dyes can potentially cause serious environmental and human health problems as many dyes used in industrial processes are quite stable against photo-bleaching and are also resistant to aerobic digestion because of their structural complexity and large molecular size (Dincer et al., 2007). In addition, many dyes are highly visible in water at low concentrations (less than 1 mg/L for some dyes), which is enough to present an aesthetic problem (Low et al. 2012). The malachite green (MG) and methylene blue (MB) dyes are basic cationic dyes mostly used in the textile industry, manufacturing of paints, printing inks, leather, wool, jute and silk due to its low cost, easy availability, efficacy and lack of a proper alternatives (Zhang et al., 2008; Chakraborty et al., 2011). The MG and MB dye have been considered as a persistent recalcitrant organic molecule in the environment as it is poorly metabolized by the microbes (Chakraborty et al., 2011; Shayesteh et al., 2015). In addition to it, the MG and MB dye are found to be relatively more carcinogenic, genotoxic, mutagenic, and teratogenic as compared to anionic dyes due to its aromatic ring with delocalized electrons (Shayesteh et al., 2015). If these dyes are absorbed in higher amounts through the skin, it can cause skin irritation, digestive tract irritation, respiratory and kidney failures (Ahmad, 2009; Shayesteh et al., 2015). Therefore, the complete elimination of cationic dyes from the dye-laden industrial effluents and other aqueous solutions is most desirable before its discharge in water bodies. Several physico-chemical and biological methods have been employed to remove the dyes from wastewater (Lee et al., 2007). Activated carbon has good adsorption capacity but it is considered an expensive adsorbent. This has led many workers to search for cheap and

efficient alternative adsorbents. A number of non-conventional and low cost agro-wastes like palm ash, bottom ash, fly ash, bagasse fly ash and rice husk etc. (Ahmad et al., 2007; Dincer et al., 2007; Janos et al., 2003; Gupta et al., 2003; Malik and Saha 2003) have been tried for the removal of dyes from their aqueous solutions.

Since India is the major producer of mentha (mint) waste in the world followed by China and Brazil, it produces mentha crop waste to the tune of approximately 1.8 to 2.0 tonnes $acre^{-1}yr^{-1}$ (Singh et al., 2010). Dried mentha plant waste is often used as fuel for steam distillation of mentha oil or else the mentha plant residues are left in the field with no subsequent application. The resulting plant ash is left behind as by-product with no subsequent application. *Mentha Piperita* plant ash (MPA) is an unattended waste byproduct of Mentha distillation industry and it is easily available in plenty in the vicinity of the industrial plant. Thus, MPA with no additional cost and pretreatmnent can be applied for removal of cationic dyes (MG and MB) as it has highly negatively charged surface. The characteristic features of MPA was determined which supported the sorption coupled electrochemical reduction of cationic dyes. The physico-chemical nature of adsorption and recovery of the dyes by using suitable desorbing agents are the additional reasons for the selection of this material (MPA).

Therefore, the main objective of present study was to evaluate the sorption and reduction potential of MPA as a low price efficient adsorbent for the removal of cationic dyes (MG and MB) from aqueous solutions.

5.2. Materials and Methods

Batch adsorption experiments were conducted as a function of contact time, adsorbent doses, pH, initial dye concentration and temperature to investigate the adsorption potential of MPA in the removal of basic cationic dyes. The adsorbent material (MPA) was characterized by using various instrumental techniques (FTIR, SEM, EDX, BET,

TGA, and XRD) to investigate the various physicochemical characteristics of MPA as described earlier. Further, Cyclic Voltammetry analysis of MPA after adsorption of cationic dyes (MG and MB) was carried out to analyze surface adsorption coupled with reductive electron transfer process. The surface adsorption coupled with reduction of cationic dyes was particularly investigated in the present study. Adsorption kinetics (Pseuo-first order, Pseudo-second order kinetic model, Intra-particle diffusion model) and adsorption isotherms (Langmuir and Freundlich) were applied on time-dependent experimental data to find the best fitted kinetic and adsorption model for the sorption of cationic dyes onto MPA. For removal of the cationic dyes by MPA, the detailed methodology including chemicals and solutions; preparation and characterization of MPA; adsorption/desorption experiments, equilibrium, kinetic and thermodynamic studies have been described earlier in Chapter-3-Materials and Methods.

A. Removal of malachite green (MG) dye by Mentha Plant Ash (MPA)

5.3. Results and Discussions

5.3.1. IR-spectroscopy (FTIR) of MPA before and after adsorption of MG dye

The FTIR spectra (Fig. 5.1) of the adsorbent (MPA) before and after adsorption of MG dye was obtained between 4000 to 500 cm^{-1} to study the surface characteristics of adsorbent. The recorded IR spectrum of dye loaded MPA sample showed bending and stretching vibrations of different functional groups which might be involved in the adsorption process of MG as given in Table 5.1. A large number peaks indicating the presence of varied functional groups on the adsorption surface of MPA particles might be responsible for the electronegative nature of adsorption surface. The changes in IR absorption peaks appearing at 3424.8, 2514.0 and 1795.6 cm^{-1} assigned to N–H stretching of amine, O–H stretching of carboxylic acid and C=O stretching of acid

chloride, indicated the role played by these functional groups in dye binding on the MPA surface (Farhan, 2015; Mohan, 2005).

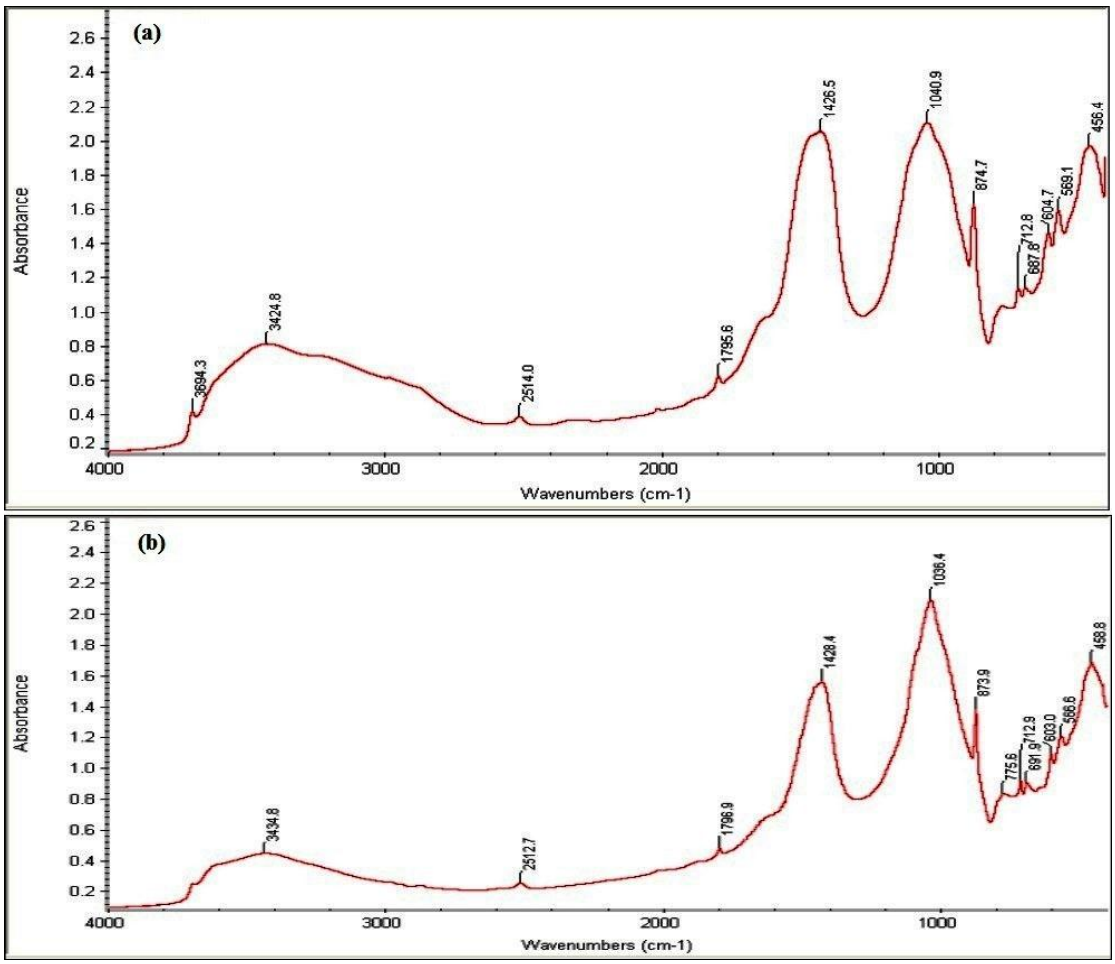

Fig. 5.1. FTIR (Mid) stack image of MPA (a) before and (b) after adsorption of MG dye at pH 6.0.

The results on IR absorption peak of MPA due to the presence of O–H stretching of alcohol after adsorption of MG dye and a new IR peak (755.6 cm^{-1}) appeared due to the aromatic –CH stretching vibrations (Ramola et al., 2014). The IR peaks at wavenumber 3694.3 cm^{-1} assigned to O–H stretching of alcohol (Mohrig et al., 2006) and completely disappeared after the treatment of MPA adsorbent due to the binding of MG dye molecules with hydroxyl group. The changes in IR peaks at wavenumber of 1426.5, 1040.9 and 874.7 cm^{-1} assigned to C–O stretching of carbonyl group, C–O stretching of ester and CO_3^{2-} group, respectively, which involved in the adsorption of MG dye onto MPA (Poletto et al., 2012; Mohrig et al., 2006; Smidt and Schwanninger, 2005).

Further, the IR peak at wavenumber 712.8 and 569.1 cm^{-1} assigned to CO_3^{2-} group and Alkyl halide (–C–Cl) stretch, respectively, which might be involved in surface adsorption due to the C=O stretching and bending (Smidt and Schwanninger, 2005; Akerholm et al., 2004). The observed IR peaks indicate the functional groups on the surfaces of MPA adsorbent which may drift from the their original wavelength due to different modifications of heat treatment during ash generation which might be responsible for eliminating or rearranging functional groups on MPA surface.

Table 5.1. FTIR Wavenumber (cm^{-1}) of MPA before and after adsorption of MG dye.

Observed frequency in (cm^{-1}) of MPA adsorbent			
Frequency range in cm^{-1}	Before adsorption of MG dye	After adsorption of MG dye	Band assignment
3800–3550	3694.3	0	O–H group (Mohrig et al., 2006)
3550–3250	3424.8	3434.8	N–H stretch of amine (Farhan, 2015)
3200–2500	2514.0	2512.7	O–H of carboxylic group (Mohan, 2005)
1815–1770	1795.6	1796.9	C=O stretch of acid chloride (Mohan, 2005)
1435 –1405	1426.5	1428.4	C–O of carbonyl group (Poletto et al., 2012)
1300 –1000	1040.9	1036.4	C–O stretching of ester (Mohrig et al., 2006)
875 – 602	874.7	873.9	$–CO_3^{2-}$ (Smidt and Schwanninger, 2005)
794 – 752	0	755.6	Aromatic –CH stretch (Ramola et al., 2014)
770 – 620	712.8	712.9	$–CO_3^{2-}$ (Smidt and Schwanninger, 2005)
500 – 600	569.1	566.6	–C–Cl group (Akerholm et al., 2004)

5.3.2. Cyclic Voltammetric analysis of MG dye in presence of MPA

Cyclic voltammetry analysis was carried out to see whether a rapid decolourization of MG dye in the presence of MPA was simply adsorption of dye or something else. The cyclic voltammetry test was performed on the MG dye solution obtained after treatment of MPA adsorbent. The cyclic voltammogram of MG dye (Fig. 5.2) in the electrolytic solution showed a well-defined redox couple.

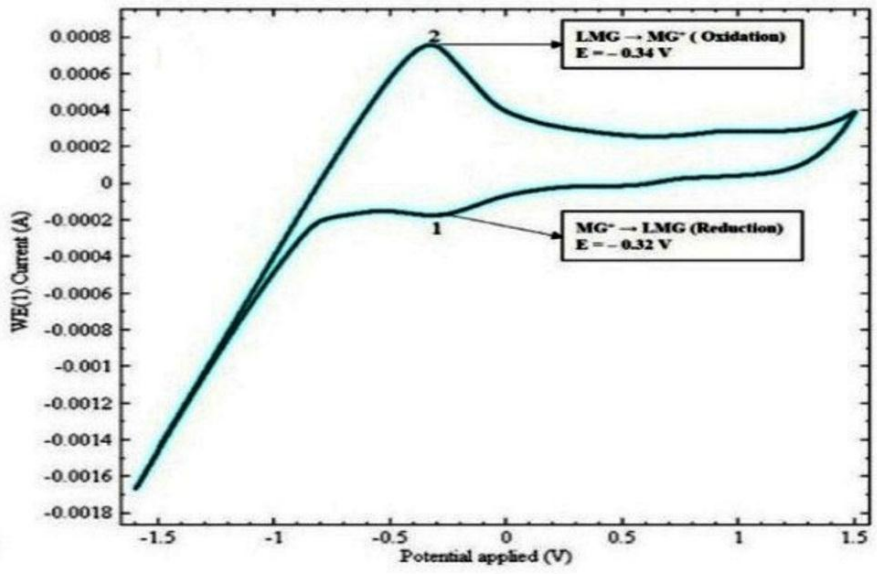

Fig. 5.2. Cyclic voltammogram of MG dye treated with MPA adsorbent [Potential range from -1.5V to +1.5 V (Ag/AgCl); Scan rate 100 m/V].

Results of the cyclic voltammetry (CV) test showed cathodic and anodic activities of MG dye in aqueous solution, indicating reduction of MG dye by MPA particles involves electron transfer process (Ngamukot et al., 2006). In the cyclic voltammogram of MG dye, the peak 1 (cathodic) appearing at approximately –0.32V was assigned to the reduction of MG^+ to neutral leuco malachite green (LMG) by one electron transfer reaction (Ngamukot et al., 2006), where peak 2 (anodic) at –0.34V might be related to oxidation of neutral LMG to MG^+. The coupled redox reaction for MG dye in the CV test suggested that MG^+ cations adsorbed on the surface of MPA particles were changed to LMG through a reversible electron transfer reaction. The several minerals and

surface active ligands in MPA might be contributing as electron donors for adsorbent mediated reduction of MG dye. Earlier, workers have also demonstrated a similar electron transfer process involved in the reduction of MG dye (Ngamukot et al., 2006).

5.3.3. Factors affecting adsorption of MG dye

5.3.3.1. Effect of contact time

The dye uptake was studied as a function of time using initial dye concentration of 50 mg L^{-1}, adsorbent dosage of 0.1g/100 mL. The result (Fig. 5.3 (a)) showed that the dye binding by MPA initially occurred at a faster rate, (7.18 mg $g^{-1}min^{-1}$) up to first five minutes of incubation and resulted into removal of 72.86 % dye within 5 minutes. Thereafter, dye adsorption continued till the first 45 min at a slower rate, perhaps due to non-availability of adsorption sites on the surface of adsorbent. The relative increase in the removal of dye after 45 minutes was insignificant. A rapid rate of dye adsorption at the initial contact time could be attributed to availability of large number of adsorbent sites. Earlier, it has been demonstrated that slow adsorption rate after initial rapid phase could be due to saturation of available adsorption sites and decrease in the number of adsorption sites on the adsorbent (Saha et al., 2010; Chakraborty et al., 2011). Similar pattern of observations on time-dependent dye removal were reported by earlier workers for the removal of cationic MG dye by pumice stone and clayey soil of Indian origin as a low cost adsorbents (Shayesteh et al., 2016; Saha et al., 2010). Chakraborty et al. (2011) also reported similar results for the removal of cationic crystal violet dye by using NaOH-modified rice husk as adsorbent.

5.3.3.2. Effect of adsorbent dose

The adsorption capacity is greatly influenced by the dose of MPA (adsorbent) in removal of MG dye from aqueous solution. The amount of dye adsorbed by MPA was studied as a function of adsorbent doses (0.05 to 0.3g/100 mL) at 50 mg L^{-1} dye

concentration for 45 min. Results (Fig. 5.3 (b)) showed that the dye uptake increased from 28.81 to 43.11 mg g^{-1} with increase in adsorbent dose from 0.05 to 0.3g/100 mL. A rapid phase of dose-dependent increase in dye removal occurred up to 0.1 g/100 mL dose of MPA and this was followed a sluggish phase of dye removal between 0.1 to 0.3 g/100 mL of dose of adsorbent. The maximum dye removal, at an adsorbent dose of 0.1 g/100 mL, was found to be 36.86 mg g^{-1}. As the number of available adsorption sites increased in a dose-dependent manner, the rate of dye removal also increased (Ahmad, 2009). A sluggish increase in dye binding at higher doses of adsorbent (0.1 to 0.3 g/100 mL) may be due to less availability of dye molecules per unit concentration of adsorbent. Otherwise it may state that the clustering of adsorbent particles per unit volume might be hindering the free mobility of the dye molecules approaching to the binding sites on the surface of adsorbent (Garg et al., 2003). Similar observations on dose-dependent dye removal were reported by earlier workers in the removal of cystal violet dye by the coniferous pinus bark powder (CPBP) and treated saw dust as adsorbents (Ahmad, 2009; Garg et al., 2003).

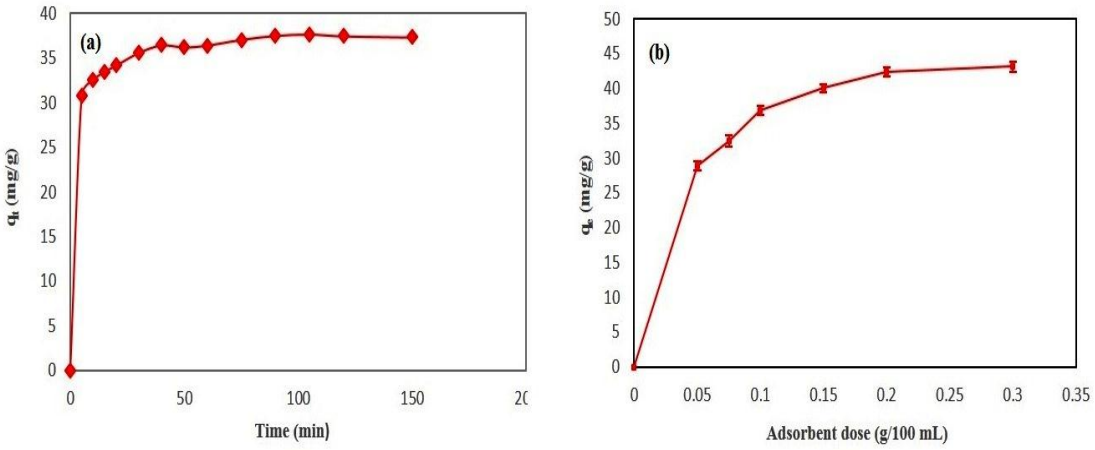

Fig. 5.3. Effect of (a) contact time and (b) adsorbent dosage on MG dye uptake (mg g^{-1}) by MPA [Dye concentration 50 mg/L, time 150 min, adsorbent concentration 0.1 g/100 mL, pH 6.0, temperature 30° C].

5.3.3.3. Effect of pH

The pH of the dye solution can influence the surface potential of the adsorbent as well as the chemistry of adsorbate molecules (Shayesteh et al., 2015). In the present study, the effect of pH condition (4.0 – 10.0) on the sorption of MG dye by MPA was studied using different inorganic buffers (20 mM), constant dye concentration (50 mg L^{-1}) and dose of adsorbent (0.1 g/100 mL). The results (Fig. 5.4 (a)) showed that the amount of dye adsorbed at equilibrium (q_e) increased from 32.41 to 46.21 mg g^{-1} with increase in pH from 4.0 to 10.0, respectively. The results showed least adsorption of MG dye at acidic pH 4.0 perhaps due to reduction in the electronegative moieties on the adsorbent surface (MPA). Besides, protonation of the MG dye molecules at acidic pH might be inhibiting the active binding between the adsorbent and dye molecules. A high rate of dye removal at pH 10.0 could be due to increase in the negatively charged moieties on the surface of the adsorbent, which facilitate the binding of cationic MG dye. An increase in electrostatic interaction between the dye molecule and surface binding ligands is responsible for an initial fast rate of dye adsorption (Mittal et al., 2010). Earlier, workers have also demonstrated a high rate of MG dye removal at pH 10.0 by spent tea active carbon (Akar et al., 2013).

5.3.3.4. Effect of initial dye concentration

The effect of initial dye concentration on the adsorption capacity of MPA depends on the availability of dye molecules and surface binding sites of MPA particles. The extent of dye removal is greatly influenced by initial dye concentration in aqueous solution. In the present study, the effect of different initial concentration of MG (20 to 100 mg L^{-1}) was studied on the adsorption of MG dye for 45 min at fixed adsorbent dosage (0.1g/100 mL) at room temperature and pH 6.0. The results (Fig. 5.4(b)) showed initially a very rapid process upto 5 min, followed by slowing down of the process with increase in the contact time up to 45 min, perhaps due to non-availability of adsorption

sites on the surface of adsorbent (Saha et al., 2010). Further removal of dye after 45 minutes was found to be insignificant. The equilibrium stage and maximum uptake of total amount of MG dye was found to occur within 45 minutes at different concentration of MG dye. A rapid rate of dye adsorption at the initial contact time could be attributed to availability of a large number of adsorption sites. The rate of dye binding increased in a concentration-dependent manner and the saturation concentration of dye at equilibrium (q_e) was found to increase from 14.73 to 73.03 mg g^{-1} with increase in the initial dye concentration from 20 to 100 mg L^{-1}. An increase in adsorption capacity of MPA with increase in MG dye concentrations, might be due to relatively higher rate of mass transfer (Bulut and Aydin, 2006). But the sluggish increase in the rate of dye adsorption at higher concentration could be attributed to a limiting dose of adsorbent (Garg et al., 2003).

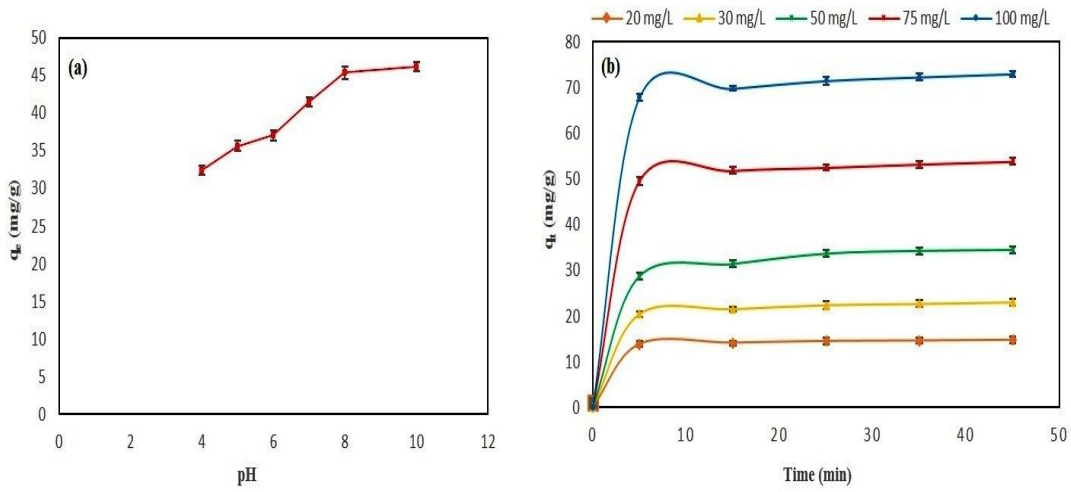

Fig. 5.4. Effect of (a) pH and (b) initial dye concentration on the amount adsorbed (mg g-1) of MG dye by MPA [Dye concentration 50 mg/L, adsorbent concentration 0.1 g/100 mL, time 45 min, temperature 30º C].

The rate of dye binding increased in a concentration dependent manner, exhibiting rate saturation 100 mg L^{-1} concentration of MG dye. The increase in initial dye concentration provided rapid increase as it overcame all mass transfer resistances of the dye between the aqueous and solid phase (Hameed et al., 2008). But the rate saturation

at higher concentration of dye was due to sorbent as rate limiting factor. Similar results were reported by other investigators for the removal of malachite green (Garg et al., 2003).

5.3.4. Adsorption isotherms

The Langmuir constants (q_{max} and b) and Freundlich constants (K_F and n) were calculated from the slope and intercept of the linear plots of $1/q_e$ versus $1/C_e$ (Fig. 5.5 (a)) and log q_e vs. log C_e (Fig. 5.5 (b)) respectively and presented in Table 5.2 along with the correlation coefficient R^2. The high value of correlation coefficient R^2 (0.989) showed the applicability of Langmuir isotherm model for equilibrium adsorption and fitted well to the experimental data for the sorption of MG onto MPA. The maximum monolayer sorption capacity (q_{max}) according to Langmuir isotherm model was found to be 322.58 mg g^{-1} at room temperature. A comparison of adsorption capacities of previously reported adsorbents with MPA (Table 5.3) showed higher adsorption capacity of MPA than other reported adsorbents.

Comparatively low value of correlation coefficient R^2 (0.981) showed poor agreement of experimental data with Freundlich isotherm model. The value of n (1.067) indicated favorable adsorption process (Chakraborty et al., 2012). It has been suggested that the value of constant n between 1 and 10 represent beneficial sorption process (Ho and Mckay, 1998). The value of K_F was found to be 0.327, representing the adsorption coefficient for dye binding.

The calculated value of separation factor (R_L) was used to express the shape of Langmuir isotherm. The value of separation factor (R_L) described the trend of the adsorption process, which is either unfavorable ($R_L > 1$), favorable ($0 < R_L < 1$), linear ($R_L = 1$) or irreversible ($R_L = 0$) (Ma et al., 2015). The values of R_L (Table 5.4) were in the range of 0.98 – 0.91 at different concentration of MG (20 to 100 mg g^{-1}) at room

temperature, which indicated favorable adsorption of MG dye onto MPA. The value of R_L between 0 and 1was indicative of favorable adsorption with greater affinity of MPA particles towards adsorbate molecules (Ma et al., 2015; Hameed et al., 2008).

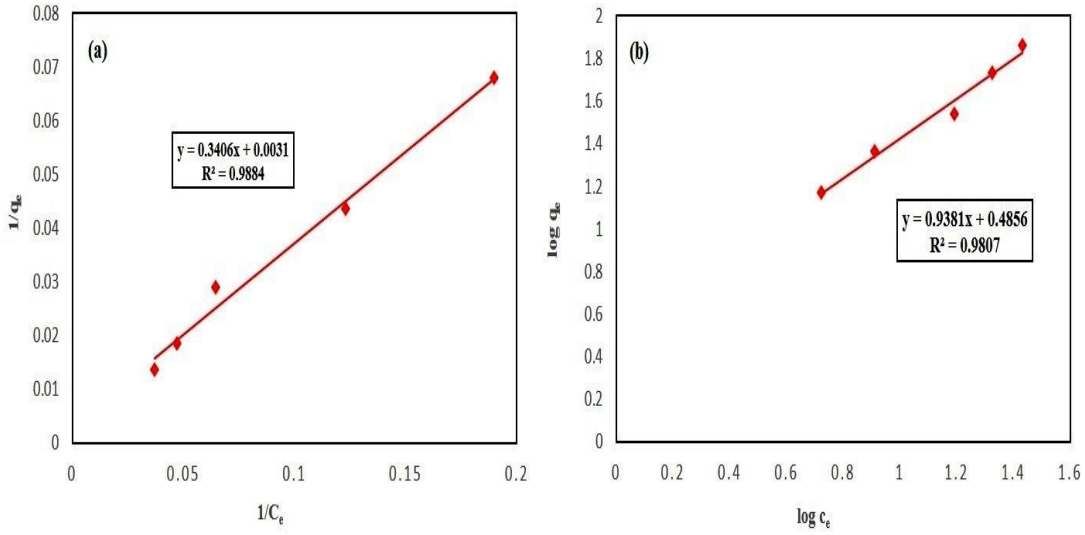

Fig. 5.5. Adsorption isotherms (a) Langmuir and (b) Freundlich equilibrium model for the sorption process of MG dye onto MPA [Dye concentration 20 – 100 mg/L, adsorbent concentration 0.1 g/100 mL, pH 6.0, time 45 min, temperature 30º C].

Table 5.2. Values of isotherm constants for the sorption of MG dye onto MPA adsorbent.

Langmuir constants			**Freundlich constants**		
q_m (mg g^{-1})	b (L mg^{-1})	R^2	Adsorption intensity (n)	Adsorption coefficient K_F (mg/g)	R^2
322.58	0.00106	0.989	1.066	0.3269	0.981

Table 5.3. Comparison of adsorption capacity of MPA with other reported agro and plant wastes based adsorbents for the sorption of MG dye.

Adsorbents	q_{max} (mg/g)	pH	Temp (K)	References
Potato leaves	33.3	7	303	(Gupta et al., 2011)
Potato peel	32.39	4	298	(Guechi and Hamdaoui, 2011)
Ginger waste	84	-	-	(Ahmad and Kumar, 2010)
Anona squamosa seed	25.91	6	300	(Santhi et al., 2011)
Oil palm trunk fibre	149	-	-	(Hameed and El-Khaiary, 2008)
Platanus vulgaris leaves	85.47	-	-	(Hamdaouia et al., 2008)
Chlorella biomass	18.4	7	298	(Tsai and Chen, 2010)
Borassus bark carbon	20.7	6	303	(Arivoli et al., 2009)
Tamarind fruit shell	1.95	5	303	(Saha et al., 2010)
Mentha Plant Ash (MPA)	322.58	6	303	This study

Table 5.4. Separation factor (R_L) at different dye concentration for MPA.

Initial concentration (mg L^{-1})	Seperation factor (R_L)
20	0.98
30	0.97
50	0.95
75	0.93
100	0.91

5.3.5. Adsorption kinetics

The Lagergren's first order rate constants k_1 and q_e were calculated from the slope and intercept of the plot between log ($q_e - q_t$) versus t (Fig. 5.6 (a)) and listed in Table 5.5

along with the correlation coefficient (R^2). The values of the correlation coefficients (R^2< 0.99) indicated that pseudo-first order kinetic model did not fit in well with the experimental data. It was found that calculated q_e values were far apart from the experimental q_e values. These results suggested that pseudo-first order kinetic model was not a suitable model to describe the adsorption process of MG onto MPA (Wang et al., 2010).

The value of Pseudo-second order constant k_2 and q_e were calculated from the slope and intercept of the plot t/q_t vs. t (Fig. 5.6 (b)) and presented in Table 5.5 along with their correlation coefficients. The comparatively high values of correlation coefficients (R^2>0.99) at different concentration of dye were much closer to unity, and calculated q_e values were also fairly closer to experimental value of q_e. These results indicated that kinetic data fitted very well to the pseudo-second order kinetic model at room temperature. Similar phenomenon were reported in sorption of basic dye onto activated carbon prepared from rattan saw dust (Hameed et al., 2007).

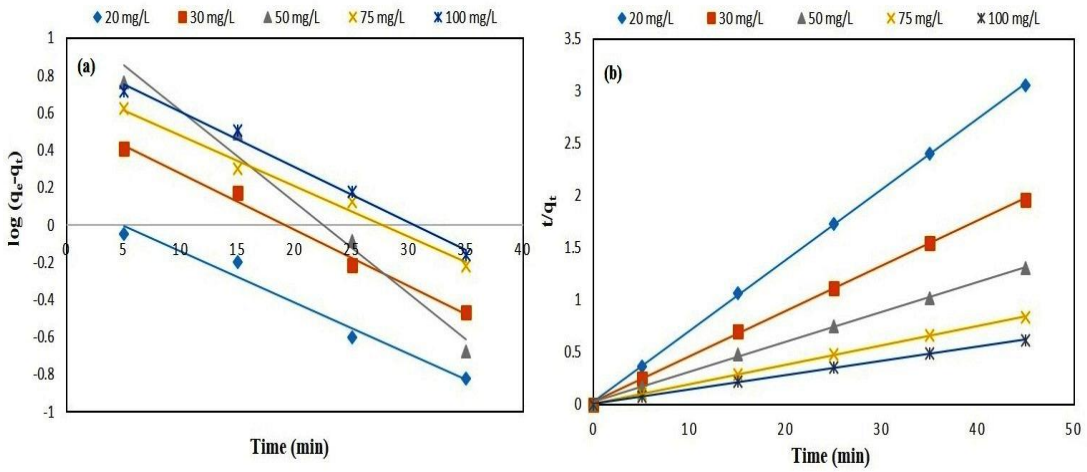

Fig. 5.6. Adsorption kinetics (a) Pseudo-first order and (b) Pseudo-second order kinetic model for the sorption of MG dye onto MPA [pH 6.0, adsorbent concentration 0.1g/100 mL, Time 45 min, dye concentration 20 – 100 mg/L, temperature 30º C].

The rate constant K_{id} and intercept C were evaluated from the slope and intercept of the plot of q_t versus $t^{1/2}$ (Weber and Morris, 1962). The plot of q_t versus $t^{1/2}$ (Fig. 5.7 (a))

showed linear regression and passes through the origin at each concentration, indicated that intra particle diffusion could be the rate controlling step. The calculated parameters of intra-particle diffusion model are presented in Table 5.6. The intercept C of the linear plot reflects boundary layer diffusion. The larger the value of C, greater the contribution of the surface sorption as rate controlling step (Hameed et al., 2008). When the linear plot at every concentration did not pass over the origin, this was the indicative of some degree of involvement of boundary layer in controlling diffusion, not only intra-particle diffusion (Alzaydien, 2009; Hameed et al., 2008). A high value of initial adsorption rate *h* (200.04 mg/g min) for MPA at rate saturating concentration of dye (100 mg L^{-1}) indicated that the sorption of MG dye onto MPA might be carried out through surface interchange reactions until the surface functional sites were occupied (Ma et al., 2015). The *h* value increased from 45.05 to 200.04 mg/g min with increase in the initial concentration of MG dye (Table 5.6), perhaps it would be due to increase in dye binding with increasing concentration of dye (Hameed et al., 2008; Kumar, 2006).

Table 5.5. Kinetic parameters at different dye concentration in the sorption of MG dye onto MPA.

Conc (mg/L)	**Exp. q_e (mg/g)**	**First-order kinetics**			**Second order kinetics**		
		k_1 (1/min)	Cal. q_e (mg/g)	R^2	k_2 (mg/g min)	Cal. q_e (mg/g)	R^2
20	14.73	0.064	1.35	0.973	0.208	14.75	0 .999
30	22.99	0.069	3.78	0.991	0.078	23.1	0.999
50	34.49	0.113	12.59	0.975	0.035	34.97	0.999
75	53.83	0.063	5.63	0.986	0.051	53.77	0.999
100	73.03	0.069	7.94	0.989	0.038	73	0.999

Table 5.6. The calculated parameters of intra-particle diffusion model at different dye concentration in removal of MG dye by MPA.

Intra-particle diffusion model			
h (mg/g min)	K_{id} (mg/g $min^{1/2}$)	C	R^2
45.05	0.21	13.36	0.979
41.35	0.58	19.25	0.979
42.57	1.36	26.09	0.945
147.1	0.91	47.88	0.973
200.04	1.19	65.3	0.991

5.3.6. Activation energy

The activation energy for the surface adsorption of MG dye onto MPA was calculated from the slope of Arrheniums plot of lnk vs. 1/T (Fig. 5.7 (b)). The activation energy (*Ea*) involved in the surface binding of MPA was calculated as 1.24 kJ mol^{-1}, which confirmed the sorption process was physisorption as well as non-activated chemisorption. In physisorption, the activation energy is usually not more than 4.2 kJ mol^{-1} since the forces involved in physi-sorption are weakened at the equilibrium and sorption is rapidly attained because the energy requirements is small (Chowdhury and Saha, 2010). In chemisorption, activation energy is of the same magnitude as the heat of chemical reactions. A small value of *Ea* indicated non-activated chemisorption which occurs very rapidly (Chowdhury and Saha, 2010). Earlier, it has been demonstrated that adsorption of dye molecules and toxic heavy metal ions onto various low cost adsorbents is attributable to a physico-chemical adsorption process (Chowdhury and Saha, 2010).

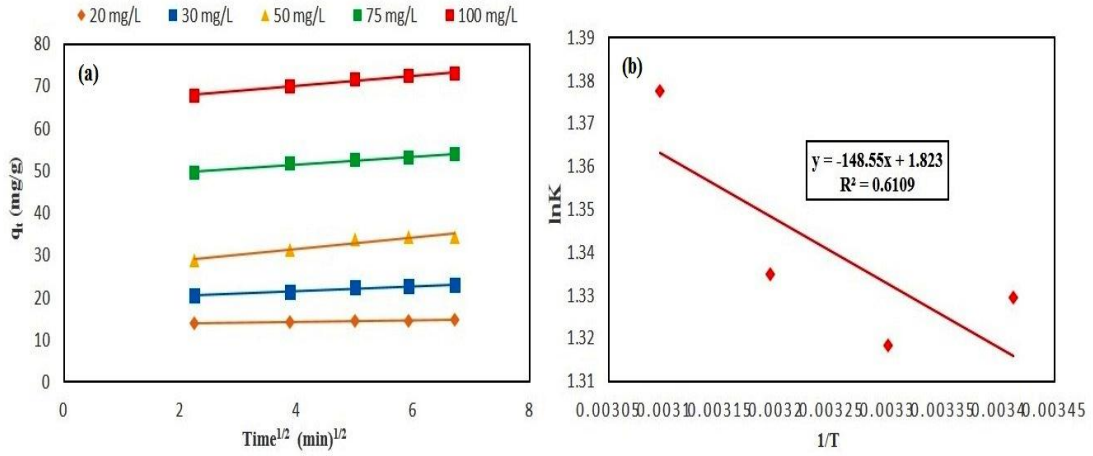

Fig. 5.7. (a) Intra-particle diffusion model for different MG dye concentration and (b) Arrhenius plot for the sorption of MG dye onto MPA [Adsorbent concentration 0.1g/100 mL, pH 6.0, Time 45 min, dye concentration 20 – 100 mg/L].

5.3.7. Thermodynamic studies for sorption of MG dye

The calculated value of thermodynamic parameters ($\Delta G°$, $\Delta H°$ and $\Delta S°$) are given in Table 5.7. The dye binding by MPA was recorded at different temperature from 293 to 323 K. The Gibb's free energy change ($\Delta G°$) was found to be negative at all the selected temperature for sorption of MG onto MPA, which indicated the feasibility and spontaneity of the adsorption process. An increase in the negative value of $\Delta G°$ from -2.453 to -2.919 kJ/mol with an increase in temperature from 293 to 323 K indicated that the adsorption process was more favorable at lower temperature. The Gibb's free energy change with negative value ($-\Delta G°$) for adsorption shows favourable adsorption (Baek et al., 2010). The value of $\Delta H°$ and $\Delta S°$ were determined from the slope and intercept of the plot of lnkc vs. 1/T (Fig. 5.8). The positive low value of $\Delta H°$ (1.925 kJ/mol) indicated that adsorption process was endothermic and possible interaction between sorbent and adsorbate molecules was physical in nature (Ghasemi and Asadpour, 2007). In case of MG sorption by MPA might be acquiring energy from hydration energy where adsorbate species has to displace more than one water

molecules for their adsorption and result in the endothermicity of the adsorption process (Ahmad and Kumar, 2010). The positive entropy change, ΔS^0 (14.872 J/mol K) might be related to the hydration of cationic dye molecules and release of water molecules during sorption from surrounding of the dye molecules contributing to increase in the degree of freedom of the water molecules (Baek et al., 2010; Ghasemi and Asadpour, 2007).

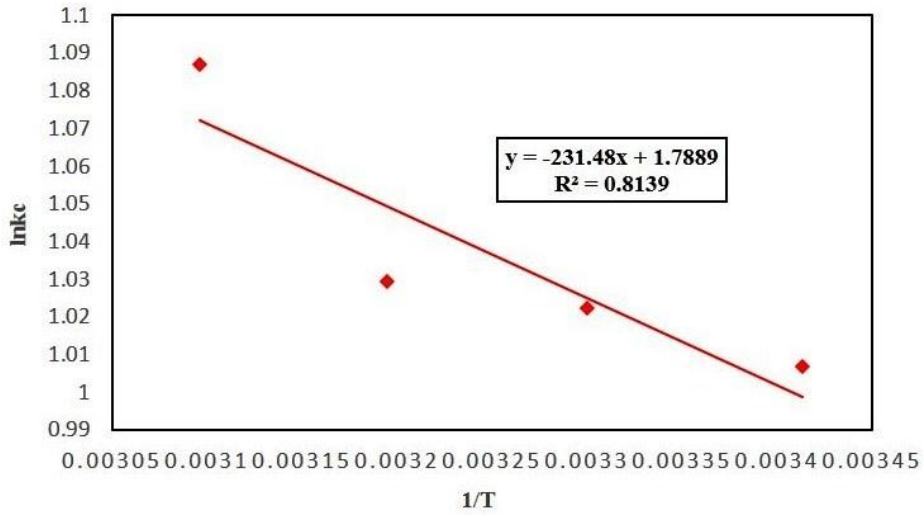

Fig. 5.8. Vont'hoff plot for the calculation of thermodynamic parameters in removal of MG dye by MPA [Initial dye concentration 50 mg/L, adsorbent concentration 0.1g/100 mL, Time 45 min, pH 6.0].

Table 5.7. Thermodynamic parameters at different temperature for the sorption of MG dye onto MPA.

T(K)	ΔG°(kJ/mol)	ΔH° (kJ/mol)	ΔS° (J/mol K)
293	-2.453	1.925	14.872
303	-2.576		
313	-2.679		
323	-2.919		

5.3.8. Desorption of MG dye

A study on dye desorption can be more helpful in order to confirm the possible sorption mechanisms as well as the potential recovery of the adsorbent for its repeated use in the

sorption process. In the present study, the desorbing solutions of mineral acids (1N HCl and H_2SO_4) were found to be more effective in desorption of MG dye from dye loaded MPA adsorbent as compared to other desorbing agents (Table 5.8). A high percentage desorption (49.55%) of MG dye by mineral acid (HCl) indicated that the dye was adsorbed onto MPA by a physico-chemical sorption process as suggested by earlier workers (Mall et al., 2006). The desorbing agent (HCl) reduced the pH of solution and hence, at acidic pH (> 5.0), the surface of MPA becomes more protonated and the attachment between dye molecules and MPA is weakened due to electrostatic repulsion as MG is positively charged dye. The lowest percentage of desorption (6.53%) was observed with 1N of NaOH as desorbing solution perhaps on account of strong affinity of the adsorbent for the cationic adsorbate at alkaline pH. Desorption process is always inversely proportional to bond strength of adsorbed material, a strong interaction between the dye and MPA could be the reason for weak desorption of MG dye (Rawat and Singh, 2017).

Table 5.8. Percent desorption (%) of MG dye by different desorbing agents.

Desorbing solution (1N)	**Amount of dye desorbed ($mg\ g^{-1}$)**	**Percent desorption (%)**
HCl	18.05	49.55
H_2SO_4	10.15	27.87
CH_3COOH	4.77	13.09
NaOH	2.38	6.53
H_2O	5.38	14.76

B. Removal of methylene blue (MB) dye by Mentha Plant Ash (MPA)

5.4. Results and Discussions

5.4.1. IR-Spectroscopy (FTIR) of MPA before and after adsorption of MB dye

The FTIR spectra (4000 to 500 cm^{-1}) of MPA were compared before and after adsorption of MB dye (Fig. 5.9). The results displayed the participation of several fuctional groups present on the surface of MPA particles (Table 5.9). The result on IR absorption spectrum of MPA due to MB dye binding showed increased absorption area bend as well as shift in the IR peaks at wavenumbers 3434.9, 1436.4 and 1034.7 cm^{-1}. These results indicate the role of N–H stretching of amine (Farhan, 2015; Mary et al., 2016), C–H variable alkenes groups (Shi et al., 2014) and C–C and C–O vibrations in esters (Shi et al., 2014; Ding et al., 2016), which played crucial role in MB dye binding by MPA particles. The IR absorption peak at 1795.7 and 1642.0 cm^{-1}, assigned to C=O for carboxyl groups and C=C stretching of aromatic group in lignin (Poletto et al., 2012), respectively. The IR peaks at wavenumber 1642.0 cm^{-1} was completely disappeared after the treatment of MPA adsorbent due to C=C stretching of aromatic group in lignin for the binding of MB dye molecules. The changes in IR peaks at wavenumber of 2514.9, 874.7 and 712.8 cm^{-1} assigned to O–H stretching of carboxylic group and CO_3^{2-} group, respectively, which involved in the adsorption of MB dye onto the surface of MPA particles (Mohan, 2005; Smidt and Schwanninger, 2005). Further, the IR peak at wavenumber 688.0 and 569.9 cm^{-1} assigned to C–H phenyl rings and Alkyl halide (–C–Cl) stretch, respectively, which might be involved in surface adsorption due to the C–H and C–Cl stretching and bending (Ramola et al., 2014; Akerholm et al., 2004). The overall results on IR spectra of MPA after adsorption of MB dye exhibit that hydroxyl, ester, amine, phenyl, carboxyl and carbonyl groups are

the surface functional moieties, not only contributing to negative charge on surface of MPA, but are actively participated in the binding of cationic MB dye.

Table 5.9. FTIR Wavenumber (cm^{-1}) of MPA before and after adsorption of MB dye.

Observed frequency in (cm^{-1}) of MPA adsorbent			
Frequency range (cm^{-1})	Before adsorption of MB dye	After adsorption of MB dye	Band assignment
3550–3250	3434.9	3435.6	N–H stretching of amine (Farhan, 2015)
3200–2500	2514.9	2514.5	O–H of carboxylic group (Mohan, 2005)
1815–1770	1797.2	1795.7	C=O stretch of acid chloride (Mohan, 2005)
1620 – 1680	1642.0	0	–C=C– aromatic group (Poletto et al., 2012)
1435 –1405	1436.4	1434.0	C–H alkenes groups (Shi et al., 2014)
1300 –1000	1034.7	1036.2	C–O stretch of ester (Mohrig et al., 2006)
875 – 602	875.1	874.7	CO_3^{2-} (Smidt and Schwanninger, 2005)
674 – 686	688.0	685.9	C–H phenyl rings (Ramola et al., 2014)
770 – 620	712.8	711.7	CO_3^{2-} (Smidt and Schwanninger, 2005)
500 – 600	569.0	569.9	–C–Cl group (Akerholm et al., 2004)

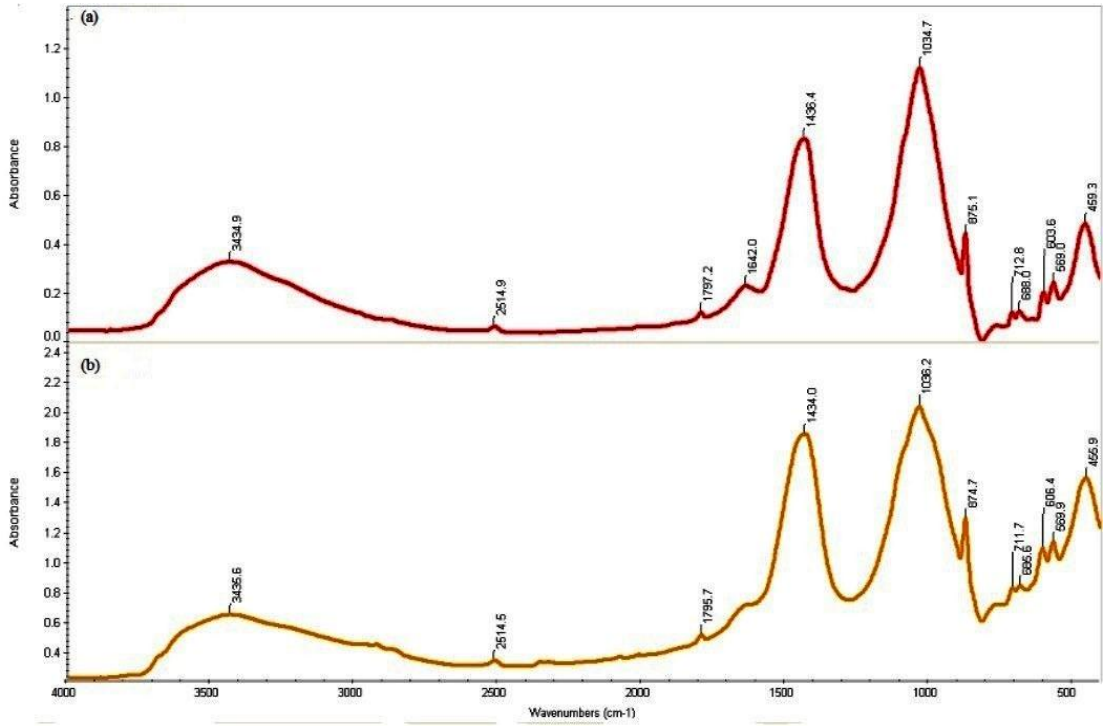

Fig. 5.9. FTIR spectra of MPA (a) after (b) before adsorption of MB dye.

5.4.2. Cyclic voltametric analysis of MB dye in presence of MPA

Cyclic voltametric analysis was carried out to see whether a rapid decolourization of MB dye in the presence of MPA was simply adsorption of dye or something else. The Cyclic voltametric (CV) test was performed on the MB dye solution obtained after treatment of MPA adsorbent.The cyclic voltammograms of MB dye in the electrolytic solution showed a well-defined redox couple. Results on CV tests showed cathodic (reduction) and anodic (oxidation) activities in MB dye solution, emphasizing that the reduction of MB dye by MPA particles through electron transfer process (Farsi and Hosseini 2013). In cyclic voltammogram of MB dye, the cathodic peak 1 and anodic peak 2 appearing at approximately –0.52V and –0.38V (Fig. 5.10) can be assigned to the reduction of MB^+ to Leucomethylene blue (LMB) and oxidation of LMB to MB^+, respectively, indicating reversible nature redox process in MB dye solution after treatment of MPA. The coupled redox reaction for MB dye in CV test suggested that

MB^+ cations adsorbed on the surface of MPA particles were changed to LMB through reductive process. The several minerals and surface active ligands of MPA might be contributing as electron donor.

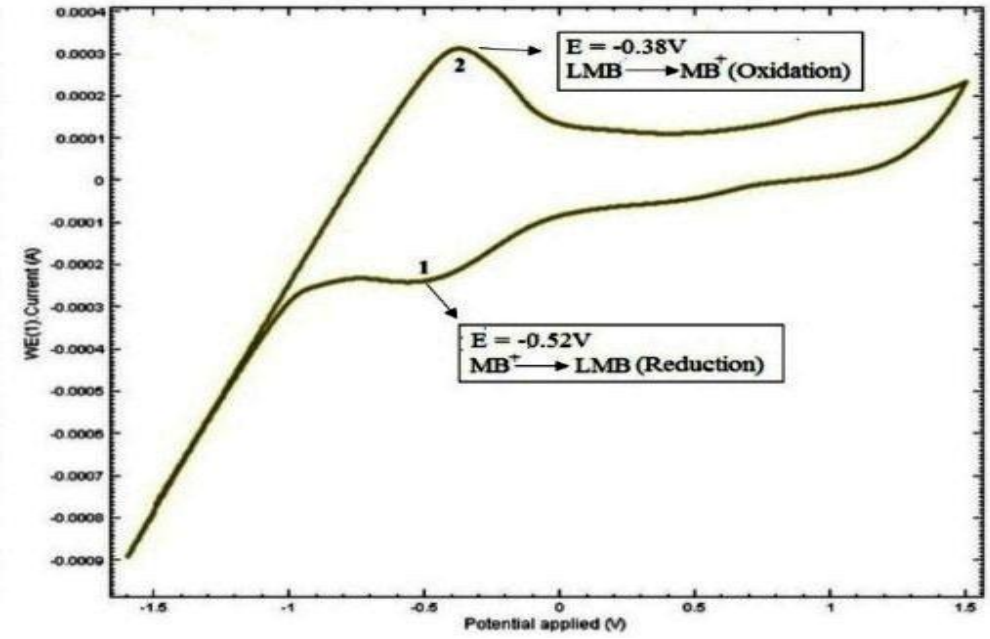

Fig. 5.10. Cyclic Voltammogram of MB dye after treatment with MPA [Potential range = –1.5V to +1.5V; Scan rate = 100 mVs^{-1} and step potential = 0.002V].

5.4.3. Factors affecting adsorption of MB dye

5.4.3.1. Effect of contact time

The adsorption of MB dye was studied as a function of time using initial dye concentration of 25 mg L^{-1}, adsorbent dosage of 0.1g/100 mL. The result (Fig. 5.11 (a)) showed that the dye adsorption by MPA initially occurred at a faster rate, (18.67 mg g^{-1}) up to first five minutes of incubation and resulted into removal of 74.68 % dye within 5 minutes. Thereafter, dye adsorption continued till the first 15 min at a slower rate, perhaps due to non-availability of adsorption sites on the surface of adsorbent. The relative increase in the removal of dye after 15 minutes was insignificant. A rapid rate of dye adsorption at the initial contact time could be attributed to availability of large number of adsorbent sites. Earlier, it has been demonstrated that slow adsorption rate

after initial rapid phase could be due to saturation of available adsorption sites and decrease in the number of adsorption sites on the adsorbent (Saha et al., 2010; Chakraborty et al., 2011). Earlier, workers have demonstrated similar observation for the removal of cationic dyes by pumice stone as a low cost adsorbent (Shayesteh et al., 2016). Hameed et al. (2009) studied the adsorption of basic methylene blue dye from aqueous solution using pine apple stem (PS) and reported similar trend of adsorption as a function of time.

5.4.3.2. Effect of adsorbent dose

The adsorption capacity is greatly influenced by the dose of MPA (adsorbent) in removal of MB dye from aqueous solution. The amount of dye adsorbed by MPA was studied as a function of adsorbent doses (0.5 to 3 g/L) at 25 mg L^{-1} dye concentration for 30 min at room temperature. Results (Fig. 5.11 (b)) showed that the dye uptake increased from 15.02 to 24.41 mg g^{-1} with increase in adsorbent dose from 0.5 to 3 g/L. A rapid phase of dose-dependent increase in dye removal occurred up to 1 g/L dose of MPA and this was followed a sluggish phase of dye removal between 1 to 3 g/L of dose of adsorbent. The maximum dye removal, at an adsorbent dose of 1 g/L, was found to be 20.65 mg g^{-1}. As the number of available adsorption sites increased in a dose-dependent manner, the rate of dye removal also increased (Ahmad, 2009). A sluggish increase in dye binding at higher doses of adsorbent (1 to 3 g/L) may be due to less availability of dye molecules per unit concentration of adsorbent. Otherwise it may state that the clustering of adsorbent particles per unit volume might be hindering the free mobility of the dye molecules approaching to the binding sites on the surface of adsorbent (Garg et al., 2003). Earlier, workers have also demonstrated an increasing trend of dose dependent MB dye removal by pine apple stem (Hameed et al., 2009).

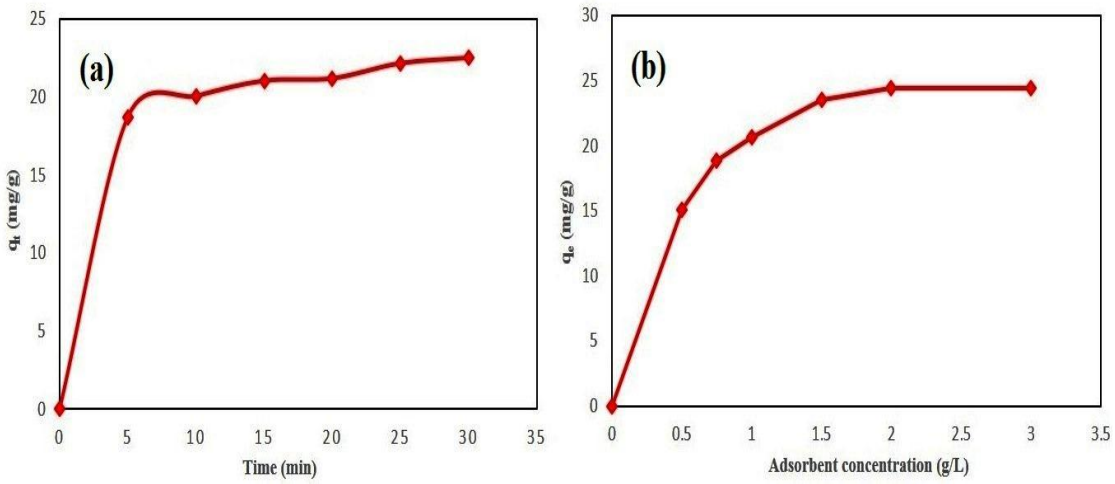

Fig. 5.11. Effect of (a) contact time and (b) adsorbent concentration on MB dye adsorption by MPA [Initial dye concentration 25 mg L^{-1}, time 30 min, pH 7.0, adsorbent concentration 0.1g/100 mL].

5.4.3.3. Effect of initial dye concentration

The effect of initial dye concentration on the adsorption capacity of MPA depends on the availability of dye molecules and surface binding sites of MPA particles. The extent of dye removal is greatly influenced by initial dye concentration in aqueous solution. In the present study, the effect of different initial concentration of MB (5 to 50 mg L^{-1}) was studied on the adsorption of MB dye for 45 min at fixed adsorbent dosage (0.1g/100 mL) at room temperature and pH 7.0. The results (Fig. 5.12) showed initially a very rapid process upto 5 min, followed by slowing down of the process with increase in the contact time up to 30 min, perhaps due to non-availability of adsorption sites on the surface of adsorbent (Saha et al., 2010). Further removal of dye after 30 minutes was found to be insignificant. The equilibrium stage and maximum uptake of total amount of MB dye was found to occur within 30 minutes at different concentration of MB dye. A rapid rate of dye adsorption at the initial contact time could be attributed to availability of a large number of adsorption sites. The rate of dye binding increased in a concentration-dependent manner and the saturation concentration of dye at equilibrium (q_e) was found to increase from 4.41 to 37.76 mg g^{-1} with increase in the

initial dye concentration from 5 to 50 mg L^{-1}. An increase in adsorption capacity of MPA with increase in MB dye concentrations, might be due to relatively higher rate of mass transfer (Bulut and Aydin, 2006). But the sluggish increase in the rate of dye adsorption at higher concentration could be attributed to a limiting dose of adsorbent (Garg et al., 2003). The rate of dye binding increased in a concentration dependent manner, exhibiting rate saturation 50 mg L^{-1} concentration of MB dye. The increase in initial dye concentration provided rapid increase as it overcame all mass transfer resistances of the dye between the aqueous and solid phase (Hameed et al., 2008). But the rate saturation at higher concentration of dye was due to sorbent as rate limiting factor. Similar results were reported by other investigators for the removal of methylene blue dye by pine apple stem and they found that the adsorption capacity of the pine apple stem was increased with an increase initial dye concentration (Hameed et al., 2009).

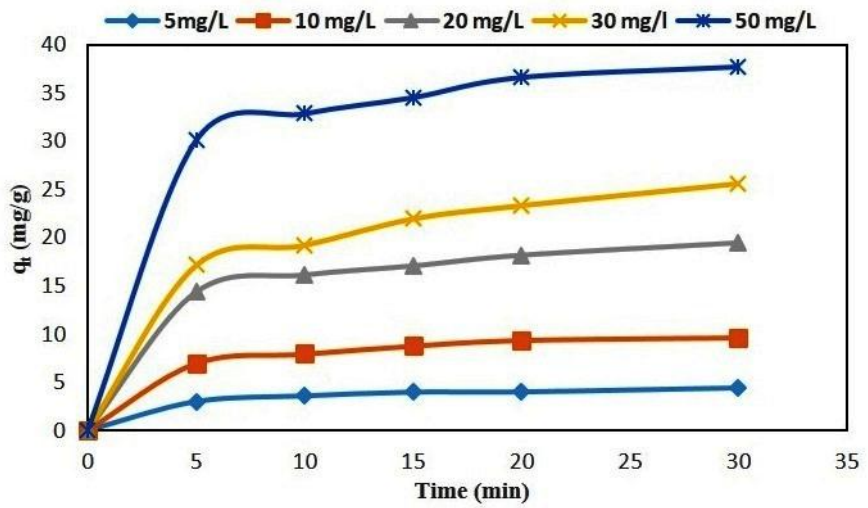

Fig. 5.12. Effect of initial dye concentration on the amount adsorbed (mg g-1) of MB by MPA [Dye concentration 5–50 mg/L, adsorbent concentration 0.1 g/100 mL, time 30 min, pH 7.0, temperature 30º C].

5.4.3.4. Effect of pH on adsorption of MB dye

The surface-potential of MPA is considered an essential factor influencing the extent of dye adsorption on the surface of any adsorbent. In order to see the role of surface charge

potential of adsorbent during the dye adsorption, the zeta potential of MPA were recorded as a function of different pH in a buffered medium. The zeta potential for the MPA adsorbent ranged from –24.3 mV at pH 4.0 to – 40.1 mV at pH 10.0 as shown in Fig. 5.13. The results on zeta potential values of MPA indicated a highly negative charged surface with little effect of pH condition. As the pH of ambient condition increases, the zeta potential of MPA became slightly more negative. A highly electronegative surface along with little effect of changing pH condition on the zeta potential suggested about larger contribution of salts and minerals in determining the zeta potential was suggested by ealier workers (Aksoy and Kaya, 2011). This could be the reason for high binding efficiency of MPA for cationinc dye like methylene blue (Bootharaju and Pradeep, 2013). Similar observations have been made by earlier workers on zeta potential of quartz powder with isoelectric point (iep) at around pH 2.0 and zeta potential ranging from – 15 mV at pH 4.0 to – 56 mV at pH 10.5 (Huang and Fuerstenau, 2001). Johnson (1999) reported that the quartz has iep at pH below 2 and the zeta potential is about –50 mV at neutral pH and – 60 mV at pH 10 in the presence of 1×10^{-3} M KCl. In the present investigation, the iep of the MPA could not be found within the selected range of pH. However, hydrated ionic radius of minerals may also affect the zeta potential; the larger is the ionic radius and thicker the layer, the value of zeta potential shifts towards negative side as in the case of MPA (Aksoy and Kaya, 2011).

Initial pH condition of the adsorbate solution can influence the chemistry of adsorbate as well as over all surface charge potential of the adsorbent (Shayesteh et al., 2015). Since variation in pH condition of the solution leads to disparity in the grade of ionization of the chemical moieties present on the surface of adsorbent as well as ionization potential of adsorbate molecule (Nandi et al., 2009). In the present work, the

adsorption of MB dye by MPA was studied, using different pH conditions (pH 4.0 to 10.0) at fixed concentration of dye (25 mg L^{-1}) and adsorbent (0.1 g/100 mL). The result (Fig. 5.13) showed that the amount of dye adsorbed by MPA at equilibrium (q_e) increased from 15.51 to 23.13 mg g^{-1}, respectively, with increase in the pH from 4.0 to 10.0.

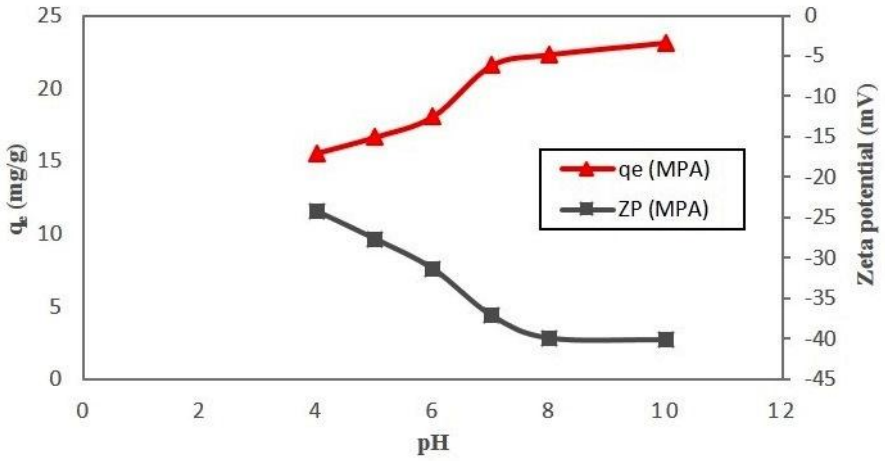

Fig. 5.13. Effect of pH on zeta potential and adsorption of MB dye by MPA [C_0 = 25 mg L^{-1}; Dose of adsorbent = 0.1 g/100 mL; Time t = 30 min; Temperature T = 303 K].

The pH dependent (pH 4.0 to 10.0) increase in the amount of dye adsorption might be attributed to increase in surface charge potential of MPA particles at different pH value. The results clearly showed reduced adsorption of dye at acidic pH (4.0), perhaps on account of reduced electronegative surface of MPA particles at acidic pH, which was perhaps unfavourable for adsorption of cationic dye. Besides, protonation of cationic MB dye molecules at acidic pH might also hinder the active binding between the adsorbents and adsorbate and thereby, reducing the adsorption capacity (Sathishkumar et al., 2012). Further, results on the pH dependent change in the zeta potential of MPA particles showed a pH dependent gradual increase in the negative value of zeta potential of adsorbent between pH 4.0 to pH 10.0, perhaps due to enhanced hydrated ionic radius contributing to negative charges on the surface. Earlier findings have also demonstrated

an increased electrostatic attraction between the positively charged dye and anionic surface of the adsorbents and thereby, facilitating initial faster rise in the adsorption of cationic dye (Mittal et al., 2010).

5.4.4. Adsorption isotherms

Adsorption isotherms were applied on equilibrium experimental data to obtain the valuable information about the distribution of MB cations on the surface of the MPA particles and calculate its adsorption capacity (mg g^{-1}). The results showed that both Langmuir and Freundlich adsorption isotherms (Fig. 5.14 (a) and (b)) were well suited to the data on equilibrium sorption of MB dye onto MPA. It has already reported that the high ash content in MPA is indicative of more functional groups (Sewu et al., 2017) and make it appropriate for the sorption of cationic MB dye. According to Langmuir isotherm model, the q_{max} values of MPA at room temperature was calculated as 588.24 mg g^{-1}. A high q_{max} value of MPA is likely due to enhanced binding of MB dye with the large number of surface binding ligands of MPA. The electrostatic interaction and ion exchange mechanisms were involved in the binding of MB dye with the hydroxyl, carbonyl, phenyl and carboxyl functional groups disseminated on the surface of MPA particles (Sewu et al., 2017), as discussed in FTIR analysis (Fig. 5.9). The R^2 values are shown in Table 5.10 showed better applicability of Langmuir as well as Freundlich isotherm to describe MPA for equilibrium adsorption and fitted well to the equilibrium adsorption data of MB dye. The adsorbent MPA had high affinity for MB dye adsorption supported by R_L values (Table 5.11). The calculated R_L values of MPA (0.94 to 0.61) at different dye concentration (5 to 50 mg g^{-1}) indicated favorable adsorption process. The R_L values between 0 and 1 were indicative of favourable adsorption with more affinity of MPA particles towards dye molecules (Hema and Arivoli, 2007; Ma et al., 2015). A high R^2 values and value of $1/n < 1$ for MPA (0.838) in Freundlich

isotherm on MB adsorption also confirmed the role of chemisorption on the heterogeneous surface of MPA. The q_{max} values of different sorbent materials, as given in Table 5.12, were used to compare our results. A comparison of adsorption capacity of different adsorbents suggested that MPA are better adsorbents than many other reported adsorbents.

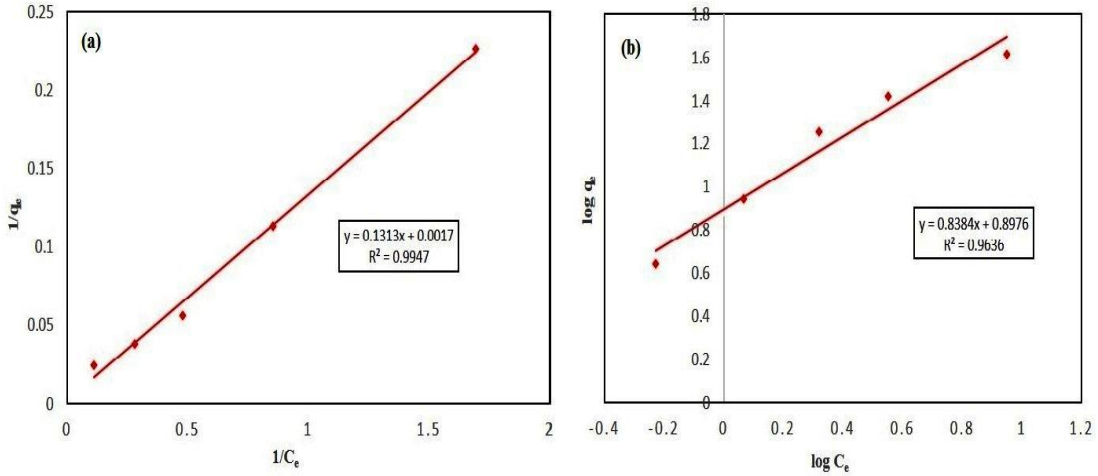

Fig. 5.14. Adsorption isotherms (a) Langmuir and (b) Freundlich model in biosorption of MB dye onto MPA [C_0 = 5 – 50 mg L^{-1}; pH = 7.0; Dose of adsorbent = 0.1 g/100 mL; Time t = 30 min; Temperature T = 303 K].

Table 5.10. Equilibrium adsorption parameters for the sorption of MB dye onto MPA.

Langmuir isotherm			**Freundlich isotherm**		
q_{max} (mg g^{-1})	b (L mg^{-1})	R^2	K_F (mg g^{-1})	1/n	R^2
588.24	0.013	0.995	0.127	0.838	0.964

Table 5.11. Separation factor (R_L) of MPA at different MB dye concentration.

Initial concentration (mg L^{-1})	**Seperation factor (R_L)**
5	0.94
10	0.89
20	0.8
30	0.73
50	0.61

Table 5.12. Comparison of maximum adsorption capacity (q_{max}) of MPA with other reported agro and plant waste based adsorbents for MB dye removal.

Adsorbents	q_{max} (mg g^{-1})	References
Kenaf fibre char	22.7	(Mahmoud et al., 2012)
Coconut bunch waste	70.92	(Hameed et al., 2008)
Anaerobic granular sludge biochar	90.91	(Shi et al., 2014)
Palm kernel fibre	95.4	(El-Sayed, 2011)
Eucalyptus bark biochar	104.2	(Dawood et al., 2016)
Wheat straw biochar	12.03	(Liu et al., 2012)
Biochar ash	178	(Ozbay et al., 2013)
Mentha Plant Ash (MPA)	588.24	Present study

5.4.5. Adsorption kinetics

The study on adsorption kinetics was performed in order to examine the adsorption mechanisms involved in the removal of MB dye by MPA. The kinetic experimental data at different dye concentration (5 – 50 mg L^{-1}), and the non-linear fits of pseudo-first and second order kinetic models are displayed in Fig. 5.15 (a) and (b). All the calculated kinetic parameters, correlation coefficients (R^2) are presented in Table 5.13. It can be confirmed from the pseudo-first order kinetic parameters, the values of R^2 and cal. q_e suggested that pseudo-first order kinetic model did not fit in well with the experimental data for the adsorption of MB dye onto MPA. From the second order kinetic parameters, it was confirmed that the pseudo-second order kinetic model was the well fitted model with comparatively high R^2 values at different concentration of MB dye and closer values of cal. q_e to exp. q_e. The fit of this model clearly indicated that the rate of adsorption of MB dye onto MPA was almost a controlled chemisorption

process, which involved sharing of electrons between dye molecules and surface of MPA (Foo and Hameed, 2012).

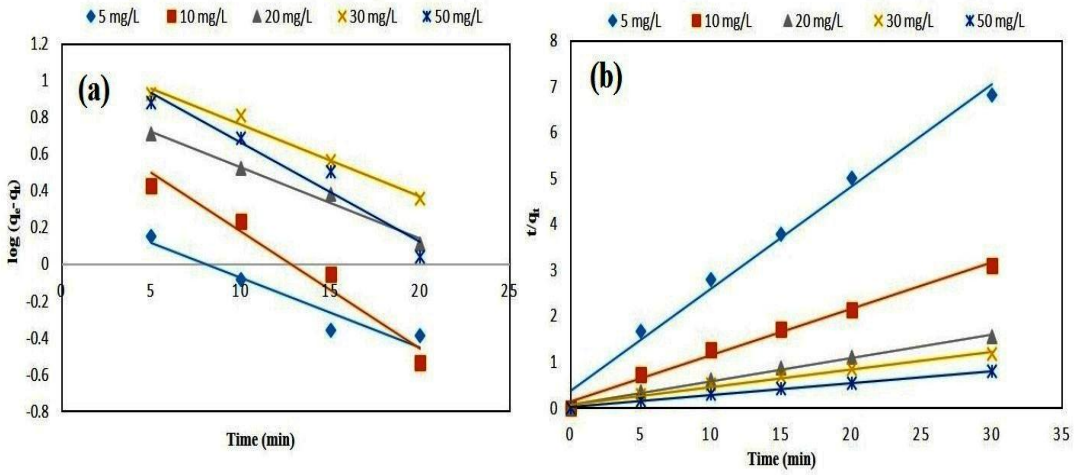

Fig. 5.15. Adsorption kinetics (a) Pseudo-first and (b) second order kinetic model in removal of MB dye by MPA [C_0 = 5 – 50 mg L^{-1}; pH = 7.0; Dose of adsorbent = 0.1 g/100 mL; Time t = 0 – 30 min; Temperature T = 303 K].

Table 5.13. Kinetic parameters for the sorption of MB dye onto MPA at different initial dye concentration.

Conc (mg/L)	**Exp. q_e (mg/g)**	**First-order kinetics**			**Second order kinetics**			**Initial adsorption rate (*h*)**
		K_1 (mg g^{-1} min^{-1})	Cal. q_e (mg g^{-1})	R^2	K_2 (mg g^{-1} min^{-1})	Cal. q_e (mg g^{-1})	R^2	*h* (mg g^{-1} min^{-1})
5	3.76	0.087	2.02	0.926	0.132	4.49	0.991	2.67
10	7.32	0.147	6.55	0.961	0.069	9.94	0.993	6.82
20	14.01	0.089	8.23	0.984	0.035	19.76	0.992	13.57
30	22.12	0.091	14.26	0.985	0.019	26.32	0.984	12.52
50	34.49	0.124	16.09	0.943	0.026	38.32	0.997	37.74

The initial adsorption rate (*h*) values were increased with increase in the MB dye concentration from 5 to 50 mg L^{-1} (Table 5.13). An increasing trend of *h* values with

the dye concentration might be due to increase in dye binding with increasing concentration of dye (Hema and Arivoli, 2008; Kumar, 2006). High *h* values for MPA (37.74 mg g^{-1} min^{-1}) at rate saturating concentration of dye indicated that the adsorption of MB dye molecules onto the surface of MPA might be carried out through surface interchange reactions until all the functional binding sites were occupied (Ma et al., 2015).

5.4.6. Activation energy

Activation energy (*Ea*) provides an important information about the type of sorption process (physical and chemical adsorption). The activation energy (*Ea*) involved in the surface adsorption of MB dye by MPA was calculated from the slope of Arrheniums plot between lnK versus 1/T (Fig. 5.16). The activation energy of the surface binding process was calculated to be 14.90 kJ mol^{-1} for dye binding by MPA, which confirmed the physico-chemical sorption process. The lower value of activation energies (>4 kJ/mol) have been reported to be responsible for physical adsorption, while higher value of *Ea* in the present study suggested for either activated chemisorption or combination of both physical and activated chemisorption as suggested earlier (Chowdhury and Saha, 2010).

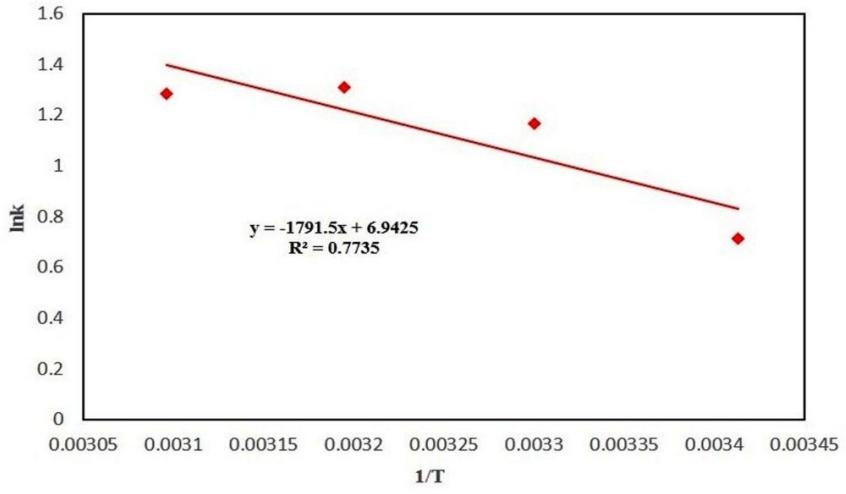

Fig. 5.16. Arrhenius plot for the calculation of activation energy (*Ea*) in removal of MB dye by MPA.

5.4.7. Thermodynamic studies

In the present experiment, the dye binding by the MPA adsorbent was recorded at different temperature from 293 to 323 K. The amount of dye adsorption by MPA was increased from 16.64 to 22.03 mg g^{-1}, with rise in temperature, indicated endothermic adsorption process, where increased kinetic mobility of dye molecules to the active binding might have have enhanced with increase in temperature. On the other hand, a decline in the dye adsorption with the increasing temperature, an indicator of exothermic adsorption process, might be due to decrease in adsorptive forces between the dye molecules and active binding sites as suggested earlier (Salleh et al., 2011). In the present investigation, temperature dependent increase in dye removal capacity of the adsorbents could be due to enhanced number of surface active centers available for adsorption (Mohan et al., 2002). Results in Table 5.14 showed negative values of ΔG° for MPA from -1.676 to -5.381 kJ/mol at all the chosen temperature, which showed that the adsorption of MB dye onto MPA particles was thermodynamically feasible and spontaneous (Baek et al., 2010). The free energy change (ΔG°) with negative value for adsorption supported that view that the removal of MB dye by MPA was favourable adsorption process. An increase in negative value of ΔG° with rising temperature specified that the process of adsorption was more favourable at lower temperature (Chowdhury and Saha, 2010). The Von't Hoff plot for MPA (Fig. 5.17) was used to determine the enthalpy (ΔH°) and entropy (ΔS°) values. The results showed positive values of ΔH° for MPA (35.82 KJ mol^{-1}), indicating that the adsorption process was endothermic and nature of interaction between MPA particles and dye molecules was physico-chemical process (Ghasemi and Asadpour, 2007). The endothermic nature of MB adsorption by surface moieties on MPA particles might be deriving the required energy from hydration shell of dye molecules (Ahmad and Kumar, 2010). The positive

values of ΔS° for MPA (128.42 J mol^{-1} K^{-1}) was supporting involvement of hydration energy with the cationic dye and the same was released during the sorption of dye molecules, contributing to an increase in the degree of freedom of the water molecules (Ghasemi and Asadpour, 2007; Baek et al., 2010).

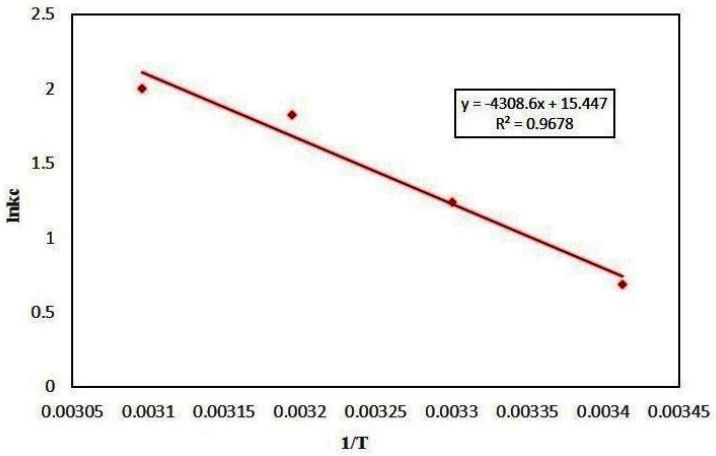

Fig. 5.17. Vont'Hoff plot for the calculation of thermodynamic parameters in removal of MB dye by MPA [Temperature range = 293 – 323 K; C_0 = 25 mg L^{-1}; pH = 7.0; Dose of adsorbent = 0.1g/100 mL; Time t = 30 min].

Table 5.14. Thermodynamic parameters for the sorption of MB dye onto MPA at different temperature.

T(K)	ΔG°(kJ mol^{-1})	ΔH° (kJ mol^{-1})	ΔS° (J mol^{-1} K^{-1})
293	-1.676	35.82	128.42
303	-3.124		
313	-4.749		
323	-5.381		

5.4.8. Desorption of MB dye

A study on MB dye desorption can be more helpful in order to confirm the nature of sorption process as well as the recovery of the MPA for its repeated use in the sorption process. Desorption of dye is proportional to the bond strength (e.g., covalent and ionic bond) as well as the frequency of the weak forces of attraction (e.g., dipole–dipole interactions and Van der Waals forces) established between the adsorbent particles and

the adsorbate molecules (Bouaziz et al., 2017). The desorbing solutions of mineral acids (0.1 N HCl and H_2SO_4) were found to be more effective in desorption of MB dye from dye loaded MPA as compared to other desorbing agents (Table 5.15). A high percentage desorption (53.71 %) of MB dye by mineral acid (HCl) indicated that the dye was adsorbed onto MPA by a physico-chemical sorption process as suggested earlier workers (Mall et al., 2006). The desorbing agent (HCl) reduced the pH of solution and hence, at acidic pH, the surface of MPA become more protonated and the attachment between dye molecules and MPA is weakened due to electrostatic repulsion as MB is a cationic dye (Mall et al., 2006). The lowest percentage of desorption was observed with 0.1N NaOH as desorbing solution perhaps on account of strong affinity of the adsorbent for the cationic adsorbate at alkaline pH. Desorption process is always inversely proportional to bond strength of adsorbed material, a strong interaction between the dye and MPA could be the reason for weak desorption of MB dye (Mall et al., 2006).

Table 5.15. Percent desorption (%) of MB dye by different desorbing agents.

Desorption solution (0.1 N)	**Amount of dye desorbed (mg/g)**	**% desorption**
CH_3COOH	3.38	18.6
H_2SO_4	6.37	35.06
HCl	9.76	53.71
H_2O	3.78	20.8
NaOH	2.16	11.89

CHAPTER- VI

Removal of Cr(VI) by Mentha Plant Ash (MPA)

6.1. Introduction

Hexavalent chromium Cr(VI) is an extremely toxic pollutant found in industrial wastewater and it has high toxicity potential to cause carcinogenesis and mutation in all living beings including human and animals. The US Environmental Protection Agency (USEPA) has notified that the Cr(VI) is one of the top-most toxic contaminant of aqueous systems (Pang et al., 2011). Various anthropogenic activities such as electroplating, metal finishing, chromate production, mining, leather tanning and etc. are mainly responsible for the release of large amount of chromium containing wastewater in the natural environment (Samania et al., 2010). Therefore, developing an effective and low cost treatment technology for the removal of Cr(VI) from the aqueous systems is of prime concern to environmentalist and other research groups. During the last few years, a number of physico-chemical treatment methods such as coagulation, adsorption, oxidation-reduction, electrochemical precipitation, ion exchange and reverse osmosis have been successfully used for detoxification of Cr(VI) in aqueous systems (Gu et al., 2012). Among these treatment methods, adsorption has been considered as one of the most suitable and efficient method due to its availability of wide resource materials, easy operation, high adsorption efficiency and easy recovery process. During the last few years, a number of adsorbents such as zeolites, organic resins, chitosan, clay minerals, agricultural wastes and fly ash have been used for the removal of different toxic metal ions from aqueous solutions (Gao et al., 2013; Lee et al., 2013; Kumric et al., 2013; Gupta et al., 2003). Among the various reported adsorbents, the adsorbent materials having large number of organic functional groups are more capable in adsorption of metal ions as indicated by earlier workers (Lam et al., 2007). The surface functional groups like hydroxyl, carboxyl, amine, carbonyl, thiol groups and etc., play a crucial role in heavy metal adsorption due to their higher binding

affinity for the metal ions to form complex during sorption process (Sud et al., 2008). Generally, the surface protonation of the adsorbent materials under the acidic condition is mainly involved in electrostatic interactions with different oxyanionic forms of Cr(VI) and thus, acidic pH condition is very helpful in the removal of Cr(VI) from aqueous solutions (Pang et al., 2011a). A number of previous studies suggested that the surface modification of organic functional groups of adsorbents can enhance their adsorption potential to a great extent in removal of metal ions. Therefore, selecting a most suitable organic materials is of prime concern to researchers in developing highly efficient adsorbents for the removal of Cr(VI).

Adsorbent MPA, a waste byproduct of mentha oil distillation unit, contain various organic functional groups such as carboxyl, carbonyl, hydroxyl and amine groups on its surface and these functional groups may play a crucial role in adsorption and modification of Cr(VI) to detoxify the aqueous solution. Therefore, the main objective of present study was to evaluate the sorption and redox potential of MPA as a low cost efficient adsorbent for the removal of Cr(VI) from aqueous solutions.

6.2. Materials and Methods

Batch adsorption experiments were conducted as a function of contact time, adsorbent doses, pH and initial Cr(VI) concentration to evaluate nature and sorption efficiency of MPA in removal of Cr(VI). The adsorbent material (MPA) was characterized by using various instrumental techniques to determine physicochemical properties of various ligands present on the surface of MPA as described earlier in Chapter-3. Further, X-Ray Photoelectron Spectroscopy (XPS) and Cyclic Voltammetry analysis of MPA after adsorption of Cr(VI) was carried out to analyze the interaction of functional groups and Cr(VI) on the surface of adsorbent. Adsorption kinetics, equilibrium adsorption isotherms and thermodynamic studies were carried out to explain the nature of

adsorption process and to define the applicability of various isotherms and kinetic models for the Cr(VI) sorption efficiency of MPA. The detailed methodology including chemicals and solutions; preparation and characterization of MPA; batch adsorption experiments; equilibrium, kinetic and thermodynamic studies have been described earlier in Chapter-3. The redox state of chromium during interaction with adsorbent was studied by cyclic voltammetry.

6.3. Results and Discussions

6.3.1. IR-spectroscopy (FTIR) of MPA before and after adsorption of Cr(VI)

The FTIR spectra (Fig. 6.1.) of adsorbent (MPA) before and after adsorption of Cr(VI) were compared to study the role of various surface functional groups in the binding of Cr(VI) metal ions. The results displayed the participation of several functional groups such as hydroxyl, ester, amine, phenyl, carboxyl and carbonyl in the binding of Cr(VI) metal ions on the surface of MPA particles. Few major drastic changes were found to occur in the IR absorption characteristics due to presence of Cr(VI). The changes in the different surface functional groups of MPA adsorbent after adsorption of Cr(VI) showed changes in IR peaks at wavenumbers 3635.6 and 1797 cm^{-1} assigned to O−H and C=O stretching of hydroxyl and carbonate groups (Mary et al., 2016). The Cr(VI) induced alterations in the IR peak at wavenumbers 1434 and 1036 cm^{-1} were due to involvement of carboxylic group, C−C stretching and C−O stretching of ether, ester and phenolic group in the Cr(VI) binding (Shi et al., 2014). Further, the IR absorption peaks at wavenumbers 874 and 685 cm^{-1} contributed by C−H stretching of aromatics and phenyl groups (Shi et al., 2014), respectively, play important role in the Cr(VI) binding. The other surface ligands such as C−H, O−H, C−O, C=O and phenyl groups are also found to be involved in metal ion binding as depicted in Fig. 6.1.

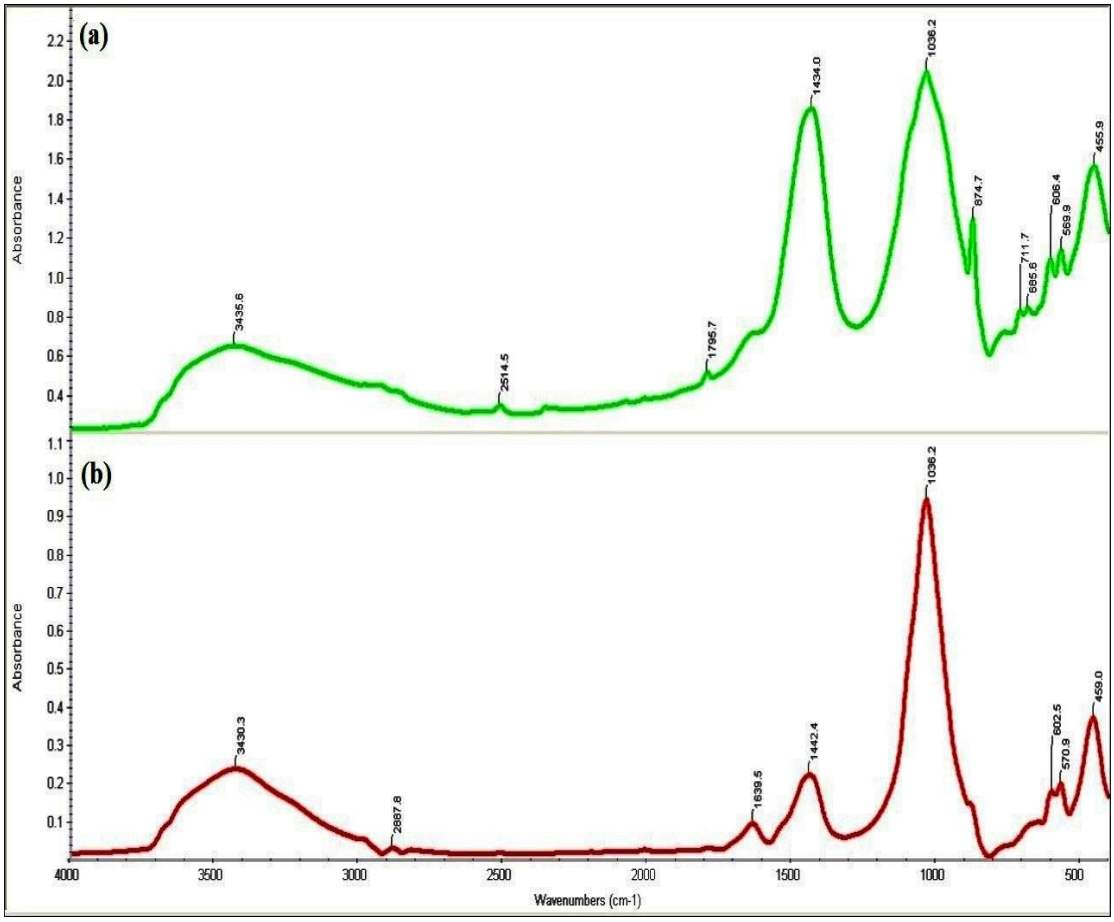

Fig. 6.1. IR-spectra of MPA (a) before and (b) after adsorption of Cr(VI) at pH 3.0.

The changes in IR absorption peaks at 3435.6 and 1434 cm^{-1}, assigned to hydroxyl group (O−H stretching) and methylene group (C−H bending), respectively, indicated the important role played by these functional groups in Cr(VI) removal by MPA particles (Mary et al., 2016). The IR peaks at wavenumber 874.7, 711.7 and 685.6 cm^{-1} assigned to alkene group (=C−H bending), amide V group and alkyl halide (C−Cl stretch), were completely lost after adsorption of Cr(VI). The emergence of new IR peaks at wavenumber 1639.5 and 2887.8 cm^{-1} were assigned to amide I group (NH_2^-) and alkyl group (C−H stretch) indicating the formation of new bonds between the surface ligands and Cr(VI) ions. The IR absorption peaks at wavenumber 2514.5 and 1795.7 cm^{-1}, characteristic of carboxylic group (O−H stretch) and carbonate anion (CO_3^{2-}), respectively, also disappeared after adsorption of Cr(VI) ions onto the surface

of MPA. These results indicated a strong interaction between organic functional groups on the surface of MPA adsorbent and Cr(VI) metal (Poletto et al., 2012). The changes in IR absorption peaks at wavenumbers 1434 and 1442 cm^{-1} associated with methylene group ($=CH_2$) and methyl group ($R-CH_3$) of lipids, could be due to steric hinderances caused due to adsorption of Cr(VI). The overall results on IR spectra of MPA after adsorption of Cr(VI) exhibit that hydroxyl, ester, amine, phenyl, carboxyl and carbonyl groups are the surface functional moieties which actively participated in the binding of Cr(VI) metal.

6.3.2. Cyclic Voltammetry: Reduction mechanisms of Cr(VI)

Cyclic voltammetry analysis was carried out to see whether a rapid color change of Cr(VI) solution (orange to pale green) in the presence of MPA adsorbent was associated with chemical transformation of Cr(VI) metal ions or not. The Cyclic Voltammetry test was performed on the Cr(VI) solution treated with MPA adsorbent for 190 min at 30ºC. The electrochemical behavior of Cr(VI) was analyzed over a potential range from -1.5V to +1.5 V (Ag/AgCl) with scan rate of 100 mV^{-1}. The cyclic voltammogram of Cr(VI) in the electrolytic solution exhibited two well-defined redox couple as shown in Fig 6.2. Results on Cyclic Voltammetry test showed cathodic (reduction) and anodic (oxidation) activities in the Cr(VI) metal ion solution, emphasizing that the reduction of Cr(VI) by MPA adsorbent particles through electron transfer process (Wyantutia et al., 20015). As we can see in Fig. 6.2., the redox couple (2) exhibited the redox reaction of Cr(VI) and Cr(III), whereas the redox reaction of Cr(III) and Cr(II) was indicated by redox couple (1). The cathodic peak (2d) in redox couple (2) appearing at 0.56V in the cyclic voltammogram was assigned to reduction of Cr(VI) to Cr(III). Similarly, the cathodic peak (1b) in the redox couple (1) appearing at -0.18V was assigned to reduction of Cr(III) to Cr (II).

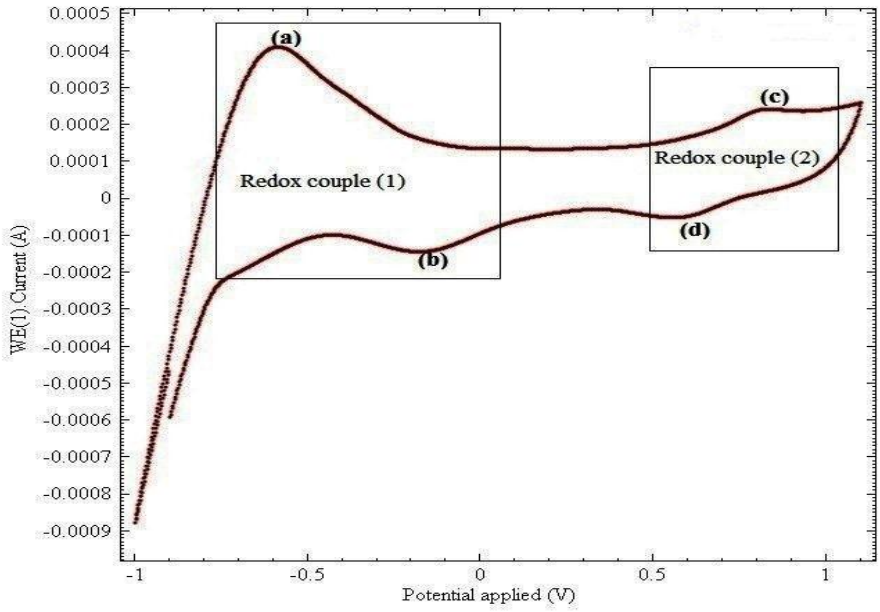

Fig. 6.2. Cyclic voltammogram of Cr(VI) solution treated with MPA [Potential range from -1.5V to +1.5 V (Ag/AgCl); Scan rate 100 m/V].

The anodic peak appearing at +0.8V in the redox couple (2c) could be assigned to oxidation of Cr(III) to Cr(II), whereas peak appearing at -0.60V in redox couple (1a) was assigned to oxidation Cr(II) to Cr(III). The coupled redox reaction for Cr(VI) in cyclic voltammetry test suggested that Cr(VI) metal ions adsorbed on the surface of MPA particles were reduced to Cr(III) and Cr(II) through reductive process (Liu et al., 2008). The several minerals and surface active ligands of MPA might be contributing one electron as electron donor for the reduction of Cr(VI) in step wise electron transfer reaction. The second step involving the reduction of Cr(III) was found to be slow, because the reduced Cr(III) was present in the form of a complex (chromium chloride complex) surrounded by neutral ligands (water and anions) octahedrally (Saha et al., 2011). Thus, the high residual concentration of Cr(III) in the solution required higher redox current for the reduction of Cr(III) to Cr(II) in redox couple (1) of cyclic voltammogram. Further, the redox couple (1) and (2) were found to be respectively

quasi-reversible and irreversible in nature (Liu et al., 2008). The slow and fast reaction involved in reduction of Cr(VI) to Cr(III) and Cr(II) are given as follows:

(i) $Cr^{6+} + 3e^{-} \rightarrow Cr^{3+}$ (Fast reaction)

(ii) $Cr^{3+} + e^{-} \rightarrow Cr^{2+}$ (Slow reaction, $1e^{-}$ transfer reaction)

6.3.3. X-Ray Photoelectron Spectroscopy (XPS): Removal mechanism of Cr(VI)

In order to analyze the chemical redox reaction occurred during adsorption of Cr(VI) onto the surface of MPA, it was essential to perform the analysis of chromium species present on the surface of adsorbent. The sorption mechanisms of Cr(VI) and presence of its reduced forms on the surface of MPA after adsorption were examined using X-Ray Photoelectron Spectroscopy (XPS) techniques. The XPS spectrum of MPA after adsorption of Cr(VI) was recorded to identify the possible chromium species present on the surface of adsorbent. The Cr 2p peaks in the binding energy range (0 – 1200 eV) and (570 – 595 eV) were analyzed as recorded in the spectrums given in the Fig. 6.3(a) and 6.3(b), respectively. The binding energy in the range of 572–581 eV and 582–591 eV correspond to Cr 2p3/2 and Cr 2p1/2 orbitals, respectively (Wu et al., 2009). Generally in Cr 2p XPS spectrum, hexavalent state (Cr(VI)) of chromium are characterized by higher binding energy such as 578.1 eV (CrO_3) and 579.2 eV ($K_2Cr_2O_7$) (Fathima et al., 2005), while the characteristics peak at binding energy 577.0 – 578.0 eV and 586.0 – 588.0 eV corresponds to Cr(III) form (Gu et al., 2012). In the present study, the binding energy (eV) peaks of Cr $2p_{3/2}$ and Cr $2p_{1/2}$ were detected at around 579.2, 588.8, 577.6, 588.0, 576.8 and 585.6 eV in the XPS spectrum of MPA after adsorption of Cr(VI). The band at binding energy 579.2 eV (Cr $2p_{3/2}$) and 588.8 eV (Cr $2p_{1/2}$) were assigned to Cr(VI) forms whereas the peaks at binding energies of 577.6 eV (Cr $2p_{3/2}$) and 588.0 eV (Cr $2p_{1/2}$) were assigned to Cr(III) forms of chromium

(Wu et al., 2009). Further, the next two peaks at binding energy of 576.8 eV (Cr $2p_{3/2}$) and 585.6 eV (Cr $2p_{1/2}$) were indicative of Cr(II) forms on the surface of MPA adsorbent. Therefore, the presence of Cr(III) and Cr(II) forms on surface of MPA particles indicated that the adsorbed Cr(VI) metal ions onto the surface of MPA was partially reduced to Cr(III) and Cr(II) forms during sorption process.

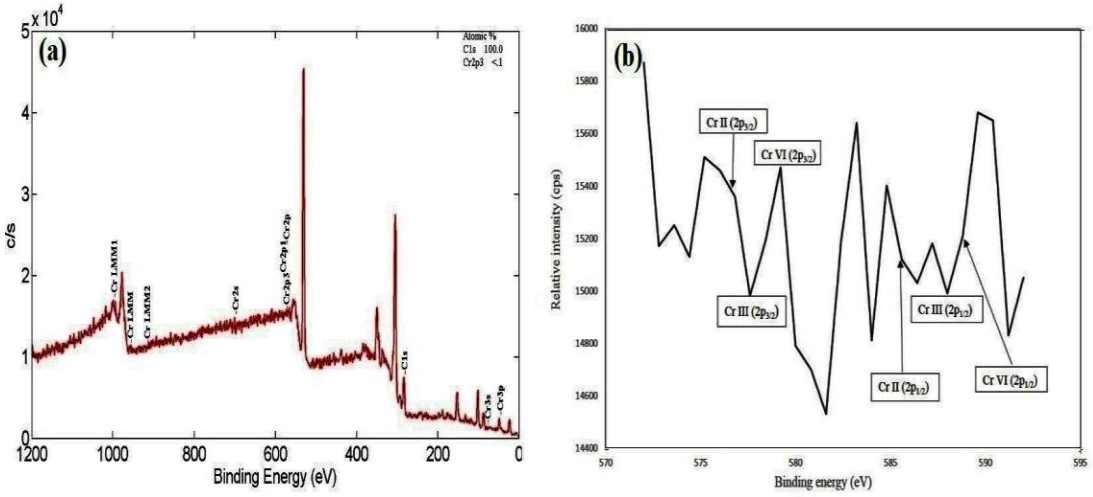

Fig. 6.3. XPS Cr 2p spectra of MPA in binding energy range (a) from 0 to 1200 eV and (b) from 570 to 595 eV after adsorption of Cr(VI).

The reduction of toxic Cr(VI) to less toxic Cr(III) and Cr(II) forms might be due to the reactive electron donor groups (−OH,−NH2,−COOH and >C=O) present on the surface of MPA. The removal mechanisms of Cr(VI) from aqueous solution by using MPA seems to be the combination of both surface adsorption and reduction of Cr(VI). The nitrogen atoms of amine groups, if protonated in acidic condition (pH 3.0), might be involved in bond formation with negatively charged $HCrO_4^-$ ions due to electrostatic attraction. After being adsorbed onto the surface of MPA particles, the Cr(VI) was partially reduced to Cr(III) and Cr(II) forms and subsequently, the reduced forms of Cr(III) and Cr(II) were released into the aqueous solution due to the electrostatic repulsion. But some of the Cr(III) and Cr(II) metal ions were still bound with the surface of MPA adsorbent, perhaps due to complex bonding with the nitrogen atoms of amine

group in MPA. It has been reported that positively charged Cr(III) and Cr(II) metal ions form coordinate bond with lone pair electron of nitrogen atom. Another possible explanation for the removal of Cr(VI) could be adsorption of Cr(III) and Cr(II) metal ions onto MPA particles due to its mesoporous structure and electronegative nature. Therefore, it has been concluded that the removal mechanism of Cr(VI) by MPA was dominated by both electrostatic adsorption and reduction process.

6.3.4. Factors affecting adsorption of Cr(VI)

6.3.4.1. Effect of adsorbent dose

The sorption capacity is greatly influenced by the dose of adsorbent (MPA) in removal of Cr(VI) from aqueous solution. The percent removal of Cr(VI) from aqueous solution by MPA as adsorbent was studied at varying adsorbent doses (0.1 to 0.5g/100 mL) and fixed concentration of Cr(VI) (10 mg L^{-1}). The rate of Cr(VI) adsorption was studied for 90 min at pH 3.0. As can be seen in Fig. 6.4(a), the percent removal of Cr(VI) was increased from 47.9 to 70.1 % with increase in the dose of adsorbent from 0.1 to 0.5 g/100 mL. A time dependent adsorption showed a rapid phase of dose-dependent increase in removal of Cr(VI) metal which continued to occur up to 0.2 g/100 mL dose of MPA and that was followed by a sluggish phase of Cr(VI) removal between 0.2 to 0.5 g/100 mL of adsorbent dose. Initially a faster rate of Cr(VI) adsorption might be the result of increase in number of available adsorption sites with increase in dose of adsorbent. A sluggish increase in Cr(VI) metal ion removal at higher doses of adsorbent (0.2 to 0.5 g/100 mL) might be due to reduced availability of metal ions binding sites per unit concentration of adsorbent. Otherwise this could be interpreted as clustering of adsorbent particles per unit volume which might be hindering the free mobility of the metal ions to adsorption sites and might be termed as shadowing effect of adsorbent on the accessibility of adsorbate (Guo et al., 2017).

6.3.4.2. Effect of pH

The pH of the solution was found to be an important controlling factor in the adsorption of Cr(VI), as the charge density of the adsorbent surface and adsorbate species are mainly dependent on pH of the aqueous medium. In order to see the effect of pH on Cr(VI) adsorption, batch adsorption experiments were carried out by varying the pH of the aqueous solution (pH 3.0 to 8.0) at an initial concentration of Cr(VI) at 10 mg L^{-1} and adsorbent concentration of 0.1 g/100 mL. The effects of pH condition of the solution on percent removal of Cr(VI) has been shown in Fig. 6.4(b). The results showed that the percent removal of Cr(VI) decreased from 46.8 to 29.9 % with increase in pH from 3.0 to 8.0, indicating that low pH range (pH 3.0–4.0) was more favorable for the binding of Cr(VI) metal ions onto MPA particles. The pH dependent Cr(VI) removal might be related to surface functional groups of MPA adsorbent and chemistry of the Cr(VI) metal ions in the aqueous solution (Guo et al., 2017; Gupta et al., 2001). Usually the Cr(VI) has different forms such as CrO_4^{2-}, $HCrO_4^-$, $Cr_2O_7^{2-}$ in wastewater, which are directly associated with pH of the wastewater as suggested by earlier workers (Chen et al., 2010). Based on the FTIR results, it was observed that the surface of MPA particles contains various functional groups such as hydroxyl, amine, ester, carbonyl and carboxylic groups, which are actively involved in the binding of Cr(VI) metal ions. At acidic pH conditions (pH 3.0–4.0), the surface functional groups of MPA particles become protonated and the protonated functional groups complex with Cr(VI) metal ions forms that mainly existed in solution as species of $HCrO_4^-$ and $Cr_2O_7^{2-}$ through an electrostatic attraction and ion exchange process. On the other hand, at alkaline pH conditions, the negatively charged surface of MPA particles was not suitable to bind with Cr(VI) metal ions. Generally, at neutral (pH 7.0) and alkaline pH conditions, Cr(VI) mainly exists in the form of $CrO4^{2-}$ anions which is repelled by negative surface

charge on MPA. Thus, at higher pH values, the electrostatic repulsion between the adsorbent surface and chromate species decreased the overall rate of Cr(VI) removal from aqueous solution.

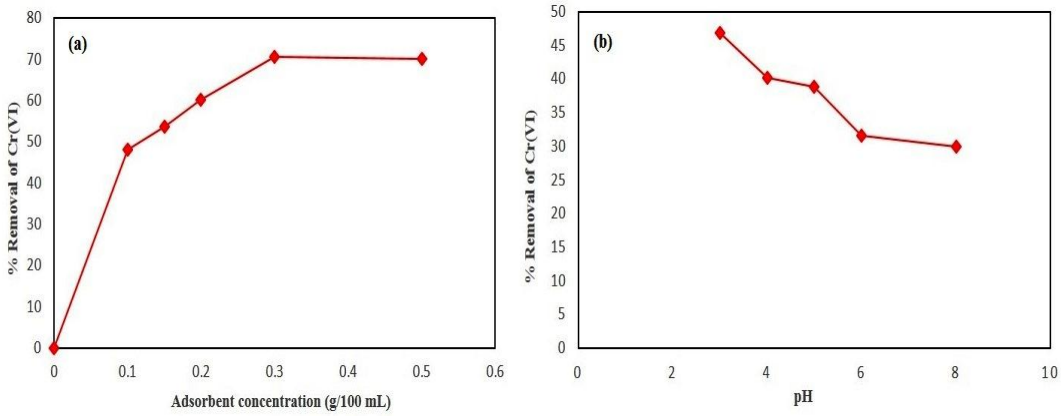

Fig. 6.4. Effect of (a) adsorbent dose and (b) pH on percentage removal of Cr(VI) using MPA [initial Cr(VI) concentration 10 mg/L, Time 90 min, Adsorbent concentration 0.1g/100 mL, temperature 303 K].

6.3.4.3. Effect of initial Cr(VI) concentration and contact time

The effect of initial Cr(VI) concentration on the adsorption capacity of MPA depends on the availability of metal ions and surface binding sites of MPA particles. The extent of Cr(VI) removal is greatly influenced by the initial metal ion concentration in aqueous solution. In the present study, the effect of different initial Cr(VI) concentration (10–50 mg L^{-1}) was studied on the adsorption of Cr(VI) for 90 min at a fixed dose of adsorbent (0.1 g/100 mL) at room temperature and pH 3.0. The results in Fig. 6.5 on the adsorption of Cr(VI) by MPA at different metal ion concentration showed initially a rapid sorption process up to 30 min, followed by sluggish sorption process with increase in the contact time up to 90 min, perhaps due to saturation of adsorption sites on the surface of adsorbent (Guo et al., 2017). Further, the removal of Cr(VI) after 90 minutes was found to be insignificant. A fast rate of metal ion adsorption at the initial contact time might be attributed to the availability of a large number of adsorption sites. The rate of metal ion adsorption increased in a concentration-dependent manner and the saturating

concentration of Cr(VI) at equilibrium (q_e) was found to be between 5.1 to 6.01 mg g^{-1} with increase in the initial metal ion concentration from 10 to 50 mg L^{-1}. An increase in adsorption capacity of MPA with increase in Cr(VI) concentrations, might be due to relatively higher rate of mass transfer (Thirumavalavan et al., 2012). But the sluggish increase in the rate of metal ion adsorption at higher concentration could be attributed to a limiting dose of adsorbent (Thirumavalavan et al., 2012).

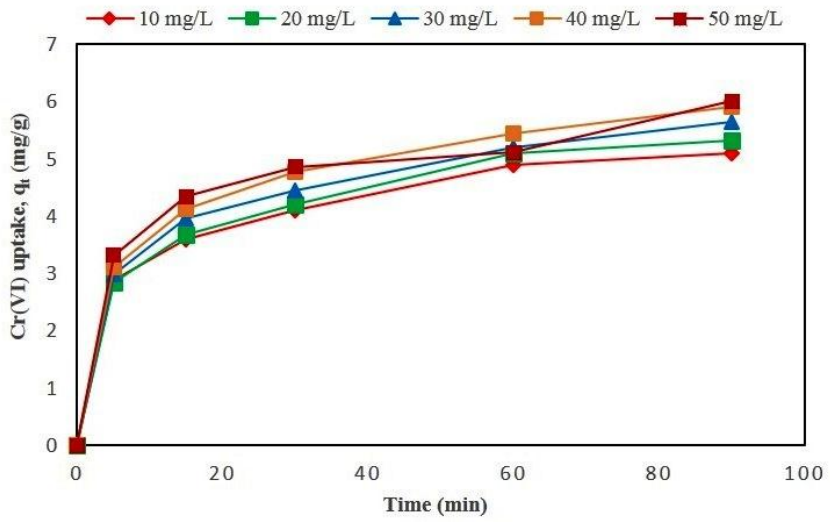

Fig. 6.5. Effect of initial Cr(VI) concentration on adsorption capacity (mg/g) per unit concentration of MPA [Adsorbent concentration 0.1 g/100 mL, pH 3.0, Time 90 min, temperature 303 K].

6.3.5. Adsorption kinetics

Adsorption kinetics not only helpful in determination of rate of sorption process but also provides insights into possible reaction mechanisms involved in the removal of Cr(VI) from aqueous solution. Pseudo-first order (Fig. 6.6(a)) and Pseudo-second order kinetic model (Fig. 6.6(b)) were applied on experimental data to analyze the adsorption kinetics for the sorption of Cr(VI) onto MPA adsorbent. The sorption kinetics of Cr(VI) by MPA adsorbent was studied as a function of varying time intervals at different initial concentrations of Cr(VI). The calculated kinetic parameters at different initial Cr(VI) concentrations could describe the sorption process of Cr(VI) by MPA as listed in Table 6.1. Results (Table 6.1) showed that adsorption data fitted well to the Pseudo-second

order kinetic model (R^2 >0.99) than to pseudo-first order kinetic model (R^2 >0.91). The experimental q_e values (equilibrium adsorption capacity) were in close agreement with the calculated q_e values derived from the pseudo-second order model, whereas the q_e values calculated from the pseudo-first order model were not in good agreement with the experimental q_e values. Further, the results indicated that the rate constant (k_2) decreased with the increase in the initial Cr(VI) concentration (Table 6.1), which is a typical behavior for the sorption process fitting to pseudo-second order kinetic model as reported in earlier studies on the adsorption (Abbas et al., 2014; Konicki et al., 2013). The results on pseudo-second order adsorption kinetics implied that the sorption of Cr(VI) was an almost controlled chemisorption process. It has been demonstrated that the pseudo-second-order kinetic model is based on the supposition that the rate-controlling step in the sorption process is the surface adsorption by valence forces through sharing or exchanging of electrons between adsorbent particles and adsorbate molecules (Pang et al., 2011).

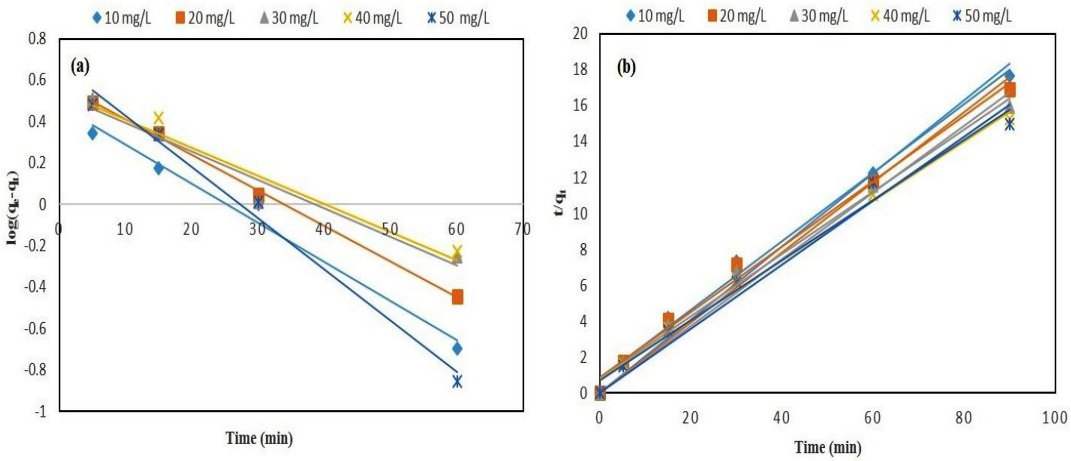

Fig. 6.6. Adsorption kinetics (a) Pseudo-first order and (b) Pseudo-second order kinetic model for the sorption of Cr(VI) onto MPA [Time 90 min, pH 3.0, adsorbent concentration 0.1 g/100 mL, initial Cr(VI) concentration 10 to 50 mg/L].

Table 6.1. First and second order kinetic parameters for the sorption of Cr(VI) onto MPA adsorbent.

Conc. (mg/L)	q_e, exp. (mg/g)	Pseudo-first order kinetics			Pseudo-second order kinetics		
		k_1 (1/min)	q_e, cal. (mg/g)	R^2	k_2 (mg/g min)	q_e, cal (mg/g)	R^2
10	5.1	0.069	1.45	0.954	0.212	4.98	0.999
20	6.01	0.075	2.91	0.912	0.098	6.12	0.987
30	7.12	0.121	11.23	0.963	0.039	7.02	0.988
40	7.98	0.059	2.93	0.972	0.069	8.01	0.995
50	8.12	0.071	13.12	0.921	0.048	8.08	0.997

6.3.6. Adsorption isotherms

Adsorption isotherms (Langmuir and Freundlich) were applied on equilibrium experimental data to obtain the valuable information about the monolayer chemisorption of Cr(VI) metal ions on the surface of the MPA particles and determine adsorption capacity (mg g^{-1}). The results showed that both Langmuir and Freundlich adsorption isotherms (Fig. 6.7) were fitted well with the data on equilibrium sorption of Cr(VI) onto MPA particles. It has already been reported that the high mineral content in MPA indicating more surface functional groups on the surface and make it appropriate for the sorption of Cr(VI) metal ions (Guo et al., 2017). According to Langmuir isotherm model, the maximum monolayer adsorption capacity (q_{max}) of MPA at room temperature (30ºC) and pH 3.0 was calculated as 8.63 mg g^{-1}. The q_{max} value of MPA represents single layer surface adsorption of Cr(VI) metal ions and maximum binding of Cr(VI) with the large number of oxygen containing functional groups present

on the surface of MPA as described earlier in IR-Spectroscopy (FTIR) of MPA. An electrostatic interaction and ion exchange mechanisms might be involved in the binding of Cr(VI) metal ions with the hydroxyl, carbonyl, phenyl and carboxyl functional groups disseminated on the surface of MPA particles (Guo et al., 2017).

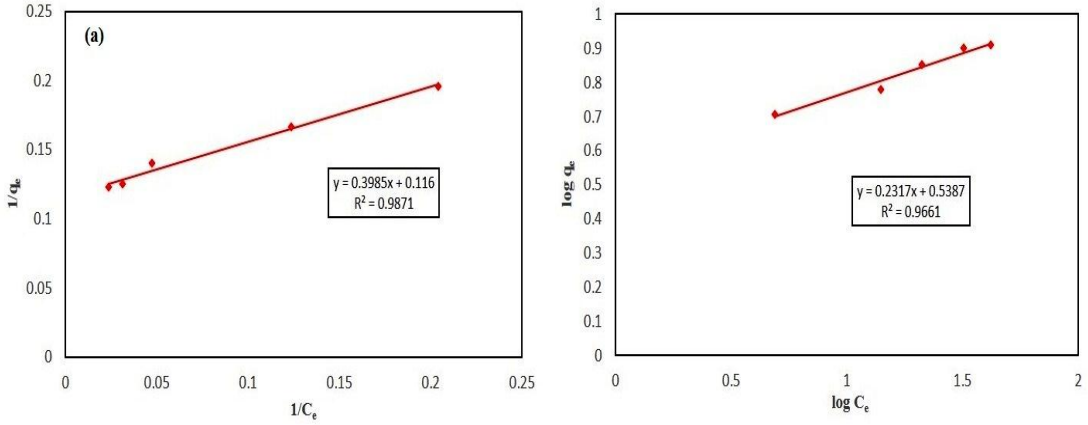

Fig. 6.7. Adsorption isotherms (a) Langmuir and (b) Freundlich model for the sorption of Cr(VI) [adsorbent concentration 0.1g/100 mL, pH 3.0, Time 90 min, initial Cr(VI) concentration range 10 to 50 mg/L].

The regression coefficient (R^2) values in both the adsorption isotherms are shown in Table 6.2. The R^2 values indicated better applicability of Langmuir as well as Freundlich isotherms to describe the nature of MPA adsorbent for equilibrium adsorption and fitted well to the equilibrium adsorption data of Cr(VI). MPA adsorbent had strong affinity for Cr(VI) adsorption supported by R_L values (Table 6.3). The calculated R_L values of MPA (0.451 to 0.592) at different Cr(VI) concentration (10 to 50 mg g^{-1}) indicated favorable adsorption process (Hameed et al., 2008). The R_L values between 0 and 1 indicated a favourable adsorption with more affinity of MPA particles towards Cr(VI) metal ions. The high R^2 values and value of $1/n < 1$ for MPA (0.2318) in Freundlich isotherm also confirmed the role of chemisorption on the heterogeneous surface of MPA particles (Guo et al., 2017). The q_{max} values of different sorbent materials in removal of Cr(VI), as given in Table 6.4, were used to compare the q_{max}

value of MPA. A comparison of adsorption capacity of different adsorbents suggested that MPA is better adsorbent than many other reported adsorbents.

Table 6.2. Langmuir and Freundlich constants for the sorption of Cr(VI) onto MPA adsorbent.

Langmuir isotherm			**Freundlich isotherm**		
q_{max} (mg g^{-1})	b (L mg^{-1})	R^2	1/n	K_F (mg g^{-1})	R^2
8.63	0.04623	0.988	0.2318	0.2892	0.967

Table 6.3. Separation factor (R_L) at different Cr(VI) concentration for MPA.

Initial concentration (mg L^{-1})	**Seperation factor (R_L)**
10	0.451
20	0.521
30	0.695
40	0.393
50	0.592

Table 6.4. A list of adsorbents including MPA and their adsorption capacities for the removal of Cr(VI).

Adsorbents	**q_{max} (mg g^{-1})**	**References**
Almond	10.62	Dakiky et al. (2002)
Carbon slurry	25.60	Singh and Tiwari (1997)
Coconut husk fibres	29.0	Hamadi et al. (2001)
Paper mill sludge	7.4	Calace et al. (2002)
Olive cake	33.44	Dakiky et al. (2002)
Coal	6.78	Dakiky et al. (2002)
Saw dust	15.82	Dakiky et al. (2002)
Almond pine needles	21.50	Dakiky et al. (2002)
Mentha Plant Ash (MPA)	8.63	Present Study

6.3.7. Thermodynamic studies for the sorption of Cr(VI)

In the present experiment, the Cr(VI) binding by the adsorbent (MPA) was recorded as a function of varying temperature (293.15 to 323.15 K) at 10 mg L^{-1} of initial Cr(VI) concentration and pH 3.0 for 90 min. The amount of Cr(VI) adsorption by MPA increased from 5.1 to 6.9 mg g^{-1} with rise in temperature, which indicated endothermic adsorption process. An increase in temperature can enhance kinetic mobility of Cr(VI) metal ions and accelerates active binding of sorbate with adsorbent (Salleh et al., 2011). On the other hand, a decline in the Cr(VI) adsorption with the increasing temperature is an indicator of exothermic adsorption process which may be due to decrease in adsorptive forces between the metal ions and active binding sites as suggested earlier (Salleh et al., 2011). In the present investigation, temperature dependent increase in Cr(VI) adsorption by MPA could be due to increase in kinetic mobility of Cr(VI) and enhanced number of surface active ligands available for adsorption (Mohan et al., 2002). Results in Table 6.5 showed negative values of $\Delta G°$ from -0.0974 to -2.1486 kJ/mol at all the chosen temperature, which showed that the adsorption of Cr(VI) onto MPA particles was thermodynamically feasible and spontaneous process (Baek et al., 2010). The free energy change ($\Delta G°$) with negative value for adsorption supported the view that the removal of Cr(VI) by MPA was a favourable adsorption process. An increase in negative value of $\Delta G°$ with rising temperature specified that the process of adsorption was more favourable at lower temperature (Chowdhury and Saha, 2010). The Von't Hoff plot for MPA (Fig. 6.8) was used to determine the enthalpy ($\Delta H°$) and entropy ($\Delta S°$) values. The results showed positive values of $\Delta H°$ (19.65 KJ mol^{-1}**)** for MPA, indicating that the adsorption process was endothermic and nature of interaction between MPA particles and Cr(VI) metal ions was physico-chemisorption process (Ghasemi and Asadpour, 2007). The endothermic nature of Cr(VI) adsorption by MPA

particles indicated that bonding energy might be deriving the required energy from hydration shell of Cr(VI) metal ions (Ahmad and Kumar, 2010). The positive values of ΔS° for MPA (67.56 J mol^{-1} K^{-1}) was supporting involvement of hydration energy of the Cr(VI) metal ions in the metal bonding released during the sorption of metal ions. Thus, increase in entropy might be contributing to an increase in the degree of freedom of the water molecules as suggested earlier (Ghasemi and Asadpour, 2007; Baek et al., 2010).

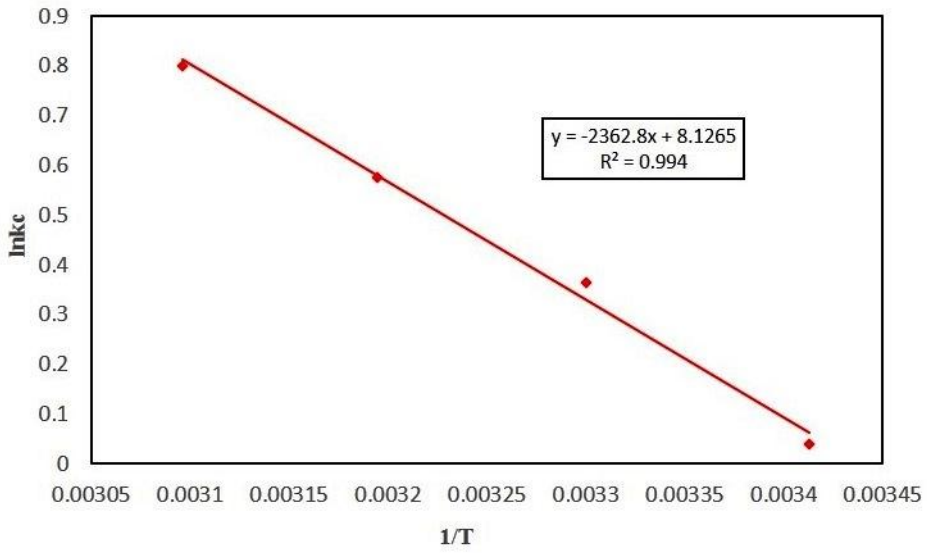

Fig. 6.8. Vont'hoff plot for the calculation of thermodynamic parameters in removal of Cr(VI) by MPA [initial Cr(VI) concentration 10 mg/L, Time 90 min, pH 3.0, adsorbent concentration 0.1g/100 mL].

Table 6.5. Thermodynamic parameters for the sorption of Cr(VI) onto MPA.

T(K)	ΔG°(kJ/mol)	ΔH° (kJ/mol)	ΔS° (J/mol K)
293	-0.09745	19.65	67.56
303	-0.91688		
313	-1.49726		
323	-2.14866		

CHAPTER-VII

General Discussions

The chemically rough surface of MPA particles with heterogenous structure of pores as confirmed by SEM analysis, played a crucial role in monolayer and multilayer adsorption of cationic dyes (MG and MB) and Cr(VI). Presence of small heterogenous layers of pores on the surface of MPA particles might be due to the volatilization and decomposition of various biomolecules present in the plant waste material. Generally, the waste plant materials contain high content of volatile matter and low lignin content which directly affects the formation of heterogenous pore stuctures on the surface of adsorbent particles (Lehmann et al., 2011). The complex and fibrous structures of MPA particles might be more helpful in adsorption of dyes and Cr(VI), which developed due to aggregation of various cellulosic structures and mineral compounds during combustion of plant waste material at higher temperature (850ºC) as suggested by other workers (Yargicoglu et al., 2014; Fernandez et al., 2012). The variation in particle surface, shrinking and splitting of MPA particles was observed due to volatization of organic matter during thermal combustion (450 – 800 ºC). A chemically rough surface of MPA particles might be due to presence of high content of Si minerals as indicated in EDX analysis. The mineral composition of MPA included a very high content of C, O, Mg, Cl, K, Si, Fe and Ca, which were exceptionally higher in the MPA than that reported in other adsorbents (Lehmann et al., 2011).

In the BET analysis of adsorbent, the shape of the N_2 adsorption/desorption isotherm matches the Type IV shape of adsorption isotherm (IUPAC classification), indicating a mesoporous structure of MPA. An important characteristic of Type IV isotherm corresponds with monolayer-multilayer adsorption and are indicative of relatively strong interaction between adsorbent surface and adsorbate as suggested by earlier investigators (Sing et al., 1985). In the present study, the small BET specific surface area of MPA (7.169 m^2 g^{-1}) might be due to filling of pores largely with resins and

minerals, which interfere with the diffusion of nitrogen molecules (Rawat and Singh, 2017). The pore size distribution of MPA particles, as determined by BJH plot, was found to be in the range of 3–25 nm, indicating mesoporous nature of the adsorbent. The pore diameter of particles ranging between 2 to 50 nm, indicated a mesoporous nature of adsorbent material (Sing et al., 1985). The results derived from BET and BJH methods suggested that the adsorbent (MPA) was mesoporous material, which played crucial role in adsorption of dyes and heavy metals as suggested by the earlier investigators (Sing et al., 1985; Rawat and Singh, 2017).

Presence of low boiling volatile organic matter, moisture content, the residual content of hemicellulose, cellulose and lignin in the MPA were played an important role in the binding of dyes molecules and Cr(VI) metal ions. Since the biomolecules (hemicellulose, cellulose and lignin) contain a number of oxygen containing functional groups which favour binding of cationic dyes and Cr(VI) as suggested by earlier workers (Guo et al., 2017; Qi et al., 2010). In thermogravimetric analysis (TGA), the first phase of weight loss was related to release of H_2O molecules and low boiling volatile organic matter (Zhang et al., 2006). The second phase of weight loss during thermal change (180 – 700°C) assigned to the decomposition of hemicellulose (200 – 300°C), cellulose (300 – 400°C) and lignin (200 – 700°C) and their conversion to CO_2, CO and CH_4 (Liu et al., 2012). The third phase of weight loss during thermal change (700 – 850°C) might be related to decomposition of lignin (160 – 900°C). It has been reported that decomposition of calcite ($CaCO_3$) and release of CO_2 result into greater thermal stability of material during the third phase of weight loss (Qi et al., 2010). Different stages of weight loss during thermal decomposition were indicative of changes in organic and inorganic contents of MPA which helps in the assessment of type of surface functional groups present in a biomolecules.

The presence of silica clay minerals such as calcite, quartz, sylvite and dolomite were confirmed in the XRD pattern of MPA adsorbent. The intense sharp peaks at 3.36Å indicated well crystalline form of quartz was present in higher amount as compared to other minerals present in MPA (Yuan et al., 2011). An increase in the peak intensity at 4.53 and 3.03 Å in the XRD pattern of MPA with increase in temperature from 450 to 850ºC, also suggested that high content of crystalline cellulose and calcite were present in MPA. It has been reported that the adsorption potential of sorbents is mainly dependent on the net negative charges present on the silica clay minerals of sorbents (Elmoubarki et al., 2015). The negative charges on MPA favoured adsorption of positively charged cationic dyes (MG and MB). An exchangeable ions in clay minerals were found to play a vital role in the removal of cationic dyes and Cr(VI) through adsorption and ion exchange process (Eren, 2010). The most common ions in clay minerals of MPA included H^+, K^+, Na^+, Ca^{2+}, Mg^{2+}, NH_4^+, Cl^-, SO_4^{2-}, PO_4^{3-} and NO_3^- which exhibited a strong attraction towards the cationic dyes and Cr(VI) metal ions as suggested by the earlier workers (Crini, 2006).

The values of zeta potential of MPA particles (–37.1 mV) at neutral pH 7.0 indicated a highly negatively charged sorption surface of MPA particles with little effect of pH condition. As the ambient pH condition increases, the zeta potential of MPA became slightly more negative. A highly electronegative surface along with little effect of changing pH condition on the zeta potential indicated about larger contribution of salts and minerals in determining the zeta potential (Aksoy and Kaya, 2011). This could be the reason for high binding efficiency of MPA for cationic dyes (MG and MB) and Cr(VI) metal ions (Bootharaju and Pradeep, 2013). Similar observations have been made by earlier workers on zeta potential of quartz powder with isoelectric point (iep)

at around pH 2.0 and zeta potential ranging from –15 mV at pH 4.0 to –56 mV at pH 10.5 (Huang and Fuerstenau, 2001).

The IR-spectra (FTIR) of MPA exhibited stretching vibration of various functional groups such as O−H carboxylic groups, aliphatic C–H stretching vibration of methyl groups and C− O stretching of C–OH group (Ding et al., 2016), which largely contributed to more electronegative surface of MPA adsorbent. Different IR absorption peaks in the IR absorption spectrum of MPA indicated a crucial role of C–H deformation, C–C and C–O stretching of ester and phenyl group, strong bend in C–H phenyl rings, in determining a high negative zeta potential values of MPA particles (Shi et al., 2014). The IR peaks at wavenumbers 3435.6, 1797, 1434 and 1036 cm^{-1} correspond to O–H stretching of carboxyl group (Mary et al., 2016), C=O stretching of carboxyl groups (Ding et al., 2016), C–H variable alkenes groups, C–C and C–O vibrations in esters, ether or phenol (Shi et al., 2014), respectively. These surface functional groups of MPA might be playing an active role in an electrostatic attraction of the cationic dye molecules and Cr(VI) metal ions. The overall results on IR spectra of MPA exhibited that hydroxyl, ester, amine, phenyl, carboxyl and carbonyl groups were the main surface functional moieties, not only contributing to negative charge on surface of MPA, but may be actively involved in the binding of cationic dyes and Cr(VI) metal ions as suggested by other workers (Shi et al., 2014; Ding et al., 2016).

The cyclic voltammograms of cationic dyes (MG and MB) and Cr(VI) in the electrolytic solution showed a well-defined redox couples. In cyclic voltammetry (CV) test, the cathodic (reduction) and anodic (oxidation) activities in solution of cationic dyes and Cr(VI) metal in the presence of MPA, emphasized that the reduction of cationic dyes/Cr(VI) by MPA particles through one electron transfer process (Ngamukot et al., 2006; Farsi and Hosseini 2013; Wyantutia et al., 20015). In the cyclic

voltammograms of MG and MB dyes, the peak 1 (cathodic) appearing at approximately –0.32V and –0.52V were assigned to the reduction of MG^+ to neutral leuco malachite green (LMG) and reduction of MB^+ to Leucomethylene blue (LMB), respectively, by one electron transfer reaction, whereas peak 2 (anodic) at –0.34V and –0.38V might be related to oxidation of neutral LMG to MG^+ and LMB to MB^+, respectively, indicating reversible nature of redox process for both MG and MB dye solution in the presence of MPA (Ngamukot et al., 2006). Further, the presence of two well-defined redox couple in the cyclic voltammogram of Cr(VI) exhibited the redox reactions of Cr(VI) to Cr(III) and Cr(III) to Cr(II). The second step involved in the reduction of Cr(III) to Cr(II) was found to be slower, because the reduced Cr(III) was present in a complex form (chromium chloride complex) surrounded by neutral ligands (water and anions) octahedrally (Saha et al., 2011). The residual concentration of Cr(III) and Cr(II) in the solution become high and therefore, redox current was high as recorded in redox couple (1) of cyclic voltammogram. Further, the redox couple (1) and (2) were found to be respectively quasi-reversible and irreversible in nature (Liu et al., 2008). The coupled redox reaction for cationic dyes in CV test suggested that MG^+ and MB^+ cations adsorbed on the surface of MPA particles were changed to LMG and LMB, respectively, through reductive process (Ngamukot et al., 2006; Farsi and Hosseini 2013). Further, the coupled redox reaction for Cr(VI) suggested that Cr(VI) metal ions adsorbed on the surface of MPA particles were partially reduced to less toxic Cr(III) and Cr(II) through reductive process (Liu et al., 2008). The several minerals and surface active ligands of MPA might be contributing as electron donor and the reduction of cationic dyes and Cr(VI) occurred through step wise electron transfer reaction.

The XPS analysis also showed the presence of Cr(III) and Cr(II) forms on surface of MPA particles after adsorption which indicated that the adsorbed Cr(VI) metal ions

onto the surface of MPA was partially reduced to Cr(III) and Cr(II) forms during sorption process. The reduction of toxic Cr(VI) to less toxic forms of Cr(III) and Cr(II) might be due to the presence of reactive electron donor groups (−OH,−NH_2,−COOH and >C=O) present on the surface of MPA. The removal mechanisms of Cr(VI) from aqueous solution by using MPA seems to be the combination of both surface adsorption and reduction of Cr(VI). The nitrogen atoms of amine groups get protonated at acidic condition (pH 3.0) and the protonated nitrogen atoms might be involved in bond formation with negatively charged $HCrO_4^-$ ions by electrostatic attraction. After being adsorbed onto the surface of MPA particles, the Cr(VI) was partially reduced to Cr(III) and Cr(II) forms and subsequently, the reduced forms Cr(III) and Cr(II) were released into the aqueous solution due to the electrostatic repulsion. But some of the Cr(III) and Cr(II) metal ions were still bound on the surface of MPA adsorbent, which can be explained in terms of protonated amine group in MPA adsorbent at acidic pH can form coordinate bond with positively charged Cr(III) and Cr(II) metal ions due to presence of lone pair electrons of nitrogen atoms (Fathima et al., 2005). Another possible explanation for removal of Cr by MPA particles might be due to ability of mesoporous MPA to adsorb Cr(III) and Cr(II) metal ions. Therefore, it has been concluded that the removal mechanism of Cr(VI) by MPA was dominated by both electrostatic adsorption and reduction process.

The effect of contact time on removal of cationic dyes and Cr(VI) by MPA from the ambient aqueous medium played a key role in determining equilibrium time and amount of dye/metal ion adsorbed at equilibrium stage. The adsorption of MG and MB dyes by MPA initially occurred at a faster rate, up to first five minutes of incubation and resulted into removal of 72.86 and 74.68 % dye, respectively. Further, the adsorption of Cr(VI) by MPA showed initially a rapid sorption process up to 30 min,

followed by sluggish phase of the Cr sorption process with increase in the contact time from 30 min to 90 min. Further, the removal of Cr(VI) after 90 minutes was found to be insignificant. A rapid rate of initial dye/metal ion removal by MPA could be due to maximum availability of vacant binding sites on the surface of adsorbent, ensuring high efficiency of dye/metal ion removal as suggested by earlier workers (Sen and Sarzali, 2008, Guo et al., 2017). The subsequent stage of slower rate of dye/heavy metal removal after certain time could be attributed to less availability of binding ligands on the surface of MPA. Ansari and Mosayebzadeh (2010) have reported that the sorption capacity increases with increase in contact time to a certain limit, but further increase in contact time does not increase the adsorption capacity due to saturation of all the active sites within a short span on the surface of adsorbent. Earlier, workers have also demonstrated an initial fast phase, followed by slow phase of dye/metal ion adsorption onto adsorbents due to saturation of available adsorption sites (Shayesteh et al., 2016; Guo et al., 2017).

The removal of cationic dyes and Cr(VI) by MPA was highly dependent on the dose of adsorbent added to the solution. A rapid phase of dose-dependent increase in MG and MB dye removal occurred up to 0.1 g/100 mL dose of MPA and this was followed by sluggish phase of dye removal between 0.1 to 0.3 g/100 mL of dose of adsorbent. But in case of Cr(VI) removal by MPA, a rapid phase of dose-dependent increase in Cr(VI) removal occurred up to 0.2 g/100 mL dose of MPA and this was followed a sluggish phase of Cr(VI) removal between 0.2 to 0.5 g/100 mL of dose of adsorbent. It has been suggested that number of available adsorption sites increases in a dose-dependent manner, the rate of dye and heavy metal removal also increases (Ahmad, 2009). A sluggish increase in the removal of cationic dyes and Cr(VI) at higher doses of adsorbent may be due to less availability of adsorbate molecules per unit concentration

of adsorbent (Guo et al., 2017). It may otherwise be said that clustering of adsorbent particles per unit volume might be hindering the free mobility of the adsorbate molecules approaching to the adsorption sites on the surface of adsorbent (Garg et al., 2003; Guo et al., 2017).

The results on pH dependent MG and MB dye removal showed relatively lesser adsorption of dyes at acidic pH (4.0) and gradual increase in the removal of dye between pH 4.0 to pH 10.0. Thus, the initial pH condition of the dye and heavy metal solution can influence the chemistry of both dye/metal ions as well as overall surface charge potential of the adsorbent (Shayesteh et al., 2015). It has been reported that variation in pH condition of the solution leads to variation in the degree of ionization of the chemical moieties on the surface of the adsorbent as well as ionization potential of adsorbate molecule (Nandi et al., 2009). The least adsorption of MG and MB dyes at acidic pH 4.0, perhaps due to protonation of the electronegative moieties on the surface of adsorbent (MPA) at acidic pH, was not favourable for the adsorption of cationic dyes. Besides, protonation of MG and MB dye molecules at acidic pH may also hinders the active binding between the adsorbent particles and adsorbate molecules and thereby, reducing the adsorption capacity (Ncibi et al., 2007). A high rate of dye removal at alkaline pH could be due to increase in the net negative charge of adsorption sites on the surface of the adsorbent, which facilitates the adsorption of cationic MG and MB dyes. Earlier, workers have also demonstrated a high rate of dye removal at pH 10.0 by spent tea active carbon (Akar et al., 2013). Earlier findings also demonstrated that an increase in electrostatic interaction between the dye molecule and surface binding ligands was responsible for faster rate of dye adsorption (Mittal et al., 2010). But in case of Cr(VI) adsorption by MPA, the percent removal of Cr(VI) was decreased from 50.16% to 27.84% with increase in pH from 3.0 to 8.0, exhibiting that low pH range

(pH 2.0–3.0) was more favorable for the binding of Cr(VI) metal ions onto the MPA particles. Thus, the pH dependent Cr(VI) removal could be related to surface functional groups of MPA and the chemistry of Cr(VI) (Guo et al., 2017; Gupta et al., 2001). It is well known that the Cr(VI) exists in different forms such as CrO_4^{2-}, $HCrO_4^-$, $Cr_2O_7^{2-}$ in wastewater, which are directly associated with pH of the wastewater (Chen et al., 2010). Based on the FTIR findings, it was observed that the surface of MPA contains various functional groups such as hydroxyl, amine, ester, carbonyl and carboxylic groups, which are actively involved in the binding of Cr(VI) metal ions. At lower pH 3.0 and 4.0, the surface functional groups become positively charged and complex with Cr(VI) metal ions that mainly existed in the anionic $HCrO_4^-$ and $Cr_2O_7^{2-}$ forms through ion exchange and electrostatic attraction (Chen et al., 2010). On the other hand, at higher pH conditions, the surface of MPA become negative charged, which was not suitable to bind with anionic Cr(VI) metal ions. Generally, at neutral (pH 7.0) and alkaline pH, Cr(VI) in the solution exists only in the form of $CrO4^{2-}$ (Gupta et al., 2001). The increase in OH^- group with the increase in pH of the solution, results into electrostatic repulsion of $CrO4^{2-}$. However, at higher pH values, the electrostatic repulsion between the adsorbent surface and chromate species could lower the rate of removal of Cr(VI) from aqueous solution as suggested by earlier workers (Guo et al., 2017).

The effect of initial dye/metal ion concentration on the adsorption capacity of MPA was also dependent on the availability of adsorbate molecules (dye/heavy metal) in aqueous solution as well as surface binding ligands on MPA particles. The removal of MG and MB dyes by MPA showed initial concentration dependent rapid increase in the rate of dye removal up to 15 min, followed by slowing down of the process with increase in the contact time up to 30 min, perhaps due to less availability of free adsorption sites

on the surface of adsorbent (Saha et al., 2010). Further removal of dye after 30 minutes was found to be insignificant. At different initial dye concentration, the equilibrium stage and maximum uptake of total amount of MG and MB dyes were observed within 45 and 30 min, respectively. In removal of Cr(VI) by MPA, the adsorption of Cr(VI) at different metal ion concentration showed initially a rapid sorption process up to 60 min, followed by slowing down of the sorption process with increase in the contact time up to 90 min, perhaps due to less availability of adsorption sites on the surface of adsorbent (Guo et al., 2017). The rate of Cr(VI) metal ions binding increased in a concentration-dependent manner and the rate saturating concentration of Cr(VI) at equilibrium (q_e) increased from 4.9 to 7.98 mg g^{-1} with increase in the initial metal ion concentration from 10 to 50 mg L^{-1}. With increasing concentration of cationic dyes and Cr(VI), the percentage removal efficiency of MPA declined, perhaps due to relatively higher driving force for mass transfer (Bulut and Aydin, 2006). At higher concentrations of dye and heavy metal, the removal efficiency declined, perhaps due to reduced availability of adsorption sites on the surface of MPA as well as mass transfer resistances between the aqueous and solid phase (Hameed et al., 2008). The increase in initial dye/metal ion concentration provided rapid increase in the dye/metal removal as it overcame all mass transfer resistances between the aqueous and solid phase. But the sluggish rise in the rate of dye/metal removal at higher concentration was due to sorbent as rate limiting factor as reported by other investigators (Yagub et al., 2012; Garg et al., 2003; Guo et al., 2017).

The study on adsorption kinetics indicated that the removal of cationic dyes (MG and MB) and Cr(VI) by MPA was a physico-chemisorption process as indicated by kinetic parameters derived from the Pseudo-second order kinetic model, the values of R^2 and calculated q_e values. The pseudo-first order kinetic model did not fit in well with the

experimental data for the sorption of cationic dyes and Cr(VI) onto MPA. From the kinetic parameters, it was confirmed that the pseudo-second order kinetic model was the best fitted model for the sorption of cationic dyes and Cr(VI) with comparatively high R^2 values at different concentration of cationic dyes/Cr(VI). The values of cal. q_e was closer to exp. q_e values which clearly indicated that the rate of adsorption of dye and heavy metal onto MPA was almost a controlled physico-chemisorption process, which involved sharing of electrons between adsorbate molecules and surface active ligands of MPA particles (Hameed et al., 2008). It was observed that initial adsorption rate (*h*) increased with increase in the dye/metal ion concentration. An increasing trend of *h* values with the dye/metal ion concentration suggested an increase in dye/metal ion binding with increasing concentration of dye and heavy metal in aqueous solution (Kumar, 2006). A higher *h* values for MPA at rate saturating concentration of dye and heavy metal indicated that the adsorption of cationic dyes and Cr(VI) onto the surface of MPA was carried out through surface interchange reactions until all the functional binding sites were occupied (Ma et al., 2015). Similar results have been reported by other investigators in removal of dyes and heavy metals (Guo et al., 2017; Kumar, 2006).

Equilibrium adsorption studies (Langmuir and Freundlich isotherms) on removal of cationic dyes (MG and MB) and Cr(VI) by MPA indicated that the both Langmuir and Freundlich adsorption isotherms fitted well to the data on equilibrium sorption of cationic dyes and Cr(VI). The regression coefficient (R^2) values showed better applicability of Langmuir as well as Freundlich isotherm to describe MPA for equilibrium adsorption and fitted well to the equilibrium adsorption data of cationic dyes/Cr(VI). According to Langmuir isotherm model, the q_{max} values of MPA for the removal of MG and MB dye at room temperature were calculated as 322.58 and 588.24

mg g^{-1}, respectively, but in case of Cr(VI) removal, it was found to be 8.68 mg g^{-1}. A high q_{max} value of MPA in removal of cationic dyes (MG and MB) was obviously due to enhanced binding of cationic dye molecules with the large number of surface binding ligands of MPA. It has already been reported that the high ash content in MPA adsorbent was indicative of more surface functional groups and thus, making it more suitable for the binding of cationic dyes and Cr(VI) metal ions (Sewu et al., 2017). An electrostatic interactions and ion exchange mechanisms were mainly involved in the binding of cationic dyes and Cr(VI) metal ions by MPA particles (Sewu et al., 2017). MPA had comparatively higher affinity for dye/metal ion adsorption supported by R_L values. The calculated R_L values of MPA at different dye/metal ion concentration indicated favorable adsorption process. The R_L values between 0 and 1 were indicative of favourable adsorption with more affinity of adsorbent particles towards dye/metal ions (Hema and Arivoli, 2008; Ma et al., 2015). The higher R^2 values and value of 1/n < 1 for MPA in Freundlich adsorption isotherm also confirmed the role of chemisorption on the heterogeneous surface of MPA. Similar results on adsorption isotherms for the removal of cationic dyes and Cr(VI) have been reported by the earlier workers (Ma et al., 2015; Guo et al., 2017). A comparison of adsorption capacity of different adsorbents suggested that MPA was better adsorbent than many other reported biosorbents.

The thermodynamic studies on removal of cationic dyes and Cr(VI) by the MPA at different temperature from 293.15 to 323.15 K indicated that the amount of dye/metal ions adsorption by MPA was found to increase with rise in temperature, which increased the kinetic mobility of dye/Cr(VI) metal ions to the active sorption sites. It may be concluded the dye/metal adsorption by MPA was endothermic process. In the present investigation, temperature dependent increase in the sorption capacity of MPA

in removal of cationic dyes (MG and MB) and Cr(VI) could be due to their free kinetic mobility and increase in sorptive forces as suggested by other investigators (Salleh et al., 2011; Mohan et al., 2002). The negative values of ΔG° at all the chosen temperature indicated that the adsorption of cationic dyes and Cr(VI) onto MPA was thermodynamically feasible and spontaneous process (Baek et al., 2010). The free energy change (ΔG°) with negative value for adsorption supported that the removal of dye/heavy metal by MPA was favourable adsorption process. An increase in negative value of ΔG° with rising temperature specified that the process of adsorption was more favourable at lower temperature (Chowdhury and Saha, 2010). The positive values of ΔH° for MPA indicated that the adsorption process was endothermic and nature of interaction between adsorbent particles and dye/metal ions was physico-chemical process (Ghasemi and Asadpour, 2007). The endothermic nature of dye and heavy metal adsorption by surface moieties on MPA particles might be deriving the energy released as hydration energy surrounding the dye and metal ions as suggested by Ahmad and Kumar (2010). A positive value of ΔS° for MPA also supported the assumption of involvement of hydration energy which was released during the sorption of dye and heavy metal, and thus, it contributed to an increase in the degree of freedom of the water molecules (Ghasemi and Asadpour, 2007; Baek et al., 2010).

In the present investigation, adsorption and reduction potential of adsorbent (MPA) derived from distilled mentha plant waste was analyzed for removal of cationic dyes (MG and MB) and Cr(VI) from their aqueous solutions. The present study simply confirmed the interaction of cationic dyes and Cr(VI) with MPA involved both chemisorption as well as reduction of toxicants as evident from the schematic flow chart given in Fig 7.1. The other factors influencing the sorption of dyes (MG and MB) and Cr metal were contact time, pH, adsorbent dose, initial concentration and temperature.

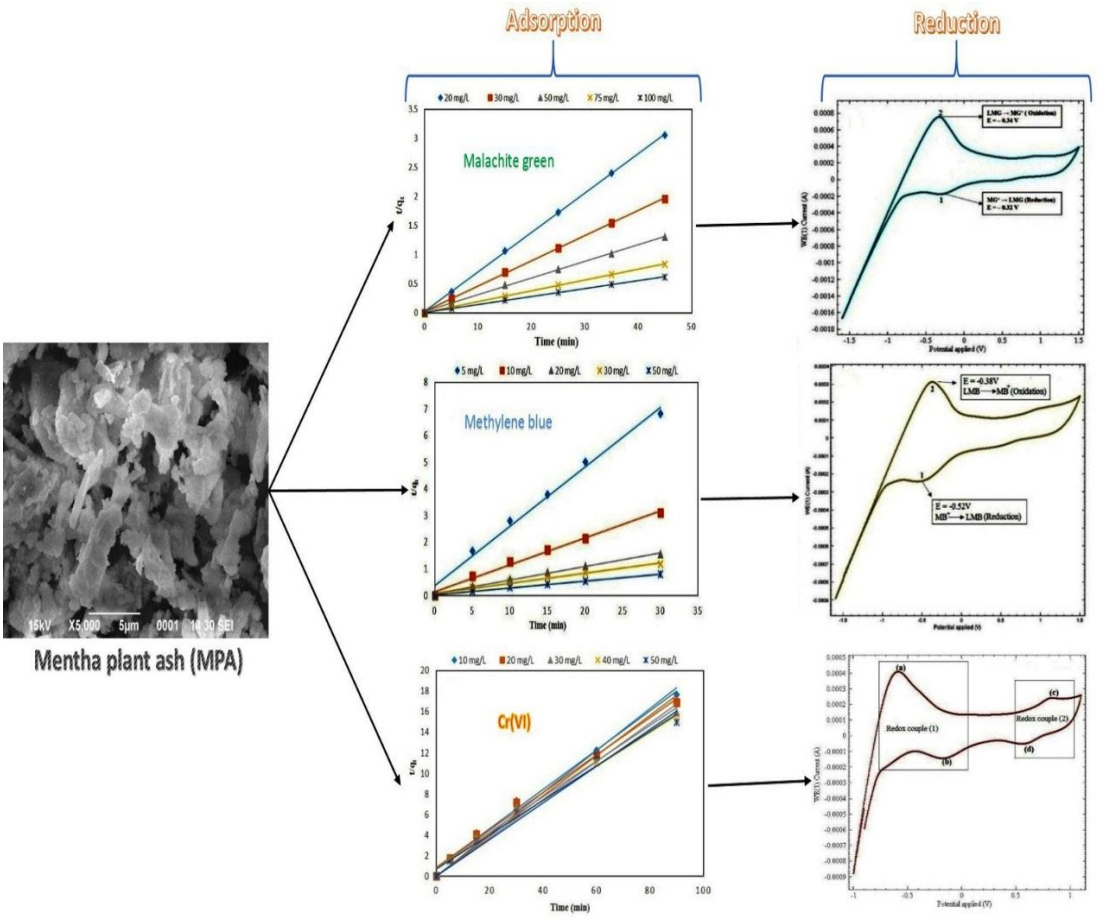

Fig. 7.1. A schematic diagram representing adsorption and reduction potential of MPA in removal of cationic dyes (MG and MB) and Cr(VI) from their aqueous solutions.

The FTIR, XRD and SEM analysis of adsorbent MPA showed the presence of various organic ligands and minerals contributing to the net negative charge on the surface which facilitated the adsorption of cationic dye and Cr metal. During the sorption, it was confirmed that the bonding of dyes/Cr(VI) involved transfer of electrons, leading to one electron transfer based reduction as evident from the results of cyclic voltammetry and XPS analysis of MPA before and after bonding of dyes/Cr(VI) with MPA. This unique character of MPA as sorbent with adsorption/reduction potential can be useful tool for treatment of industrial wastewater, particularly wastewater loaded with dyes or chromium metals. This study on MPA offers immense potential of MPA application as a cheaper and ecofriendly tool for wastewater treatment.

CHAPTER-VIII

Summary and Conclusions

8.1. Summary

The present investigation covers the potential application of mentha plant ash (MPA) derived from distilled mentha plant waste as an efficient adsorbent in removal of basic cationic dyes (MG and MB) and Cr(VI) from their aqueous solutions. Mentha (mint) plant ash, a dumping waste was collected from local mentha oil distillation units, Barabanki, Uttar Pradesh, India. Prior to use, MPA was homogenized to a fine powder and the resulting powder was sieved (< 0.21 mm) by using 70-mesh size sieve so that all the particles were of almost of uniform size. The various physico-chemical characteristics of MPA as an adsorbent were determined using Zeta Potential Analyzer, Scanning Electron Microscope (SEM), Energy dispersive X-Ray Spectroscopy (EDX), X-Ray Photoelectron Spectroscopy (XPS), Brunauer-Emmett-Teller (BET), Fourier Transform Infrared Spectroscopy (FTIR), X-Ray Diffraction (XRD), Thermo gravimetric Analyzer (TGA) and Cyclic Voltammetry. BET specific surface area, total pore volume and average pore diameter of MPA particles were also analyzed. Presence of low boiling volatile organic matter, moisture content, hemicellulose, cellulose and lignin in the MPA adsorbent were confirmed by thermo-gravimetric analysis (TGA) and various surface functional groups by IR-Spectroscopy (FTIR). The IR-spectra of MPA exhibit that hydroxyl, ester, amine, phenyl, carboxyl and carbonyl groups are the surface functional moieties, not only contributing to negative charge on surface of adsorbent, but may be actively involved in the binding of cationic dyes and Cr(VI) metal ions. The value of zeta potential of MPA particles at neutral pH (pH 7.0) was determined as −37.1 mV, indicating a highly negatively charged sorption surface of MPA particles. A highly electronegative surface along with little effect of changing pH condition on the zeta potential suggested about larger contribution of salts and minerals in determining the zeta potential of adsorbent (MPA). This could be the reason for high

binding efficiency of MPA for cationic dyes (MG and MB) and Cr(VI) metal ions. The shape of the N_2 adsorption/desorption isotherm matches the Type IV shape of adsorption isotherm (IUPAC classification), indicating a mesoporous structure of MPA particles. The characteristics of Type IV isotherm correspond with monolayer-multilayer adsorption and are indicative of relatively strong interaction between adsorbent surface and adsorbate molecules. The BET specific surface area of MPA was found to be 7.169 m^2 g^{-1}. A pore diameter in MPA particles between 2 to 50 nm indicates a mesoporous material. The presence of clay minerals such as calcite, quartz, sylvite and dolomite were confirmed in the XRD pattern of MPA. SEM image of MPA showed irregular surface with heterogenous pore structures on the surface of MPA particles. The EDX analysis of the MPA exhibited chemically rough surface of MPA particles was due to major contribution of Mg, Cl, K, Si, Fe, Ca C, O and Al content. The cyclic voltammetry analysis of cationic dyes (MG and MB) and Cr(VI) showed a reversible, coupled redox reaction at the interface of dye/metal ions and MPA particles. Further, the Cr 2p peaks in the binding energy range (0 – 1200 eV) and (570 – 595 eV) were analyzed in recorded XPS spectrum of MPA after adsorption of Cr(VI). The binding energy in the range of 572–581 eV and 582–591 eV corresponds to Cr 2p3/2 and Cr 2p1/2 orbitals, respectively. The binding energy (eV) peaks of Cr $2p_{3/2}$ and Cr $2p_{1/2}$ were detected at around 579.2, 588.8, 577.6, 588.0, 576.8 and 585.6 eV in the recorded XPS spectrums and these peaks were assigned to Cr(VI), Cr(III) and Cr(II) forms.

Adsorption behavior of MPA in removal of basic cationic dyes (MG and MB) from aqueous solutions was analyzed as a function of different pH (4.0 – 10.0), initial dye concentration (20 – 100 mg/L for MG and 5 – 50 mg/L for MB), contact time (0 – 45 min for MG; 0 – 30 min for MB), dose of adsorbent (0.05 – 0.3 g/100 mL of MPA) and

temperature (20 – 50°C). Similarly, the sorption of Cr(VI) by MPA was carried out as a function of different contact time (0 – 90 min), adsorbent dose (0.1 – 0.5g/100 mL), pH condition (pH 3.0 – 9.0) and initial Cr(VI) concentration (10 – 50 mg L^{-1}) to define the optimum conditions for the adsorption of Cr(VI). The MG and MB dye removal by MPA initially occurred at a faster rate, corresponding to 72.86 and 74.68 % removal with in 5 min, respectively. Similarly, the adsorption of Cr(VI) at different metal ion concentration by MPA showed initially a rapid sorption process up to 30 min, followed by slowing down of the sorption process with increase in the contact time up to 90 min. A rapid rate of initial dye/heavy metal removal by MPA could be due to maximum availability of vacant binding sites on the surface of adsorbent, ensuring high efficiency of dye/heavy metal removal. The maximum MG and MB dye removal, at an adsorbent dose of 0.1 g/100 mL, was found to be 36.86 and 20.65 mg g^{-1}, respectively. A rapid phase of dose-dependent increase in Cr(VI) metal ion removal was found to occur up to 0.2 g/100 mL dose of MPA and this was followed by a sluggish phase of Cr(VI) removal between 0.2 to 0.5 g/100 mL of dose of adsorbent. In the present study, the biphasic pattern of dose dependent dye/heavy metal removal could be interpreted in terms of initial dose dependent rapid dye/heavy metal removal due to enhanced availability of binding ligands and larger surface area, while sluggish phase of dye/heavy metal removal might be the overlapping and shadowing effect of excess MPA particles on binding ligands and thereby, resulting into reduced accessibility of the dye molecules/metal ions to the active site. The adsorption efficiency of MPA adsorbent in removal of cationic dyes was found to increase with gradual increase in pH (pH 4.0 – 10.0), whereas the acidic condition (pH 3.0) was favorable for the maximum adsorption of Cr(VI) by MPA. Adsorbent material (MPA) was found to be more effective in removal of cationic dyes and Cr(VI) in the pH range (pH 6.0 – 10.0)

and (pH 3.0 – 4.0), respectively, due to combined action of physico-chemisorption and a reductive electron transfer reactions. Equilibrium adsorption isotherms (Langmuir and Freundlich) were applied on equilibrium adsorption data of cationic dyes and Cr(VI) and results showed monolayer physico-chemisorption of cationic dyes and Cr(VI), followed by both Langmuir and Freundlich adsorption isotherms. The maximum monolayer adsorption capacity (q_{max}) of MPA in removal of MG and MB dye was found to be 322.58 and 588.24 mg g^{-1}, respectively. In Cr(VI) removal by MPA, the q_{max} value was found to be 8.63 mg g^{-1}. The separation factor (R_L) values were between 0 and 1, indicating a favorable adsorption of cationic dyes and Cr(VI) onto MPA. Pseudo-first order, pseudo-second order kinetics and intra-particle diffusion model were analyzed at different concentration of cationic dyes and Cr(VI). The adsorption kinetic data fitted well with the pseudo-second order kinetics as the value of calculated q_e in this model was found to be very close to experimental value of q_e. Activation energy (*Ea*) calculated for the surface binding of MB (14.90 kJ.mol^{-1}) and MG dye (1.24 kJ mol^{-1}) indicated that the dye binding by MPA was energetically favorable physico-chemical sorption process. The values of Gibbs free energy (ΔG°), entropy (ΔS°) and enthalpy (ΔH°) for the sorption of cationic dyes and Cr(VI) onto MPA indicated that adsorption of dye/heavy metal by MPA was endothermic and spontaneous in nature. Further, use of desorbing agents like 0.1 N solution of HCl, H_2SO_4, CH_3COOH, NaOH and H_2O exhibited better recovery of MG and MB dye from the MPA in the presence of HCl and H_2SO_4 than CH_3COOH, NaOH and H_2O. Present investigation revealed that removal of cationic dyes and Cr(VI) was due to synergistic action of physico-chemisorption coupled with reductive electron transfer mechanism.

8.2. Conclusions

The main conclusions of the present study are given as follows:

- Mentha plant ash (MPA), is a low cost material available in plenty as a waste byproduct around the mentha oil distillation unit, which can be used as an efficient adsorbent in removal of cationic dyes (MG and MB) and Cr(VI) from waste water without any kind of pre-treatment.
- The zeta potential analysis of adsorbent (MPA) indicated a highly negatively charged surface with little effect of pH condition. The values of zeta potential of MPA at neutral pH 7.0 were found to be -37.1 mV. A highly electronegative surface along with little effect of changing pH condition on the zeta potential suggested about larger contribution of salts and minerals in determining the zeta potential of MPA. This could be the reason for high binding efficiency of MPA for cationic dyes and Cr(VI).
- The shape of the N_2 adsorption/desorption isotherm measured on MPA matches the Type IV shape of adsorption isotherm (IUPAC classification), indicating a mesoporous structure of MPA adsorbent. The specific features of Type IV isotherm correspond with monolayer-multilayer adsorption and are indicative of relatively strong interaction between adsorbent particles and adsorbate molecules. The BET specific surface area, total pore volume and average pore diameter of MPA were found to be 7.169 $m^2 g^{-1}$, 3.414 $cm^3 g^{-1}$ and 12.915 nm, respectively.
- FTIR analysis of MPA showed a number of IR peaks, indicating the presence of various surface functional groups (amine, phenyl, hydroxyl, carbonyl and carboxyl groups etc.) on the surface of MPA adsorbent. The changes in the IR-peaks after dye/metal ions binding with MPA indicated a strong interaction between the adsorbate molecules and binding ligands present on the surface of MPA.

- The minerals such as calcite, quartz, crystalline cellulose and dolomite were the main crystalline phases present in MPA adsorbent. The XRD pattern and a high carbonates content in adsorbent material (MPA) suggested that different carbonates forms were the main alkaline constituents in the MPA adsorbent derived from mentha plant waste at the high temperature (800ºC).
- The biomolecules such as cellulose, hemicellulose, lignin and low boiling organic matter were abundantly present in adsorbent material (MPA). Since the biomolecules contain a number of oxygen containing functional groups and these were found to play a crucial role in the sorption of cationic dyes and Cr(VI).
- The cyclic voltammetric analysis of cationic dyes (MG and MB) and Cr(VI) after adsorption indicated a reversible, redox coupled electrochemical reduction of dye/metal ion mediated by MPA. Thus, the MPA mediated decolourization of dye and heavy metal at higher concentrations involves both physico-chemisorption as well as electrochemical reduction of cationic dyes and Cr(VI).
- The XPS analysis of MPA after adsorption of Cr(VI) indicated a partial reduction of Cr(VI) to Cr(III) and Cr(II) under acidic conditions (pH 3.0). Further, the results on XPS analysis suggested that the mechanism of Cr(VI) removal by MPA was dominated by both the electrostatic adsorption and reduction under acidic conditions (pH 3.0). The reduction of toxic Cr(VI) to less toxic Cr(III) and Cr(II) was likely due to the reactive hydroxyl (–OH) and amine ($–NH_2$) electron donors present on the surface of MPA particles.
- The process of cationic dyes and Cr(VI) adsorption was found to be dependent on initial dye/metal ion concentration, dose of adsorbent, pH, contact time and temperature. All the process optimizing parameters were found to play an

important role in defining the optimum conditions for the sorption of cationic dyes and Cr(VI.

- The amount of dye/metal ion adsorption by MPA was found to increase with increasing contact time and the maximum adsorption efficiency of MPA in removal of cationic dyes and Cr(VI) was achieved in 45 min for malachite green, 30 min for methylene blue and 90 min for Cr(VI).
- An increase in the pH of the solution, increased the sorption efficiency of MPA in removal of cationic dyes (MG and MB) from aqueous solution whereas the sorption efficiency of MPA in removal of Cr(VI) was found to decrease with increase in pH of the solution. The maximum adsorption capacity of MPA was obtained at pH 6.0 for MG, pH 7.0 for MB and pH 3.0 for Cr(VI) at room temperature.
- The adsorption capacity of MPA was found to increase with increase in the dose of adsorbent in removal of cationic dyes and Cr(VI) from aqueous solutions. The optimum doses of MPA to achieve maximum adsorption efficiency were found to be 0.1g/100 mL for cationic dyes (MG and MB) and 0.3 g/100 mL for Cr(VI).
- An increase in the initial concentrations of MG, MB dye and Cr(VI) in the solutions increased the adsorption efficiency of MPA. But their corresponding percentage removal of cationic dyes and Cr(VI) decreased with increase in the concentrations of dye and heavy metal.
- The studies on adsorption isotherms showed well-fitting of equilibrium adsorption data to both Langmuir and Freundlich isotherm model for the sorption of cationic dyes and Cr(VI) onto MPA. The well-fitting of equilibrium

adsorption data to both Langmuir and Freundlich isotherm model indicates monolayer physico-chemisorption of cationic dyes and Cr(VI).

- The maximum monolayer adsorption capacity (q_{max}) of MPA at room temperature for the sorption of MG and MB dye were found to be 322.56 and 588.24 mg g^{-1}, respectively. A high q_{max} value of MPA in the sorption of cationic dyes was likely due to enhanced binding of MG and MB dye molecules with the large number of surface binding ligands of MPA.
- The values of separation factor or equilibrium parameter (R_L) for the sorption of cationic dyes and Cr(VI) onto the surface of MPA were found in between 0 and 1, which indicated favorable adsorption of cationic dyes and Cr(VI).
- The kinetic studies on adsorption of cationic dyes and Cr(VI) showed that experimental adsorption data fitted quite well to Pseudo-second order kinetic model. Further, the fit of this model clearly indicated that the rate of adsorption of dyes and Cr(VI) onto MPA adsorbent was almost a controlled chemisorption process, which involved sharing of electrons between dyes/metal ions and surface of adsorbent particles.
- Studies on the thermodynamic factors ($\Delta H°$, $\Delta S°$ and $\Delta G°$) for the sorption of cationic dyes and Cr(VI) onto MPA clearly indicated the feasible, spontaneous and endothermic nature of physico-chemisorption process.
- Further, the added advantage associated with MPA is that the resource material for ash, is easily available in plenty as a byproduct of mentha oil distillation units. Finally, it was concluded that the MPA, without any pre-treatment, is cheap, ecofriendly adsorbent material exhibiting great adsorption/reduction potential for the removal of the cationic dyes and Cr(VI), which can be prove to be better than any costly commercial adsorbents available in the market. The

practical applicability of MPA as a low cost adsorbent for the removal of cationic dyes and Cr(VI) from their aqueous solutions has been conclusively proved.

References

Abbas, M., Kaddour, S., Trari, M. (2014) Kinetic and equilibrium studies of cobalt adsorption on apricot stone activated carbon. J. Ind. Eng. Chem. 20, 745–751.

Abid, M.F., Zablouk, M.A., Alameer, A.M.A. (2012) Experimental study of dye removal from industrial wastewater by membrane technologies of reverse osmosis and nanofiltration. Iranian Journal of Environmental Health Science and Engineering 9, 1–9.

Abechi, E.S., Gimba, C.E., Uzairu, A., Kagbu, J.A. (2011) Kinetics of adsorption of methylene blue onto activated carbon prepared from palm kernel shell. Arch. Appl. Sci. Res. 3, 154–164.

Ahmad, R. (2009) Studies on adsorption of crystal violet dye from aqueous solution onto coniferous pinus bark powder (CPBP). J. Hazard. Mater. 171, 767–773.

Ahmad, A.A., Hameed, B.H., Aziz, N. (2007) Adsorption of direct dye on palm ash: Kinetic and equilibrium modeling. J. Hazard. Mater. 141, 70–76.

Ahmad, M.A., Alrozi, R. (2011) Removal of malachite green dye from aqueous solution using rambutan peel-based activated carbon: Equilibrium, kinetic and thermodynamic studies. Chem. Eng. J. 171, 510–516.

Ahmad, R., Kumar, R. (2010) Adsorption studies of hazardous malachite green onto treated ginger waste. J. Env. Manag. 91, 1032–1038.

Akar, E., Altinişik, A., Seki, Y. (2013) Using of activated carbon produced from spent tea leaves for the removal of malachite green from aqueous solution. Eco. Eng. 52, 19–27.

Akerholm, M., Hinterstoisser, B., Salmen, L. (2004) Characterization of the crystalline structure of cellulose using static and dynamic FT-IR spectroscopy. Carbohy. Res. 339, 569–578.

Aksoy, Y.Y., Kaya, A. (2011) A study of factors affecting on the zeta potential of kaolinite and quartz powder. Environ. Earth Sci. 62, 697–705.

Aksu, Z., Kutsal, T. (1990) A comparative study for biosorption characeteristics of heavy metal ions with *C. vulgaris.* Environ. Technol. 11, 979–987.

Aksu, Z., Ozer, D., Ekiz, H., Kutsal, T., Calar, A. (1996) Investigation of biosorption of chromium(VI) on *C. crispate* in two staged batch reactor. Environ. Technol. 17, 215–220.

Al-Degs, Y., Khraisheh, M.A.M., Allen, S.J., Ahmad, M.N. (2003) Effect of carbon surface chemistry on the removal of reactive dyes from textile effluent. Water Res 34, 927–935.

Al-Jlil, S.A., Alharbi, O.A. (2010) Comparative study on the use of reverse osmosis and adsorption process for heavy metals removal from wastewater in Saudi Arabia. Research Journal of Environmental Sciences, 4, 400–406.

Allen, S.J., Koumanova, B. (2003) Decolourization of water/wastewater using adsorption. J. Univ. Chem. Technol. Metall. 40, 175–192.

Ali, I., Asim, M., Khan, T.A. (2012) Low cost adsorbents for the removal of organic pollutants from wastewater. J. Environ. Manag. 113, 170–183.

Alothman, Z.A. (2012) A Review: Fundamental aspects of silicate mesoporous materials. Materials, 5, 2874–2902.

Alyuz, B., Veli, S. (2009) Kinetics and equilibrium studies for the removal of nickel and zinc from aqueous solutions by ion exchange resins. J. Hazard. Mater. 167, 482–488.

Alzaydien, A.S. (2009) Adsorption of methylene blue from aqueous solution onto a low cost natural Jordanian Tripoli. Am. J. Environ. Sci. 5, 197–208.

Aman, T., Kazi, A.A., Sabri, M.U., Bano, Q. (2008) Potato peels as solid waste for the removal of heavy metal copper(II) from waste water/industrial effluent. Colloids Surf. B: Biointerfaces, 63, 116–121.

Anjum, A., Lokeswari, P., Kaur, M., Datta, M. (2011) Removal of As(III) from aqueous solutions using montmorillonite. Journal of Analytical Sciences, Methods and Instrumentation, 1, 25–30.

Annadurai, G., Juang, R.S., Lee, D.J. (2002) Use of cellulose-based wastes for adsorption of dyes from aqueous solutions. J. Hazard. Mater. 92, 263–274.

Ansari, R., Mosayebzadeh, Z. (2010) Removal of basic dye methylene blue from aqueous solutions using sawdust and sawdust coated with polypyrrole. J. Iran. Chem. Soc. 7, 339–350.

Arfaoui, S., Srasra, N.F., Srasra, E. (2008) Modelling of the adsorption of the chromium ion by modified clays. Desalination, 222, 474–481.

Arivoli, S., Hema, M., Martin, P., Prasath, D. (2009) Adsorption of malachite green onto carbon prepared from borassus bark. Arab. J. Sci. Eng. 34, 31–42.

Aydın, H., Bulut, Y., Yerlikaya, C. (2008) Removal of copper (II) from aqueous solution by adsorption onto low-cost adsorbents. J. Environ. Manag. 87, 37–45.

Aygun, A., Yenisoy-Karakas, S., Duman, I. (2003) Production of granular activated carbon from fruit stones and nutshells and evaluation of their physical, chemical and adsorption properties. Microporous Mesoporous Mater. 66, 189–195.

Aziz, H.A., Adlan, M.N., Ariffin, K.S. (2008) Heavy metals (Cd, Pb, Zn, Ni, Cu and Cr(III)) removal from water in Malaysia: Post treatment by high quality limestone. Bioresour. Technol. 99, 1578–1583.

AWWA and ASCE (2012) Water treatment plant design, 5th Edition, McGraw-Hill Inc. New York.

Babarinde, N.A.A., Babalola, J.O., Sanni, R.A. (2006) Biosorption of lead ions from aqueous solution by maize leaf. Int. J. Phy. Sci. 1, 23–26.

Babel, S., Kurniawan, T.A. (2003) Low-cost adsorbents for heavy metals uptake from contaminated water: A review. J. Hazard. Mater. 97, 219–243.

Babu, P.E.J., Kumar, V., Visvanathan, R. (2010) Equilibrium and kinetic study for the removal of malachite green using activated carbon prepared from *Borassus flabellofer male flower*. Asia-Pacific Journal of Chemical Engineering, 5, 465–472.

Baccar, R., Blanquez, P., Bouzid, J., Feki, M., Attiya, H., Sarra, M. (2013) Modeling of adsorption isotherms and kinetics of a tannery dye onto an activated carbon prepared from an agricultural by-product. Fuel Process. Technol. 106, 408–415.

Baek, M.H., Ijagbemi, C.O.S.J., Kim, D.S. (2010) Removal of malachite green from aqueous solution using degreased coffee bean. J. Hazard. Mater. 176, 820–828.

Banat, I.M., Nigam, P., Singh, D., Marchant, R. (1996) Microbial decolorization of textile-dye-containing effluents: a review. Bioresour. Technol. 58, 217–227.

Bajpai, A.K., Rajpoot, M. (1999) Adsorption techniques: A review. J. Sci. Ind. Res. 58, 844–860.

Bangash, F.K., Alam, S. (2009) Adsorption of acid blue 1 on activated carbon produced from the wood of *Ailanthus altissima.* Brazilian J. Chem. Eng. 26, 275–285.

Barakat, M.A. (2011) New trends in removing heavy metals from industrial wastewater. Arab. J. Chem. 4, 361–377.

Barbooti, M.M., Mohamed, T.J., Hussein, A.A., Abas, F.O. (2004) Optimization of pyrolysis conditions of scrap tires under inert gas atmosphere. J. Anal. Appl. Pyrolysis, 72, 165–170.

Barceloux, D.G. (1999) Chromium. Journal of Toxicology -Clinical Toxicology, 37, 173–194.

Basar, C.A. (2003) Effect of presence of ions on surface characteristics of surfactant modified powdered activated carbon (PAC). Appl. Surf. Sci. 218, 169–174.

Basar, C.A., Onal, Y., Kilicer, T., Eren, D. (2005) Adsorptions of high concentration malachite green by two activated carbons having different porous structures. J. Hazard. Mater. 127, 73–80.

Behnajady, M.A., Modirshahla, N., Ghanbary, F. (2007) A kinetic model for the decolorization of C. I. Acid yellow 23 by Fenton process. J. Hazard. Mater. 148, 98–102.

Bektas, N., Aydın, S., and Oncel, M.S. (2011) The adsorption of arsenic ions using beidellite, zeolite, and sepiolite clays: A study of kinetic, equilibrium and thermodynamics. Sep. Sci. Technol. 46, 1005–1016.

Bello, O.S., Adegoke, K.A., Akinyunni, O.O. (2017) Preparation and characterization of a novel adsorbent from *Moringa oleifera* leaf. Appl. Water Sci. 7, 1295–1305.

Bello, O.S., Adelaide, O.M., Hammed, M.A., Popoola, O.A.M. (2010) Kinetic and equilibrium studies of methylene blue removal from aqueous solution by adsorption on treated sawdust. Macedonian J. Chem. Eng. 29, 77–85.

Bello, O.S., Olusegun, O.A., Njoku, V.O. (2013) Fly ash: An alternative to powdered activated carbon for the removal of eosin dye from aqueous solutions. Bull. Chem. Soc. Ethiop. 27, 191–204.

Benaissa, H. (2005) Removal of acid dyes from aqueous solutions using orange peel as a sorbent material. Ninth International Water Technology Conference, IWTC9, Sharm El-Sheikh, Egypt, pp., 1175–1185.

Bhatnagar, A., Sillanpaa, M. (2010) Utilization of agro-industrial and municipal waste materials as potential adsorbents for water treatment—a review. Chem. Eng. J. 157, 277–296.

Bhatnagar, A., Minorcha, A.K., Sillanpaa, M. (2010) Adsorptive removal of cobalt from aqueous solution by utilizing lemon peel as a biosorbent. Biochem. Eng. J. 48, 181–186.

Bhatnagar, A., Vilar, V.J.P., Botelho, C.M.S., Boaventura, R.A.R. (2011) A review of the use of redmud as adsorbent for the removal of toxic pollutants from water and wastewater. Environ. Technol. 32, 231–249.

Bhatti, H.N., Nasir, A.W., Hanif, M.A. (2010) Efficacy of *Daucas carota L.* waste biomass for the removal of chromium from aqueous solutions. Desalination, 253, 78–87.

BIS (2012) Drinking water specification (IS: 10500), New Delhi.

Bootharaju, M.S., Pradeep, T. (2013) Facile and rapid synthesis of a dithiol-protected Ag_7 quantum cluster for selective adsorption of cationic dyes. Langmuir 29, 8125–8132.

Bouaziz, F., Koubaa, M., Kallel, F., Ghorbel, R.E., Chaabouni, S.E. (2017) Adsorptive removal of malachite green from aqueous solutions by almond gum: Kinetic study and equilibrium isotherms. International Journal of Biological Macromolecules 105, 56–65

Bouyarmane, H., El-Asri, S., Rami, A., Roux, C., Mahly, M.A., Saoiabi, A., Coradin, T., Laghzizil, A. (2010) Pyridine and phenol removal using natural and synthetic apatites as low cost sorbents, influence of porosity and surface interaction. J. Hazard. Mater. 181, 736–741.

Brunauer, S., Deming, L.S., Deming, W.E., Teller, E. (1940) "On a Theory of the van der Waals Adsorption of Gases," J. Am. Chem. Soc. 62, 1723–1732.

Buasri, A., Chaiyut, N., Tapang, K., Jaroensin, S., Panphrom, S. (2012) Equilibrium and kinetic studies of biosorption of Zn(II) ions from wastewater using modified corncob. APCBEE Procedia 3, 60–64.

Bulut, Y., Aydin, H. (2006) A kinetics and thermodynamics study of methylene blue adsorption on wheat shells. Desalination, 194, 259–267.

Calace, N., Muro, D.A., Nardi, E., Petronio, B.M., Pietroletti, M. (2002) Adsorption isotherms for describing heavy metal retention in paper mill sludges. Ind. Eng. Chem. Res. 41, 5491–5497.

Cao, X., Ma, L., Gao, B., Harris, W. (2009) Dairy-manure derived biochar effectively sorbs lead and atrazine. Environ. Sci. Technol. 43, 3285–3291.

Cao, X.Y., Yue, Q.Y., Song, L.Y., Li, M., Zhao, Y.C. (2007) The performance and application of fly ash modified by PDMDAAC. J. Hazard. Mater. 147, 133–138.

Chakraborty, S., Chowdhury, S., Saha, P.D. (2011) Adsorption of crystal violet from aqueous solution onto NaOH-modified rice husk. Carbohydr. Polym. 86, 1533–1541.

Chakraborty, S., Chowdhury, S., Saha, P.D. (2012) Insight into biosorption equilibrium, kinetics and thermodynamics of crystal violet onto *Ananas comosus* (pineapple) leaf powder. Appl. Water Sci. 2, 135–141.

Chakravarti, A.K., Chowdhury, S.B., Chakrabarty, S., Chakrabarty, T., Mukherjee, D.C. (1995) Liquid membrane multiple emulsion process of chromium (VI) separation from wastewaters. Colloids Surf. A: Physicochem. Eng. Aspects, 103, 59–71.

Chang, Q., Zhang, M., Wang, J.X. (2009) Removal of Cu^{2+} and turbidity from wastewater by mercaptoacetyl chitosan. J. Hazard. Mater.169, 621–625.

Chang, Q., Wang, G. (2007) Study on the macromolecular coagulant PEX which traps heavy metals. Chem. Eng. Sci. 62, 4636–4643.

Chen, B., Chen, Z. (2009) Sorption of naphthalene and 1-naphthol by biochars of orange peels with different pyrolytic temperatures. Chemosphere 76, 127–133.

Chen, S.H., Yue, Q.Y., Gao, B.Y., Xu, X. (2010) Equilibrium and kinetic adsorption study of the adsorptive removal of Cr(VI) using modified wheat residue. J. Colloid Interface Sci. 349, 256–264.

Chen, T., Zhou, Z., Xu, S., et al. (2015) Adsorption behavior comparison of trivalent and hexavalent chromium on biochar derived from municipal sludge. Bioresour. Technol. 190, 388–394.

Chen, Y.-d., Lin, Y.-C., Ho, S.-H., Zhou, Y., Ren, N-qi. (2018) Highly efficient adsorption of dyes by biochar derived from pigments-extracted macroalgae pyrolyzed at different temperature. Bioresour. Technol. 259, 104–110.

Chen, Y., Zhai, S.R., Liu, N., Song, Y., An, Q.D., Song, X.W. (2013) Dye removal of activated carbons prepared from NaOH-pretreated rice husks by low-temperature solution-processed carbonization and H_3PO_4 activation. Bioresour. Technol. 144, 401–409.

Choudhary, B., Paul, D. (2018) Isotherms, kinetics and thermodynamics of hexavalent chromium removal using biochar. J. Environ. Chem. Eng. 6, 2335–2343.

Chowdhury, S., Saha, P. (2010) Sea shell powder as a new adsorbent to remove Basic Green 4 (Malachite Green) from aqueous solutions: Equilibrium, kinetic and thermodynamic studies. Chem. Eng. J. 164, 168–177.

Chung, K.T., Cerniglia C.E. (1992) Mutagenicity of azo dyes: structure-activity relationships. Mutat Res. 277, 201–220.

Cieslak-Golonka, M. (1995) Toxic and mutagenic effects of Cr(VI). Polyhedron 15, 3667–3689.

Chou, K.S., Tsai, J.C., Lo, C.T. (2001) The adsorption of Congo red and vacuum pump oil by rice hull ash, Bioresour. Technol. 78, 217–219.

Clarke, E. A., Anliker, R. (1980) Organic dyes and pigments. In The Handbook of Environmental Chemistry, Vol. 3, Part A. Anthropogenic Compounds, ed. O. Hutzinger. Springer, Heidelberg, pp. 181–215.

Clarkson, C.R., Bustin, R.M., Levy, J.H. (1997) Application of the mono/multilayer and adsorption potential theories to coal methane adsorption isotherms at elevated temperature and pressure. Carbon 35, 1689–705.

Cohen, M.D., Kargacin, B., Klein, C.B., Costa, M. (1993) Mechanisms of chromium cancerogenicity and toxicity. Crit. Rev. Toxicol. 23, 255–268.

Crini, G. (2006) Non-conventional low-cost adsorbents for dye removal: A review. Bioresour. Technol. 97, 1061–1085.

Crini, G., Peindy, H.N., Gimbert, F., Robert, C. (2007) Removal of C.I. Basic Green 4 (malachite green) from aqueous solutions by adsorption using cyclodextrin based adsorbent: kinetic and equilibrium studies. Sep. Purif. Technol. 53, 97–110.

Dakiky, M., Khamis, M., Manassra, M., Mer'eb, M. (2002) Selective adsorption of Chromium(VI) in industrial waste water using low cost abundantly available adsorbents. Adv. Environ. Res. 6, 533–540.

Dave, R.S., Dave, G.B., Mishra, V.P. (2011) Removal of Nickel from electroplating wastewater by weakly basic chelating anion exchange resins: Dowex 50x4, Dowex 50x2 and Dowex M-4195. Journal of Applied Sciences in Environmental Sanitation, 6, 39–44.

Davis, A.P., Bernstein, C., Gietka, P.M. (1995) Waste minimization in electropolishing: process control in: A.K. Sengupta (Ed.), Proceedings of the twenty seventh mid Atlantic industrial waste conference: Hazardous and industrial wastes. Lancaster, Technomic, 62–71.

Dawood, S., Sen, T.K., Phan, C. (2016) Adsorption removal of Methylene Blue (MB) dye from aqueous solution by bio-char prepared from *Eucalyptus sheathiana* bark: kinetic, equilibrium, mechanism, thermodynamic and process design. Desalin. Water Treat. 57 28964-28980.

Dermont, G., Bergeron, M., Mercier, G., Laflèche-Richer, M. (2008) Metal-Contaminated Soils, Remediation Practices and Treatment Technologies. Practice periodical of hazardous, toxic and radioactive waste management, 12, 188–209.

Demirbas, E., Kobya, M., Senturk, E., Ozkan, T. (2004) Adsorption kinetics for the removal of chromium (VI) from aqueous solutions on the activated carbons prepared from agricultural wastes. Water SA, 30, 533–539.

Demirbas, A. (2009) Agricultural based activated carbons for the removal of dyes from aqueous solutions: a review. J. Hazard. Mater. 167, 1–9.

Dhungana, T.P., Yadav, P.N. (2009) Determination of chromium tannery effluent and study of adsorption of Cr(VI) on saw dust and charcoal from sugarcane bagasses. Journal of Nepal Chemical Society, 23, 93–101.

Dialynas, E., Diamadopoulos, E. (2009) Integration of a membrane bioreactor coupled with reverse osmosis for advanced treatment of municipal wastewater. Desalination 238, 302–311.

Dincer, A.R., Gunes, Y., Karakaya, N., Gunes, E. (2007) Comparison of activated carbon and bottom ash for removal of reactive dye from aqueous solution. Bioresource Technol. 98, 834–839.

Ding, Y., Jing, D., Gong, H., Zhou, L., Yang, X. (2012) Biosorption of aquatic cadmium(II) by unmodified rice straw. Bioresour. Technol. 114, 20–25.

Ding, Z., Wan, Y., Hu, X., Wang, S., Zimmerman, A.R., Gao, B. (2016) Sorption of lead and methylene blue onto hickory biochars from different pyrolysis temperatures: Importance of physicochemical properties. J. Ind. Eng. Chem., http://dx.doi.org/10.1016/j.jiec.2016.03.035

Djouider, F. (2012) Radiolytic formation of non-toxic Cr(III) from toxic Cr(VI) in formate containing aqueous solution: A system for water treatment. J. Hazard. Mater. 223–224, 104–109.

Dong, X., Ma, L.Q., Li, Y. (2011) Characteristics and mechanisms of hexavalent chromium removal by biochar from sugar beet tailing. J. Hazard. Mater. 190, 909–915.

Elmoubarki, R., Mahjoubi, F.Z., Tounsadi, H., Moustadraf, J., Abdennouri, M., Zouhri, A., ElAlban, A., Barka, N. (2015) Adsorption of textile dyes on raw and decanted Moroccan clays: kinetics, equilibrium and thermodynamics. Water Resour. Industry 9, 16–29.

El-Sayed, G.O. (2011) Removal of methylene blue and crystal violet from aqueous solutions by palm kernel fiber. Desalination 272, 225–232.

EPA (1990) Environmental Pollution Control Alternatives. Environmental Protection Agency, Cincinnati, US.

EPA (2010) A handbook on the implementation of the regulations for water services authorities for public water supplies. Office of Environmental Enforcement, Ireland.

Eren, E. (2010) Adsorption performance and mechanism in binding of azo dye by raw bentonite. Clean Soil Air Water 38, 758–763.

Eren, E., Afsin, B. (2007) Investigation of a basic dye adsorption from aqueous solution onto raw and pre-treated sepiolite surfaces. J. Dyes Pig. 73, 162–167.

Farhan, B.S.A. (2015) Potential removal of crystal violet (CV), acid red (AR) and methyl orange (MO) from aqueous solution by magnetic nanoparticles. Int. J. Nano. Chem. 3, 97–102.

Farooq, U., Khan, M.A., Atharc, M., Kozinskia, J.A. (2011) Effect of modification of environmentally friendly bioadsorbents wheat (*Triticum aestivum*) on the biosorptive removal of cadmium (II) ions from aqueous solution. Chem. Eng. J. 171, 400–410.

Farsi, H., Hosseini, S.A. (2013) The electrochemical behaviors of methylene blue on the surface of nanostructured $NiWO_4$ prepared by co-precipitation method. J. Solid State Electrochem. 17, 2079–2086.

Fathima, N.N., Aravindhan, R., Rao, J.R., Nair, B.U. (2005) Solid waste removes toxic liquid waste: adsorption of Cr(VI) by Iron complexed protein waste. Environ. Sci. Technol. 39, 2804–2810.

Faust, S.D., Aly, O.M. (1987) Adsorption processes for water treatment. Butterworth Publishers, Stoneham.

Feng, N., Guo, X., Liang, S., Zhu, Y., Liu, J. (2011) Biosorption of heavy metals from aqueous solutions by chemically modified orange peel. J. Hazard. Mater. 185, 49–54.

Fernandez, R.G., Garcia, C.P., Lavin, A.G., de las Heras, J.L.B. (2012) Study of main combustion characteristics for biomass fuels used in boilers. Fuel Process. Technol. 103, 16–26.

Fernandez, Y., Maranon, E., Costrillon, L., Vazquez, I. (2005) Removal of Cd and Zn from inorganic industrial waste leachate by ion exchange. J. Hazard. Mater. 126, 169–175.

Fiol, N., Villaescusa, I., Martínez, M., Miralles, N., Poch, J., Serarols, J. (2006) Sorption of Pb(II), Ni(II), Cu(II) and Cd(II) from aqueous solution by olive stone waste. Sep. Purif. Technol. 50, 132–140.

Foo, K.Y., Hameed, B.H. (2012) A rapid regeneration of methylene blue dye-loaded activated carbons with microwave heating. J. Anal. Appl. Pyrolysis 98, 123–128.

Forgacsa, E., Cserhatia, T., Oros, G. (2004) Removal of synthetic dyes from wastewaters: A review. Environ. Int., 30, 953–971.

Ganguli, A., Tripathi, A.K. (2002) Bioremediation of toxic chromium from electroplating effluent by chromate-reducing *Pseudomonas aeruginosa* A2Chr in two bioreactors. Appl. Microbiol. Biotechnol. 58, 416–420.

Gao, J., Liu, F.Q., Ling, P.P., Lei, J.T., Li, L.J., Li, C.H., Li, A.M. (2013) High efficient removal of Cu(II) by a chelating resin from strong acidic solutions: complex formation and DFT certification. Chem. Eng. J. 222, 240–247.

Gao, P., Feng, Y., Zhang, Z., Liu, J., Ren, N. (2011) Comparison of competitive and synergetic adsorption of three phenolic compounds on river sediment. Environ. Pollut. 159, 2876–2881.

Garg, V.K., Gupta, R., Yadav, A.B., Kumar, R. (2003) Dye removal from aqueous solution by adsorption on treated sawdust. Bioresource Technol. 89, 121–124.

Garg, V.K., Amita, M., Kumar, R., Gupta, R. (2004) Basic dye (methylene blue) removal from simulated wastewater by adsorption using Indian Rosewood sawdust: a timber industry waste. Dyes Pig. 63, 243–250.

Ghasemi, J., Asadpour, S. (2007) Thermodynamics' study of the adsorption process of methylene blue on activated carbon at different ionic strengths. J. Chem. Therm. 39, 967–971.

Gisi, S.D., Lofrano, G., Grassi, M., Notarnicola, M. (2016) Characteristics and adsorption capacities of low-cost sorbents for wastewater treatment: A review. Sustainable Materials and Technologies, 9, 10–40.

Gomori, G. (1955) Preparation of buffers for use in enzyme studies. Methods in Enzymology, 1, 138–146.

Greene, J.C., Baughman, G.L. (1996) Effects of 46 dyes on population growth of fresh green algae *Selenastrum capricornutum*. Text. Chem. Color. 28 (4) 23.

Gu, H.B., Rapole, S.B., Sharma, J., Huang, Y.D., Cao, D.M., Colorado, H.A., Luo, Z.P., Haldolaarachchige, N., Young, D.P., Walters, B., Wei, S.Y., Guo, Z.H. (2012) Magnetic polyaniline nanocomposites towards toxic hexavalent chromium removal. RSC Adv. 2, 11007–11018.

Guechi, El-K., Hamdaoui, O. (2011) Sorption of malachite green from aqueous solution by potato peel: kinetics and equilibrium modeling using non-linear analysis method. Arab. J. Chem. http:// dx.doi.org/10.1016/j.arabjc.2011.05.011.

Guiza, S. (2017) Biosorption of heavy metal from aqueous solution using cellulosic waste orange peel. Ecol. Eng. 99, 134–140.

Guo, H., Bi, C., Zeng, C., Ma, W., Yan, L., Li, K., Wei, K. (2017) Camellia oleifera seed shell carbon as an efficient renewable bioadsorbent for the adsorption removal of hexavalent chromium and methylene blue from aqueous solution. doi:10.1016/j.molliq.2017.11.096

Guo, M.X., Qiu, G.N., Song, W.P. (2010) Poultry litter-based activated carbon for removing heavy metal ions in water. Waste Manage. 30, 308–315.

Gupta, N., Kushwaha, A.K., Chattopadhyaya, M.C. (2011) Application of potato (*Solanum tuberosum*) plant wastes for the removal of methylene blue and malachite

green dye from aqueous solution. Arab. J. Chem. http://dx.doi.org/10.1016/j.arabjc.2011.07.021

Gupta, V.K., Ali, I. (2000) Utilization of bagasse fly ash (a sugar industry waste) for the removal of copper and zinc from wastewater. Sep. Purif. Technol. 18, 131–140.

Gupta, V.K., Jain, C.K., Ali, I., Sharma, M., Saini, V.K. (2003) Removal of cadmium and nickel from wastewater using bagasse fly ash-a sugar industry waste. Water Res. 37, 4038–4044.

Gupta, V.K., Mittal, A., Krishnan, L., Gajbe, V. (2004) Adsorption kinetics and column operations for the removal and recovery of malachite green from wastewater using bottom ash. Sep. Purif. Technol. 40, 87–96.

Gupta, V.K., Pathania, D., Sharma S., Singh, P. (2013) Preparation of bio-based porous carbon by microwave assisted phosphoric acid activation and its use for adsorption of Cr (VI). J. Colloid Interface Sci. 401, 125–132.

Gupta, V.K., Shrivastava, A.K., Jain, N. (2001) Biosorption of Cr(VI) from aqueous solution by green algae spirogyra species. Water Res. 35, 4079–4085.

Gupta, V.K., Srivastava, S.K., Mohan, D. (1997) Equilibrium uptake, sorption dynamics, process optimization, and column operations for the removal and recovery of malachite green from wastewater using activated carbon and activated slag. Ind. Eng. Chem. Res. 36, 2207–2218.

Hall, K.R., Eagleton, L.C., Acrivos, A., Vermeulen, T. (1966) Pore solid diffusion kinetics in fixed bed adsorption under constant pattern conditions. Ind. Eng. Chem. Fundam. 5, 212–223.

Hamadi, N.K., Chen, X.D., Farid, M.M., Lu, M.G.Q. (2001) Adsorption kinetics for the removal of Cr(VI) from aqueous solution by adsorbents derived from used tyres and sawdust. J. Chem. Eng. 84, 95–105.

Hamdaouia, O., Saoudi, F., Chiha, M., Naffrechoux, E. (2008) Sorption of malachite green by a novel sorbent dead leaves of plane tree: Equilibrium and kinetic modelling. Chem. Eng. J. 143, 73–84.

Hameed, B.H., Ahmad, A.A. (2009) Batch adsorption of methylene blue from aqueous solution by garlic peel, an agricultural waste biomass. J. Hazard. Mater. 164, 870–875.

Hameed, B.H., Ahmad, A.L., Latiff, K.N.A. (2007) Adsorption of basic dye (methylene blue) onto activated carbon prepared from rattan sawdust. Dyes Pig. 75, 143–149.

Hameed, B.H., El-Khaiary, M.I. (2008) Removal of basic dye from aqueous medium using a novel agricultural waste material: pumpkin seed hull. J. Hazard. Mater. 155, 601–609.

Hameed, B.H., Krishni, R.R., Sata, S.A. (2009) A novel agricultural waste adsorbent for the removal of cationic dye from aqueous solutions. J. Hazard. Mater. 162, 305–311.

Hameed, B.H., Din, A.T.M., Ahmad, A.L. (2007) Adsorption of methylene blue onto bamboo-based activated carbon: Kinetics and equilibrium studies. J. Hazard. Mater. 141, 819–825.

Hameed, B.H., Mahmoud, D.K., Ahmad, A.L. (2008) Equilibrium modeling and kinetic studies on the adsorption of basic dye by a low-cost adsorbent: Coconut (*Cocos nucifera*) bunch waste. J. Hazard. Mater. 158, 65–72.

Hameed, B.H., Mahmoud, D.K., Ahmad, A.L. (2008a) Sorption equilibrium and kinetics of basic dye from aqueous solution using banana stalk waste. J. Hazard. Mater. 158, 499–506.

Han, R., Zhang, L., Song, C., Zhang, M., Zhu, H., Zhang, L. (2010) Characterization of modified wheat straw, kinetic and equilibrium study about copper ion and methylene blue adsorption in batch mode. Carbohyr. Polym. 79, 1140–1149.

Han, R., Zou, W., Yu, W., Cheng, S., Wang, Y., Shi, J. (2007) Biosorption of methylene blue from aqueous solution by fallen Phoenix tree's leaves. J. Hazard. Mater. 141, 156–162.

Hao, O.J., Kim, H., Chiang, P.C. (2000) Decolorization of wastewater. Critical Reviews in Environmental Science and Technology, 30, 449–505.

Hawari, A.H., Mulligan, C.N. (2006) Heavy metals uptake mechanisms in a fixed-bed column by calcium-treated anaerobic biomass. Process Biochem. 41, 187–198.

Heidmann, I., Calmano, W. (2008) Removal of Zn(II), Cu(II), Ni(II), Ag(I) and Cr(VI) present in aqueous solutions by aluminium electrocoagulation. J. Hazard. Mater. 152, 934–941.

Hema, M., Arivoli, S. (2007) Comparative study on the adsorption kinetics and thermodynamics of dyes onto acid activated low cost carbon. Int. J. Phys. Sci. 2, 10–17.

Hossain, M.A., Ngo, H.H., Guo, W.S., Setiadi, T. (2012) Adsorption and desorption of copper(II) ions onto garden grass. Bioresour. Technol. 121, 386–395.

Ho, Y.S., McKay, E. (2000) The kinetics of sorption of divalent metal ions onto *sphagnum* moss peat. Water Res. 34, 735–742.

Ho, Y.S., Mckay, G. (1998) Sorption of dye from aqueous solution by peat. Chem. Eng. J. 70, 115–124.

Hunger, K. (2003) Industrial Dyes, Chemistry, Properties, Applications. Wiley-VCH, Weinheim, Germany, 2003, pp. 1–10.

Huang, P., Fuerstenau, D.W. (2001) The effect of the adsorption of lead and cadmium ions on the interfacial behavior of quartz and talc. Coll. Surf. A Physicochem. Eng. Asp. 177, 147–156.

Husain, Q., Jan, U. (2000) Detoxification of phenols and aromatic amines from polluted wastewater by using phenol oxidases. J. Sci. Ind. Res. 59, 286–293.

Inyang, M., Gao, B., Zimmerman, A., Zhang, M., Chen, H. (2014) Synthesis, characterization, and dye sorption ability of carbon nanotube–biochar nanocomposites. Chem. Eng. J. 236, 39–46.

Iqbal, M., Saeed, A., Kalim, I. (2009) Characterization of adsorptive capacity and investigation of mechanism of Cu^{2+}, Ni^{2+} and Zn^{2+} adsorption on mango peel waste from constituted metal solution and genuine electroplating effluent. Sep. Sci. Technol. 44, 3770–3791.

IUPAC (1982) Manual of Symbols and Terminology of Colloid Surface. Butterworths, London, p. 1.

Jalali, M., Aboulghazi, F. (2013) Sunflower stalk, an agricultural waste, as an adsorbent for the removal of lead and cadmium from aqueous solutions. J. Mater. Cycles Waste Manag. 15, 548–555.

Janos, P., Buchtova, H., Ryznarova, M. (2003) Sorption of dyes from aqueous solutions onto fly ash. Water res. 37, 4938–4944.

Jimoh, T.O., Iyaka, Y.A., Nubaye, M.M. (2012) Sorption Study of Co (II), Cu(II) and Pb(II) ions removal from aqueous solution by adsorption on Flamboyant Flower (*Delonix regia*). Am. J. Chem. 2, 165–170.

Johnson, P.R. (1999) A comparison of streaming and micro-electrophoresis methods for obtaining the zeta potential of granular porous media surfaces. J. Coll. Interface Sci. 209, 264–267.

Juang, R.S., Wu, F.C., Tseng, R.L. (2002) Characterization and use of activated carbons prepared from bagasses for liquid-phase adsorption. Colloids Surf. A Physicochem. Eng. Asp. 201, 191–199.

Jung, R., Steinle, D., Anliker, R. (1992) A compilation of genotoxicity and carcinogenicity data on aromatic aminosulphonic acids. Food Chem. Toxicol. 30, 633–660.

Kadirvelu, K., Karthika, C., Vennilamani, N., Pattabhi, S. (2005) Activated carbon from industrial solid waste as an adsorbent for the removal of Rhodamine-B from aqueous solution: Kinetic and equilibrium studies. Chemosphere, 60, 1009–1017.

Kadirvelu, K., Kavipriya, M., Karthika, V., Radhika, M., Vennilamani, N., Pattabhi, S. (2003) Utilization of various agricultural wastes for activated carbon preparation and application for the removal of dyes and metal ions from aqueous solutions. Bioresource Technol. 87, 129–132.

Kaikake, K., Hoaki, K., Sunada, H., Dhakal, R.P., Baba, Y. (2007) Removal characteristics of metal ions using degreased coffee beans: adsorption equilibrium of Cd(II). Bioresour. Technol. 98, 2787–2791.

Kannan, N., Sundaram, M.M. (2001) Kinetics and mechanism of removal of methylene blue by adsorption on various carbons—a comparative study. Dyes Pigment, 51, 25–40.

Kapoor, K.L. (2009) A textbook of physical chemistry, 3rd Edition (Volume 2), MacMillian Publishers Limited, India.

Karthikeyan, K.G., Elliott, H.A., Cannon, F.S. (1996) Enhanced metal removal from wastewater by coagulant addition. In Proceedings of 50th Purdue Industrial Waste Conference 50, 259–267.

Khaled, A., El Nemr, A., El-Sikaily, A., Abdelwahab, O. (2009) Removal of Direct N Blue-106 from artificial textile dye effluent using activated carbon from orange peel: Adsorption isotherm and kinetic studies. J. Hazard. Mater. 165, 100–110.

Khandegar, V., Saroha, A.K. (2013) Electrocoagulation for the treatment of textile industry effluent: A review. J. Environ. Manage. 128, 949–963.

Khare, P., Goyal, D.K. (2013) Effect of high and low rank char on soil quality and carbon sequestration. Ecol. Eng. 52, 161–166.

Khattri, S.D., Singh, M.K. (2012) Use of Sagaun sawdust as an adsorbent for the removal of crystal violet dye from simulated wastewater. Env. Prog. Sustain. Ener. 31, 435–442.

Khattri, S.D., Singh, M.K. (2009) Colour removal from synthetic dye wastewater using a biosolid sorbent. Water Air Soil Pollut. 120, 283–294.

Khouni, I., Marrot, B., Moulin, P., Amar, R.B. (2011) Decolourization of the reconstituted textile effluent by different process treatments: Enzymatic catalysis, coagulation/flocculation and nanofiltration processes. Desalination, 268, 27–37.

Kiernan, J.A. (2001) Classification and naming of dyes, stains and fluorochromes. Biotech Histochem. 76, 261–278.

Kibe, K., Takahashi, M., Kameya, T., Urano, K. (2000) Adsorption equilibriums of principal herbicides on paddy soils in Japan. Sci. Total Environ. 263, 115–125.

Kim, K.H., Kim, J.Y, Cho, T.S., Choi, J.W. (2012) Influence of pyrolysis temperature on physicochemical properties of biochar obtained from the fast pyrolysis of pitch pine (*Pinus rigida*). Bioresour. Technol. 118, 158–162.

Kizito, S. Wu, S., Kipkemoi Kirui, W., Lei, M., Lu, Q., Bah, H., Dong, R. (2015) Evaluation of slow pyrolyzed wood and rice husks biochar for adsorption of ammonium nitrogen from piggery manure anaerobic digestate slurry. Sci. Total Environ. 505, 102–112.

Komnitsas, K.A., Zaharaki, D. (2016) Morphology of modified biochar and its potential for phenol removal from aqueous solutions. Front. Environ. Sci. 4, 1–11.

Konicki, W., Sibera, D., Mijowska, E., Lendzion-Bielun, Z., Narkiewicz, U. (2013) Equilibrium and kinetic studies on acid dye Acid Red 88 adsorption by magnetic ZnFe2O4 spinel ferrite nanoparticles. J. Colloid. Interf. Sci. 398, 152–160.

Kongsricharoern, N., Polprasert, C. (1996) Chromium removal by a bipolar electrochemical precipitation process. Water Sci. Technol. 34, 109–116.

Koroki, M., Saito, S., Hashimoto, H., Yamada, T., Aoyoma, M. (2010) Removal of Cr(VI) from aqueous solutions by the clum of bamboo grass treated with concentrated sulfuric acid. Environ. Chem. Lett. 8, 197–207.

Krishnan, K.A., Sreejalekshmi, K.G., Baiju, R.S. (2011) Nickel (II) adsorption onto biomass based activated carbon obtained from sugarcane bagasse pith. Bioresour. Technol. 102, 10239–10247.

Krishnan, S., Rawindran, H., Sinnathambi, C.M., Lim, J.W. (2017) Comparison of various advanced oxidation processes used in remediation of industrial wastewater laden with recalcitrant pollutants. Materials Science and Engineering, doi:10.1088/1757-899X/206/1/012089

Ku, Y., Jung, I.L. (2001) Photocatalytic reduction of Cr(VI) in aqueous solutions by UV irradiation with the presence of titanium dioxide. Water Res. 35, 135–142.

Kumar, K.V. (2006) Linear and non-linear regression analysis for the sorption kinetics of methylene blue onto activated carbon. J. Hazard. Mater. 137, 1538–1544.

Kumar, P.S., Ramalingam, S., Kirupha, S.D., Murugesan, A., Vidhyadevi, T., Sivanesan, S. (2011) Adsorption behavior of nickel(II) onto cashew nut shell: equilibrium, thermodynamics, kinetics, mechanism and process design. Chem. Eng. J. 167, 122–131.

Kumar, R., Ahmad, R. (2011) Biosorption of hazardous crystal violet dye from aqueous solution onto treated ginger waste TGW. Desalination, 265, 112–118.

Kumric, K.R., Dukic, A.B., Trtic-Petrovic, T.M., Vukelic, N.S., Stojanovic, Z., Grbovic Novakovic, J.D., Matovic, L.L. (2013) Simultaneous removal of divalent heavy metals from aqueous solutions using raw and mechanochemically treated interstratified montmorillonite/kaolinite clay. Ind. Eng. Chem. Res. 52, 7930–7939.

Lai, K.C., Lo, I.M. (2008) Removal of chromium (VI) by acid-washed zero-valent iron under various ground water geochemistry conditions. Environ. Sci. Technol. 42, 1238–1244.

Lam, K.F., Yeung, K.L., Mckay, A.G. (2007) Efficient approach for Cd^{2+} and Ni^{2+} removal and recovery using mesoporous adsorbent with tunable selectivity. Environ. Sci. Technol. 41, 3329–3334.

Langmuir, I. (1918) The adsorption of gases on plane surfaces of glass, mica and platinum. J. Am. Chem. Soc. 40, 1361–1403.

Lee, C.K., Liu, S.S., Juang, L.C., Wang, C.C., Lin, K.S., Lyu, M.D. (2007) Application of MCM-41 for dyes removal from wastewater. J. Hazard. Mater. 147, 997–1005.

Lee, D.W., Lim, C., Israelachvili, J.N., Hwang, D.S. (2013) Strong adhesion and cohesion of chitosan in aqueous solutions. Langmuir, 29, 14222–14229.

Lehmann, J., Rillig, M.C., Thies, J., Masiello, C.A., Hockaday, W.C., Crowley, D. (2011) Biochar effects on soil biota-A review. Soil Biol. Biochem. 43, 1812–1836.

Li, X., Tang, Y., Xuan, Z., Liu, Y., Luo, F. (2007) Study on the preparation of orange peel cellulose adsorbents and biosorption of Cd^{2+} from aqueous solution. Sep. Purif. Technol. 55, 69–75.

Li, Y., Du, Q., Liu, T., Sun, J., Wang, Y., Wu, S., Wang, Z., Xia, Y., Xia, L. (2013) Methylene blue adsorption on graphene oxide/calcium alginate composites. Carbohydr. Polym. 95, 501–507.

Lima, R.O.A., Bazo, A.P., Salvadori, D.M.F., Rech, C.M., Oliveira, D.P., Umbuzeiro, G.A. (2007) Mutagenic and carcinogenic potential of a textile azo dye processing plant effluent that impacts a drinking water source. Mutat. Res., Genet. Toxicol. Environ. Mutagen. 626, 53–60.

Liu, B., Lu, L., Wang, M., Zi, Y. (2008) A study of nanostructured gold modified glassy carbon electrode for the determination of trace Cr(VI). J. Chem. Sci. 120, 493–498.

Liu, W., Liu, Y., Tao, Y., Yu, Y., Jiang, H., Lian, H. (2014) Comparative study of adsorption of Pb(II) on native garlic peel and mercerized garlic peel. Environ. Sci. Pollut. Res. 21, 2054–2063.

Liu, Y., Liu, Y.I. (2007) Biosorption isotherms, kinetics and thermodynamics. Sep. Purif. technol. 61, 229–242.

Liu, Z., Quek, A., Hoekman, S.K., Srinivasan, M.P., Balasubramanian, R. (2012) Thermogravimetric investigation of hydrochar-lignite co-combustion. Bioresour. Technol. 123, 646–652.

Losso, J. N., Khachatryan, A., Ogawa, M., Godber, J.S., Shih, F. (2005) Random centroid optimization of phosphatidylglycerol stabilized lutein-enriched oil-in-water emulsions at acidic pH. Food Chemistry, 92, 737–744.

Low, K.S., Lee, C.K. (1990) The removal of cationic dyes using coconut husk as an adsorbent. Pertanika, 132, 221–228.

Low, F.C.F., Wu, T.Y., Teh, C.Y., Juan, J.C., Balasubramanian, N. (2012) Investigation into photocatalytic decolorisation of CI Reactive Black 5 using titanium dioxide nanopowder. Coloration Technology 128, 44–50.

Lu, H., Zhang, W., Yang, Y., Huang, X., Wang, S., Qiu, R. (2012) Relative distribution of Pb^{2+} sorption mechanisms by sludge-derived biochar. Water Res. 46, 854–862.

Lundh, M., Jonsson, L., Dahlquist, J. (2000) Experimental studies of the fluid dynamics in the separation zone in dissolved air flotation. Water Res. 34, 21–30.

Lyu, H., Gao, B., He, F., Zimmerman, A.R., Ding, C., Tang, J., Crittenden, J.C. (2018) Experimental and modeling investigations of ball-milled biochar for the removal of aqueous methylene blue. Chem. Eng. J. 335, 110–119.

Ma, H., Li, J.B., Liu, W.W., Miao, M., Cheng, B.J., Zhu, S.W. (2015) Novel synthesis of a versatile magnetic adsorbent derived from corncob for dye removal. Bioresour. Technol. 190, 13–20.

Mahmoud, D.K., Salleh, M.A.M., Karim, W.A.W.A., Idris, A., Abidin, Z.Z. (2012) Batch adsorption of basic dye using acid treated kenaf fibre char: equilibrium, kinetic and thermodynamic studies. Chem. Eng. J. 181–182, 449–457.

Malarvizhi, T.S., Santhi, T. (2013) Demineralised lignite fly ash for the removal of Zn (II) ions from aqueous Solution. J. Water Res. Protect. 5, 72–81.

Malik, P.K. (2003) Use of activated carbons prepared from sawdust and rice-husk for adsorption of acidic dyes: a case study of acid yellow 36. Dyes Pig. 56, 243–250.

Malik, P.K., Saha, S.K. (2003) Oxidation of direct dyes with hydrogen peroxide using ferrous ion as catalyst. Sep. Puri. Technol. 31, 241–250.

Malik, R., Ramteke, D.S., Wate, S.R. (2007) Adsorption of malachite green on groundnut shell waste based powdered activated carbon. Waste Manag. 27, 1129–1138.

Mall, I.D., Srivastava, V.C., Agarwal, N.K. (2006) Removal of Orange-G and Methyl Violet dyes by adsorption onto bagasse fly ash – Kinetic study and equilibrium isotherm analysis. Dyes Pig. 69, 210–223.

Manya, J.J. (2012) Pyrolysis for biochar purposes: a review to establish current knowledge gaps and research needs. Environ. Sci. Technol. 46, 7939–7954.

Marc, R. (1996) Asian textile dye makers are a growing power in changing market. CEN North East News Bureau 73, 10–12.

Markandeya, S.P.S., Mohan, D. (2017) Toxicity of disperse dyes and its removal from wastewater using various adsorbents: a review. Research Journal of Environmental Toxicology, 11, 72–89.

Mary, G.S., Sugumaran, P., Niveditha, S., Ramalakshmi, B., Ravichandran, P., Seshadri, S. (2016) Production, characterization and evaluation of biochar from pod

(*Pisum sativum*), leaf (*Brassica oleracea*) and peel (*Citrus sinensis*) wastes. Int. J. Recycl. Org. Waste Agric. 5, 43–53.

McQuarrie, D.A. (1997) Physical Chemistry: A molecular Approach. Sausalito: University Science Books.

Memon, J.R., Memon, S.Q., Bhanger, M.I., El-Turki, A., Keith, R., Allen, G.C.H. (2009) Banana peel: a green and economical sorbent for the selective removal of Cr(VI) from industrial wastewater. Colloids Surf. B Biointerfaces 70, 232–237.

Metcalf and Eddy (2004) Wastewater engineering, treatment and reuse, 4th Edition, TATA-McGraw Hill Publishing Company Limited, New Delhi.

Meyer, S., Glaser, B., Quicker, P. (2011) Technical, economical, and climate-related aspects of biochar production technologies: a literature review. Environ. Sci. Technol. 45, 9473–9483.

Mishra, G., Tripathy, M. (1993) A critical review of the treatment for decolorization of textile effluent. Colourage 40, 35–38.

Mittal, A., Krishnan, L., Gupta, V.K. (2005) Removal and recovery of malachite green from wastewater using an agricultural waste material, de-oiled soya. Sep. Purif. Technol. 43, 125–133.

Mittal, A., Mittal, J., Malviya, A., Kaur, D., Gupta, V.K. (2010) Adsorption of hazardous crystal violet from waste water by waste materials. J. Colloid Interface Sci., 343, 463–473.

Moghadam, M., Nasirizadeh, N., Dashti, Z., Babanezhad, E. (2013) Removal of Fe(II) from aqueous solution using pomegranate peel carbon: Equilibrium and kinetic studies. Int. J. Ind. Chem. 4, 1–6.

Mohammadi, H., Gholami, M., Rahimi, M. (2009) Application and optimization in Chromium-contaminated wastewater treatment of the reverse osmosis technology. Desalination and Water Treatment, 9, 229–233.

Mohan, J. (2005) Organic spectroscopy principles and applications. Second ed., Narosa Publishing House, New Delhi.

Mohan, S.V., Rao, N.C., Karthikeyan, J. (2002) Adsorptive removal of direct azo dye from aqueous phase onto coal based sorbents: A kinetic and mechanistic study. J. Hazard. Mater. 90, 189–204.

Mohanty, K., Naidu, J.T., Meikap, B.C., Biswas, M.N. (2006) Removal of crystal violet from waste water by activated carbons prepared from rice husk. Ind. Eng. Chem. Res. 45, 5165–5171.

Mohrig, J.R., Hammond, C.N., Schatz, P.F. (2006) Techniques in Organic Chemistry, 3rd ed., W. H. Freeman and Company, New York.

Mohsen-Nia, M., Montazeri, P., Modaress, H. (2007) Removal of Cu^{2+} and Ni^{2+} from wastewater with a chelating agent and reverse osmosis processes. Desalination 217, 276–281.

Mondal, S. (2008) Methods of dye removal from dye house effluent-an overview. Environ. Eng. Sci. 25, 383–396.

Morillo, E., Undabeytia, T., Maqueda, C., Ramos, A. (2000) Glyphosate adsorption on soils of different characteristics, influence of copper addition. Chemosphere 40, 103–107.

Namasivayam, C., Kavitha, D. (2002) Removal of Congo red from water by adsorption on to activated carbon prepared from coir pith, an agricultural solid waste. Dyes Pigment 54, 47–58.

Namasivayam, C., Kumar, M.D., Selvi, K., Begum, R.A., Vanathi, T., Yamuna, R.T. (2001) Waste coir pith – A potential biomass for the treatment of dyeing wastewaters. Biomass Bioener. 6, 477–483.

Nandi, B.K., Goswami, A., Purkait, M.K. (2009) Removal of cationic dyes from aqueous solutions by kaolin: Kinetic and equilibrium studies. Appl. Clay Sci. 42, 583–590.

Nasuha, N., Hameed, B.H., Din, A.T.M. (2010) Rejected tea as a potential low-cost adsorbent for the removal of methylene blue. J. Hazard. Mater. 175, 126–132.

Nautiyal, P., Subramanian, K.A., Dastidar, M.G. (2016) Adsorptive removal of dye using biochar derived from residual algae after in-situ transesterification: Alternate use of waste of biodiesel industry. J. Environ. Manage. 182, 187–197.

Nava, Y.F., Ulmanu, M., Anger, I., Maranon, E., Castrillon, L. (2011) Use of granular bentonite in the removal of Mercury(II), Cadmium(II) and Lead(II) from aqueous solutions. Water Air Soil Pollution, 215, 239–249.

Ncibi, M.C., Mahjoub, B., Seffen, M. (2007) Kinetic and equilibrium studies of methylene blue biosorption by *Posidonia oceanic* (L.) fibres. J. Hazard. Mater. 139, 280–285.

Ngamukot, P., Charoenraks, T., Chailapakul, O., Motomizu, S., Chuanuwatanakul, S. (2006) Cost-effective flow cell for the determination of malachite green and leucomalachite green at a boron-doped diamond thin-film electrode. Analytical Sciences 22, 111–116.

Nigam, P., Singh, D., Marchant, R. (1995) An investi-gation of the biodegradation of textile dyes by aerobic and anaerobic microorganisms. In Environmental Bio-

technology: Principles and Applications, ed. M. Moo-Young. Kluwer Academic, The Netherlands, pp. 278–292.

Nigam, P., Armour, G., Banat, I.M., Singh, D and Marchant, R. (2000) Physical removal of textile dyes from effluents and solid- state fermentation of dye adsorbed agricultural residues. Bioresour. Technol., 72, 219–226.

Novotny, C., Dias, N., Kapanen, A., Malachova, K., Vandrovcova, M., Itavarra, M., Lima, N. (2006) Comparative use of bacterial, algal and protozoan tests to study toxicity of azo and anthraquinone dyes. Chemosphere, 63, 1436–1442.

Nriagu, J.O., Nieboer, E. (1988) Chromium in the natural and human Environment. Wiley, New York.

Ofomaja, A.E., Ho, Y.S. (2007) Equilibrium sorption of anionic dye from aqueous solution by palm kernel fibre as sorbent. Dyes Pig. 74, 60–66.

Oladipo, A.A., Ifebajo, A.O. (2018) Highly efficient magnetic chicken bone biochar for removal of tetracycline and fluorescent dye from wastewater: Two-stage adsorber analysis. J. Environ. Manage. 209, 9–16.

Önal, Y. (2006) Kinetics of adsorption of dyes from aqueous solution using activated carbon prepared from waste apricot. J. Hazard. Mater. 137, 1719–1728.

Onal, Y., Akmil-Basar, C., Eren, D., SarIcI-O zdemir, C., Depci, T. (2006) Adsorption kinetics of Malachite green onto activated carbon prepared from Tunc¸bilek lignite. J. Hazard. Mater. 128, 150–157.

Ong, S.T., Lee, C.K., Zainal, Z. (2007) Removal of basic and reactive dyes using ethylenediamine modified rice hull. Bioresource Technol. 98, 2792–2799.

O'Neill, C., Hawkes, F.R., Hawkes, D.L., Lourenço, N.D., Pinheiro, H.M., Delée, W. (1999) Colour in textile effluents – sources, measurements, discharge consents and simulation: A review. J. Chem. Technol. Biotechnol. 74, 1009–1018.

Opperman, D.J., van Heerden, E. (2007) Aerobic Cr(VI) reduction by *Thermus scotoductus* strain SA-Journal of Applied Microbiology, 103, 1907–1913.

Osma, J.F., Saravia, V., Toca-Herrera, J.L., Couto, S.R. (2007) Sunflower seed shells: a novel and effective low-cost adsorbent for the removal of the diazo dye Reactive Black 5 from aqueous solutions. J. Hazard. Mater. 147, 900–905.

Outridge, P.M., Scheuhammer, A.M. (1993) Bioaccumulation and toxicology of chromium: Implications for wildlife. J. Contam. Toxicol. 130, 31–37.

Ozbay, I., Ozdemir, U., Ozbay, B., Veli, S. (2013) Kinetic, thermodynamic and equilibrium studies for adsorption of azo reactive dye onto a novel waste adsorbent: charcoal ash. Desalin. Water Treat. 51, 6091–6100.

Ozdes, D., Duran, C., Senturk, H.B. (2011) Adsorptive removal of Cd(II) and Pb(II) ions from aqueous solutions by using Turkish illitic clay. J. Environ. Manage. 92, 3082–3090.

Padmesh, T.V.N., Vijayaraghavan, K., Sekaran, G., Velan, M. (2005) Batch and column studies on biosorption of acid dyes on fresh water macro algae *Azolla filiculoides*. J. Hazard. Mater. 125, 121–129.

Pagilla, K., Canter, L.W. (1999) Laboratory studies on remediation of chromium contaminated soils. J. Environ. Eng. 125, 243–248.

Palmer, C.D., Puls, R.W. (1994) Natural Attenuation of Hexavalent Chromium in Ground Water and Soils, U.S. EPA Ground Water Issue Paper, EPA/540/5-94/505 (U.S. EPA, Office of Research and Development, Washington).

Pang, F.M., Teng, S.P., Teng, T.T., Omar, A.K.M. (2009) Heavy metals removal by hydroxide precipitation and coagulation-flocculation methods from aqueous solutions. Water Quality Research Journal of Canada, 44, 174–183.

Pang, Y., Zeng, G.M., Tang, L., Zhang, Y., Liu, Y.Y., Lei, X.X., Li, Z., Zhang, J.C., Liu, Z.F., Xiong, Y.Q., (2011) Preparation and application of stability enhanced magnetic nanoparticles for rapid removal of Cr(VI). Chem. Eng. J. 175, 222–227.

Pang, Y., Zeng, G.M., Tang, L., Zhang, Y., Liu, Y.Y., Lei, X.X., Li, Z., Zhang, J.C., Xie, G.X. (2011a) PEI-grafted magnetic porous powder for highly effective adsorption of heavy metal ions. Desalination 281, 278–284.

Parab, H., Joshi, S., Shenoy, N., Lali, A., Sharma, U.S., Sudersanan, M. (2006) Determination of kinetic and equilibrium parameters of the batch adsorption of Co(II), Cr(III) and Ni(II) onto coir pith. Process Biochem. 41, 609–615.

Parab, H., Suderesan, M., Pathare, N., Vaze, B. (2009) Use of agroindustrial wastes for removal of basic dyes from aqueous solutions. Clean 37, 963–969.

Parmar, M., Thakur, L.S. (2013) Heavy metal Cu, Ni and Zn: Toxicity, health hazards and their removal techniques by low cost adsorbents - A short review. International Journal of Plant, Animal and Environmental Sciences, 3, 143–157.

Pearce, C.I., Lloyd, J.R., Guthrie, J.T. (2003) The removal of colour from textile wastewater using whole bacterial cells: a review. Dyes Pig. 58, 179–196.

Pehlivan, E., Altun, T., Parlayici, S. (2012) Modified barley straw as a potential biosorbent for removal of copper ions from aqueous solution. Food Chem. 135, 2229–2234.

Petrilli, F.L., Deflora, S. (1977) Toxicity and Mutagenicity of Hexavalent Chromium on *Salmonella typhimurium*. Appl. Environ. Microbiol. 33, 805–809.

Poletto, M., Zattera, A.J., Santana, R.M.C. (2012) Structural differences between wood species: Evidence from chemical composition, FTIR spectroscopy and thermogravimetric analysis. J. Appl. Polym. Sc., 126, 336–343.

Porkodi, K., Kumar, K.V. (2007) Equilibrium kinetics and mechanism modeling and simulation of basic and acid dyes sorption onto jute fiber carbon: Eosin yellow malachite green and crystal violet single component systems. J. Hazard. Mater. 143, 311–327.

Qi, Y.F., Yue, Q.Y., Han, S.X., Yue, M., Gao, B.Y., Yu, H., Shao, T. (2010) Preparation and mechanism of ultra-lightweight ceramics produced from sewage sludge. J. Hazard. Mater. 176, 76–84.

Qiu, Y., Zheng, Z., Zhou, Z., Sheng, G.D. (2009) Effectiveness and mechanisms of dye adsorption on a straw-based biochar. Bioresour. Technol. 100, 5348–5351.

Rajeswari, S., Namasivayam, C., Kadirvelu, K. (2001) Orange peel as an adsorbent in the removal of Acid violet 17 acid dye from aqueous solutions. Waste. Manag. 21, 105–110.

Ramola, S., Mishra, T., Rana, G., Srivastava, R.K. (2014) Characterization and pollutant removal efficiency of biochar derived from baggase, bamboo and tyre. Env. Monitor. Asses. 186, 9023–9039.

Rawat, A.P., Singh, D.P. (2017) Kinetic and thermodynamic study on adsorption characteristics of ash derived from distilled waste of aromatic crop *Mentha piperita*: a low-cost, efficient adsorbent for crystal violet removal. Desalination Water Treat. 84, 225–236.

Reznik, S.G., Katz, I., Dosoretz, C.G. (2008) Removal of dissolved organic matter by granular activated carbon adsorption as a pretreatment to reverse osmosis of membrane bioreactor effluents. Water Resour. 42, 1595–1605.

Robinson, T., McMullan, G., Marchant, R., Nigam, P. (2001) Remediation of dyes in textile effuent: a critical review on current treatment technologies with a proposed alternative. Bioresour. Technol. 77, 247–255.

Saeed, A., Sharif, M., Iqbal, M. (2010) Application potential of grapefruit peel as dye sorbent: Kinetics, equilibrium and mechanism of crystal violet adsorption. J. Hazard. Mater. 179, 564–572.

Saha, P.D., Chowdhury, S., Mondal, M., Sinha, K. (2012) Biosorption of Direct Red 28 (Congo red) from aqueous solutions by eggshells: Batch and column studies. Sep. Sci. Technol. 47, 112–123.

Saha, P., Chowdhury, S., Gupta, S., Kumar, I. (2010) Insight into adsorption equilibrium, kinetics and thermodynamics of malachite green onto clayey soil of Indian origin. Chem. Eng. J. 165, 874–882.

Saha, R., Mukherjee, K., Saha, I., Ghosh, A., Ghosh, S., Saha, B. (2013) Removal of hexavalent chromium from water by adsorption on mosambi (*Citrus limetta*) peel. Res. Chem. Intermed. 39, 2245–2257.

Saha, R., Nandi, R., Saha, B. (2011) Sources and toxicity of hexavalent chromium. J. Coord. Chem. 64, 1782–1806.

Salleh, M.A.M., Mahmoud, D.K., Karim, W.A.W.A., Idris, A. (2011) Cationic and anionic dye adsorption by agricultural solid wastes: a comprehensive review. Desalination 280, 1–13.

Samania, M.R., Borgheib, S.M., Oladc, A., Chaichid, M.J. (2010) Removal of chromium from aqueous solution using polyaniline-poly ethylene glycol composite. J. Hazard. Mater. 184, 248–254.

Sampera, E., Rodrigueza, M., De la Rubia, M.A., Prats, D. (2009) Removal of metal ions at low concentration by micellar-enhanced ultrafiltration (MEUF) using sodium dodecyl sulfate (SDS) and linear alkylbenzene sulfonate (LAS). Sep. Purif. Technol. 65, 337–342.

Saner, G. (1980) Chromium in Nutrition and Diseases. Alan R Liss Inc., New York.

Santhi, T., Manonmani, S., Smitha, T. (2011) Kinetics and isotherm studies on cationic dyes adsorption onto *Annona squamosa* seed activated carbon. Int. J. Eng. Sci. Technol. 2, 287–295.

Sarin, V., Pant, K.K. (2006) Removal of chromium from industrial waste by using eucalyptus bark. Bioresour. Technol. 97, 15–20.

Sathishkumar, P., Arulkumar, M., Palvannan, T. (2012) Utilization of agro-industrial waste *Jatropha curcas* pods as an activated carbon for the adsorption of reactive dye Remazol Brilliant Blue R (RBBR). J. Clean. Prod. 22, 67–75.

Schulz, H., Baranska, M. (2007) Identification and quantification of valuable plant substances by IR and Raman spectroscopy. Vib. Spectrosc., 43, 13–25.

Sciban, M.B., Klasnja, M.T., Antov, M.G. (2011) Study of the biosorption of different heavy metal ions onto kraft lignin. Ecol. Eng. 37, 2092–2095.

Seaman, J.C., Bertsch, P.M., Schwallie, L. (1999) In situ Cr(VI) reduction within coarse-textured, oxide-coated soil and aquifer systems using Fe(II) solutions. Environ. Sci. Technol. 33, 938–944.

Selvaraj, K., Manonmani, S., Pattabhi, S. (2003) Removal of hexavalent chromium using distillery sludge. Bioresour. Technol. 89, 207–211.

Senthilkumaar, S., Kalaamani, P., Subburaam, C.V. (2006) Liquid phase adsorption of crystal violet onto activated carbons derived from male flowers of coconut tree. J Hazard. Mater. 136, 800–808.

Sen, T.K., Sarzali, M.V. (2008) Removal of cadmium metal ion ($Cd^{2+)}$ from its aqueous solution by aluminium oxide (Al_2O_3): A kinetic and equilibrium study. Chem. Eng. J. 142, 256–262.

Sewu, D.D., Boakye, P., Woo, S.H. (2017) Highly efficient adsorption of cationic dye by biochar produced with Korean cabbage waste. Bioresour. Technol. 224, 206–213.

Shahalam, A.M., Al-Harthy, A., Al-Zawhry, A. (2002) Feed water pretreatment in RO systems in the Middle East. Desalination 150, 235–245.

Sharma, S.K., Sanghi, R. (2012) Advances in water treatment and pollution prevention, Springer, Dordrecht, Netherlands.

Shayesteh, H., Kelishami, A.R., Norouzbeigi, R. (2015) Adsorption of malachite green and crystal violet cationic dyes from aqueous solution using pumice stone as a low-cost adsorbent: Kinetic, equilibrium and thermodynamic studies, Desalination and Water Treatment, 57, 12822–12831.

Shi, L., Wei, D., Ngo, H.H., Guo, W., Du, B., Wei, Q. (2015) Application of anaerobic granular sludge for competitive biosorption of methylene blue and Pb(II): Fluorescence and response surface methodology. Bioresour. Technol. 194, 297–304.

Shi, L., Zhang, G., Wei, D., Yan, T., Xue, X., Shi, S., Wei, Q. (2014) Preparation and utilization of anaerobic granular sludge-based biochar for the adsorption of methylene blue from aqueous solutions. J. Mol. Liq., 198, 334–340.

Shibi, I.G., Anirudhan, T.S. (2006) Polymer-grafted banana (*Musa paradisiaca*) stalk as an adsorbent for the removal of lead(II) and cadmium(II) ions from aqueous solutions: kinetic and equilibrium studies. J. Chem. Technol. Biotechnol. 81, 433–444.

Sing, K.S.W., Everett, D.H., Haul, R.A.W., Moscou, L., Pierotti, R.A., Rouquerol, J., Siemieniewska, T. (1985) Reporting physisorption data for gas/solid systems with special reference to the determination of surface area and porosity. Pure and Applied Chemistry, 57, 603–619.

Singh, B., Singh, B.P., Cowie, A.L. (2010) Characterizaion and evaluation of biochars for their application as a soil amendment. Australian Journal of Soil Research 48, 516–525.

Singh, J., Mishra, N.S., Umba, Banerjee, S., C. Sharma, Y. (2011) "Comparative study of physical characteristics of raw and modified sawdust for their use as adsorbents for removal of acid dye". Bio Resources, 6, 2732–2743.

Singh, K.P., Mohan, D., Sinha, S., Tondon, G.S., Gosh, D. (2003) Color removal from wastewater using low-cost activated carbon derived from agricultural waste material. Ind. Eng. Chem. Res. 42, 1965–1976.

Singh, S. M., Gangwar, G. R., Prakash, O., Rachna (2010) Biocomposting of extracted peppermint plant residue (*Mentha piperita*) using red worm, *Eisenia fetida* and its effect on the growth of *Vigna mungo* (Urad). Journal of Applied and Natural Science 2, 305–312.

Singh, V.K., Tiwari, P.N. (1997) Removal and recovery of chromium (VI) from industrial wastewater. J. Chem. Technol. Biotechnol. 69, 376–382.

Sivakumar, P., Palanisamy, N. (2010) Mechanistic study of dye adsorption on to a novel non-conventional low-cost adsorbent. Adv. Appl. Sci. Res. 1, 58–65.

Smidt, E., Schwanninger, M. (2005) Characterization of waste materials using FT-IR Spectroscopy – Process monitoring and quality assessment. Spectro. Lett. 38, 247–270.

Sobhanardakani, S., Parvizimosaed, H., Olyaie, E. (2013) Heavy metals removal from wastewaters using organic solid waste—rice husk. Environ. Sci. Pollut. Res. 20, 5265–5271.

Soliman, E.M., Ahmad, S.A., Fadl, A.A. (2011) Reactivity of sugarcane bagasse as a natural solid phase extractor for selective removal of Fe(III) and heavy metal ions from natural water samples. Arab. J. Chem. 4, 63–70.

Sonawane, G.H., Shrivastava, V.S. (2009) Kinetics of decolourization of malachite green from aqueous medium by maize cob (Zea maize): an agricultural solid waste. Desalination 247, 430–441.

Stolz, A. (2001) Basic and applied aspects in the microbial degradation of azo dyes. Appl. Microbiol. Biotechnol. 56, 69–80.

Sud, D., Mahajan, G., Kaur, M.P. (2008) Agricultural waste material as potential adsorbent for sequestering heavy metal ions from aqueous solutions: a review. Bioresour. Technol. 99, 6017–6027.

Sun, L., Wan, S., Luo, W. (2013) Biochars prepared from anaerobic digestion residue, palm bark, and eucalyptus for adsorption of cationic methylene blue dye: Characterization, equilibrium, and kinetic studies. Bioresour. Technol. 140, 406–413.

Sun, Q., Yang, L. (2003) The adsorption of basic dyes from aqueous solution on modified peat-resin particle. Water Res. 37, 1535–1544.

Suwandi, A.C., Indraswati, N., Ismadji, S. (2012) Adsorption of N-methylated diaminotriphenylmethane dye (Malachite green) on natural rarasaponin modified kaolin. Desalination and Water Treatment, 41, 342–355.

Tan, X., Liu, Y., Zeng, G., Wang, X., Hu, X., Gu, Y., Yang, Z. (2015) Application of biochar for the removal of pollutants from aqueous solutions. Chemosphere 125, 70–85.

Tasaso, P. (2014) Adsorption of copper using pomelo peel and depectinated pomelo peel. J. Clean Energy Technol. 2, 154–157.

Tavlieva, M.P., Genieva, S.V., Georgieva, V.G., Vlaev, L.T. (2013) Kinetic study of brilliant green adsorption from aqueous solution onto white rice husk ash. J. Colloid Interface Sci. 409, 112–122.

Thirumavalavan, M., Lai, Y.L., Lee, J.F. (2011) Fourier transform infrared spectroscopic analysis of fruit peels before and after the adsorption of heavy metal ions from aqueous solution. J. Chem. Eng. Data 56, 2249–2255.

Tiravanti, G., Petruzzelli, D., Passiono, R. (1997) Pretreatment of tannery wastewaters by an ion exchange process for Cr(III) removal and recovery. Water Sci. Technol. 36, 197–207.

Tofan, L., Teodosiu, C., Paduraru, C., Wenkert, R. (2013) Cobalt (II) removal from aqueous solutions by natural hemp fibers: batch and fixed-bed column studies. Appl. Surf. Sci., doi:10.1016/j.apsusc.2013.06.151

Tsai, W.T., Chang, C.Y., Lin, M.C., Chien, S.F., Sun, H.F., Hsieh, M.F. (2001) Adsorption of acid dye onto activated carbons prepared from agricultural waste bagasse by $ZnCl_2$ activation. Chemosphere, 45, 51–58.

Tsai, W.T., Chen, H.R. (2010) Removal of malachite green from aqueous solution using low-cost chlorella-based biomass. J. Hazard. Mater. 175, 844–849.

Tyagi, O.D., Yadav, M.S., Yadav, M. (2002) A Textbook of Synthetic Dyes. 67, Anmol-PVT. LTD.

UN-Water (2013) Factsheet on water scarcity. www.UNWater.org

UNICEF, FAO and SaciWATERs (2013) Water in India, situation and prospects, New Delhi.

USEPA (1995) Profile of fabricated metal products industry. Office of Compliance, Office of Enforcement and Compliance Assurance, Washington, D.C.

USEPA (2012) Drinking water standards and health advisories, Office of Water, Washington, D.C.

Van der Zee, F.P., Bisschops, I.A., Blanchard, V.G., Bouwman, R.H., Lettinga, G., Field, J.A. (2003) The contribution of biotic and abiotic processes during azo dye reduction in anaerobic sludge. Water Res. 37, 3098–3109.

Vadivelan, V., Kumar, K.V. (2005) Equilibrium, kinetics, mechanism, and process design for the sorption of methylene blue onto rice husk. Colloid Interface Sci. 286, 90–100.

Verma, A.K., Raghukumar, C., Verma, P., Shouche, Y.S., Naik, C.G. (2010) Four marine-derived fungi for bioremediation of raw textile mill effluents. Biodegradation, 21, 217–233.

Verma, A.K., Dash, R.R., Bhunia, P. (2012) A review on chemical coagulation/flocculation technologies for removal of colour from textile wastewaters. J. Environ. Manage. 93, 154–168.

Verma, V.K., Mishra, A.K. (2008) Removal of dyes using low cost adsorbents. Ind. J. Chem. Tech.15, 140–145.

Wang, C., Gu, L., Liu, X., Zhang, X., Cao, L., Hu, X. (2016) Sorption behavior of Cr(VI) on pineapple-peel-derived biochar and the influence of coexisting pyrene. Int. Biodeterior. Biodegrad. 111, 78–84.

Wang, L.K., Chen, J.P., Hung, Y.T., Shammas, N.K. (2009) Heavy metals in the environment. CRC press, Boca Raton.

Wang, Y.Q., Zhang, Z., Qin, L., Liu, Y.H. (2012) Adsorption of Thorium from aqueous solution by HDTMA+-pillared bentonite. Journal of Radioanalytical and Nuclear Chemistry, 293, 519–528.

Wang, X.S., Liu, X., Wen, L., Zhou, Y., Li, Z. (2008) Comparison of basic dye crystal violet removal from aqueous solution by low-cost biosorbents. Sep. Sci. Technol. 43, 3712–3731.

Wang, Z.H., Xiang, B., Cheng, R.M., Li, Y.J. (2010) Behaviors and mechanism of acid dyes sorption onto diethylenetriamine-modified native and enzymatic hydrolysis starch. J. Hazard. Mater. 183, 224–232.

Waranusantigul, P., Pokethitiyook, P., Kruatrachue, M., Upatham, E.S. (2003) Kinetics of basic dye methylene blue biosorption by giant duck week *Spirodela polyrrhiza*. Environ. Poll. 385, 92.

Wawrzkiewicz, M. (2012) Comparison of the efficiency of Amberlite IRA 478RF for acid, reactive and direct dyes removal from aqueous media and wastewaters. Industrial and Engineering Chemistry Research, 51, 8069–8078.

Weber, W.J., Morris, J.C. (1962) Advances in water pollution research: Removal of biologically resistant pollutant from waste water by adsorption. International Conference on Water Pollution Symposium. Vol. 2. Pergamon, Oxford, pp. 231–266.

Wen, Y., Tang, Z., Chen, Y., Gu, Y. (2011) Adsorption of Cr(VI) from aqueous solutions using chitosan-coated fly ash composite as biosorbent. Chem. Eng. J. 175, 110–116.

World Health Organization (1988) Environmental Health Criteria 61, Chromium, WHO, Geneva.

WHO (2011) Guidelines for drinking water quality, 4th Edition, Geneva.

Wu, S.J., Liou, T.H., Mi, F.L. (2009) Synthesis of zero-valent copper–chitosan nanocomposites and their application for treatment of hexavalent chromium. Bioresour. Technol. 100, 4348–4353.

Wyantutia, S., Hartatia, Y.W., Panataranib, C., Tjokronegoroa, R. (2015) Cyclic Voltammetric Study of Chromium (VI) and Chromium (III) on the Gold Nanoparticles-Modified Glassy Carbon Electrode. Procedia Chemistry 17, 170–176.

Xuejiang, W., Ling, C., Siqing, X., Jianfu, Z., Chovelon, J.M., Renault, N.J. (2006) Biosorption of Cu (II) and Pb (II) from aqueous solutions by dried activated sludge. Mineral. Eng., 19, 968–971.

Xu, Y., Chen, B. (2013) Investigation of thermodynamic parameters in the pyrolysis conversion of biomass and manure to biochars using thermogravimetric analysis. Bioresour. Technol. 146, 485–493.

Yadav, D., Kapur, M., Kumar, P., Mondal, M.K. (2015) Adsorptive removal of phosphate from aqueous solution using rice husk and fruit juice residue. Process. Saf. Environ. 94, 402–409.

Yagub, M.T., Sen, T.K., Ang, H.M. (2013) Removal of cationic dye methylene blue (MB) from aqueous solution by ground raw and base modified pine cone powder. Environ. Earth. Sci. doi: 10.1007/s12665-013-2555-0.

Yagub, M.T., Sen, T.K., Ang, H.M. (2012) Equilibrium, kinetics and thermodynamics of methylene blue adsorption by pine tree leaves. Water Air Soil Pollut. 223, 5267–5282.

Yakout, S.M. (2015) Monitoring the changes of chemical properties of rice straw – derived biochars modified by different oxidizing agents and their adsorptive performance for organics. Bioremediation J. 19, 171–182.

Yang, P., Guo, D.B., Chen, Z.H., et al. (2017) Removal of Cr (VI) from aqueous solution using magnetic biochar synthesized by a single step method. J. Dispersion Sci. Technol. 38, 1665–1674.

Yargicoglu, E.N., Sadasivam, B.Y., Reddy, K.R., Spokas, K. (2014) Physical and chemical characterization of waste wood derived biochars. Waste Manage. 36, 256–268.

Yuan, J-H., Xu, R-K., Zhang, H. (2011) The forms of alkalis in the biochar produced from crop residues at different temperatures. Bioresour. Technol. 102, 3488–3497.

Yuvaraja, G., Krishnaiah, N., Subbaiah, M.V., Krishnaiah, A. (2014) Biosorption of Pb (II) from aqueous solution by Solanum melongena leaf powder as a low-cost biosorbent prepared from agricultural waste. Colloids Surf. B 114, 75–81.

Zhang, J., Li, Y., Zhang, C., Jing, Y. (2008) Adsorption of malachite green from aqueous solution onto carbon prepared from Arundo donax root. J. Hazard. Mater. 150, 774–782.

Zhang, S.W., Zeng, M.Y., Li, J.X., Li, J.J., Xu, Z., Wang, X.K. (2014) Porous magnetic carbon sheets from biomass as an adsorbent for the fast removal of organic pollutants from aqueous solution. J. Mater. Chem., 2, 4391.

Zhang, X., Lv, L., Qin, Y., Xu, M., Jia, X., Chen, Z. (2018) Removal of aqueous Cr(VI) by a magnetic biochar derived from *Melia azedarach* wood. Bioresour. Technol. 256, 1–10.

Zhang, Z., Yan, X., Tian, B., Yu, C., Tu, B., Zhu, G., Qiu, S., Zhao, D. (2006) Synthesis of ordered small pore mesoporous silicates with tailorable pore structures and sizes by polyoxyethylene alkyl amine surfactant. Micropor. Mesopor. Mat. 90, 23–31.

Zhao, N., Yin, Z., Liu, F., Zhang, M., Lv, Y., Hao, Z., Pan, G., Zhang, J. (2018) Environmentally persistent free radicals mediated removal of Cr(VI) from highly saline water by corn straw biochars. Bioresour. Technol. 260, 294–301.

Zheng, L., Zhu, C., Dang, Z., Zhang, H., Yi, X., Liu, C. (2012) Preparation of cellulose derived from corn stalk and its application for cadmium ion adsorption from aqueous solution. Carbohydr. Polym. 90, 1008–1015.

Zhou, L., Liu, Y., Liu, S., et al. (2016) Investigation of the adsorption-reduction mechanisms of hexavalent chromium by ramie biochars of different pyrolytic temperatures. Bioresour. Technol. 218, 351–359.

Zhou, X., Korenaga, T., Takahashi, T., Moriwake, T., Shinoda, S. (1993) A process monitoring/controlling system for the treatment of wastewater containing Cr(VI). Water Res. 27, 1049–1054.

Zhu, L., Ma, J. (2008) Simultaneous removal of acid dye and cationic surfactant from water by bentonite in one-step process. Chem. Eng. J. 139, 503–509.

Zou, W., Zhao, L., Zhu, L. (2012) Efficient uranium(VI) biosorption on grapefruit peel: Kinetic study and thermodynamic parameters. J. Radioanal. Nucl. Chem. 292, 1303–1315.

Research Publications

1. **Patent Application Publication-** Name of Inventors: **Abhay Prakash Rawat** and D. P. Singh; Title of the invention: *Mentha piperita* plant ash (MPA) adsorbent for the removal of dyes and heavy metals. Intellectual Property India, Application No. : 2716/DEL/2015, Journal No. 40/2016, Publication date: 23/09/2016.
2. **Abhay Prakash Rawat** and D. P. Singh (2017). Kinetic and thermodynamic study on adsorption characteristics of ash derived from distilled waste of aromatic crop *Mentha piperita*: a low-cost efficient adsorbent for crystal violet removal. Desalination and Water Treatment, 84, 225–236; doi: 10.5004/dwt.2017.21072
3. **Abhay Prakash Rawat** and D. P. Singh (2018). Decolourization of malachite green dye by mentha plant biochar (MPB): a combined action of adsorption and electrochemical reduction processes. Water Science and Technology, 77, 1734-1743; DOI: 10.2166/wst.2018.059
4. Prem Chandra, **Abhay Prakash Rawat** and D. P. Singh (2016). Isolation of alkaliphilic bacterium Citricoccus alkalitolerans CSB1: an efficient bio-sorbent for bioremediation of tannery waste water. Cellular and Molecular Biology, 62:3; doi:10.4172/1165-158X.1000135
5. **Abhay Prakash Rawat** and D. P. Singh (2018). Synergistic action of surface adsorption and reductive properties of mentha biochars prepared at different pyrolysis temperature in removal of methylene blue dye from aqueous media. Separation Science and Technology (Communicated).
6. **Abhay Prakash Rawat** and D. P. Singh (2018). Synergistic adsorption and reduction of hexavalent chromium using mentha plant ash (MPA) as a biosorbent. Journal of Hazardous materials (Communicated).

Papers presented in Conferences

1. Presented a paper on the title ‘‘Equilibrium, kinetic and thermodynamic study on adsorption characteristics of mentha activated carbon (MAC) in removal of methyl orange dye’’ in the National Conference on “*Biodegradation of wildlife, Environment and Biodiversity*” organized by Gandhi Faiz-E-Aam (P.G.) College, Shahjahanpur held during 19th – 20th March, 2017.
2. Presented a paper on the title “Removal of malachite green dye from aqueous solution using mentha plant biochar (MPB) as a biosorbent” in national symposium on “Biodiversity and natural resources for sustainable development & 37th annual session of Academy of Environmental Biology” organized by Department of Zoology, Chaudhary Charan Singh University, Meerut, (U.P.), India during 24-26th November, 2017.
3. Presented a paper on the title “Organic and inorganic contaminants removal from wastewater using low-cost adsorbents” in the workshop on “Socio-environmental Dimensions of Rejuvenating River Gomti” organized by the Department of Environmental Science, Babasaheb Bhimrao Ambedkar University (BBAU), Lucknow, (U.P.), India held on 23rd April, 2018.